Heart Holes and Breath Holds: Influence of Sex and Intracardiac Shunt on Pulmonary Gas Exchange Efficiency and Association of Vascular Mediators on Blunted Hypoxic Pulmonary Vasoconstriction in Apnea Divers

by

Tyler Kelly

A dissertation accepted and approved in partial fulfillment of the

requirements for the degree of

Doctor of Philosophy

in Human Physiology

Dissertation Committee:

Dr. Andrew Lovering, PhD, Chair

Dr. Ashley Walker, PhD, Core Member

Dr. William Cornwell, MD, Non-UO Member

Dr. Rachel Lord, PhD, Non-UO Member

Dr. Joshua Snodgrass, PhD, Institutional Representative

University of Oregon

Fall 2023

DISSERTATION ABSTRACT

Tyler Kelly

Doctor of Philosophy in Human Physiology

Title: Heart Holes and Breath Holds: Influence of Sex and Intracardiac Shunt on Pulmonary Gas Exchange Efficiency and Association of Vascular Mediators on Blunted Hypoxic Pulmonary Vasoconstriction in Apnea Divers

Patent foramen ovale (PFO) has been documented in humans since Galen reported their existence approximately 2000 years ago. PFO has been associated with a variety of negative outcomes such as impaired ventilatory acclimatization to altitude and increased risk for high altitude pulmonary edema. However, the degree to which PFO impacts pulmonary gas exchange efficiency has remained under debate.

Apnea diving presents unique challenges to the cardiopulmonary system. These challenges arise from the combination of physiological stressors created by diving, ranging from increased central venous pressure to severe hypoxia during the final ascent phase a dive. These unique stressors have created unique physiological adaptations in apnea divers.

In Chapter IV the interaction of sex and PFO size, as determined by saline contrast echocardiography, is explored in participants at rest and while participating in moderate to strenuous exercise. The data in this chapter show that in females, but not males, with large PFO there is a significant impairment in pulmonary gas exchange efficiency. Additional work in Chapter V shows that percutaneous closure of PFO improves pulmonary gas exchange efficiency in women.

Chapter VI examined the prevalence of PFO in apnea divers to non-diving controls, finding that divers are significantly more likely to have a PFO. Chapter VII utilized a 20- to 30-

minute hypoxic challenge to investigate changes in pulmonary resistance in divers vs non diving controls. This chapter shows that apnea divers had a severely blunted increase in pulmonary resistance in response to hypoxia. Chapter VIII investigated potential mediators of pulmonary vascular tone in apnea divers and individuals breathing 11.5% oxygen for 7 to 10 hours, as well as whether there were differences in the circulating inflammatory milieu. The data presented in this chapter shows that apnea divers do not have greater bioavailability of nitric oxide nor greater endothelin-1 levels compared to non-diving controls.

This dissertation includes previously published co-authored material as well previously unpublished co-authored material.

CURRICULUM VITAE

NAME OF AUTHOR: Tyler Kelly

GRADUATE AND UNDERGRADUATE SCHOOLS ATTENDED:

University of Oregon, Eugene
California State University, East Bay
California State University, Chico

DEGREES AWARDED:

Doctor of Philosophy, Human Physiology, 2023, University of Oregon
Master of Science, Kinesiology, 2016, California State University
Bachelor of Science, Exercise Physiology, 2009, California State University

AREAS OF SPECIAL INTEREST:

Hypoxic Pulmonary Vasoconstriction
Exercise Physiology
Environmental Physiology
Pulmonary Gas Exchange

PROFESSIONAL EXPERIENCE:

Graduate Teaching Fellow, Department of Human Physiology, University of Oregon, September 2018-December 2023

Research Assistant, Department of Human Physiology, University of Oregon, September 2018-December 2023

Program Lead, United States Anti-Doping Agency, September 2016-September 2018

GRANTS, AWARDS, AND HONORS:

Eugene & Clarissa Evonuk Memorial Graduate Fellowship in Environmental or Stress Physiology, Department of Human Physiology, University of Oregon, June 2022

PUBLICATIONS:

Kelly T, **Brown C**, **Bryant-Ekstrand M**, **Lord R**, **Dawkins T**, **Drane A**, **Futral JE**, **Barak O**, **Dragun T**, **Stembridge M**, **Spajić B**, **Drviš I**, **Duke JW**, **Ainslie PN**, **Foster GE**, **Dujic Z**, **Lovering AT**. Blunted hypoxic pulmonary vasoconstriction in apnoea divers. *Experimental Physiology* 107: 1225–1240, 2022. doi: 10.1113/EP090326.

Kelly T, **Patrician A**, **Bryant-Ekstrand M**, **Brown C**, **Gasho C**, **Caldwell HG**, **Lord RN**, **Dawkins T**, **Drane A**, **Stembridge M**, **Dragun T**, **Barak O**, **Spajić B**, **Drviš I**, **Duke JW**, **Foster GE**, **Ainslie PN**, **Dujić Ž**, **Lovering AT**. High prevalence of patent foramen ovale in recreational to elite breath hold divers.

Lovering AT, **Kelly TS**, **DiMarco KG**, **Bradbury KE**, **Charkoudian N**. Implications of a patent foramen ovale for environmental physiology and pathophysiology: do we know the 'hole' story? *The Journal of Physiology* 600: 1541–1553, 2022. doi: 10.1113/JP281108.

Kelly T, Bryant-Ekstrand M, Bradbury K, DiMarco K, Betts A, Kysar J, Futral JE, Goodman RD, Hawn JA, Gladstone IM, Duke JW, Elliott JE, Lovering AT. Impaired pulmonary gas exchange efficiency and blunted ventilation during exercise in some women, but not men, with patent foramen ovale. *The Journal of Physiology* (**In revision**) 2023

ACKNOWLEDGMENTS

This dissertation represents the culmination of several years of work in the Cardiopulmonary and Respiratory Physiology Lab at the University of Oregon. While this dissertation is presented as my work, it would not have been possible without the assistance, advice, and effort of the dozens of collaborators who contributed to the research contained herein.

I would like to acknowledge Dr. Lovering who has invested countless hours in guiding my development as a scientist and researcher. I would also like to thank the members of my committee for their time, insight, and support through the dissertation process. I would also like to thank the members of the Cardiopulmonary and Respiratory Physiology Lab, particularly my fellow graduate students without whom the arterial line studies I depended on for multiple chapters simply couldn't have happened. I would also like to thank Ms. Bryant-Ekstrand for her reliability and enthusiasm, both of which were great contributors to my success. Additionally, I would like to thank Drs. Hawn, Yang, and Padgett for their assistance in placing radial arterial catheters for gas exchange studies, as well as the excellent echocardiographers we were fortunate enough to work with, both in Eugene and during our field studies in Croatia. Additionally, Dr. Gladstone's calm and composed presence during stressful studies was invaluable. I would also like to acknowledge the staff of the Department of Human Physiology, who's knowledge and expertise was essential at navigating the numerous deadlines and milestones involved in completing the PhD program.

Lastly, I would like to thank my family and my friends within the graduate program. Without their ongoing support, whether in the form of laughing off a bad day over a beer or

encouragement to continue through challenges outside my control, completing this dissertation would have been infinitely more challenging. Thank you.

TABLE OF CONTENTS

LIST OF FIGURES

Figure Page

LIST OF TABLES

Table Page

LIST OF EQUATIONS

Equation Page

CHAPTER I

INTRODUCTION

Movement of blood through the body can be divided into two primary circuits. The first consists of systemic circulation, where well-oxygenated blood arrives in the left atrium, moves to the left ventricle, and is then pumped to the many tissues of the body. The second, and more relevant to this dissertation, is pulmonary circulation. Blood from the body, high in carbon dioxide and low in oxygen, arrives in the right atrium, flows to the right ventricle, and is then pumped to the lungs. Once in the lungs this blood undergoes pulmonary gas exchange, offloading carbon dioxide and taking on oxygen, before arriving in the left atria to be delivered into the systemic circulation.

The importance of pulmonary circulation and pulmonary gas exchange should be obvious, and there have evolved mechanisms which serve to maximize the efficacy thereof. One of the most important of these mechanisms is hypoxic pulmonary vasoconstriction (HPV), whereby blood vessels flowing to poorly oxygenated areas of the lungs are subject to a reduction in their diameter, increasing resistance in these vessels and redirecting the flow of blood to better ventilated portions of the lungs. In situations where only small portions of the lung suffer from poor oxygenation, matching ventilation with perfusion is an effective mechanism to maximize the exchange of oxygen and carbon dioxide between the alveolar air and blood.

The efficiency of this gas exchange can also indirectly be harmed by right-to-left shunt, where blood returning from the systemic circulation bypasses the pulmonary circulation and directly re-enters the systemic circulation without undergoing pulmonary gas exchange, creating a source of venous admixture. This venous admixture has the effect of lowering the average oxygen content of systemic blood at sea level and when breathing hyperoxic gas concentrations.

A certain degree of shunt and venous admixture is expected, and derives from normal human anatomy, such as the bronchial and thebesian circulations which drain directly into the pulmonary veins and left atria, respectively. However, other sources of right-to-left shunt can exist, such as patent foramen ovale (PFO), and exacerbate venous admixture.

This dissertation has two primary objectives: 1) determine how a PFO influences pulmonary gas exchange efficiency and 2) determine how apnea diving, a form of chronic intermittent hypoxia, alters HPV. To accomplish the first objective, I will characterize how the presence of PFO impacts pulmonary gas exchange efficiency in women and men. I will subsequently examine how closure of the PFO, through a medical intervention, alters pulmonary gas exchange efficiency thereby directly demonstrating how this source of shunt impacts pulmonary gas exchange efficiency. To accomplish the second primary objective, I will characterize how apnea diving influences HPV in apnea divers and controls. I will subsequently use serum from apnea divers to investigate the influence of circulating inflammatory factors on nitric oxide and endothelin-1 release on HPV.

HISTORICAL PERSPECTIVE

One of the first physiologists, Claudius Galen is often remembered for his work as a physician to Roman gladiators as well as a succession of Roman emperors. His explanations for how the heart, lungs, and circulatory system functioned were considered definitive for nearly 1500 years after his death. Galen believed that blood was generated in the liver and distributed by veins, while air was absorbed by the lungs and distributed by blood in the arteries. According to Galen, blood was able to move from the veins into arteries in the heart by passing through tiny, invisible holes in the septum dividing the left and right heart (1). It wasn't until William Harvey's 1628 publication of *Exercitatio Anatomica de Motu Cordis et Sanguinis in Animalibus*,

which translated to English means *Anatomical Exercises on the Motion of the Heart and Blood in Animals*, that Galen's understanding was superseded and the concept of a circulatory, as opposed to open-ended, system was established.

Galen also described the physiological closure of PFO at birth. However, it was not until 1,300 years later, in 1513 that the polymath Leonardo da Vinci described and importantly illustrated the patent foramen ovale (2). In his dissections of human cadavers, da Vinci noted that there sometimes occurred a "perforating channel" between the atria of the heart and illustrated his findings in *Quadernii d'Anatomia* (da Vinci, 1952 as cited in Shoja et al., 2013). However, sometimes this process of closure and sealing fails either partially or completely, resulting in a patent foramen ovale. One of the earliest studies of the prevalence of PFO was carried out by Fawcett and Blachford, who reported a frequency of PFO of approximately 30% in deceased subjects over age 10. Interestingly, women had a slightly higher prevalence of PFO compared to men (Fawcett & Blachford, 1900).

Pulmonary exchange of gases was originally thought to be due to active secretion of oxygen from the lungs into the pulmonary capillaries, a stance supported by giants in the field such as Christian Bohr and J.S. Haldane (5). It wasn't until Bohr's student, August Krogh, developed an accurate tonometer that it could be shown that arterial pressure of oxygen was always lower than alveolar pressure of oxygen (6), showing that the lungs did not secrete oxygen. This finding would be confirmed by Marie Krogh, who developed an accurate method to determine the diffusing capacity of the lung and demonstrated that Bohr and Haldane significantly underestimated how much oxygen could diffuse across the lung (5).

The first recordings of pulmonary arterial pressure, made in the 1850s, showed that interruption of ventilation resulted in an increased pulmonary vascular pressure that reversed

upon resumption of ventilation (Beutner, 1852 as cited in Young et al., 2019). One of the earliest descriptions of the constriction of the pulmonary vasculature in response to low levels of oxygen was by German physician Ernst von Romberg in 1891, who described autopsy findings of "pulmonary vascular sclerosis" (9, 10). In 1946 von Euler and Liljestrand published their landmark paper showing a clear relationship between inspired concentrations of oxygen and increases in pulmonary arterial pressure. Reducing the fraction of inspired oxygen to 10-11% "invariably" resulted in an increase in pulmonary arterial pressure (11). Von Euler and Liljestrand accurately attributed this increase in pulmonary arterial pressure to vasoconstriction, and accurately hypothesized that this HPV functioned to ensure blood was redirected to perfuse the best-ventilated portions of the lung and away from poorly ventilated portions.

BACKGROUND AND SIGNIFICANCE

Pulmonary Gas Exchange Efficiency and Diffusion Limitation

One of the most crucial functions of the lungs, and the one most people are familiar with, is the exchange of oxygen and carbon dioxide between blood and air within the lungs. How well this function is performed is described as pulmonary gas exchange efficiency and is quantified as the difference in the partial pressure of oxygen between the alveoli and arterial blood ($A\text{-}aDO_2$). There are three factors which can worsen pulmonary gas exchange efficiency (e.g. widen $A\text{-}aDO_2$): diffusion limitation, ventilation-perfusion (V/Q) matching, and right-to-left shunt (12). Diffusion limitation refers to any impairment in the ability of oxygen and carbon dioxide to diffuse across the alveolar and capillary tissues. While there are multiple factors which can influence the ability of gases to diffuse across the lung, in a healthy person resting at sea level it is unlikely for diffusion limitation to meaningfully impair pulmonary gas exchange efficiency. It takes approximately 0.25 seconds for gasses to fully equilibrate between the capillary and

alveoli, which is much less than the 0.8 seconds an erythrocyte spends in the pulmonary capillary (12). The exception to this is highly endurance trained individuals with extremely high cardiac outputs. These individuals may circulate blood so rapidly through the pulmonary vasculature that erythrocytes pass through pulmonary capillaries in less than 0.25 seconds, potentially preventing full equilibration of gases and leading to diffusion limitation. However, this is a rare exception, and most individuals experience no diffusion limitation at sea level, even while exercising at or near maximal capacity. The impact of diffusion limitation can be eliminated by breathing a sufficiently hyperoxic mixture, ensuring that the diffusion gradient between the alveolar air and capillary blood is great enough that full equilibration can occur regardless of exercise-induced reductions in pulmonary capillary transit time.

Ventilation-Perfusion Matching, Stimulus PO_2, HPV

Under normoxic conditions, ventilation and perfusion in the upright lung are relatively well-matched. During inspiration, ventilated alveoli expand, causing distension of extra-alveolar vessels through mechanical tethering of these vessels to lung parenchyma (13). This has the beneficial effect of increasing blood flow to those alveoli which are ventilated. Additionally, which portion of the lung is well-perfused can be controlled through vasoconstriction of the pulmonary arterioles. The quantity of blood which flows through a vessel is a function of the pressure gradient between the beginning and end of that vessel and the resistance of that vessel. Constriction of a pulmonary arteriole increases resistance in that vessel, reducing flow through that vessel for any given pressure gradient. A major influencer of pulmonary vascular resistance is the stimulus PO_2. The stimulus PO_2 is a combination of the PAO_2 of alveoli perfused by that vessel and the mixed venous PO_2 ($P\bar{v}O_2$) in the pulmonary artery. The contribution of these sources to the stimulus PO_2 is not equal – PAO_2 accounts for $2/3^{rd}$ of the stimulus PO_2 owing to

the relatively larger surface area of the alveolus compared to the capillary (14). Thus, an alveolus with low PO_2 causes constriction in the pulmonary arterial vessels leading to that alveolus and reducing blood flow to that poorly ventilated alveolus. This phenomenon is classified as HPV. As mentioned above, at or near sea level, this is an important mechanism to ensure that blood flows to the portions of the lung which are receiving fresh, relatively high oxygen air. However, in situations where *all* regions of the lung have a low PAO_2, pulmonary vasoconstriction can increase in all areas of the lung. Instead of redirecting bloodflow, this has the undesirable effect of increasing the total pulmonary resistance thereby requiring the right ventricle to pump harder to overcome a greater afterload.

Shunt

The third factor which can widen the $A\text{-}aDO_2$ is shunt. Shunt represents the portion of cardiac output which does not undergo gas exchange. This could mean that this blood flows through blood vessels in portions of the lung which are unventilated, or more frequently, bloodflow that bypasses the pulmonary circulation completely. This can also occur as part of normal anatomy, where some circulations drain directly into the pulmonary veins and left atria, such as the bronchial and thebesian circulations, respectively. A common source of intracardiac shunt is the PFO, which can allow for blood to flow directly from the right to left atrium. In situations where right atrial pressure exceeds left atrial pressure, such as immediately after releasing a Valsalva maneuver, blood may pass through this channel traveling from the right atrium to the left atrium. Right to left blood flow shunted through a PFO also has the potential to reduce arterial PO_2 at sea level due to the significantly lower PO_2 in mixed venous blood compared to the PO_2 in the arterial blood. Even a relatively small degree of shunt can meaningfully reduce PaO_2 if the difference between PaO_2 and $P\bar{v}O_2$ is great enough. However,

the closer P_vO_2 is to P_aO_2, the less impact the venous admixture will have on arterial oxygen saturation, such as occurs at high altitude (15). As blood flow through a PFO is dependent on inter-atrial pressure gradients, circumstances which increase right atrial pressure relative to left atrial pressure have the potential to increase the amount of blood flowing through a PFO. When pulmonary vascular pressure increases, such as during global HPV, the right ventricle and right atrium must operate at higher pressures to create the necessary pressure gradient to continue pumping blood through the pulmonary circuit. The increased right heart pressure and resultant elevation in right atrial pressure may, in some situations, be enough to facilitate right-to-left shunting through the PFO, resulting in worse pulmonary gas exchange efficiency.

Sex and Gas Exchange/Ventilation

Sex also plays a role in respiratory function and pulmonary gas exchange efficiency. Lung size is closely associated with height, and since men are on average taller than women, men also have greater average lung size (16). However, even when matched for height, men have larger lungs than women (17). Men and women also have different chest cavity geometry, which given that the lung expands to fill the chest cavity, may allow for greater lung capacity in men compared to women (18). Women may also display different respiratory mechanics compared to men (19). Women have a smaller airway area compared to men, even after adjusting for total lung capacity (20) as well as lower maximal flow rates and a greater frequency of being flow-limited during exercise (21, 22). Women may also have reduced diffusing capacity compared to men of the same age (23), though this may be a function of lung structure. When expressed as a function of alveolar volume, women no longer display impairments in diffusing capacity (24, 25). Women have been shown to be more likely to experience exercise-induced arterial hypoxemia caused at least in part by these differences in respiratory mechanics

(26). Additionally, women have been shown to be more likely to develop exercise-induced arterial hypoxemia and having a greater power of breathing for a given ventilation (26). Additionally, smaller airways necessitate greater changes in intrathoracic pressure to overcome increased airway resistance to achieve a given flow rate. These greater swings in intrathoracic pressure may have the potential to impact venous return and right atrial pressure, potentially making it more likely to have blood flow through a PFO in women.

Intermittent Hypoxia

Forms of intermittent hypoxia, particularly sleep apnea, have commonly been associated with a variety of negative outcomes such as hypertension and atherosclerosis (27). In sleep apnea, a cessation of breathing results in a reduction in arterial PO_2 and O_2 saturation. This leads to increased sympathetic autonomic activation, arousal, resumption of breathing, and return to sleep. This process can cycle dozens, hundreds, or thousands of times each night. In contrast to the negative sequelae of sleep apnea, other forms of intermittent hypoxia have been associated with reduced blood pressure (28) and suppression of proinflammatory mediators (29, 30) in addition to a wide variety of other positive sequelae (27). This apparent contradiction in the harm/benefit of intermittent hypoxia may be a result of the "hypoxic dose", or the product of the severity, duration, and frequency of the hypoxic challenge. In broad terms, available data suggest that highly frequent and highly severe hypoxic doses may lead to pathological outcomes, whereas doses that are infrequent and more moderate in the level of hypoxia may lead to beneficial outcomes. However, the potential benefits of intermittent and what may constitute appropriate "dosing" remain largely unexplored.

Diving Physiology

Breath hold diving presents a variety of challenges to the cardiopulmonary system. With immersion in water, there is a translocation of blood from the periphery to the thorax, increasing central venous volume and central venous pressure. As divers descend, for every 10m of depth there is a doubling of hydrostatic pressure and a halving of the gas volume in the lung, and gas solubility increases (31). The combination of decreasing lung volumes and increased blood volume in the thorax has the potential to drastically elevate pulmonary vascular pressure and right ventricular afterload. The right ventricle, when compared to the left ventricle, is meant to pump against a low-pressure circuit, and increases in right ventricular afterload frequently lead to right ventricular dysfunction, which can be detected by ultrasound measurements of tricuspid annular plane systolic excursion (TAPSE) (32). Additionally, the partial pressure of gases increases as hydrostatic pressure increases. This results in arterial hyperoxia as the diver proceeds to the nadir of their dive (33). However, the diver continues to consume oxygen during their dive, and the decreases in hydrostatic pressure as the diver ascends combined with oxygen consumption can result in PO_2 values that are dangerously low (34). Because these fluctuations in blood gases are driven by hydrostatic pressure, these dangerously low PO_2 values are not apparent until the very end of a dive and only for a short period. Divers nonetheless experience a severe and rapid-onset hypoxia, which becomes intermittent given the repetitive nature of apnea diving training, or spear fishing. It remains unknown whether this form of chronic intermittent hypoxia results in negative sequelae like other forms of chronic intermittent hypoxia such as sleep apnea.

Pulmonary Vascular Tone, Nitric Oxide, and Endothelin-1

As mentioned earlier, hypoxia can be a stimulus for contraction in the pulmonary vasculature. There are also numerous mechanisms which oppose vasoconstriction and relax or

dilate the pulmonary vessels. For the purposes of this dissertation, nitric oxide-mediated vasodilation is the most important. Nitric Oxide (NO) is a reactive oxygen species produced from a family of enzymes found throughout the body. This nitric oxide synthases (NOS) produce nitric oxide through the conversion of L-citrulline to L-arginine, releasing NO in the process. In the case of endothelial NOS (eNOS), found in vascular endothelium, NO then diffuses from the endothelial cell into the vascular smooth muscle where a series of reactions leads to reduction of intracellular calcium and vasodilation. Some inflammatory cytokines can interfere with this pathway by inhibiting eNOS expression (35, 36), and metabolic products associated with hypoxia can also impair generation of NO by eNOS (37). Thus, NO and eNOS have important roles in the regulation of pulmonary vascular tone and can interact with both inflammatory cytokines and hypoxia to modulate pulmonary vascular tone.

Whereas eNOS and NO function to reduce vasoconstriction, endothelins function to increase vasoconstriction. Endothelins, of which there are 3, are a class of peptides which are produced by endothelial cells and active in smooth muscle and endothelial cells. Endothelin-1 (ET-1) is the most important endothelin in regards to regulation of vascular tone, and unlike ET-2 and ET-3, is found in vascular endothelial cells (38). ET1 binds to ET_A receptors in smooth muscle cells and ET_B receptors in endothelial cells (39). Interestingly, the function of ET-1 is highly variable based on the receptor it binds to. When ET-1 binds to ET_A, the result is increased vasoconstriction, but when ET-1 binds to ET_B, the end result is vasodilation. However, the affinity of ET_A for ET-1 is much higher than that of ET_B, and at physiological concentrations, ET-1 acts as a potent vasoconstrictor and inhibitor of endothelial NO production. As such, balance between NO and ET-1 (among other vasoactive substances) is critical in regulating vascular tone.

PFO Closure and Exercise

As a source of shunt, the PFO has the potential to decrease arterial oxygen saturation and therefore decrease arterial oxygen content (CaO_2). Reductions in CaO_2 have the potential to impair exercise performance through both central and peripheral pathways. Lack of oxygen delivery to the brain has been associated with fatigue during exercise (40). This may be a function of reduced interstitial PO_2 caused by a mismatch between cerebral oxygen demand and oxygen supplied by cerebral blood flow(41). Delivery of oxygen to the brain is a function of CaO_2 and the volume of cerebral blood flow. While moderate intensity exercise increases cerebral blood flow, exercise intensities greater than approximately 70% of VO_{2Max} result in relative decrease in cerebral blood flow (42). During strenuous exercise, hyperventilation may reduce cerebral blood flow (43). The combination of reduced CaO_2 caused by PFO and reduced cerebral blood flow caused by strenuous exercise has the potential to reduce oxygen delivery to the brain and the potential to induce or exacerbate central fatigue during exercise. If reductions in cerebral blood flow limit oxygen delivery to the brain during high intensity exercise, this may drop interstitial PO_2 beyond a poorly-defined "critical limit", resulting in central fatigue (41).

While the above constellation of findings suggests the potential for PFO to alter central fatigue during strenuous exercise , the PFO is unlikely to impair oxygen delivery to the brain at rest, as brain blood flow can increase to compensate for any decrements in CaO_2 and maintain cerebral oxygen delivery. Peripherally, decreased CaO_2 reduces oxygen delivery to working muscles at a given volume of blood flow which in turn may potentially decrease the ability of those muscles to continue to exercise. Additionally, if those with PFO have increased ventilation at a given workload to maintain CaO_2, this would necessitate increased bloodflow to the respiratory muscles at this workload. This results in "respiratory steal", as the increased fraction

of cardiac output flowing to respiratory muscles reduces blood flow to locomotor muscles. Consequently, closing the PFO has the potential to improve exercise capacity by increasing CaO_2, reducing respiratory steal, and improving oxygen delivery.

STATEMENT OF PROBLEM

It is known that the PFO is a relatively common source of right-to-left intracardiac shunt, and has the potential to impair pulmonary gas exchange efficiency at rest (44, 45). The degree of shunt through PFO is also impacted by alterations in venous return and associated alterations in right atrial pressure (46). It has been reported that pulmonary gas exchange efficiency is worse in women than in men (26, 47), but the presence or absence of PFO in the women in these studies was not known. Thus, it is currently unknown how the presence and size of a PFO interact to impact pulmonary gas exchange efficiency within a given sex. It also unknown whether percutaneous closure of a PFO will improve pulmonary gas exchange efficiency or exercise capacity.

It is known that apnea diving creates unique challenges to the cardiopulmonary system due to the complex interactions between the mammalian diving response, changes in barometric pressure associated with diving, as well as intermittent hyperoxia and hypoxia (31). The thoracic shift in blood caused by peripheral vasoconstriction as part of the mammalian diving response combined with increases in barometric pressure can increase pulmonary vascular pressure, while the rapid and severe hypoxia associated with the late ascent phase creates a strong stimulus for HPV and increased pulmonary resistance. Both situations require increased right-heart work to maintain a given cardiac output. However, it is unknown if increases in pulmonary vascular pressure associated with apnea diving result in greater right-heart dysfunction. At the commencement of these projects, it was also unknown whether the stresses on the

cardiopulmonary system associated with apnea diving made conditions more favorable for the detection of PFO in apnea divers. We have since shown that PFO is detected at higher rates in apnea divers compared to non-diving controls (48), though the reasons for this difference remain unclear.

Lastly, it is known that some forms of intermittent hypoxia, such as sleep apnea, lead to a variety of negative sequela, including elevated circulating inflammatory cytokines (49–51). In turn, inflammation is known to interfere with eNOS expression and activity, leading to reductions in bioavailable nitric oxide (35, 52). It is also known that the hypoxic "dose," i.e., severity, frequency, and duration of the exposure, modulates whether adaptations are detrimental or beneficial (27). However, it is unknown if the intermittent hypoxia of apnea diving leads to beneficial or detrimental cardiopulmonary adaptations. It is also unknown whether the intermittent hypoxia of apnea diving may influence circulating inflammation and the bioavailability of nitric oxide.

PURPOSE AND HYPOTHESES

The purposes of this dissertation was to 1) determine if PFO size influences pulmonary gas exchange efficiency in men and women and investigate whether percutaneous closure of PFO improves pulmonary gas exchange efficiency and subsequently, exercise capacity; 2) determine if the PFO is more prevalent in apnea divers, and characterize the effect of the chronic intermittent hypoxia of apnea diving on HPV, levels of circulating vascular inflammation and/or the influence of apnea diver serum on eNOS and ET-1 activity in the pulmonary vasculature. To perform these investigations, I proposed the following questions and aims.

Aim #1

Previous work has shown that a PFO may act as an intracardiac right-to-left shunt during situations where right atrial pressure is elevated above left atrial pressure, such as end inspiration during diastole. Conceptually, a larger PFO allows for more shunt, allowing for a larger impact on pulmonary gas exchange efficiency (i.e., widening of $AaDO_2$). Females have smaller diameter airways, necessitating greater changes in intrathoracic pressure for the same quantity of ventilation compared to males. This likely results in greater fluctuations in right atrial pressure, potentially resulting in more shunting through the PFO. However, the effect of PFO size on pulmonary gas exchange efficiency at rest and during exercise has not been characterized in men and women. Therefore **Aim #1** tested the hypothesis that pulmonary gas exchange efficiency would be worse in those with large PFO.

Aim #2

Previous work has shown that a PFO may act as an intracardiac right-to-left shunt during situations where right atrial pressure is elevated above left atrial pressure, such as end expiration during diastole. It follows then that percutaneous closure of PFO prevents this shunting completely or near-completely, reducing venous admixture and improving pulmonary gas exchange efficiency and thereby improving exercise capacity. Therefor **Aim #2** tested the hypothesis that percutaneous closure of PFO would (A) improve pulmonary gas exchange efficiency and (B) improve exercise capacity by increasing CaO_2, when compared to before PFO closure.

Aim #3

Apnea diving results in significant elevations in pulmonary artery pressure due to the combination of lung compression and translocation of blood from the periphery into the thorax,

creating significant stress on the cardiopulmonary system. The PFO may act as a "pressure relief valve", limiting the increase in pulmonary vasculature pressures and allowing for deeper or more frequent dives, resulting in those with PFO "self-selecting" for apnea diving. Additionally, during the final portions of the ascent phase of the dive alveolar and mixed venous PO_2s rapidly decrease, creating a strong stimulus for HPV and another pathway for increasing stress on the cardiopulmonary system. Increased stress on the cardiopulmonary system may lead to increased right heart work and right ventricular dysfunction. Thus, **Aim #3** tested the hypotheses that (A) PFO would be more prevalent in apnea divers compared to non-diving controls, (B) apnea divers will have a greater total pulmonary resistance compared to non-diving controls, and (C) that apnea divers would have increased right ventricular dysfunction (e.g. reduced TAPSE) when compared to non-diving controls.

Aim #4

Preliminary data from our lab has shown that inflammatory cytokines are elevated in response to several hours of hypoxia, and that IL-6, IL-8, IL12p70, IL-17A and IL-23 are positively correlated with increased pulmonary pressure and resistance in response to the same hypoxic stimulus. However, there have been no studies examining whether *in vivo* NO production and release is correlated with these circulating inflammatory cytokines and PASP in response to several hours of hypoxia (11.5% O_2). Therefore, **Aim #4** tested the hypothesis that (A) plasma from subjects with the lowest cytokine levels and increases in PASP in response to 10 hours of breathing 11.5% O_2 will have the highest levels of plasma nitric oxide and lowest levels of endothelin-1 and (B) serum from apnea divers with lower HPV and cytokine levels will have greater levels of serum nitric oxide and lower levels of endothelin-1 compared to serum from non-diving controls with greater HPV and elevated cytokines.

Chapter IV is under review with the *Journal of Physiology* and was co-authored with Mohini Bryant-Ekstrand, Karleigh Bradbury, Kaitlyn DiMarco, Aaron Betts, Jacob Kysar, Joel E. Futral, Randall D. Goodman, Jerald A. Hawn, Igor M. Gladstone, Joseph W. Duke, Jonathen E. Elliott, and Andrew T. Lovering. Chapter V is in preparation for submission to the *Journal of Physiology* and was co-authored with Karleigh Bradbury, Kaitlyn DiMarco, Aaron Betts, Joel E. Futral, Jacob Kysar, Jerold A. Hawn and Andrew T. Lovering. Chapter VI is published in the *Journal of Science and Medicine in Sport* and was co-authored with Alexander Patrician, Mohini Bryant-Ekstrand, Courtney Brown, Christopher Gasho, Hannah G. Caldwell, Rachel N. Lord, Tony Dawkins, Aimee Drane, Michael Stembridge, Tanja Dragun, Otto Barak, Boris Spacjíc, Ivan Drviš, Joseph W. Duke, Glen E. Foster, Philip N. Ainslie, Željko Dujić, and Andrew T. Lovering. Chapter VII is published in the *Journal of Experimental Physiology* and was co-authored with Courtney Brown, Mohini Bryant-Ekstrand, Rachel Lord, Tony Dawkins, Aimee Drane, Joel E Futral, Otto Barak, Tanja Dragun, Michael Stembridge, Boris Spajić, Ivan Drviš, Joseph W. Duke, Philip N. Ainslie, Glen E. Foster, Željko Dujić, and Andrew T. Lovering. Chapter VIII was co-authored with Kaitlyn DiMarco, Abigail Cullen, Ashley Walker, and Andrew T. Lovering.

CHAPTER II

REVIEW OF THE LITERATURE

INTRODUCTION

The goal of this review of relevant literature is to present a comprehensive understanding of pulmonary gas exchange and how pulmonary gas exchange efficiency can be impaired by shunt, as well as briefly describing how sex assigned at birth influences respiratory physiology. The next section of this review of the literature provides an explanation for how pulmonary vascular tone is regulated by vasoactive factors, primarily nitric oxide and endothelin-1, as well as how pulmonary vascular tone changes in response to alveolar hypoxia. Additionally, this review of the literature presents information on how certain inflammatory cytokines can moderate the regulation of pulmonary vascular tone by disrupting nitric oxide synthesis. Finally, this review of the literature synthesizes these areas of information to characterize the unique challenges to cardiopulmonary physiology presented by apnea diving and the associated chronic intermittent hypoxia and hyperoxia.

PULMONARY GAS EXCHANGE

The transfer of gases from alveolar air to blood within the pulmonary capillaries, and vice-versa, is described as pulmonary gas exchange. The two primary gasses of interest are oxygen which diffuses from alveolar air to capillary blood, and carbon dioxide, which diffuses from capillary blood into alveolar air. As the site of gas exchange is the alveolar/capillary interface, alveolar ventilation ($\dot{V}_A$) is an important factor to consider. $\dot{V}_A$ represents the portion of ventilation ($\dot{V}_E$) that reaches the alveoli and takes into account the effects of $\dot{V}_E$ that never reaches the alveoli (i.e., dead space). $\dot{V}_A$ cannot be directly measured, and so must be calculated from the alveolar ventilation equation:

$$\dot{V}_A = \frac{\dot{V}CO_2 \times k}{PACO_2}$$

Equation 2.1. Alveolar Ventilation

Where $\dot{V}CO_2$ represents the volume of CO_2 production, $PACO_2$ represents the alveolar partial pressure of carbon dioxide, and k is a constant which accounts that the other variables in the equation are conventionally measured at different temperatures, pressures, and humidities (53), and is equal to 863 mmHg at 37°C. While k varies according to temperature, within the physiological range of temperatures 863 mm Hg is an appropriate value for k. Due to the diffusing capacity for CO_2 between approximately 20 times greater than that of oxygen, there is never a diffusion limitation for CO_2 (12), and we can assume that measured arterial CO_2 ($PaCO_2$) is equal to $PACO_2$.

Alveolar ventilation, ultimately, regulates alveolar PO_2 (PAO_2). However, similar to $\dot{V}_A$, PAO_2 cannot be directly measured and must be calculated. This is done utilizing the alveolar gas equation (54):

$$PAO_2 = [(P_B - e^{0.05894809 \times T_B + 1.689589}) \times FIO_2] - PaCO_2 \times [FIO_2 + \frac{(1 - FIO_2)}{RER}]$$

Equation 2.2. Alveolar Gas Equation

Where P_B represents ambient barometric pressure minus water vapor pressure, T_B represents measured body temperature, FIO_2 represents the fraction of inspired oxygen, $PaCO_2$ represents arterial CO_2, and RER represents the respiratory exchange ratio. $PaCO_2$ can be measured directly utilizing arterial blood samples and a blood gas analyzer, while RER can be calculated from measurements of $\dot{V}O_2$ and $\dot{V}CO_2$ obtained using a metabolic cart.

When the calculated PAO_2 is compared against PaO_2 measured by arterial sampling and blood gas analysis, the resulting difference is the definition and quantification of pulmonary gas exchange efficiency, or the alveolar-arterial difference in O_2 ($AaDO_2$). An $AaDO_2$ of 0 reflects perfect pulmonary gas exchange efficiency, and any value greater than zero reflects some degree of impairment. While theoretically pulmonary gas exchange may be perfectly efficient, pulmonary gas exchange is almost always impaired to some degree, for reasons which will be discussed below. While physiologically impossible, $AaDO_2$ may also be calculated to be a negative due to accumulations of small errors in the measured values. Potential factors which impair pulmonary gas exchange efficiency are a limitation in the ability of gasses to diffuse between the alveoli and capillaries within the given transit time of blood flow through the capillaries (diffusion limitation), alveolar ventilation-to-perfusion ($\dot{V}_A/\dot{Q}$) mismatch, and right-to-left shunt.

At rest, the time it takes for a single red blood cell to transit the length of a pulmonary capillary is approximately 0.8 seconds, whereas the time it takes for gasses to equilibrate between alveoli and capillary blood is approximately 0.2 seconds (12). Thus, under normal resting conditions, there is more than adequate time for complete gas exchange to occur. When cardiac output increases due to a perturbation such as exercise, pulmonary capillary time would theoretically decrease, possibly to the point of not allowing sufficient time for gasses to equilibrate – indeed, at extremely high cardiac outputs (> 25 L/min) pulmonary capillary transit time may decrease to the point that complete equilibration is not possible (55). However, at sea level, this situation occurs only in the very highest trained athletes who can sustain a cardiac output of > 25L/min. Outside of this elite population, increases in left atrial wedge pressure results in distension and recruitment of pulmonary capillaries (56). This combination results in a

preservation of pulmonary capillary transit time of >0.5 seconds, ensuring that diffusion limitation is not a meaningful contributor to pulmonary gas exchange inefficiency.

Ensuring that the pulmonary capillaries surrounding ventilated alveoli receive appropriate bloodflow (i.e., $\dot{V}_A/\dot{Q}$ matching) is fundamental to ensuring the appropriate exchange of gases and ensuring the prevention of arterial hypoxemia. While this is, to some degree, managed by bronchodilation in response to elevated $PACO_2$ (57), the majority of adjustments to ensure adequate $\dot{V}_A/\dot{Q}$ matching are the result of vasoconstriction to poorly ventilated alveoli through HPV. This mechanism, discussed in more detail below, increases the resistance in pulmonary arterioles feeding capillaries surrounding poorly ventilated alveoli, redirecting bloodflow to well-ventilated alveoli. While this mechanism is effective at redirecting blood from poorly ventilated areas of the lung to well-ventilated areas, there is a distribution of ventilation and perfusion across the lung where upper portions of the lung are relatively over-ventilated for their perfusion (high $\dot{V}_A/\dot{Q}$) and lower portions of the lung are over-perfused for their ventilation (low $\dot{V}_A/\dot{Q}$), leading to a $\dot{V}_A/\dot{Q}$ of approximately 0.8 when the lung is considered as a whole. Despite this slight $\dot{V}_A/\dot{Q}$ inequality across the whole lung, $\dot{V}_A/\dot{Q}$ mismatch is likely to be only a minor contributor to pulmonary gas exchange impairments in healthy lungs at sea level.

At rest, diffusion limitation and $\dot{V}_A/\dot{Q}$ matching are unlikely to meaningfully impair pulmonary gas exchange efficiency. However during exercise exceedingly high cardiac outputs may result in diffusion limitation, but this is limited to only the most elite athletes. $\dot{V}_A/\dot{Q}$ mismatch has also been suggested as a cause for some degree of gas exchange impairment during exercise, though increases in $\dot{V}_A/\dot{Q}$ from exercise are “relatively slight” (58) and not all studies have shown increased $\dot{V}_A/\dot{Q}$ mismatch during exercise (59), while others have shown effects at only extremely high ventilations and cardiac outputs (60). In contrast to diffusion

limitation and $\dot{V}_A/\dot{Q}$ matching, which appear to minimally contribute to gas exchange efficiency except at very high rates of exercise,, anatomical shunt *must* contribute to pulmonary gas exchange inefficiency to some degree at all exercise levels and at rest. Bronchial and thebesian circulations, as part of normal anatomy, drain directly into the left atrium resulting in approximately 0.5% shunt (61). This unavoidably introduces blood with low PO_2 into the systemic circulation and reduces PaO_2, unavoidably increasing $AaDO_2$ (61, 62). Any right-to-left shunt beyond this normally occurring anatomical shunt, such as PFO, will further impair pulmonary gas exchange efficiency and increase the $AaDO_2$. Prevalence studies of PFO have shown that up to 35-40% of the population may have a PFO (63, 64) and thus may be subject to increased shunt and worse pulmonary gas exchange efficiency.

Unlike normal anatomic shunt from bronchial and Thebesian circulations which occur with every heartbeat, shunt though a PFO is dependent upon the relative pressure gradient between the right and left atria and will only occur when right atrial pressure exceeds left atrial pressure. In a normal physiological state, left atrial pressure is greater than right atrial pressure, preventing flow through the PFO (65). However, this pressure gradient may undergo reversal for brief periods, such as end-inspiration during early ventricular diastole or during isovolumic ventricular contraction, allowing spontaneous blood flow through the PFO (65, 66). Similar right-to-left atrial pressure gradients can be created by utilizing a Valsalva release maneuver to transiently increase venous return and is used to aid in the detection of PFO by transthoracic saline contrast echocardiography. Right atrial pressure can also be increased when pulmonary resistance is high, resulting in a buildup of ‘backpressure’ due to increased right ventricular afterload, ultimately increasing right atrial pressure. This can occur with a variety of disease

states which result in pulmonary hypertension, or through lung-wide pulmonary hypoxia leading HPV which significantly increases pulmonary resistance.

Sex Differences in Respiratory Physiology

For decades, our understanding of the human respiratory system and physiology was based primarily on male anatomy. However, it has more recently come to be appreciated that female respiratory anatomy, as well as respiratory physiology, differs significantly from that of males. Across the lifespan, female lungs are smaller and less massive compared to male lungs (67). Females have smaller conducting airways compared to men, resulting in greater airway resistance, and also have a higher power (work) and oxygen cost of breathing (68–70). This becomes increasingly important with increasing exercise workloads, as females are more likely to become flow limited during strenuous exercise when $\dot{V}_E$ exceeds 50-70 L/min (68, 71). Various breathing strategies may be employed to minimize flow limitation, such as hyperinflation or tachypneic breathing, but these strategies may also impair the ability to exercise by increasing the metabolic demand of respiratory muscles or reducing alveolar ventilation (70). Hyperinflation results in operating on the flat portion of the pressure-volume curve, whereby for a given change in volume a much greater change in pressure is required. Creating that pressure change requires greater recruitment of respiratory muscles and places a greater metabolic demand upon the respiratory muscles. The combination of recruiting more respiratory muscles and demanding more activity from those muscles increases the oxygen demand of the respiratory system. The metaboreflex of respiratory muscles during exercise can initiate a sympathetic response causing vasoconstriction to exercising skeletal muscle (72), though the inspiratory muscle metaboreflex may be blunted in females compared to males (73). Hyperinflation may also lead to increased intrathoracic pressure and reduced venous return (74), in turn reducing

cardiac output and oxygen delivery to skeletal muscle (75). Tachypneic breathing results in a greater portion of deadspace in each breath, reducing $\dot{V}_A$ and reducing PAO_2, potentially leading to arterial hypoxemia.

PULMONARY TONE, NITRIC OXIDE, AND ENDOTHELIN-1

Maintenance of appropriate pulmonary vascular resistance is necessary to maintain the health and function of the lungs. The "normal" state of the pulmonary vasculature is to have little to no vasoconstriction, offering low resistance to blood flow. This state is maintained through a balance between vasoconstrictors, such as the potent vasoconstrictor ET-1, and vasodilators, primarily nitric oxide (NO).

ET-1 is a member of the endothelin family of peptides, but is the only member of that family which is constitutively produced by vascular endothelial cells (39). Endothelins are produced from inactive intermediates known as "big ETs" by the action of endothelin converting enzymes (ECEs) (76, 77). There are two types of ECEs, both of which are found throughout the body though vascular endothelial cells are the primary location of ECE-1, and ECE-1 produces primarily ET-1 (39). There are two receptors for ET-1, ET_A and ET_B. ET_A is located within vascular smooth muscle, while ET_B is located within vascular endothelium primarily in the kidney and only represents <15% of the ET-family receptors outside the kidney (78). *In vitro,* binding of ET-1 to ET_B promotes eNOS expression and production of NO. However, *in vivo* ET-1 binds primarily to ET_A receptors due to ET_A receptors having a high affinity for ET-1 than other endothelins, whereas ET_B binds all endothelins equally.(39, 79, 80). The location of ET_B receptors and their affinity for all endothelins suggests that ET_B receptors serve to "clear" endothelins from circulation as opposed to an active role in regulating vascular tone in humans (78). Once ET-1 binds to the ET_A receptor of vascular smoother muscle intracellular calcium

stores are released, leading to activation of L-type calcium channels and an influx of extracellular calcium causing vasoconstriction (81, 82).

For many years, it was known that there was some endothelium-derived relaxation factor responsible for smooth muscle relaxation around blood vessels. In 1987, Furchgott showed that this substance was NO (83). NO is synthesized in the body by nitric oxide synthases (NOS). There are three isoforms of NOS, named according to their general activity or tissue type in which they were originally found. These three isoforms are neuronal NOS, inducible NOS, and endothelial NOS (eNOS). It is this latter isoform which is most relevant in the regulation of pulmonary vascular tone. NO is generated by converting L-arginine to L-citrulline while consuming NADPH and in the presence of the necessary co-factor tetrahydrobiopterin (BH_4) (84). NO generated by vascular endothelium diffuses into smooth muscle cells surrounding the vessel. After diffusing to perivascular smooth muscle, NO binds guanylate cyclase leading to an increase in cGMP which in turn phosphorylates protein kinase G. The phosphorylation of protein kinase G leads to inhibition of L-type calcium channels, reducing intracellular Ca^{2+} concentrations and reduced contraction, thereby resulting in vasodilation (85). Furchgott also showed that anoxia interferes with the endothelial release of NO (86).

That low oxygen, or hypoxia, results in pulmonary vasoconstriction had been well established for decades before Furchgott's work. As discussed in the Historical Perspective, some of the first recordings of pulmonary arterial pressure, made in the 1850s, showed the link between adequate ventilation and pulmonary vascular pressure (Beutner, 1852 as cited in Sylvester et al., 2012). Von Euler and Liljestrand would later show that the degree of constriction of the pulmonary vessels was directly related to oxygen levels within the lung. The degree of this vasoconstriction is based on the stimulus PO_2. Stimulus PO_2 is the combination of

both PAO_2 and mixed venous PO_2, with the greater contribution coming from PAO_2 due partially to the vascular wall geometry but more significantly due to O_2 exchange between alveolar gas and blood within the small pulmonary arteries (88). While it has been clear for some time that HPV takes place within smooth muscle cells of the pulmonary arterioles, the sensor for hypoxia has yet to be definitively identified. An alveolar oxygen sensor was proposed and investigated, but ruled out due to failure of tissue PO_2 tension curves relating mixed venous PO_2 and PAO_2 to intersect the isobaric tension line (88). Potential oxygen sensors for HPV include mitochondria and $K_{v1.5}$ channels. However, the location and exact identity of the sensor responsible for initiating HPV remain open to debate.

Mechanism of Oxygen Sensing and Initiation of HPV

A likely candidate for the oxygen sensor in HPV is the mitochondria due to the mitochondria being a source of reactive oxygen species (ROS), as well as the primary source of oxygen consumption within pulmonary vascular smooth muscle (89). ROS refers to a class of molecules which contain an unpaired electron on the oxygen atom, include molecules such as superoxide, and are capable of influencing the cellular redox state as well as directly acting on calcium channels (90). There is active debate as to whether an increase or decrease in mitochondrial ROS signals for HPV, or if alterations in cellular redox state associated with ROS initiate HPV (91–94).

Mitochondria can produce ROS at multiple sites along the mitochondrial electron transport chain (METC). Approximately 3% of electron flux through the METC is lost to the formation of superoxide (O_2^-), primarily occurring in complexes I and III of the METC (87, 90). Superoxide can also be transported to the cytosol via voltage-dependent anion channels (95). Inhibition of METC complex I and III resulted in decreased ROS production, caused

vasoconstriction in normoxia and inhibited further hypoxic vasoconstriction (89). It was hypothesized that redox-sensitive cysteine bridges of potassium channels were the targets of the altered cellular redox state caused by decreased mitochondrial ROS release (90), and that inhibition of these channels led to activation of L-type calcium channels and vasoconstriction (96, 97).

However, measurement of ROS in intact lungs during hypoxia presents several problems, ranging from non-specificity and reactivity of the ROS fluorescent probes, the short lifespan of ROS, and compartmentalization of ROS production (90). Other data has suggested that hypoxia may lead to an increase in ROS, and that this increase in ROS triggers HPV. For example, an increase in reactive oxygen species (ROS) generated from mitochondria could occur in hypoxia due to the proximal METC becoming reduced, the concentration of electron donors increasing, and the concentration of O_2 falling (as reviewed in Sylvester et al., 2012). Studies which report an increase in ROS were primarily performed in isolated pulmonary artery smooth muscle cells and utilized dichlorofluorescein to detect ROS. Determination of whether an increase or decrease in ROS may contribute to signaling for HPV has been further complicated due to other proteins which release ROS, such as NADPH oxidase (as reviewed in Sylvester et al., 2012). Administration of antioxidants supports the conclusion that an increase in ROS generated from mitochondria signals for HPV and have been shown to inhibit HPV. It is thought that the increase in ROS would result in opening of Ca^{2+} channels in the smooth muscle cell membrane as well as Ca^{2+} release from the sarcoplasmic reticulum, resulting in vasoconstriction (as reviewed in Sylvester et al., 2012).

Hypoxia Impairs NO Synthesis

Hypoxia can also interfere with NO synthesis by interfering with eNOS. NOS utilizes O_2 as a substrate to produce NO, so a reduction in available O_2 can inhibit this reaction from occurring. NO production has been shown to be reduced by half in response to low oxygen, and the K_m of eNOS is almost entirely dependent on O_2 concentration (98). In the endothelium, superoxide produced by mitochondria can react with NO to form peroxynitrate which in turn can oxidize BH_4 and lead to eNOS uncoupling (99, 100). Uncoupled eNOS will produce superoxide instead of NO (101, 102), leading to further formation of peroxynitrate and oxidation of numerous intracellular proteins (103).

In addition to hypoxia interfering with eNOS expression and NO synthesis, hypoxia can also lead to increased levels of ET-1. Murine models have shown that 4-weeks of hypoxia increases ET-1 and ET-1 receptor expression in the lungs and pulmonary arteries (104) and that chronic intermittent hypoxia increased plasma ET-1 levels and mean arterial pressure (105–107). Similar results have been shown in humans, where 30 minutes of moderate hypoxia (SaO_2 = 75-80%) resulted in a nearly 3-fold increase in plasma ET-1 levels (108). Studies in humans have also shown a doubling of plasma ET-1 levels following rapid ascent from low-altitude to high altitude (4559m) and an inverse correlation to arterial PO_2 (109, 110). Plasma ET-1 levels also decreased upon administration of supplemental oxygen (109). These findings illustrate a clear connection between various forms of hypoxia and increasing levels of ET-1.

Hypoxia Increases Inflammation.

Hypoxia can also lead to increases in inflammatory cytokines which interfere with eNOS expression. A mouse model of hypoxic pulmonary hypertension utilizing wild-type and IL-17 knockout mice showed that IL-17 knockout prevented any increases in right-ventricular systolic pressure (RVSP) in response to 4 weeks of hypoxia (111). Interestingly, this study also showed

a restoration of hypoxic pulmonary hypertension when knockout mice were treated with recombinant mouse IL-17. In cultured endothelial cells, hypoxia elevated levels of IL-6 (112). IL-6 directly regulates eNOS expression and activity (as reviewed in Didion, 2017; Hung et al., 2010). TNF-α is also upregulated by hypoxia (35, 114) and has been shown to impair expression of eNOS mRNA (35). Thus, circulating inflammation may also mediate the eNOS response to hypoxia.

Inflammation and ET-1

The increases in inflammation associated with hypoxia can lead to increases in ET-1 in addition to the suppression of NO activity. ET-1 transcription can be increased by a variety of cytokines including IL-2, IL-1β, TNFα and IFN-β (115–117). Many of these cytokines are also increased by hypoxia, illustrating the link between hypoxia and ET-1. Interestingly, ET-1 can also have a proinflammatory effect, stimulating the production of a variety of cytokines such as IL-6, IL-8, and IL-1 (116, 118). ET-1 has also been shown to increase the generation of ROS, particularly superoxide (119, 120), a potential secondary mechanism for ET-1 promoting vasoconstriction via interference with eNOS activity in addition to ET-1's effects on calcium channels.

In summary, global lung hypoxia results in significant increases in pulmonary vascular resistance through two pathways – hypoxia results in smooth muscle contraction in pulmonary arteries through HPV, and hypoxia can lead to reduction in bioavailable NO which impairs vasodilation. The degree of HPV is highly variable between individuals. This has been shown in mechanically ventilated dogs (121) and in sheep (122) and in humans (Grünig et al., 2000; as reviewed Swenson, 2013). Despite the significant inter-individual variability in HPV, the intra-individual variability is relatively low, and HPV remains consistent in an individual exposed to

the same hypoxic stimulus. The high degree of inter-individual variability may be explained by differing levels of circulating inflammatory cytokines potentiating the hypoxic response, differing levels of ROS generation by mitochondria, or differing levels of antioxidants mediating the hypoxic response.

Additionally, HPV is not without potentially negative consequences. The increase in pulmonary vascular resistance through these pathways causes an increase in afterload for the right ventricle (as reviewed in Bogaard et al., 2009; Naeije & Dedobbeleer, 2013). In turn, the right ventricle can become dysfunctional, leading to dilation and failure. Additionally, increased pulmonary vascular and right heart pressures may lead to a buildup of "backpressure" to the right atrium, increasing right atrial pressure. If true, this would potentially reverse the pressure gradient between the atria. In situations where blood flow between the atria is possible, such as when a PFO is present, this will increase right-to-left shunt through the PFO. In this scenario, the PFO may serve as a "pressure relief valve," reducing the quantity of blood pumped to the pulmonary vasculature thereby reducing pulmonary vascular pressure but also potentially making pulmonary gas exchange worse.

CARDIOPULMONARY PHYSIOLOGY OF APNEA DIVING

There are many models of hypoxia which generally fall into two categories – persistent hypoxia (such as living at high altitude) and intermittent hypoxia, such as that experienced by apnea divers. One of the most common examples of intermittent hypoxia in humans is obstructive sleep apnea. This is a chronic intermittent hypoxic model characterized by frequent episodes of severe hypoxia (F_IO_2 of 2-8%, and up to 2,400 cycle of hypoxia per day). This model has shown a variety of negative sequelae, such as elevated systemic (127, 128) and pulmonary vascular pressures (129), elevated inflammatory cytokines (130), elevated sympathetic activation

(131), and right ventricular hypertrophy (McGuire & Bradford, 2001; as reviewed in Navarrete-Opazo & Mitchell, 2014). In contrast, models of intermittent hypoxia which use either a less severe or less frequent hypoxic dose have shown reductions in systemic blood pressure (28, 132) and to have no elevation in circulating inflammatory cytokines (as reviewed in Navarrete-Opazo & Mitchell, 2014; Serebrovskaya et al., 2011). As such, models of intermittent hypoxia which differ from sleep apnea in their severity and frequency may shed new light on the cardiopulmonary responses to hypoxia.

Apnea diving represents one such alternate model of intermittent hypoxia. Apnea diving as a form of subsistence and commercial seafood gathering has been practiced by some cultures, such as the Ama (a population of primarily female divers in Korea and Japan who have historically dove to harvest shellfish), for hundreds to thousands of years. It is also frequently practiced both recreationally (such as spearfishing) and competitively (such as competing for depth, time, or distance). The physiology of diving is a complex interplay of many systems and is altered according to the depth and duration of the diver. The interplay of physiological systems is described by the mammalian dive reflex. This reflex stems from stimulation of the face and nose with cold water. This reflex results in a parasympathetically mediated decrease in heart rate, reducing cardiac output. This is concomitant with sympathetically mediated peripheral vasoconstriction to maintain mean arterial pressure (133). The peripheral vasoconstriction results in a translocation of blood from the periphery to the thorax, increasing central venous volume and central venous pressure. The combination of bradycardia and hemodynamic shifts are thought to reduce total oxygen consumption while prioritizing oxygen delivery to the brain (134).

Apnea diving for depth introduces even more challenges. A depth dive can be divided into two basic phases: the dive phase and the ascent phase. The dive phase consists of the duration of the dive from initial submersion until the nadir of the dive is reached, while the ascent phase covers the period from the nadir until the diver is once again able to breathe above the surface of the water. The changes in barometric pressure during both the dive and ascent phases have significant impacts on blood gas concentrations and pulmonary vascular pressures.

From the surface to the nadir of the dive, the barometric pressure increases, doubling every 10m below the surface of the water. As the gas held in the lungs during an apnea dive is compressible, this results in a decrease in lung volume as the depth of the dive increases, causing the lungs to compress to residual volume at a depth of 40-50m (31). This compression of the lung and reduction in lung volume causes reduction in mechanical distension and recruitment of pulmonary vessels. Simultaneously, the compression of the gases within the lung increases the partial pressure of gases within the lung such that at 10m depth, the partial pressures of gasses within the lung and blood are approximately double that at the surface. Interestingly, intermittent hyperoxia has been shown to be able to induce activation of some of the same cellular cascades (such as activation of HIF) as hypoxia due to fluctuations in cellular oxygen levels (as reviewed in Hadanny & Efrati, 2020), a phenomenon known as the hyperoxic-hypoxic paradox. In clinical practice, increased F_IO_2 is combined with hyperbaria to elevate PaO_2 in excess of 1500 mm Hg (135) – roughly equivalent to what would be expected in an apnea diver at approximately 100m depth. The subsequent fluctuation in PaO_2 when F_IO_2 and barometric pressure return to normal is hypothesized to activate HIF-1 (136). The fluctuation in PaO_2 as a diver progresses from surface to nadir to surface may function similarly thereby activating HIFs. HIFs regulate a variety of target genes related to pulmonary vascular tone, and HIF-mediated

changes in energy metabolism of pulmonary arterial smooth muscle and endothelial cells are implicated in elevated pulmonary vascular pressures (137). Intermittent hyperoxia has additionally been shown to induce mitochondrial biogenesis in a mouse model (138). Increased mitochondrial biogenesis has the potential to alter the redox state of the cell, which is a proposed mechanism of oxygen sensing for the initiation of HPV.

While some direct measures of arterial blood gasses have failed to show the expected increase in PaO_2 and $PaCO_2$ associated with apnea diving (33), most measures of PaO_2 and $PaCO_2$ in simulated wet dives (139) and during actual apnea dives (33, 140, 141) show that diving increases PaO_2 and $PaCO_2$ as expected an in accordance with Boyle's law (as reviewed in Paganini et al., 2022; Patrician et al., 2021). It is unclear why two of the divers in Bosco's 2018 work did not increase blood gas pressures as expected, though hypotheses include ventilation/perfusion mismatch and right-to-left intrapulmonary shunting due to atelectasis caused by significant reduction in lung volume (33). Despite these anomalous findings, apnea divers should generally be thought of as hyperoxic and hypercapnic for the majority of both the descent and ascent phases of an apneic dive, though this is also influenced by the length of the dive and VO_2, both of which can alter the expected PaO_2.

Unsurprisingly, during the ascent phase the changes in barometric pressure are reversed from those during the descent phase. As the diver ascends from the nadir of their dive, barometric pressure decreases, allowing lung volume to increase (31) subsequently causing blood gas pressures to decrease as well. For every 10m of ascent, the partial pressure of gases is reduced by half. This is particularly relevant during the final portion of the ascent phase. Since oxygen will have been consumed for the duration of the apnea, PaO_2 can rapidly drop to levels incapable of supporting consciousness during the final portions of the ascent phase. The P_aO_2 of

a diver who dove to 150m can be as low as low as 25 mmHg upon surfacing (143). This results in a phenomenon known as shallow water blackout, a result of this rapid and sudden drop in oxygen levels and has resulted in multiple apnea diving fatalities. This drastic decrease in gas pressures also creates a strong stimulus for HPV. During the final phase of ascent, this strong HPV stimulus may result in a transient increase in right atrial pressure as outlined above, allowing for right-to-left intracardiac shunt if a PFO is present.

CHAPTER III

METHODS

INFORMED CONSENT

The University of Oregon Institutional Review Board formally approved the studies and protocols contained within this dissertation (Chapters IV-VIII). For Chapters VI, VII, and VIII, the Institutional Review Board of the University of Split Medical School also formally approved the research protocols. Prior to enrollment in all studies, procedures and risks were discussed with every participant and written informed consent was obtained from all participants.

ECHOCARDIOPHIC SCREENING

For all data collected in Eugene, Oregon echocardiography was performed by professional ultrasonographers (Eben Futral, RDCS, MBA; Douglas Elton, RDCS; Freddy Garcia, RDCS). For data collected in Split, Croatia echocardiography was performed by researchers from Cardiff Metropolitan University (Dr. Aimee Drane, PhD, Dr. Tony Dawkins, PhD, Dr. Rachel Lord, PhD). A three-lead ECG was placed and participants were positioned in the left lateral decubitus position in a reclining chair, with their head resting on their left arm. For a small number of participants in Chapters IV and V, technical complications required a 12-lead ECG routed through a metabolic system to the ultrasound machine in place of a 3-lead ECG directly connected to the machine. The left lateral decubitus position both spreads the ribs apart to and allows the heart to move anteriolaterally against the participant's ribcage, the combination of which allows for optimal imaging of the heart in an apical 4-chamber view. Screening began with a comprehensive inspection of the structure and function of the heart to rule out any cardiac abnormalities or obvious pathologies. Screening includes evaluation of right heart function

through tricuspid annular plane systolic excursion (TAPSE) and estimations of right atrial pressure in accordance with American Society of Echocardiography guidelines (144).

Detection of Patent Foramen Ovale

Ultrasound detection of PFO was performed contiguous with echocardiographic screening. Prior to positioning the subject in the reclining chair, a 22 gauge intravenous catheter was aseptically placed into the antecubital fossa of the arm, an extension set and three-way stopcock attached, and patency of the catheter was confirmed. Participants were then positioned in the left lateral decubitus position as described above. A 10 mL syringe was filled with approximately 5 mL of sterile saline and then attached to one of the open stopcock ports. A 10 mL syringe filled with approximately 1 mL of air was attached to other open part, and saline was mixed vigorously between the syringes to create agitated saline contrast. While a 4-chamber apical view of the heart was maintained, the contrast was injected into the antecubital vein and observed entering the right atrium. Bubbles which appeared in either the left atrium or left ventricle within three cardiac cycles was considered positive for PFO. A "bubble score" of 0 to 5 was assigned based on the quantity of bubbles which appeared in the left heart following contrast injection, where a score of 0 represented no bubbles crossing and a score of 5 was assigned when the left ventricle was completely opacified with contrast. This process was completed with the participant completing a Valsalva maneuver whereby the participant bears down against a closed glottis to increase intrathoracic and intraabdominal pressure. This increase in pressure temporarily restricts venous return to the right atrium. Upon release of the Valsalva, a large bolus of venous blood returns to the right atrium, transiently increasing right atrial pressure over left atrial pressure, and facilitating flow through a PFO if one is present. A

bubble score of 3, corresponding to ≥ 12 bubbles crossing into the left heart, is considered to be a "large" PFO, while a score of 1 or 2 is considered a "small" PFO (145).

Pulmonary Artery Systolic Pressure

The most accurate method of determining pulmonary vascular pressures utilizes a catheter threaded into the pulmonary artery. However, this method is highly invasive and beyond the scope of the campus research facilities. However, non-invasive calculation of pulmonary artery systolic pressure (PASP) can be accomplished utilizing continuous wave Doppler ultrasound. This method correlates well with direct measures (146–148). Continuous wave Doppler ultrasound is used to measure the peak velocity of blood regurgitated through the tricuspid valve (TR_{Vel}). Ultrasound can also be used to estimate right atrial pressure (P_{RA}) by performing the "sniff test" of the inferior vena cava (IVC), which evaluates collapsibility of the IVC. According to 2010 American Society of Echocardiography guidelines suggested that an IVC collapse of >50% during the sniff test was indicative of "normal" P_{RA} and should be estimated at 0-5 mm Hg, while a dilated IVC with normal collapse should be considered "mildly elevated" P_{RA} of 6-10 mm Hg, whereas a failure of the IVC to collapse >50% the P_{RA} is "usually between" 10 and 15 mm Hg (144). These guidelines were slightly revised in 2015 (149), and P_{RA} values are instead recommended to be estimated at 3 mm Hg for "normal" P_{RA}, 8 mm Hg for an "indeterminate" sniff test, and 15 mm Hg when the IVC is dilated and fails to collapse > 50%. Participant data collected as part of the AltitudeOMICS studies and included in Chapter 4 utilized the 2010 guidelines, whereas all other participants in Chapter 4 and other chapters utilized the 2015 guidelines. In all cases, the modified Bernoulli equation was used to calculated PASP (144):

$$PASP = 4v^2 + P_{RA}$$

Equation 3.1. Pulmonary Artery Systolic Pressure

Where v is the measured TR_{Vel} and P_{RA} is estimated as described above. In some participants, the TR_{Vel} is difficult to visualize with ultrasound. In these cases, a small volume of agitated saline contrast was created as described above and injected to aid in visualization of the tricuspid regurgitation jet and measurement of TR_{Vel}.

Stroke Volume and Cardiac Output

Stroke volume (SV) was calculated from ultrasound measurements of left ventricular outflow tract velocity-time integral ($LVOT_{VTI}$) and left ventricular outflow tract cross sectional area ($LVOT_{CSA}$) utilizing the modified Simpson's approach (149):

$$SV = LVOT_{VTI} \times LVOT_{CSA}$$

Equation 3.2. Stroke Volume

Cardiac output ($\dot{Q}$) was then calculated as the product of SV and heart rate:

$$\dot{Q} = SV \times HR$$

Equation 3.3. Cardiac Output

$LVOT_{VTI}$ is assessed utilizing pulsed wave Doppler echocardiography. This method measures the velocity of the outflow tract just below the tricuspid valve

Comprehensive Echocardiogram

As part of echocardiographic screening participants in all studies, except for participants only included in Chapter VII, underwent a comprehensive echocardiogram. The following parameters were measured according to the standards of the American Society of Echocardiography: right ventricular wall (RV Wall) thickness (cm), right ventricle internal diameter in diastole (RVID), right ventricular end diastolic (RVED) area (cm^2) and right

ventricular end systolic (RVES) area (cm^2) to calculate right ventricular area fraction (%RVAF), left ventricular end-diastolic volume (LVEDV, mL), left ventricular end-systolic volume (LVESV, mL), left ventricle internal diameter in diastole (LVIDD), left ventricular posterior wall thickness (LVPW), left ventricle internal diameter in systole (LVIDs), left atrial diameter (LA), pulmonary valve velocity (PV peak velocity, m/s), pulmonary insufficiency end-diastolic (PIED) gradient (mm Hg) to calculate pulmonary artery end diastolic pressure (PAEDP; mm Hg), aortic valve peak velocity (AoV peak velocity, m/s) to calculate aortic valve area (AVA; cm^2), interventricular septum (IVS), aortic root (AORT), left ventricular outflow tract (LVOT) diameter, and tricuspid annular plane systolic excursion (TAPSE) (144, 149, 150). These measurements examine the structural and functional health of the heart, and allow us to ensure that 1) stress to the cardiopulmonary system through exercise, hypoxia, or the combination of the two is safe for the participant and 2) there are no baseline structural or functional deficits that may confound our results.

PULMONARY FUNCTION TESTING

Forced Vital Capacity

Forced Vital Capacity (FVC) is the maximum volume of air a participant is able to exhale with a maximal effort. This pulmonary test was performed according to the guidelines of the American Thoracic Society and European Respiratory Society (ATS/ERS) (151) which standardize the administration, performance, and evaluation of the FVC maneuver. The participant was given a noseclip and instructed to breathe through a mouthpiece attached to a pneumotachometer to measure airflow. After several normal tidal breaths, the participant is instructed to exhale “all the way” (e.g. to residual volume (RV)), followed by a sharp, large inhalation to total lung capacity which is immediately exhaled as forcibly as possible. To meet

ATS/ERS criteria, this exhalation must last between 6 and 15 seconds. The volume of expired air is equal to the FVC. ATS/ERS criteria require three successful trials where the FVC measurements are within 0.15 L of each other to meet reproducibility criteria.

The FVC maneuver also provides the forced expiratory volume in the first second (FEV_1). FEV_1 can be compared to FVC to establish the FEV_1/FVC ratio, which is approximately 0.80 in a healthy individual with no impairments in pulmonary function. Obstructive airway conditions can reduce the FEV_1, therefor reducing the FEV_1/FVC ratio. It should also be noted that the measurement of FEV_1 is dependent on a forceful exhalation and therefor is dependent on participant effort. The FVC maneuver can also provide measurement of the flow rate during the effort independent portion of a forceful exhalation, which is mainly controlled by the physical properties of the lung. This is called the mid-expiratory flow from 25% to 75% of the maximal forceful exhalation (FEF_{25-75}).

Slow Vital Capacity

The slow vital capacity (SVC) maneuver was performed after the FVC maneuver. The SVC is largely similar to the FVC, with the exception of the forced exhalation. Participants are positioned and instrumented identically to the FVC maneuver, and a minimum of four tidal breaths are collected. The participant then exhales to RV before taking a large inhalation to TLC, which is immediately followed by a "passive" exhalation to RV. Though not considered a forceful exhalation, eventually participant effort is required to continue exhalation to RV. This test is useful as the reduced exhalation rate does not require as large of an increase in thoracic pressure as the FVC maneuver. This is beneficial as the high intrathoracic pressure needed for the FVC maneuver has the potential to collapse small airways and trap gas distally to these small airways, potentially leading to a larger vital capacity measurement. The repeatability criteria for

this maneuver are similar to that of the FVC in that at least three maneuvers must completed with less than 0.15 L variance between them.

Whole-body Plethysmography

While spirometry is useful for measuring a variety of lung volumes and flows as well as calculating some capacities, it cannot evaluate total lung capacity (TLC) or functional residual capacity (FRC) due to the inability of spirometry to measure RV. Whole-body plethysmography allows for the measurement of RV, and thus calculation of TLC and FRC, through application of Boyle's Law:

$$P_1V_1 = P_2V_2$$

Equation 3.4. Boyle's Law

Where P_1 and V_1 refer to initial pressure and volume, respectively, and P_2 and V_2 represent secondary pressure and volume. Thus, the pressure and volume of a participant's thoracic cavity are related to the pressure and volume of the plethysmography enclosure. For this test, the participant is instrumented with a noseclip as with FVC and SVC maneuvers, and then enters the plethysmography enclosure which is then sealed. The participant begins breathing on a mouthpiece and pneumotachometer connected to a device which contains a series of automated shutters which are able to restrict and redirect airflow as necessary for the test. The participant places their hands on their cheeks to prevent buccal distension during panting, which has the potential to reduce the accuracy of the test. The participant then takes at least 4 tidal breaths and is then instructed to begin a series of gentle pants (fast, shallow breaths) at a rate of 70-90 breaths per minute. A shutter is then closed while the participant continues to pant against the closed shutter. After approximately 5 satisfactory pants are recorded, the shutter opens and the participant is instructed to perform an SVC maneuver. This allows for determination of the

volume of gas left in the lungs at FRC, which can then be subtracted from the expiratory reserve volume to calculate RV. RV can also be added to the measured vital capacity to arrive at a total lung capacity (TLC) calculation.

Diffusing Capacity for Carbon Monoxide

The studies in this dissertation utilized the single-breath, breath hold test for diffusing capacity of carbon monoxide. Briefly, a known concentration and volume of carbon dioxide is inhaled by the participant. After a brief breath hold of the carbon-monoxide containing gas mixture, a small volume of exhaled gas is captured and analyzed for carbon monoxide content. The volume and difference in inhalation vs exhalation carbon monoxide concentrations allows for the calculation of carbon monoxide which crossed the lung-blood interface and bound to hemoglobin. For this procedure, we used the Medgraphics Elite Plethysmograph which also has a small gas chromatograph capable of analyzing the concentration of carbon monoxide in a gas sample. The participant sits upright while breathing on a mouthpiece connected to a pneumotachometer as described above, as well as using a noseclip. After at least four tidal breaths are recorded, the participant is instructed to exhale to RV. Once at RV, a shutter opens in the plethysmograph head, allowing flow of the diffusion gas mixture (0.3% carbon monoxide, 21% oxygen, 0.5% neon, remainder nitrogen) to the participant, and the participant is instructed to take a maximal inhalation. It is important in this test that the participant inhale to at least 85% of predicted TLC to ensure accuracy. After maximal inhalation, the participant holds their breath for 8 seconds and then exhales. The initial portion (approximately 500 mL) of the exhalation is not sampled to limit the influence of dead space on measurement of diffusing capacity. A small sample of exhaled air is then taken and passed to the gas chromatograph for analysis of gas concentrations. Neon serves as an inert tracer gas, and comparisons of pre- to post-exhalation

neon concentrations provides the total volume of the alveoli (V_A). Carbon monoxide binds to hemoglobin approximately 100 times greater than oxygen, and the volume of inhaled vs exhaled carbon dioxide is used to calculate the volume of carbon monoxide which diffused from the lung into blood. The combination of these measures allows for calculation of both the diffusing capacity of carbon monoxide (DL_{CO}) and normalization of diffusing capacity to alveolar ventilation (DL_{CO}/VA), which facilitates comparison between participants of different heights/sexes.

EXERCISE TESTING

VO_{2Max} Test

The VO_{2Max} test is a frequently utilized maximal exercise test to evaluate a participants exercise capacity and oxygen consumption. In all studies involving participants exercising on a cycle ergometer, participants performed a VO_{2Max} test to measure their maximal oxygen consumption. VO_{2Max} testing was performed on a magnetically braked cycle ergometer (Lode cycle ergometer). Participants were instrumented with a forehead peripheral oxygen saturation (S_PO_2) monitor, and participants in Chapter 5 were additionally instrumented with a 12-lead ECG (MedGraphics Ultima CardiO_2). All participants were instrumented with a noseclip and mouthpiece connected to a metabolic analysis system (Medgraphics Ultima CardiO_2) for measurement (values averaged from middle 5 of last 7 breaths) of end-tidal gases ($P_{ET}O_2$, $P_{ET}CO_2$), tidal volume (V_T), minute ventilation ($\dot{V}_E$), and respiratory rate (RR). Resistance was set to 50W at the onset of exercise and increased by 25W steps every minute. Exercise testing was terminated when the participant was no longer able to pedal above 60 RPM, exceeded their age-predicted 85% heart rate maximum, or upon volitional fatigue.

6-Minute Walk Test

In addition to VO_{2Max} testing, participants in Chapter 5 also completed a 6-minute walk test. The 6-minute walk test is a sub-maximal test of exercise capacity frequently used in a clinical setting due to its simplicity and utility for individuals who may have moderate to severe exercise limitations, as well as good predictability of morbidity and mortality (152). For this test, a short distance (approximately 200 feet) was marked in the building hallway. Beginning at one end, participants completed as laps of this distance as possible in a 6-minute period. Participants were restricted to walking, and were disallowed to jog, run, or skip. Participants were instructed to "freeze" after 6 minutes of walking, and the total distance walked in 6 minutes was recorded.

PARTICIPANT INSTRUMENTATION

Intravenous Catheter

Intravenous catheters (IVs) were placed in every participant for injection of agitated saline contrast for PFO detection and TR enhancement, as well as blood draws as described below. A 20G IV (ProtectIV Plus, 20G x 1.25") was placed aseptically into the antecubital vein, usually in the non-dominant arm unless the participant requested otherwise or the veins of the non-dominant arm would have made IV placement unnecessarily challenging. After placement in the vein, the IV catheter was connected to an IV catheter extension set, which in turn was connected to a 3-way stopcock. This stopcock was utilized for injection of agitated saline as described above.

Body Core Temperature Measurements

Chapters IV and V required knowledge of a participants body core temperature at the time of arterial blood sampling for correction of blood gas values. Within the blood gas

analyzer, the electrodes which measure PO_2 and PCO_2 make these measures at 37°C. If a participants body core temperature is above or below this point, then measurements of PO_2 and PCO_2 require adjustment to account for this temperature difference. Two methods were used to measure body core temperature: esophageal probes (Mon-a-therm General Purpose Probe) and ingestible pills (HQInc., CoreTemp; VitalSense Temperature Capsule). In Chapter IV, participants were instrumented with an esophageal temperature probe. As appropriate positioning of an esophageal probe is essential for accurate temperature measurement , appropriate probe depth was calculated from the participants sitting height (153):

$$L = .0479 \times (sitting\ height) - 4.44$$

Equation 3.5. Thermal Probe Positioning

Where L is the length of probe that needs to be inserted to properly position the temperature probe tip and sitting height is the participants height will sitting on the ground against a wall. Participants were given a 3 mL syringe filled with 2% lidocaine jelly. After visual inspection of both nostrils, participants were instructed to inhale approximately 1 to 1.5 mL of lidocaine jelly through the larger nostril. After a short period to allow the lidocaine to take effect, the esophogeal probe was carefully inserted into the numbed nostril until the tip of the probe was visible in the participant's throat. Participants were then provided with a cup of water and straw and instructed to take large sips. The probe was advanced while the participant was swallowing until the probe had advanced to the pre-determined length, L. The probe was then fixed in place via taping to the participant's nose. However, not all participants are able to tolerate an esophogeal temperature probe, and an esophogeal temperature probe may not be appropriate for remote field studies. As such, participants in Chapter IV who could not tolerate a temperature probe utilized a core temperature pill. Additionally, since Chapter V built on previous work that

utilized a core temperature pill, pills continued to be used for these participants. For those participants who were given a core temperature pill, the pill was activated prior to ingestion and given to the participant immediately upon their arrival at the lab (approximately 2-3 hours prior to beginning data collection). The pill is activated via a wireless receiver, which in addition to activating the pill, also receives transmitted telemetry. Regardless of the method utilized for measuring body core temperature, measurements were taken simultaneously with each arterial blood sampling for correction of measured blood gases.

Peripheral Oxygen Saturation

Participants in Chapters IV, V, and VII were instrumented with a forehead pulse oximeter (Nellcor N600x, Covidien, Dublin, Ireland) to record estimates of peripheral arterial oxygen saturation (S_PO_2) and HR. This data was directly and continuously recorded by the metabolic system (Ultima, Medgraphics, Minneapolis, MN) in Chapters IV and V. For some participants, equipment complications prevented this recording, and instead S_PO_2 and HR were manually recorded during arterial sampling. In Chapter VII, S_PO_2 was manually recorded during ultrasound image acquisition.

The pulse oximeter adheres to the participant's forehead above the right eye, and continues a red light emitting diode (LED) and an infrared LED. The wavelengths of light reflected back from these LEDs differs depending on whether hemoglobin is saturated with oxygen or not, and the ratio between these two LEDs is used to calculate an estimate of oxygen saturation. Simultaneously, pulsatile changes in color are utilized to calculate heart rate.

Radial Arterial Catheterization

A radial arterial catheter was placed in the non-dominant wrist of participants in Chapters V and IV for arterial blood sampling and calculation of arterial blood gasses. Arterial

catheterization was performed by a licensed physician (Dr Jerry Hawn, MD; Dr Ximeng Yang, MD; Dr Richard Padgett, MD) in the Cardiopulmonary and Respiratory Physiology Lab at the University of Oregon. Prior to placement of the radial catheter, a Modified Allen's test was performed to ensure adequate collateral circulation in the hand. The Modified Allen's test is performed by palpation of the radial and ulnar arteries in the wrist. Manual pressure is then applied to occlude both arteries and the participant is coached to open and close their hand 10 times in order to evacuate blood from the hand. The occlusion of the ulnar artery is then removed, and time counted until visual perfusion of the palm of the participant's hand occurs. Visual reperfusion of the palm occurring within 7 seconds is considered a passing Modified Allen's test. Participants who failed the Modified Allen's test were excluded from the study. All radial arterial catheters were placed aseptically and utilizing sterile techniques. After verification of a passing Modified Allen's Test by the placing physician, participants were positioned supine on a medical gurney. The participant's hand was placed in a plastic support which maintained wrist flexion, and the support was kept in place for as long as the arterial catheter was present. The participants wrist was sterilized with Chloraprep (2% chlorahexadine, 70% isopropyl alcohol) and positioned on a table covered with a sterile drape. A second sterile drape with a 3 inch circular aperture was then placed such that the participants wrist was accessible through the aperture and the drape spread to create a sterile working field. A 25G needle was used to administer a small amount of anesthesia (2% lidocaine with 2% by volume nitroglycerin (5 mg/mL) to minimize vasospasm) to the catheterization site. A 20G introducer needle was used to penetrate the artery, at which point a guidewire was threaded through the needle and advanced into the radial artery. The introducer needle was then removed and a 5F catheter threaded onto the guidewire and advanced into the radial artery. A small nick was made

by scalpel into the patients skin and fascia if necessary to advance the catheter into the artery. An extension set with a 3-way stopcock pre-flushed with sterile heparinized saline was then attached to the catheter and patency of the catheter confirmed by aspiration. As patency of the arterial catheter was crucial to the ability to gather arterial samples, the arterial catheter was aspirated and flushed every 5 minutes.

Venous Blood Sampling

Venous blood was drawn via IVs placed as described above. Blood was drawn by connecting a saline-filled 10 mL syringe to one open port of the stopcock, and a plastic tube holder (colloquially known as a "wing") connected to the other open port. The catheter was aspirated using the saline-filled syringe, and once the extension line and stopcock were filled with blood, a vacutainer (BD VacuTainer) was pressed into the tube holder. Blood was collected into serum separator tubes which contain a microsilica coating to induce clotting as well as a separator gel to maintain component separation after centrifugation. After allowing blood to clot in the tubes for 30 minutes, tubes were centrifuged at 1500G for 10 minutes and serum aliquoted off. Serum was stored at -80°C until analyzed.

Plasma was collected via similar methods to serum. However, unlike serum there is no need to allow plasma to clot. As such, blood collected for plasma was collected into vacutainer (BD Vacutainer) tubes treated with EDTA, a calcium-binding agent that prevents clotting. After collection of blood into EDTA tubes, tubes were centrifuged at 1500G for 10 minutes and plasma aliquoted off. Plasma was stored at -80°C until analyzed.

Dynamic End-Tidal Forcing:

Chapter VI utilized a dynamic end-tidal forcing system to create isocapnic hypoxia in the participants. Participants breathed through a mouthpiece connected to a 2-way non-rebreathing

valve (2700 series, Hans Rudolph, Shawnee, KS, USA) for collection of end-tidal gases before and during the entire end-tidal forcing procedure. Prior to initiating the end-tidal forcing system, participants breathed on the mouthpiece for 10 minutes to establish baseline values. Once baseline was established, the end-tidal forcing system was engaged to replicate the participant breathing room air and to allow the participant to acclimate to the forcing system. After replicating room-air breathing for 5 to 10 minutes, the end-tidal forcing system was utilized to reduce the $P_{ET}O_2$ to 45 mmHg, which resulted in SpO_2 of approximately 75%, while maintaining baseline $P_{ET}CO_2$ for 30 minutes. Gases were sampled from the mouthpiece and analysed by a calibrated gas analyser (Split: ML206, ADInstruments, Colorado Springs, CO, USA; Eugene: Model 17515^A CO_2 Analyzer, Vacumed, Ventura, CA, USA; N-22M Oxygen Sensor, R-2 Flow Control, S-3A/I Oxygen Analyzer, AEI Technologies, Bastrop, Texas, USA) and respiratory flows were measured using a linear pneumotachograph (Model 4813, Hans Rudolph, Kansas City, MO, USA). Custom software (developed in Labview, Austin, TX, USA) determined breath-by-breath tidal volumes, $P_{ET}O_2$, and $P_{ET}CO_2$. The end-tidal forcing system prospectively delivered inspired gasses to clamp $P_{ET}O_2$ and $P_{ET}CO_2$ at desired levels. Independent solenoid valves delivered the necessary volumes of O_2, CO_2 and N_2 as determined by an error reduction algorithm incorporating $P_{ET}O_2$, $P_{ET}CO_2$, and inspiratory and expiratory tidal volume from the last breath (154, 155).

MEASUREMENT OF ARTERIAL BLOOD GASES

Radial Arterial Blood Draw and Analysis

Particular care is necessary to ensure that measured values of arterial blood gases are accurate. Exposure of the sample to air, such as through a bubble in the syringe, can alter the gases dissolved in the sample and this problem is particularly potent when expected gas partial

pressures within the sample differ greatly from room air such as during hypoxic or hyperoxic breathing. Arterial blood samples were collected by first wasting approximately 1 mL of blood to account for the deadspace of the combined extension set and catheter and to ensure that any saline used to flush the catheter is fully removed prior to sampling. A heparinized 3 mL syringe was then connected to the stopcock and arterial blood drawn over approximately 20 seconds. The timing and duration of the blood draw was recorded so that it could later be aligned with metabolic data. The duration of sampling allowed metabolic data to be averaged over numerous respiratory cycles. Any air bubbles in the syringe were immediately removed and then passed to the investigator analysing the arterial sample. Arterial samples were analysed utilizing either a Siemens RapidLab 248 or analysed with a Radiometer ABL90 Flex. As sampling by these pieces of equipment has the potential to introduce air bubbles, care was taken to remove any bubbles after each analysis. Samples analysed by RapidLab248 were additionally analysed for co-oximetry utilizing a Radiometer OSM-3. The ABL90 Flex also includes co-oximetry, so no additional equipment was needed for samples analysed with that platform. Arterial samples were analysed in triplicate. After analysis for blood gases and co-oximetry, arterial blood was analysed for hematocrit utilizing the microcapillary tube centrifugation method and for lactate concentration with a YSI 1500 Sport or Lactate Plus analyser. All arterial samples were corrected for body temperature and blood gas analysers were calibrated using tonometered whole blood at the start of each study day.

Tonometry

Tonometry allows for correction in day-to-day fluctuations and minor errors in measuring PO_2 and PCO_2. Samples of EDTA-treated whole blood are placed into prepared syringes, which are in turn placed into an aluminum block heated to 37°C and equilibrated with gases of known

concentrations of O_2 and CO_2 for a minimum of 60 minutes. Those samples are then analysed in triplicate, and a correction factor can be generated based on the slope of the measured vs predicted values. That correction factor is then applied to the blood gases measured during that study day. Three levels of O_2/CO_2 are utilized for the construction of each slope, and the levels of gasses used vary based on the range of values expected from arterial samples. Chapters IV and V utilized normoxic exercise, and the $\%O_2/CO_2$ utilized were 26.09/3, 10.15/2.04, and 6.12/5.1. For the hyperoxic exercise in Chapter IV, the $\%O_2/CO_2$ utilized were 26.09/3, 14.99/7.07, and 36.24/4.99.

BIOMARKER ASSAYS

Multiplex Assay

For chapter VIII, levels of various cytokines were analysed utilizing a bead based multiplex assay (Human Inflammation Panel 1, LegendPlex, BioLegend, San Diego, CA). This assay works by introducing 13 types of microbeads with differing sizes and internal fluorescence and coated with antibodies for particular analytes. When mixed with a sample, such as serum or plasma, the analytes bind to the bead antibodies. Then, biotinylated antibodies are introduced which bind to the captured antibodies, after which streptavidin-phycoerythrin (SA-PE) is added, which binds to the biotinylated antibodies. When passed through a flow cytometer, this allows for the detection of the type of antibody based on bead size and internal fluorescence, as well as quantity of the bound analyte by fluorescence of SA-PE. This particular assay measures IL-1β, IFN-α2, IFN-γ, TNF-α, MCP-1, IL-6, IL-8, IL-10, IL-12p70, IL-17A, IL-18, IL-23, and IL-33. After detection of bead size and fluorescence intensity, a standard curve can be plotted and used to interpolate analyte concentrations.

Total Nitrate and Endothelin-1 Assays

Nitric oxide is rapidly converted to nitrate in the body, making it difficult to measure directly (156) and unsuitable for measurements by enzyme-linked immunosorbent assay (ELISA). ELISAs utilize a microplate coated with a target-specific (in this case endothelin-1) antibody. Sample is then added to the microplate, and the target analyte binds to the antibody, capturing the analyte. A solution containing a detection antibody is then added, which binds to the captured analyte and forms an enzyme-antibody-target complex. A substrate solution is then added and will produce a measurable signal. The intensity of this signal can then be interpolated to determine the concentration of the analyte. While NO is too reactive and too short lived for this process, nitrate itself is stable can be utilized as a proxy measurement for nitric oxide. In Chapter VIII , ELISA was used to measure both ET-1 (Endothelin-1 Human ELISA kit, Invitrogen, Waltham, MA) and total nitrate (Total Nitric Oxide and Nitrate/Nitrite Parameter Assay Kit, R&D Systems, Minneapolis, MN).

To prepare samples for the ET-1 assay, an extraction solution was used. The extraction solution is a mixture of acetone and 0.2 mol/L hydrochloric acid and vortexed, then allowed 90 minutes at room temperature. Samples were then centrifuged at 1660g for 20 minutes at 4°C. Samples were allowed to dry over 24 hours before reconstitution with 150 μL of assay buffer. Immediately following reconstitution, samples were analysed according to the manufacturer's instructions.

To prepare samples for the total nitrate assay, centrifugal filtration was used. 500 μL of sample was added to a 10 kDA centrifugation filter (Amicon Ultra 0.5 Centrifugal Filter 10 kDa MWCO, Millipore Sigma, Rockville, MD). Samples were centrifuged at 14,000g to filter the samples, followed by inversion of the filter into a new microtube and centrifugation at 1000g for 2 minutes to extract the supernatant. Following sample preparation, supernatant was frozen at -

80°C until analysis. Frozen supernatant was thawed on ice prior to dilution and analysis according to manufacturer's instructions.

VENOUS ADMIXTURE AND SHUNT FRACTION

As mentioned previously, some degree of venous blood is mixed into arterial blood from normal anatomy, e.g. bronchial and thebesian circulation. This inherently results in some degree of pulmonary gas exchange impairment. The ratio of venous admixture necessary to arrive at a given A-aDO_2 can be calculated as venous admixture.

$$\frac{Cc'O_2 - CaO_2}{Cc'O_2 - C\bar{v}O_2}$$

Equation 3.6. Venous Admixture

Where Cc'O_2 is calculated oxygen content at the terminus of the pulmonary capillary (157), CaO_2 is arterial oxygen content, and C_VO_2 is mixed venous oxygen content. Arterial oxygen content is calculated as follows:

$$(1.34 * HbO_2 * tHb) + (PO_2 * 0.003)$$

Equation 3.7. Oxygen Content

Where HbO_2 is hemoglobin saturated with oxygen, tHb is hemoglobin concentration in mL/dL, and PO_2 is the partial pressure of oxygen. Direct calculation of mixed venous content requires invasive sampling of venous oxygen saturation which was not feasible in our lab. However, mixed venous oxygen content can be estimated:

$$C\bar{v}O_2 = \left(\left(\frac{C_aO_2}{100}\right) - \left(\frac{VO_2}{Q_T}\right)\right) * 100$$

Equation 3.8. Mixed Venous Oxygen Content

Where CaO_2 is arterial oxygen content, VO_2 is oxygen consumption, and Q_T is cardiac output. In situations where the only contributor to pulmonary gas exchange impairment is shunt, such as

when breathing a mixture of gasses where $F_IO_2 > 0.40$, the venous admixture equation instead provides a calculation of the portion of total cardiac output which must be shunted to arrive at a given A-aDO_2.

Chapter IV

IMPAIRED PULMONARY GAS EXCHANGE EFFICIENCY AND BLUNTED VENTILATION DURING EXERCISE IN SOME FEMALES, BUT NOT MALES, WITH PATENT FORAMEN OVALE

This chapter is in review with the *Journal of Physiology* and Mohini Bryant-Ekstrand, Karleigh Bradbury, Kaitlyn DiMarco, Aaron Betts, Jacob Kysar, Joel E. Futral, Randall D. Goodman, Jerold A. Hawn, Igor M. Gladstone, Joseph W. Duke, Jonathen E. Elliott and Andrew T. Lovering are co-authors. I performed the experimental work and methods were developed equally between all authors. The writing is entirely mine. Joseph W. Duke, Jonathan E. Elliott, and Andrew T. Lovering provided editorial assistance.

INTRODUCTION

In utero, the foramen ovale allows fetal blood flow to bypass the lungs. In most humans, this pathway functionally closes once the infant begins breathing due to left atrial pressure now exceeding right atrial pressure secondary to a fall in pulmonary vascular resistance and an increase in systemic vascular resistance (158, 159). Within the next few months via processes just beginning to be characterized (160), the septum primum and secundum progressively adhere forming a permanent anatomical closure of the foramen ovale. However, in approximately one third of the population permanent anatomical closure of the foramen ovale does not occur, or occurs incompletely, resulting in a “patent” foramen ovale (PFO) (63, 64, 161, 162). Accordingly, this channel allows for right-to-left shunt at times when right atrial pressure exceeds left atrial pressure, such as immediately following the release of a Valsalva maneuver or when end inspiration occurs simultaneously with diastole (44, 66).

Previous work from our laboratory has associated PFO with impaired pulmonary gas exchange efficiency at rest at sea level (44, 45) and at rest after acclimatization to high altitude (163). Work from our lab and others has associated PFO with worse O_2 desaturation in those diagnosed with obstructive sleep apnea (164) and hypoxaemia in those with chronic heart failure and pulmonary arterial hypertension (165). However, these studies only considered whether PFO was present or not, and therefore did not account for the degree of blood flow travelling through the PFO, which in part is dependent on PFO size and the pressure gradients between the left and right atria. Furthermore, one of these studies had a disproportionate number of females in the group with a PFO (163), while the other group had few females thereby complicating interpretation as to the relative impacts of sex and degree of blood flow travelling through the PFO had on previous findings. Intuitively, significant blood flow through a PFO would increase venous admixture and worsen pulmonary gas exchange efficiency. However, differences in the degree of blood flow through a PFO on pulmonary gas exchange efficiency within males and females has not been confirmed experimentally.

Thus, the purpose of the present study was to determine whether the degree of blood flow traveling through the PFO at rest was associated with worse pulmonary gas exchange efficiency and the cardiopulmonary response to exercise in males and females. We hypothesized that in response to strenuous exercise greater degrees of blood flow through the PFO would result in the greatest impairments in pulmonary gas exchange efficiency.

METHODS

This study builds on previous work published by our lab (163). Due to the imbalance of sex and presence of PFO in that study (7 of 9 females participants had PFO) it was not possible to determine if the degree of blood flow through the PFO and participant sex had an influence on

pulmonary gas exchange efficiency. Thus, the current study sought to recruit 17 additional subjects so that there would be a balanced number of males and females and balanced degrees of blood flow through the PFO. In the current study we present data from a total of 40 participants. There were 20 females, 10 with PFO, and 5 with significant blood flow through the PFO upon release of a Valsalva maneuver (bubble score ≥ 3) and 20 males, 10 with PFO, and 5 with significant blood flow through the PFO as above.

Participant Recruitment

All participants provided informed consent, and all studies were approved by the University of Oregon Institutional Review Board (IRB#s 12152011.013, 04302018.049) and conducted in accordance with the *Declaration of Helsinki*. Subsequent to providing informed consent, 37 participants were enrolled and screened for the presence of PFO, 17 participants proceeded in the study based on their combination of sex and degree of blood flow through the PFO, as determined by bubble score upon the release of a Valsalva maneuver (details follow). Participants who underwent PFO screening for other studies (UO IRB #s STUDY00000019, STUDY00000174) in the laboratory and who matched a needed combination of sex and degree of blood flow through the PFO at the time of their enrollment were invited to enroll in this study.

Study Design

After enrollment in the study, participants completed three study visits. The first visit consisted of PFO and comprehensive echocardiographic screening as well as pulmonary function testing. Participants who, after undergoing PFO screening, did not meet a needed sex and PFO size combination did not continue in the study. The second visit consisted of maximal exercise testing (VO_{2Peak}) on a cycle ergometer, as before (166). The third visit consisted of arterial blood sampling while at rest, on the cycle ergometer prior to commencing exercise, and while

exercising. Additionally, participants breathed a 50% O_2 mixture after completing exercise for quantification of shunt fraction at rest as detailed below.

PFO Screening and Echocardiogram

PFO screening was conducted via transthoracic saline contrast echocardiography as previously described (163, 167). Briefly, all ultrasound imaging (ie33, Phillips, Cambridge, USA; Philips Sonos 5500, Eindhoven, The Netherlands) and measurements were conducted by Registered Diagnostic Cardiac Ultrasonographers with >20 years of experience each (RDG, JEF). Participants were instrumented with a 22-gauge intravenous catheter in the antecubital fossa and positioned in the lateral left decubitus position, where an apical 4-chamber ultrasound view of the heart was acquired. Then, 3 mL of saline and 1 mL of air were agitated between two syringes for 10-15 seconds prior to injection. Contrast appearing in the left heart in ≤3 cardiac cycles was considered positive for presence of PFO, and the amount of contrast present was used to assign a "bubble score" (167). Bubble studies were performed with and without Valsalva release, and repeated if results were equivocal. After the release of the Valsalva, a bubble score of 0 was considered negative for PFO, a bubble score of 1-2 was considered to have a small or insignificant degree of blood flow through the PFO, while a bubble score of 3 or higher was considered indicative of large or potentially a physiologically significant degree of blood flow through the PFO (66). All participants then underwent a comprehensive ultrasound screening process to ensure participants were free of cardiac abnormalities or signs of heart disease, as before (63, 168–172).

Pulmonary Function Testing

For previously enrolled participants, pulmonary function was determined using computerized spirometry (Elite Plethysmograph, Medgraphics, St. Paul, MN) according to

American Thoracic Society/European Respiratory Society (ATS/ERS) standards (173). Lung diffusion capacity for carbon monoxide (DL_{CO}) was measured by the single-breath, breath-hold method according to ATS/ERS standards (174, 175). Lung volumes and capacities were determined using whole body plethysmography (Elite Plethysmograph, Medgraphics, St. Paul, MN) according to ATS/ERS standards (176). For newly enrolled participants, pulmonary function was determined using computerized spirometry (Elite Plethysmograph, St. Paul, MN) according to 2019 ATS/ERS standards (151) and 2017 ATS/ERS standards for single-breath, breath-hold assessment of DL_{CO} (177). Maximum voluntary ventilation (MVV) was calculated as by multiplying FEV_1 by 35 ($MVV = FEV_1 \times 35$), while breathing reserve was calculated as MVV-$\dot{V}_{E.}$ Predicted values were calculated using the Global Lung Initiative online calculator for spirometry (178) and DL_{CO} (179).

Exercise Testing

Participants completed a $\dot{V}O_{2Peak}$ test on a magnetically braked cycle ergometer (Lode cycle ergometer, Lode, Groningen, the Netherlands) while breathing on a mouthpiece connected to a metabolic analysis system (Ultima CardiO_2, Medgraphics, St. Paul, MN) for measurement (values averaged from middle 5 of last 7 breaths) of end-tidal gases ($P_{ET}O_2$, $P_{ET}CO_2$), tidal volume (V_T), minute ventilation ($\dot{V}_E$), and respiratory rate (RR). Participants were also instrumented with a forehead O_2 saturation monitor (Nellcor, Medtronic, Minneapolis, MN) for continuous tracking of heart rate (HR) and peripheral O_2 saturation (S_PO_2). Participants were instructed to maintain a cadence of 60-90 revolutions per minute. Resistance was set to 50W at the onset of exercise and increased by 25W steps every minute. Exercise testing was terminated when the participant was no longer to pedal above 60 RPM, exceeded their age-predicted 85% heart rate maximum, or upon volitional fatigue.

Arterial Line Study Instrumentation:

Participants arrived at the lab at approximately 07:00 hours and immediately ingested a core temperature pill (CorTemp HQ, Palmetto, FL) to be used for later temperature correction of arterial blood samples. A physician (JAH, IMG) placed a 20-gauge radial artery catheter in the non-dominant wrist (Arrow International, Reading, PA) under local anesthesia (2% lidocaine). Participants were additionally instrumented with an 18-gauge intravenous catheter placed into the antecubital fossa of the dominant arm, a forehead O_2 saturation monitor, and a 3-lead ECG connected to the ultrasound machine. Due to technical complications, some participants were connected to a 12-lead ECG connected to a Mortara ECG monitor (Mortara, Milwaukee, WI, USA) which was in turn routed to the ultrasound machine.

Arterial Line Study Exercise Protocol

After instrumentation participants mounted the cycle ergometer and began breathing on a mouthpiece connected to a metabolic cart (Medgraphics Ultima, Medgraphics, St. Paul, MN). Metabolic data was monitored for approximately 5 minutes until respiratory exchange ratio and end-tidal CO_2 had stabilized, at which point a pre-exercise arterial blood sample was taken. After collection of the Pre-Exercise arterial sample, participants were instructed to begin pedaling and resistance was increased to 70W. Participants were able to see and monitor their pedaling cadence and were instructed to maintain a cadence of approximately 70 revolutions per minute. Participants completed continuous exercise stages at 70, 100, 130, and 160 Watts, with each stage lasting approximately 4 minutes. Participants who, during the previously descried exercise testing, achieved a peak workload greater than 160W also attempted to complete a "Maximum" workload stage equivalent to this peak workload following completion of the 160W workload. It should be noted that no participants completed a full 4 minutes at the "Maximum"

workload, with average time spent at the "Maximum" workload being approximately 2 minutes (average 2.38 ± 0.88 minutes, range 1 min to 4.5 minutes). Exercise was terminated if participants, at any workload, were unable to maintain a pedaling cadence of at least 60RPM. Two females participants (1 PFO+, 1 PFO-) were unable to complete workloads beyond 130W. If participants felt that they would be unable to complete a workload stage, they were instructed to notify researchers with a "1 minute warning" by raising a finger, at which point measures for that workload were immediately begun. The final workloads achieved and whether or not a "1 minute warning" was given are listed in **Table 4.1**. At three and a half minutes into each workload (or upon participant giving a "1 minute warning"), arterial blood (3 ml) was anaerobically drawn over ~20 seconds while heart rate, temperature, peripheral O_2 saturation (S_PO_2), and pedaling cadence were recorded. Ultrasound images were captured as described below. Following measurements at the last completed workload, participants rested for 30 minutes. Participants were then seated on the cycle ergometer and breathed 50% O_2 from a non-rebreathing valve (Hans Rudolph 2100 Series, Shawnee, Kansas, USA). Once metabolic measurements stabilized (after ~5 minutes), an arterial sample was drawn, and ultrasound measures of cardiac output were made (to be used for the calculation of shunt fraction, detailed below). Two PFO subjects (2 females, 1 bubble score ≥ 3, 1 bubble score ≤ 2) do not have shunt fraction calculations due to feeling faint prior to the commencement of hyperoxic measures (n = 1) and unanticipated removal of the arterial catheter (n = 1).

Table 4.1 Participant Final Stages

	Females Bubble Score ≤ 2	Females Bubble Score ≥ 3	Males Bubble Score ≤ 2	Males Bubble Score ≥ 3
130W	2*			
160W	1*, 6			
190W	3*	3, 1*	1*	1*
220W		2*		
225W		1*		

Table 4.1 Participant Final Stages Continued				
	Females Bubble Score ≤ 2	Females Bubble Score ≥ 3	Males Bubble Score ≤ 2	Males Bubble Score ≥ 3
250W	1*		2	1
275W	2*		2	1
300W			3*	
325W			4*	1*
375W			3*	1*

Table 4.1: **Participant Final Stages.** The highest workload completed by participants. * = the participant was unable to complete the full duration of the listed workload. If this occurred at or below a workload of 160W, the participant did not complete further workloads. If the participant successfully completed the 160W workload and the participant felt they were able, workload was increased to the highest wattage they completed during their exercise testing.

Arterial Sample Analysis

Arterial blood samples were immediately analyzed in triplicate by a blood gas analyzer calibrated with temperature-corrected and tonometered whole blood (RapidLab 248, Siemens, Erlangen, Germany) for pH, PO_2, and PCO_2. Arterial blood gases collected during the Elliott et. al., study were corrected for core body temperature (163). Arterial blood gases collected from the additional 17 participants were tonometry and body temperature corrected (180–182). Arterial samples were also analyzed via co-oximetry (OSM-3, Radiometer, Denmark) for haemoglobin concentration (tHb), carboxyhaemoglobin (HbCO), haemoglobin saturation (HbO_2Sat) , and methylated haemoglobin (MetHb), enabling the calculation of O_2 content. Samples were analyzed for hematocrit using the capillary tube centrifugation method and for lactate (Lactate+ meter and strips, Nova Biomedical, Waltham, MA) in duplicate.

Pulmonary Artery Systolic Pressure and Cardiac Output

While arterial sampling was occurring, simultaneous ultrasound images were obtained. These images were used to measure tricuspid regurgitation velocity (TR_{Vel}) and the left ventricular outflow tract velocity time integral ($LVOT_{VTI}$), while heart rate was measured with

ECG. A small volume (<1mL) of air agitated with 3mL of saline was injected to enhance visualization of TR_{Vel} as needed. Pulmonary artery systolic pressure (PASP) was calculated from TR_{Vel} using the modified Bernoulli equation ($4v_2^2 + P_{RA}$), where v is TR_{Vel} and P_{RA} is the right atrial pressure as estimated by IVC collapse during a "sniff test" conducted as part of the ultrasound screening, as is standard. Previously enrolled (163) participants had P_{RA} estimated according to the guidelines of the American Society of Echocardiography at the time (144). Newly enrolled participants had P_{RA} estimated according to more recent guidelines (149). 1 previously enrolled participant (M, Bubble Score ≤ 2) had slightly elevated P_{RA} (8mmHg). All other participants had normal (3 mmHg) P_{RA}, regardless of when they were enrolled). $LVOT_{VTI}$ was used to calculate cardiac output (Q_T) according to the equation ($LVOT_{VTI}$ x $LVOT_{CSA}$) where $LVOT_{CSA}$ is calculated from LVOT diameter measurement collected as part of the ultrasound screening. Total pulmonary resistance (TPR) was calculated as $PASP/Q_T$ recorded in mm hg/L/min and converted to dynes/sec/cm^{-5} prior to analysis (183).

Gas Calculations

Alveolar (PAO_2) was calculated as before. (166, 169, 184). Briefly, PAO_2 was calculated using the ideal gas equation and temperature- and tonometry-corrected $PaCO_2$ and a respiratory exchange ratio (RER) averaged over the period of arterial sampling (~20 seconds). Pulmonary gas exchange efficiency (Arterial-to-alveolar difference in O_2; $AaDO_2$) was calculated at rest and during exercise as the difference between temperature- and tonometry-corrected arterial PO_2 (PaO_2) and corresponding PAO_2. Participant data from Elliott et al was calculated as previously reported (163). Measures of O_2 content were calculated using co-oximetry measured tHb and saturation calculated from the Kelman equation (157) as before (163). Mixed venous O_2 content ($C\bar{v}O_2$) was calculated using the Fick principle using measured arterial O_2 content (CaO_2), $\dot{V}O_2$,

and ultrasound derived estimates of Q_T as described earlier. Venous admixture (Q_{VA}/Q_T) and shunt fraction (Q_S/Q_T) were calculated from the shunt equation:

$$(1)\ \frac{Cc'O2-CaO2}{Cc'O2-C\bar{v}O2}\ (185).$$

Equation 3.6

Where $Cc'O_2$ is end pulmonary capillary O_2 content, CaO_2 is arterial O_2 content, and $C\bar{v}O_2$ is mixed venous O_2 content. Q_{VA}/Q_T was calculated from the metabolic data and arterial blood gasses collected at the end of each exercise workload. Q_S/Q_T was calculated from arterial blood gas analysis and metabolic data gathered while the participant was breathing 50% O_2 and seated on the cycle ergometer. This level of hyperoxia allows for collection of metabolic data while eliminating the impact of ventilation-perfusion mismatch and diffusion limitation (186) and avoids the numerous assumptions which must be made when calculating Q_s/Q_T while breathing 100% O_2 (187, 188).

Statistics

All statistical analyses were conducted in GraphPad Prism 9.4.1. We were interested in understanding how degree of blood flow through the PFO (Significant/large degree vs. Insignificant/small degree and no PFO) was associated with pulmonary gas exchange efficiency and cardiopulmonary responses to moderate to strenuous exercise within a given sex assigned at birth (i.e., males and females). Participant data was segregated according to sex, and then grouped by bubble score (≥ 3 vs ≤ 2) and analyzed separately in males and in females. Comparisons were only made within a sex, and not between sexes. Accordingly, $AaDO_2$, PAO_2, PaO_2, $PaCO_2$, $\dot{V}O_2$, $\dot{V}CO_2$, Q_{VA}/Q_T, CaO_2, CvO_2, $Cc'O_2$, V_E, V_T, Respiration Rate (RR), RER, Qc, PASP, $\dot{V}e/\dot{V}O_2$, $\dot{V}e/\dot{V}CO_2$, and TPR were analyzed by 2-way RMANOVA (Bubble Score x Workload) with Sidak's post-hoc test to compare differences between Bubble Score groups

across workloads within each sex. Additionally, ultrasound measures were not recorded in participants from the study from Elliott et al, 2015 beyond 160W, so calculations which rely on ultrasound measures (Q_{VA}/Q_T, CvO_2, Q_T, PASP, TPR) only include values up to 160W. For variables that were missing data, a mixed-effects analysis was performed with Sidak's post-hoc test for this data. This mixed-effects model uses a compound symmetry covariance matrix and is fit using Restricted Maximum Likelihood. Anthropometrics, pulmonary function, and Q_s/Q_T at 50% hyperoxia were tested for normality via Shapiro-Wilk's test. If normality was not violated, comparisons between those with bubble score ≥3 and those with bubble score ≤2 in each sex were made with Student's t-test (i.e., males were not compared against females). If normality was violated, comparisons were made with Mann-Whitney test. Data is presented as mean ± standard deviation.

RESULTS

Anthropometrics, Pulmonary Function

Females with bubble score ≥ 3 were younger than females with bubble score ≤ 2 (19.6 ± 1.3 years vs 24.4 ± 4.5 years, p = .005) (**Table 4.2**). Males with bubble score ≥ 3 had lower absolute DL_{CO} compared to males with bubble score ≤ 2 (40.62 ± 4.96 vs 46.63 ± 4.54, p = .024), but this difference was eliminated when DL_{CO} was compared as a percent of predicted value (p = .0794) (**Table 4.2**). There were no differences in DL_{CO}/V_A, either considered as an absolute value or as a percent of predicted in either males or females (**Table 4.2**).

Table 4.2. Participant Anthropometric and Pulmonary Function Measures

	Females Bubble Score ≥ 3	Females Bubble Score ≤ 2	p	Males Bubble Score ≥ 3	Males Bubble Score ≤ 2	p
n	5	15		5	15	
Age (yrs)	19.6 ± 1.3	24.4 ± 4.5	.005	25.8 ± 6.2	25.1 ± 12.9	.334
Height (cm)	169.3 ± 5.1	166.3 ± 6.2	.350	179.3 ± 4.3	180.9 ± 6.7	.271
Weight (kg):	63.1 ± 4.8	60.5 ± 6.0	.396	77.0 ± 10.5	75.5 ± 8.0	.732

Table 4.2. Participant Anthropometric and Pulmonary Function Measures Continued

	Females Bubble Score ≥ 3	Females Bubble Score ≤ 2	p	Males Bubble Score ≥ 3	Males Bubble Score ≤ 2	p
FVC (L)	4.12 ± 0.62	4.23 ± 0.82	.947	6.16 ± 0.41	5.78 ± 0.86	.275
FVC % Predicted	99.5 ± 16.5	105.4 ± 18.3	.497	110.4 ± 9.0	102.1 ± 9.9	.114
FEV1 (L)	3.55 ± 0.36	3.59 ± 0.56	.982	4.75 ± 0.36	4.82 ± 0.62	.811
FEV1 % Predicted:	98.0 ± 9.5	104.2 ± 16.3	.445	102.2 ± 7.8	102.7 ± 14.7	.486
FEV1/FVC:	.87 ± .06	.86 ± .07	.762	.77 ± .05	.84 ± .08	.092
FEV1/FVC % Predicted	98.5 ± 7.1	98.7 ± 8.0	.972	91.9 ± 4.7	99.7 ± 10.4	.129
FEF25-75 (L/s)	3.98 ± 0.64	3.84 ± 0.77	.722	4.08 ± 0.78	4.95 ± 1.31	.184
FEF25-75 % Predicted	95.2 ± 13.0	98.6 ± 21.7	.744	83.7 ± 12.9	104.9 ± 26.3	.434
SVC (L)	4.36 ± 0.64	4.06 ± 0.58	.335	6.45 ± 0.55	6.03 ± 0.80	.299
SVC % Predicted	108.1 ± 15.8	100.6 ± 12.0	.276	117.4 ± 12.4	111.0 ± 12.0	.313
IC (L)	2.82 ± 0.49	2.68 ± 0.51	.593	4.22 ± 0.58	3.86 ± 0.61	.248
IC % Predicted	112.4 ± 20.9	104.6 ± 18.8	.443	116.2 ± 20.8	108.5 ± 19.3	.454
ERV (L)	1.54 ± 0.27	1.37 ± 0.29	.251	2.66 ± 0.75	2.13 ± 0.60	.297
ERV % Predicted	111.8 ± 16.2	99.4 ± 16.7	.095	133.8 ± 31.4	119.1 ± 21.2	.056
FRC (L):	2.70 ± 0.36	2.91 ± 0.47	.375	4.19 ± 0.62	3.67 ± 0.94	.257
FRC % Predicted	99.8 ± 14.1	108.0 ± 18.3	.388	124.9 ± 19.9	109.5 ± 13.9	.115
RV (L):	1.15 ± 0.30	1.59 ± 0.44	.060	1.28 ± 0.28	1.46 ± 0.51	.469
RV % Predicted	101.3 ± 30.2	134.8 ± 38.0	.333	85.5 ± 20.3	97.8 ± 27.5	.374
TLC (L):	5.52 ± 0.82	5.55 ± 0.75	.927	7.79 ± 0.45	7.49 ± 1.04	.551
TLC % Predicted	104.1 ± 16.6	103.7 ± 12.6	.672	110.2 ± 8.3	104.8 ± 9.2	.262
RV/TLC	21.00 ± 3.67	30.06 ± 9.55	.061	15.93 ± 4.69	19.89 ± 6.37	.135
RVC/TLC % Predicted	98.5 ± 18.4	129.7 ± 34.5	.058	77.1 ± 15.4	92.3 ± 25.1	.225
DLco	27.18 ± 3.22	28.63 ± 5.53	.597	40.62 ± 4.96	46.63 ± 4.54	.024
DLco % Predicted	116.6 ± 12.7	123.1 ± 21.8	.545	121.7 ± 15.0	137.4 ± 16.5	.079
DL_{CO}/V_A	5.39 ± 1.16	5.51 ± 1.00	.743	5.56 ± 0.53	6.21 ± 0.83	.119
V_A	5.14 ± 0.68	5.19 ± 0.59	.881	7.31 ± 0.44	7.68 ± .78	.329
V_A % Predicted	102.4 ± 14.4	102.6 ± 10.7	.980	110.6 ± 3.8	113.7 ± 10.4	.529

Table 2: Anthropometric and lung function measurements were largely similar between those with bubble score ≥ 3 and those with bubble score ≤ 2, in both males and in females. Females with

bubble score ≥ 3 were slightly younger and had a larger inspiratory capacity. Males with a bubble score ≤ 3 had a lower DL_{CO} compared to males with a bubble score ≤ 2, though both groups exceed 100% of their predicted value.

Blood Gases, Q_{VA}/Q_T, Q_S/Q_T, Saturation, pH:

Females: There was a significant effect of the degree of blood flow through the PFO on $AaDO_2$ (p = .048), with significant pairwise differences at 160W (Bubble Score ≥ 3 and $AaDO_2$ = 22.6 ± 5.6 mmHg vs Bubble Score ≤ 2 and $AaDO_2$ = 14.9 ± 5.4 mmHg, p = .023) (**Figure 4.1A**). There was a significant interaction effect (Bubble Score x Workload) on PAO_2 (p < .001), though there were no pairwise differences (**Figure 4.1B**). There was a significant interaction effect (Bubble Score x Workload) on PaO_2 (p < .001) with pairwise differences at 130W (Bubble Score ≥ 3 and PaO_2 = 91.7 ± 7.8 mmHg vs Bubble Score ≤ 2 and PaO_2 = 101.4 ± 7.1 mmHg, p = .042), 160W (Bubble Score ≥ 3 and PaO_2 = 88.5 ± 7.8 mmHg vs Bubble Score ≤ 2 and PaO_2 = 102.0 ± 7.3 mmHg, p < .001), and at Max (Bubble Score ≥ 3 and PaO_2 = 91.51 ± 7.6 mmHg vs Bubble Score ≤ 2 and PaO2 = 101.9 ± 7.1 mmHg, p = .003) (**Figure 4.1C**). There was a significant interaction effect (Bubble Score x Workload) on $PaCO_2$ (p <.001) (**Figure 4.1D**). There was a significant effect of Workload on arterial O_2 saturation (p = .034), with saturation dropping slightly as Workload increased (**Figure 4.1E**). There was a significant main effect of Workload on pH (p <.001), with pH decreasing as Workload increased (**Figure 4.1F**). There was a significant interaction effect Bubble Score x Workload (p = .018) on Q_{VA}/Q_T, with pairwise differences at Pre-Ex (Bubble Score ≥ 3 1.43 ± 0.78% vs Bubble Score ≤ 2 0.21 ± 0.52%, p < .001) and 160W (BS ≥ 3 2.07 ± 0.78% vs BS ≤ 2 1.12 ± 0.68%, p = .007) (**Figure 4.2A)**. Females with Bubble Score ≥ 3 had a larger resting Q_S/Q_T (1.413 ± 0.755 % vs 0.423 ± 0.835) (p = .049) (**Figure 4.2B**)

Males: There was a main effect of Workload on $AaDO_2$ ($p < .001$), with $AaDO_2$ increasing as workload increased (**Figure 4.1A**). There was also a main effect of workload on PAO_2 ($p < .001$) which increased (**Figure 4.1B)** and PaO_2 ($p < .001$) which decreased (**Figure 4.1C**) as workload increased from Pre-Ex to Max, while $PaCO_2$ decreased as expected ($p <.001$) (**Figure 4.1D**). There was a significant interaction (Bubble Score x Workload) on O_2 saturation ($p <.001$), with significant post-hoc testing at Max (Bubble Score ≥ 3 and $SaO_2 = 97.2 \pm 0.7\%$ vs Bubble Score ≤ 2 and $SaO_2 = 95.7 \pm 1.6\%$, $p <.001$) (**Figure 4.1E**). There was a significant interaction (Bubble Score x Workload) on pH ($p = .017$), with pH decreasing more at higher workloads in males without significant blood flow through PFO (**Figure 4.1F**). There was a significant effect of Workload on Q_{VA}/Q_T ($p < .001$), with Q_{VA}/Q_T increasing as workload increased (**Figure 4.2A**). In contrast to females, there were no significant findings on resting Q_S/Q_T in males ($p = .2235$) (**Figure 4.2B**).

Figure 4.1 (next page). Blood Gases and pH (**A**) Females with significant blood flow through intracardiac shunt had significantly worse pulmonary gas exchange efficiency compared to females without significant flow through intracardiac shunt (n = 5 females with significant blood flow through PFO, 15 females with no or insignificant blood flow through PFO, 5 males with significant blood flow through PFO, 15 males with no or insignificant blood flow through PFO, $p = .048$). (**B**) There was a significant interaction effect on PAO_2 in females, where females without significant intracardiac shunt had slightly elevated PAO_2 once exercise commenced (n = 5 females significant blood flow through PFO, 15 females with no or insignificant blood flow through PFO, 5 males with significant blood flow through PFO, 15 males with no or insignificant blood flow through PFO, $p < .001$). (**C**) There was a significant interaction effect on PaO_2, and females without significant intracardiac shunt had greater PaO_2 (n = 5 females significant blood flow through PFO, 15 females with no or insignificant blood flow through PFO, 5 males with significant blood flow through PFO, 15 males with no or insignificant blood flow through PFO, $p < .001$). (D) Females with significant intracardiac shunt had greater $PaCO_2$ compared to females without significant intracardiac shunt, and this difference was greater at higher workloads (n = 5 females significant blood flow through PFO, 15 females with no or insignificant blood flow through PFO, 5 males with significant blood flow through PFO, 15 males with no or insignificant blood flow through PFO, $p < .001$). (**E**) Females with significant blood flow through intracardiac shunt had lower O_2 saturation compared to females without significant blood flow through intracardiac shunt (n = 5 females with significant blood flow

through PFO, 15 females with no or insignificant blood flow through PFO, p = .034), though there were no pairwise differences. In males, there was a significant interaction effect where O_2 saturation was similar until maximal workload (n = 5 males with significant blood flow through PFO, 15 males with no or insignificant blood flow through PFO, p < .001), where males without significant intracardiac shunt had lower saturation. † = Significant main effect of the degree of blood flow through the PFO. ‡ = Significant interaction effect (Bubble Score x Workload). * = significant pairwise difference (p < .05).

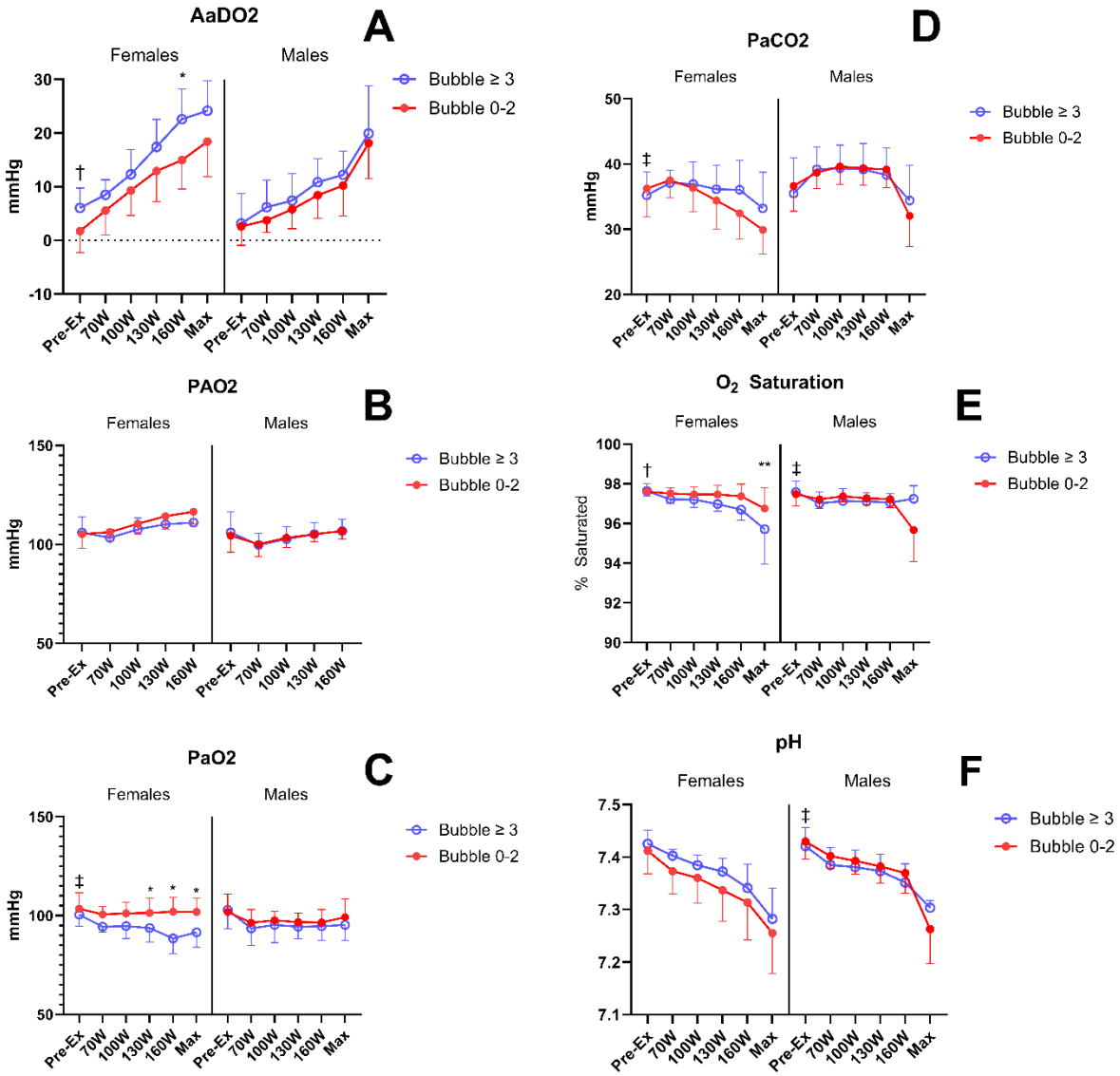

Figure 4.2. Venous Admixture and Shunt Fraction (**A**) There was a significant interaction of Workload x Bubble Score in females (n = 5 females with significant blood flow through PFO, 15 females with no or insignificant blood flow through PFO, p = .018), with specific pairwise differences at Pre-Ex (n = 5 females significant blood flow through PFO, 15 females with no or

insignificant blood flow through PFO, p <.001) and 160W (n = 4 females significant blood flow through PFO, 13 females with no or insignificant blood flow through PFO, p = .007). (**B**) Females with significant intracardiac shunt had a greater shunt fraction while breathing 50% O_2 compared to females without significant intracardiac shunt (n = 4 females significant blood flow through PFO, 14 females with no or insignificant blood flow through PFO, p = .049). ‡ = Significant interaction effect of Bubble Score x Workload (p < .05).

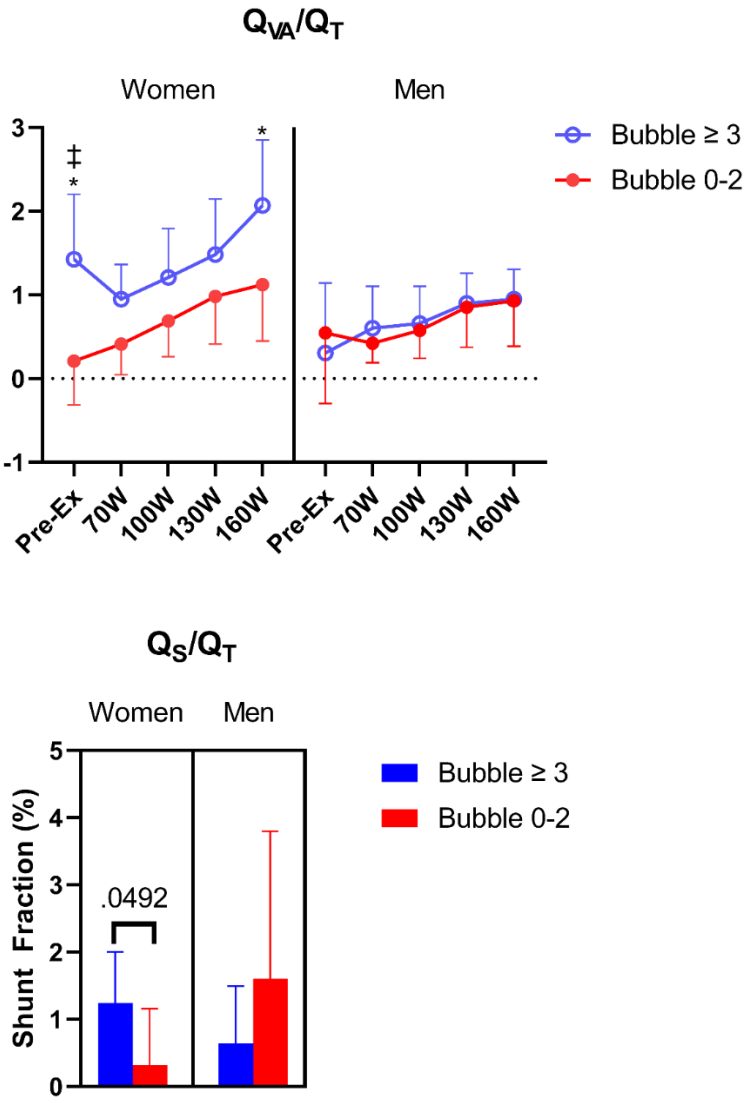

Ventilation, Tidal Volume, Respiration Rate, $\dot{V}_E/MVV$, $\dot{V}_E/\dot{V}O_2$, $\dot{V}_E/\dot{V}CO_2$*:*

Females: There was a significant main effect of the degree of blood flow through the PFO on $\dot{V}_E$ (p = .007), with significant pairwise differences at 160W (Bubble Score ≥3 and $\dot{V}_E$ =

66.14 ± 8.64 L/min vs Bubble Score ≤ 2 and $\dot{V}_E$ = 78.56 ± 61.2 L/min, p = .038) (**Figure 4.3A**). As expected, there was a significant main effect of Workload on tidal volume (p < .001) (**Figure 4.3B**), with tidal volume increasing as workload increased. Additionally, there was a significant interaction (Bubble Score x Workload) on RR (p = .022). Females with significant blood flow through PFO having a lower RR, with pairwise differences at 130W (Bubble Score ≥ 3 and RR = 27.5 ± 5.5 breaths/min vs Bubble Score ≤ 2 and RR = 42.8 ± 14.2 breaths/min p = .045) and 160W (Bubble Score ≥3 and RR = 34.1 ± 3.9 breaths/min vs Bubble Score ≤ 2 and RR = 49.2 ± 14.8 breaths/min, p = .028) (**Figure 4.3C**). As would be expected, there was a significant effect of Workload on $\dot{V}_E$/MVV (p <.001), with $\dot{V}_E$/MVV increasing as workload increased (**Figure 4.3D**). There was a significant interaction of (Bubble Score x Workload) on $\dot{V}_E/\dot{V}O_2$ (p = .002), with females who have significant flow through PFO having a greater Pre-ex $\dot{V}_E/\dot{V}O_2$ and then a lower $\dot{V}_E/\dot{V}O_2$ once they began exercising (**Figure 4.3E**). Similarly, for $\dot{V}_E/\dot{V}CO_2$, females had a significant interaction (Bubble Score x Workload) (p < .001), with significant pairwise differences at Pre-Ex (Bubble Score ≥ 3 and $\dot{V}_E/\dot{V}CO_2$ = 51.6 ± 5.3 vs Bubble Score ≤ 2 and $\dot{V}_E/\dot{V}CO_2$ = 39.2 ± 9.3, p = .002) and subsequently a lower $\dot{V}_E/\dot{V}CO_2$ during exercise (**Figure 4.3F**).

Males: There was a significant interaction (Bubble Score x Workload) on $\dot{V}_E$ (p < .001) in males, with a pairwise difference at Max (Bubble Score ≥3 and $\dot{V}_E$ = 114.37 ± 31.70 L/min vs Bubble Score ≤ 2 and $\dot{V}_E$ = 153.94 ± 22.30 L/min, p <.001) (**Figure 4.3A**). There was a significant interaction (Bubble Score x Workload) on tidal volume (p = .035), with tidal volume increasing more from Pre-Ex to Max in males without significant blood flow through PFO, although there were no significant pairwise differences (**Figure 4.3B**). As expected, there was a significant effect of Workload on Respiration Rate (p<.001), with respiration rate increasing as

workload increased (**Figure 4.3C**). There was a significant interaction (Bubble Score x Workload) on $\dot{V}_E$/MVV ($p < .001$), with a pairwise difference at Max (Bubble Score ≥ 3 and $\dot{V}_E$/MVV = 69.5 ± 20.4 vs Bubble Score ≤ 2 and $\dot{V}_E$/MVV = 89.5 ± 13.8, $p < .001$) (**Figure 4.3D**). There was a significant main effect of Workload on $\dot{V}_E/\dot{V}O_2$ ($p < .001$), with $\dot{V}_E/\dot{V}O_2$ dropping with the onset of exercise and then increasing again at Max (**Figure 4.3E**). There was a significant interaction of Workload x Bubble Score on $\dot{V}_E/\dot{V}CO_2$ ($p = .029$), with a specific pairwise difference at Pre-Ex (Bubble Score ≥ 3 and $\dot{V}_E/\dot{V}CO_2$ = 35.4 ± 3.7 vs Bubble Score ≤ 2 and $\dot{V}_E/\dot{V}CO_2$ = 43.9 ± 9.0, $p = .004$). However, once exercise began $\dot{V}_E/\dot{V}CO_2$ was similar in males regardless of Bubble Score and across workloads (**Figure 4.3F)**.

Figure 4.3 (next page). Ventilatory Data (**A**) Females with significant intracardiac shunt had reduced ventilation compared to females without significant intracardiac shunt (n = 5 females significant blood flow through PFO, 15 females with no or insignificant blood flow through PFO, p = .007), with a pairwise difference at 160W (n = 5 females with significant blood flow through PFO, 13 females with no or insignificant blood flow through PFO, p = .038). There was a significant interaction effect in males, where ventilation was similar in males with and without significant intracardiac shunt until maximal workload, where males with significant intracardiac shunt had greater ventilation (n = 5 males significant blood flow through PFO, 15 males with no or insignificant blood flow through PFO, p = <.001). (**B**) There was a significant interaction effect on tidal volume in males, where males without significant intracardiac shunt initially had smaller tidal volumes, but this was reversed with exercise (n = 5 males significant blood flow through PFO, 15 males with no or insignificant blood flow through PFO, p = .035). (**C**) There was a significant interaction on respiration rate in females, where respiration rate was similar prior to the onset of exercise, but females with significant intracardiac shunt had lower respiration rate compared to females without significant shunt once exercise began (n = 5 females significant blood flow through PFO, 15 females with no or insignificant blood flow through PFO, p = .022) with pairwise differences at 130W (n = 5 females with significant blood flow through PFO, 15 females with no or insignificant blood flow through PFO, p = .045) and 160W (n = 5 females with

significant blood flow through PFO, 13 females with no or insignificant blood flow through PFO, p = .028). (**D**) There was a significant interaction in males, where $\dot{V}_E$/MVV was similar regardless of intracardiac shunt until maximal exercise, where males without significant intracardiac shunt had greater $\dot{V}_E$/MVV (n = 5 males significant blood flow through PFO, 15 males with no or insignificant blood flow through PFO, p < .001). **(E)** There was a significant interaction in females for $\dot{V}_e/\dot{V}O_2$, where females with significant intracardiac shunt had greater $\dot{V}_E/\dot{V}O_2$ prior to exercise but had lesser $\dot{V}_E/\dot{V}O_2$ with exercise. (n = 5 females significant blood flow through PFO, 15 females with no or insignificant blood flow through PFO, p = .002). (**F**) There was a significant interaction on $\dot{V}_E/\dot{V}CO_2$ in both females and males. In females, those with significant intracardiac shunt had greater $\dot{V}_E/\dot{V}CO_2$ at pre-exercise, but this trend reversed with exercise (n = 5 females significant blood flow through PFO, 15 females with no or insignificant blood flow through PFO, p < .001). In males, $\dot{V}_E/\dot{V}CO_2$ was initially greater in males without intracardiac shunt, but was similar to males with significant intracardiac shunt with exercise (n = 5 males significant blood flow through PFO, 15 males with no or insignificant blood flow through PFO, p = .029) † = main effect of Bubble Score. ‡ = interaction effect (Bubble Score x Workload). * = significant pairwise difference (p < .05). ** = significant pairwise difference (p < .01). *** = significant pairwise difference (p < .001).

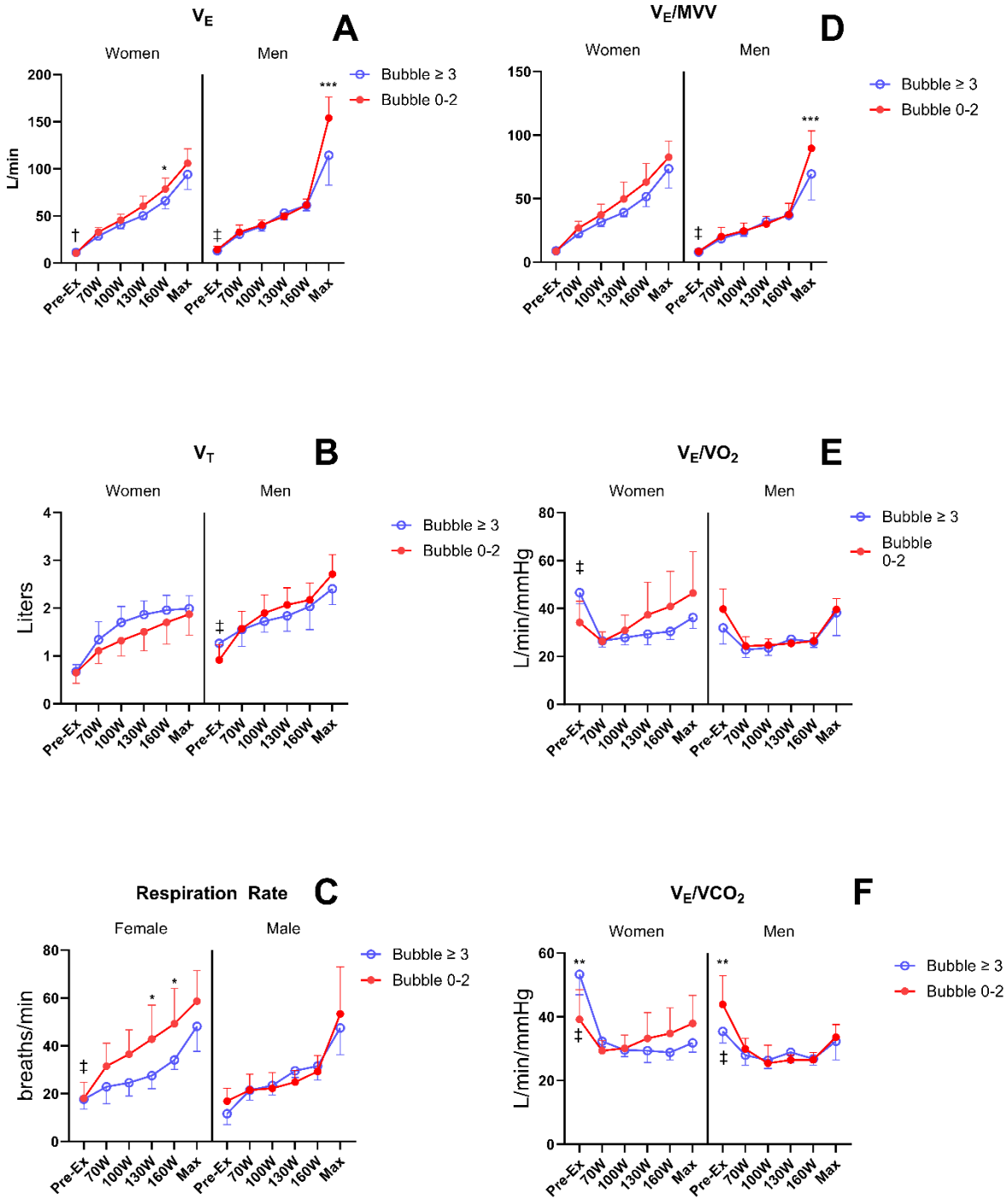
A
V_E
Women
Men
L/min
Bubble ≥ 3
Bubble 0-2
Pre-Ex
70W
100W
130W
160W
Max
D
V_E/MVV
B
V_T
Liters
C
Respiration Rate
Female
Male
breaths/min
E
V_E/VO_2
L/min/mmHg
Bubble 0-2
F
V_E/VCO_2

O_2 Content, [Hb], Q_T, PASP, TPR:

Females: There was a significant effect of Workload on haemoglobin concentration ($p < .001$), with haemoglobin increasing slightly as workload increased (**Figure 4.4A**). As expected, there was a significant effect of Workload on CaO_2 ($p < .001$) with CaO_2 increasing as Workload increased (**Figure 4.4B**). There was a significant interaction effect on CvO_2 ($p = .019$), though no specific pairwise differences (**Figure 4C**). We observed expected increases in Q_T (**Figure 4.4D**) and PASP (**Figure 4.4E**) ($p < .001$, both). Additionally, we observed the expected decrease in TPR as workload increased ($p < .001$) (**Figure 4.4F**).

Males: There was a significant interaction (Bubble Score x Workload) on haemoglobin concentration ($p < .001$), with post-hoc tests significant at Pre-Ex (Bubble Score ≥ 3 and haemoglobin = 13.9 ± 0.4 g/dL vs Bubble Score ≤ 2 and haemoglobin = 15.2 ± 0.8 g/dL, $p = .004$), 70W (Bubble Score ≥ 3 and haemoglobin = 14.3 ± 0.6 g/dL vs Bubble Score ≤ 2 and haemoglobin = 15.5 ± 0.7 g/dL, $p = .006$), 100W (Bubble Score ≥ 3 and haemoglobin = 14.2 ± 0.7 g/dL vs Bubble Score ≤ 2 and haemoglobin = 15.5 ± 0.7 g/dL, $p = .004$), and Max (Bubble Score ≥ 3 and haemoglobin = 15.1 ± 0.6 g/dL vs Bubble Score ≤ 2 and haemoglobin = 16.5 ± 0.8 g/dL, $p < .001$) (**Figure 4.4A**). As would be expected with these findings for haemoglobin concentration, there was a significant interaction (Bubble Score x Workload) on CaO_2 ($p = .023$), with post-hoc testing significant at Pre-Ex (Bubble Score ≥ 3 and $CaO_2 = 19.2 \pm 0.6$ mL/dL vs Bubble Score ≤ 2 and $CaO_2 = 21.0 \pm 1.0$ mL/dL, $p = .004$), 70W (Bubble Score ≥ 3 and $CaO_2 = 19.6 \pm 0.8$ mL/dL vs Bubble Score ≤ 2 and $CaO_2 = 21.3 \pm 1.0$ mL/dL, $p = .005$), 100W (Bubble Score ≥ 3 and $CaO_2 = 19.5 \pm 1.1$ mL/dL vs Bubble Score ≤ 2 and $CaO_2 = 21.3 \pm 0.9$ mL/dL, $p = .003$), and Max (Bubble Score ≥ 3 and $CaO_2 = 20.7 \pm 0.9$ mL/dL vs Bubble Score ≤ 2 and $CaO_2 = 22.3 \pm 1.0$ mL/dL, $p = .006$) (**Figure 4.4B**). There was a significant effect of Bubble Score on

CvO_2 ($p = .012$), though there were no specific pairwise differences (**Figure 4.4C**). There was an expected significant main effect of Workload on Q_T ($p < .001$), with Q_T increasing as workload increased. (**Figure 4.4D**). We observed the expected increase in PASP as Workload increased ($p < .001$) (**Figure 4.4E**) and the expected decrease in TPR as Workload increased ($p < .001$) (**Figure 4.4F)**.

Figure 4.4 (next page). Oxygen Content and Pulmonary Vascular Measures (**A**) In males, there was a significant interaction on haemoglobin concentration, where males without significant intracardiac shunt had greater haemoglobin concentration measured at all workloads except 130W (n = 5 males significant blood flow through PFO, 15 males with no or insignificant blood flow through PFO, $p < .001$). (**B**) There was a significant interaction effect in males on CaO_2, where males with significant intracardiac shunt had lower CaO_2, with specific differences at all workloads except 130W (n = 5 males significant blood flow through PFO, 15 males with no or insignificant blood flow through PFO, $p = .023$). (**C**) In females, there was a significant interaction effect on C_VO_2 (n = 5 females significant blood flow through PFO, 15 females with no or insignificant blood flow through PFO, $p = .019$), but there were no pairwise differences. In males there was a significant effect of bubble score on C_VO_2 (n = 5 males significant blood flow through PFO, 15 males with no or insignificant blood flow through PFO, $p < .001$), but no significant pairwise differences at any exercise load. (**D**) There was an expected increase in Q_T in both males and females as exercise workload increased ($p < .001$, both males and females). (**E**) In both males and females, TPR significantly decreased as exercise intensity increased (n = 5 males with significant blood flow through PFO, 15 males with no or insignificant blood flow through PFO, 5 females with significant blood flow through PFO, 15 females with no or insignificant blood flow through PFO, $p < .001$, both males and females). (**F**) PASP increased as workload increased in both males and females regardless of flow through intracardiac shunt (n = 5 males with significant blood flow through PFO, 15 males with no or insignificant blood flow through PFO, 5 females with significant blood flow through PFO, 15 females with no or insignificant blood flow through PFO, $p < .001$). † = Significant main effect of Bubble Score. ‡ = Significant interaction (Workload x Bubble Score). * = significant pairwise difference ($p < .05$). ** = significant pairwise difference ($p < .005$)

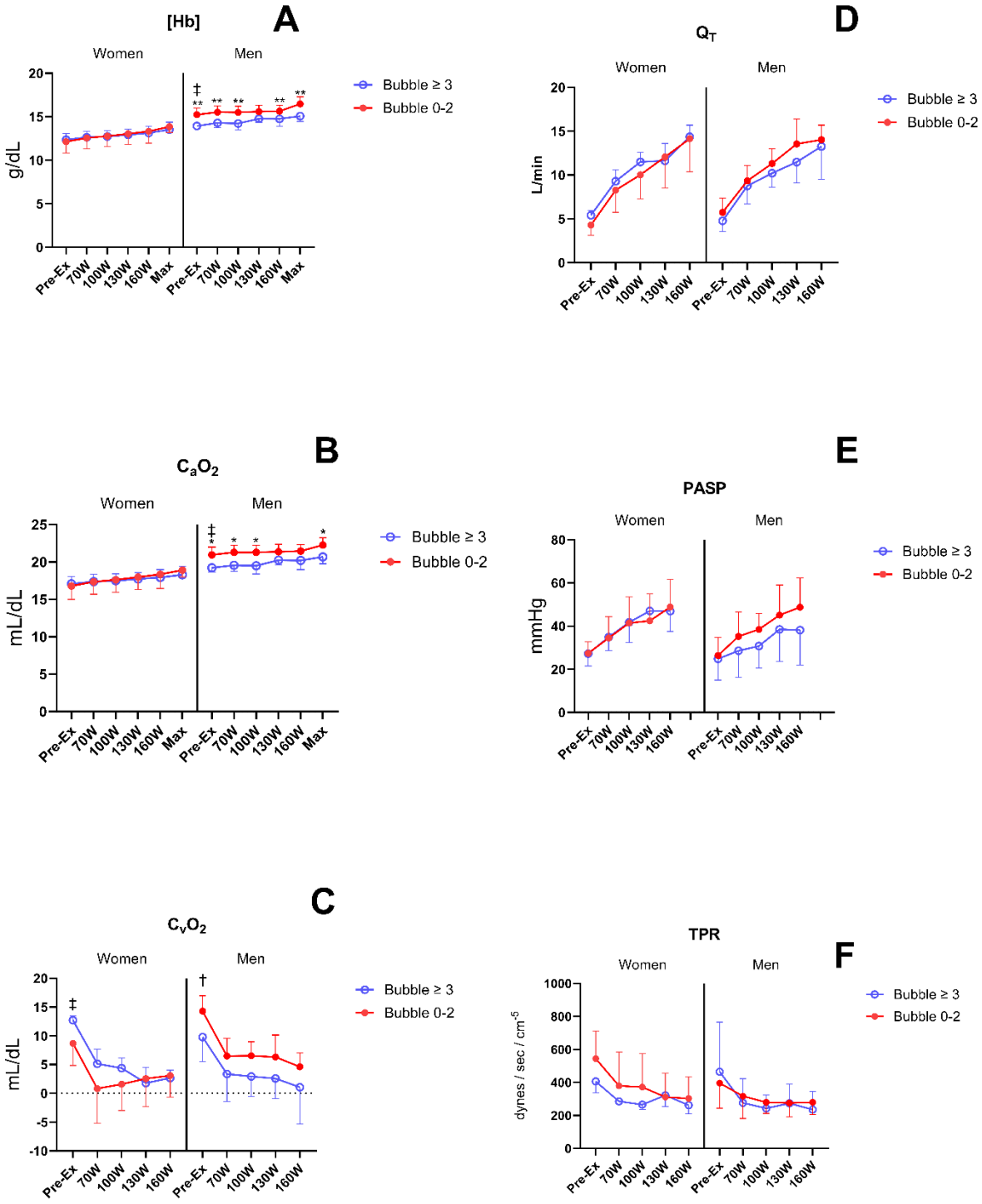
A
[Hb]
Women
Men
g/dL
Bubble ≥ 3
Bubble 0-2
Pre-Ex
70W
100W
130W
160W
Max
B
C_aO_2
mL/dL
C
C_vO_2
D
Q_T
L/min
E
PASP
mmHg
F
TPR
dynes / sec / cm^{-5}

DISCUSSION

The purpose of this study was to compare the cardiopulmonary response to moderate to strenuous exercise in those with and without significant blood blow through a common right-to-left intracardiac shunt in males and in females (i.e., the PFO). The main findings of this study were: 1) Females with significant blood flow through a PFO had wider $AaDO_2$, lower PaO_2s, and lower O_2 saturations compared to females without significant blood flow through the PFO; 2) Females with significant blood flow through a PFO had a greater degree of calculated venous admixture during exercise and a greater calculated shunt fraction at rest compared to females without significant blood flow through a PFO; 3) Females with significant blood flow through a PFO had higher $PaCO_2$, lower minute ventilation, a lower RR and reduced ventilatory equivalents for O_2 and CO_2 during exercise compared to females without significant blood flow through a PFO; 4) Males with significant blood flow through a PFO had lower haemoglobin concentrations and reduced arterial O_2 content compared to males without significant blood flow through a PFO.

The above constellation of findings suggests that significant blood flow through a PFO impairs pulmonary gas exchange efficiency through increased venous admixture reducing arterial PO_2 in females, but not in males. It is unclear why males with significant blood flow through a PFO do not also have increased venous admixture during exercise. Venous admixture in this study was the calculated amount of mixed venous blood that must bypass oxygenation in the lung and mix with fully oxygenated arterial blood to arrive at an observed $AaDO_2$ (189). Factors which may impact the calculation of venous admixture include V/Q mismatch, diffusion limitation, shunt, and drainage of the bronchial circulation into the pulmonary veins and the thebesian circulation directly into the left atrium. These normally occurring circulatory

pathways (i.e. bronchial and thebesian circulation) account for ~0.5% of venous admixture (190, 191). This is approximately the amount of venous admixture we observed at rest and during exercise in females with bubble score ≤ 2, and in males irrespective of bubble score (**Figure 4.2A**). Increases in venous admixture above ~0.5% would be expected to be caused by an additional source of shunt and in this case, an intracardiac right-to-left shunt like a PFO. Calculations of venous admixture are unable to distinguish between these sources of shunt. However, when breathing a 50% O_2 mixture, contributions to pulmonary gas exchange efficiency from ventilation/perfusion matching and diffusion limitation are prevented or greatly minimized (169, 186), meaning that any shunt calculated while breathing 50% O_2 is the result of thebesian, bronchial, intrapulmonary and intracardiac shunt – in other words, while breathing 50% O_2, Q_{VA}/Q_T equals Q_S/Q_T. By subtracting the expected contributions of thebesian and bronchial circulations, and operating under the assumption that hyperoxia minimizes the influence of intrapulmonary shunt (169), the remaining calculated shunt fraction must be from intracardiac shunt (**Figure 4.2B**). Assuming that the contributions of bronchial and thebesian circulation to shunt are equal across participants, we interpret the increased Q_S/Q_T in those with bubble score ≥ 3 as resulting from shunting through the PFO.

Pulmonary gas exchange efficiency is calculated as the difference in PO_2 between the alveoli and arterial blood. We found that in females with significant blood flow through a PFO, PAO_2 was not significantly changed compared to females without significant blood flow through PFO though there was a significant decrease in PaO_2, resulting in decreased pulmonary gas exchange efficiency. Additionally, we found that females with significant blood flow through a PFO had reduced O_2 saturation compared to females without significant flow through a PFO **(Figure 4.1E)**. While it is normal for $AaDO_2$ to increase during exercise, the weight of this

increase in $AaDO_2$ is usually caused by exercise hyperventilation increasing PAO_2 as opposed to decreases in PaO_2, which remains relatively stable under most circumstances. This is consistent with what we found in females without significant blood flow through PFO as well as males with and without significant bloodflow through PFO. While exercise hyperventilation increased PAO_2, PaO_2 did not increase due to increases in venous admixture from V/Q mismatch, diffusion limitation, and shunt. However, in females with significant bloodflow through PFO, the additional source of venous admixture from a PFO widens the $AaDO_2$ to a greater degree. The combination of a slightly (though not statistically significantly) lower PAO_2 (**Figure 4.1B**) due to a relative hypoventilation combined with a larger venous admixture results in a wider $AaDO_2$ and consequently a lower PaO_2 (**Figure 4.1C**). Venous blood mixing with arterial blood through a shunt pathway such as PFO may affect PaO_2, with the impact being larger when the difference between venous and arterial PO_2 is greatest or when relatively large volumes of venous blood mix with arterial blood. During exercise, extraction of O_2 from arterial blood is increased, resulting in lower mixed venous PO_2 and saturation compared to rest (192, 193). As such blood flow through a PFO, particularly during exercise, has the potential to meaningfully decrease PaO_2 and impair pulmonary gas exchange efficiency, particularly when combined with blunted ventilatory responses to exercise. This is consistent with our findings that females with significant blood flow through a PFO have worse pulmonary gas exchange efficiency as well as reduced arterial PO_2 and arterial O_2 saturation, and that these differences are most pronounced at higher exercise intensities when mixed venous PO_2 would be expected to be the lowest.

The reasons why females, but not males, would have significant blood flow through a PFO during exercise despite similar bubble scores upon the release of a Valsalva at rest are unclear. One possible explanation may be related to the anatomy of females' airways and sex

differences in the power of breathing. Females have smaller conducting airways compared to males irrespective of lung size (70, 194, 195), which would result in increased airway resistance per Poiseuille's equation for resistance. This has been confirmed experimentally, with work showing that females have increased resistive power of breathing (194). Given the relationship between flow and resistance, females must therefore create a greater atmospheric-to-alveolar pressure gradient to achieve the same minute ventilation compared to males. Greater swings in intrathoracic pressure to create this greater pressure gradient for breathing could transiently increase venous return through an augmented respiratory pump, resulting in transiently increased right atrial pressure, leading to a greater degree of right-to-left blood flow through intracardiac shunt such as a PFO. This may explain why females, but not males, who had bubble scores ≥ 3 at rest also had greater degrees of venous admixture as well as reductions in arterial PO_2 compared to those with bubble score ≤ 2 at rest. The PFO, while sometimes described as a "hole" in the inter-atrial septum, is in fact a short tunnel (66) and can present some amount of resistance to the flow of blood, largely determined by the radius as described above by Poiseuille's equation. In those females with a bubble score ≤ 2, the diameter of this tunnel may have been sufficiently small and therefor resistance sufficiently high to prevent significant blood flow through the PFO even with elevated ventilation and augmentation of the respiratory cardiac pump. However, no direct measures of PFO diameter were made, so this explanation remains speculative – however, work by Fenster has shown strong agreement between TTSCE bubble scores and PFO size (66). In summary, differences in respiratory system mechanics and power of breathing between males and females may influence the degree of blood flow that travels through a PFO and therefore pulmonary gas exchange efficiency. If true, then this may explain

why previous work by our group and others in this area have found inconsistent results with how and when a PFO impacts pulmonary gas exchange efficiency (44, 45, 163, 196, 197).

This explanation is also consistent with our findings that females with significant blood flow through a PFO have significantly reduced minute ventilation compared to females without significant blood flow through a PFO (**Figure 4.3A**). Females with significant blood flow through a PFO also displayed a lower respiration rate with exercise when compared to females without significant blood flow through PFO (**Figure 4.3C**). Slower, larger breaths allow for smaller and more gradual swings in thoracic pressure, which in turn would limit the swings in venous return and right to left atrial pressure gradients caused by the respiratory pump. As the degree of blood flow through a PFO, and therefore the impact of PFO on arterial PO_2 and saturation, is dependent on the pressure gradient between the right and left atria this breathing strategy could reduce that gradient, thereby reducing flow through the PFO and limiting the impact on arterial PO_2. Future studies utilizing gas formulations which reduce airway resistance (e.g., heliox) and reduce the thoracic pressure changes necessary to create a given airflow may allow for better understanding of the interaction between PFO and the effect of the respiratory pump on right and left heart pressures.

We found that there was a significant interaction effect between degree of blood flow through PFO and exercise intensity of arterial CO_2 in females where at higher exercise intensities females with significant flow through a PFO had greater $PaCO_2$ (**Figure 4.1D**) and reduced V_E (**Figure 4.3A**), suggesting a lower alveolar ventilation during exercise. We also found that females with significant blood flow through a PFO had a reduced ventilatory response for a given $\dot{V}O_2$ and $\dot{V}CO_2$ (**Figure 4.3E & F**). In males, we report a significant interaction between degree of blood flow through PFO and the ventilatory response to CO_2 (**Figure 4.3F**). However,

this difference was only apparent prior to the onset of exercise, and once exercise had commenced, the $\dot{V}_E/\dot{V}CO_2$ curves for males with and without significant blood flow through PFO are effectively identical. In females with significant blood flow through PFO there was a noticeable reduction in both $\dot{V}_E/\dot{V}O_2$ and $\dot{V}_E/\dot{V}CO_2$ with exercise. The reduced ventilation and increase $PaCO_2$ in females with significant blood flow through PFO, combined with reductions in the ventilatory response to CO_2 all suggest that females with significant blood flow through PFO have reduced sensitivity to CO_2. This is consistent with previous findings from our lab in those with PFO who had blunted ventilatory acclimatization to high altitude (163), blunted ventilatory response to acute normoxic hypercapnia while resting (198) and blunted thermal hyperpnea (199). The reasons for the blunted ventilatory responses in these individuals with a PFO are unknown but the degree of blood flow through PFO appears to also be an important factor for exercise.

Our calculations of arterial oxygen content show there was a significant interaction between workload and bubble score in males, with males who had a bubble score ≥ 3 having reduced arterial oxygen content compared to males with bubble score ≤ 2. Arterial oxygen content is primarily the product of oxygen saturation and haemoglobin concentration with a small contribution of O_2 dissolved in the plasma. We found that males with bubble score ≥ 3 had lower haemoglobin concentration compared to males with bubble score ≤ 2 (**Figure 4.4A**). Saturation was comparable in males regardless of bubble score until Max, at which point males with bubble score ≤ 2 displayed a slight decrease in saturation (**Figure 4.1E**). Decreases in O_2 saturation to ~95% at or near maximal workload at sea level are caused by increases in core body temperature and decreases in pH which right shift the oxygen haemoglobin dissociation curve, and there is significant interindividual variation. Since O_2 saturations were comparable at all

sub-maximal workloads, we believe that the elevation in haemoglobin concentration observed in males with bubble score ≤ 2 best explains the calculated differences in O_2 content (**Figures 4.4B, 4.4C**).

LIMITATIONS:

Although we did not directly measure blood flow through the PFO, our approach using bubble score ≥ 3 as a significant source of shunt has been validated with microspheres using an animal model with a surgically created perforation of the atrial septum (200). Calculations of stroke volume and therefore cardiac output were made using ultrasound. At rest, these measures are reliable performed, but may be less accurate in a human at or near maximum exercise due to combined influences of the participant moving rapidly, increased lung volumes obscuring the heart, and a greater demand for haste in capturing the ultrasound images. However, these methods have been recommended by the American Society of Echocardiography (201) and shown to be adequate for these measures at rest and during high intensity exercise (163). Likewise, there were some calculated variables, such as venous admixture which relied on assumptions that are detailed in the methods. Nevertheless, these calculated variables are used only to support the main findings of worse pulmonary gas exchange efficiency and blunted ventilatory responses to exercise which are based on sound measuring principles using gold standard approaches.

Accurate measure of P_aO_2 is a critical component of calculating the alveolar to arterial O_2 difference (A-aDO_2), which is central to our finding of impaired pulmonary gas exchange efficiency in females with significant blood flow through PFO. The most significant source of error in this measurement is the introduction of air bubbles within the syringe during arterial sampling, which have the potential to reduce measured P_aO_2 and thereby widen the A-aDO_2.

This was minimized by ensuring air bubbles which formed during sampling were contained at or near the tip of the syringe and immediately expelled, as well as ensuring positive pressure was maintained on the sample syringe during analysis to prevent the formation of bubbles during analysis. Diffusion of O_2 from the sample through the syringe, O_2 consumption by white blood cells, and O_2 consumption by the PO_2 electrode during analysis represent additional potential sources of error. We minimized the impact of O_2 diffusion and O_2 consumption by immediately analyzing arterial samples. Additionally, by correcting measurements using tonometered human blood, we minimized the impact of these potential sources of error (166, 169).

Our data showed several negative A-aDO_2 values during the Pre-Ex measurement breathing room air(4 females bubble score ≤ 2, 1 man bubble score ≥ 2, 4 males bubble score ≤ 2). Negative A-aDO_2 values are physiologically impossible, and are probably the result of very small (<1%) but cumulative errors in variables used to calculate P_AO_2 (202). These negative values ranged from -0.8 to -4.8 mmHg and are therefore most likely the result of measuring a parameter which is in most cases small using several instruments that each have a small, but non-negligible, margin of error. These values were not altered and were included in the analysis.

Lastly, several males with bubble score ≤ 2 had extremely large 50% hyperoxia Q_S/Q_T values at rest (6.63%, 5.62%, 4.20%, 4.62%). These are the largest degrees of shunt measured in any of our participants, and most likely do not reflect true shunt fraction. These large, calculated shunt fractions are likely indicative of the difficulty of arterial blood gas analysis in individuals breathing hyperoxia and the ease with which PO_2 values can change in these samples. Removal of these values did not alter the statistical findings nor our interpretation of the results of this study, and so are included for transparency.

SUMMARY AND CONCLUSION

We investigated how the degree of blood flow through a PFO impacts pulmonary gas exchange efficiency in males and females at rest and during submaximal exercise. Our results show that in females, but not males, with significant blood flow through a PFO at rest, there was a significant impairment in pulmonary gas exchange efficiency during submaximal exercise caused by decreased PaO_2. Females with significant blood flow through a PFO at rest had lower O_2 saturation, greater calculated venous admixture during exercise, and a greater shunt fraction at rest. We interpret these findings to suggest that significant blood flow through a PFO has the potential to impair pulmonary gas exchange efficiency through increased venous admixture reducing arterial PO_2 and O_2 saturation in females, but not in males. It is unclear why males with significant blood flow through PFO do not also display increased venous admixture during exercise. The reason for this may be related to an augmentation of the respiratory cardiac pump in females due to increased airway resistance and the need to generate greater alveolar-to-atmospheric pressure gradients to achieve similar minute ventilations. This may transiently increase right atrial pressure relative to left atrial pressure, facilitating flow through a PFO.

Females with significant blood flow through PFO upon release of Valsalva had increased $PaCO_2$, reduced minute ventilation, lower respiration rate, and a reduced ventilatory response for O_2 and CO_2 during exercise. We interpret these findings to suggest that females, but not males, with significant blood flow through PFO have altered ventilatory chemosensitivity to CO_2. These findings are consistent with previous findings from our lab in a different group of subjects demonstrating altered ventilatory chemosensitivity to CO_2 in those with PFO, with the caveat that our findings suggest that sex and the degree of blood flow through PFO is an important factor for ventilatory responses during exercise.

CHAPTER V

PERCUTANEOUS CLOSURE OF PATENT FORAMEN OVALE IS EFFECTIVE AT IMPROVING PULMONARY GAS EXCHANGE EFFICIENCY

This chapter is in preparation for submission to the *Journal of Applied Physiology* and Karleigh Bradbury, Kaitlyn DiMarco, Aaron Betts, Joel E. Futral, Jacob Kysar, Jerold A. Hawn, and Andrew T. Lovering are co-authors. I performed the experimental work, led the project, and the writing is entirely my own. Editorial assistance was provided by Andrew T. Lovering.

INTRODUCTION

The closure of the foramen ovale following birth was originally described by the ancient Roman healer Claudius Galen (1). During fetal development the foramen ovale, along with the ductus arteriosus, allows for fetal circulation to bypass the underdeveloped fetal lungs. This is facilitated by the right atrium having a greater pressure than the left atrial, thereby creating flow. Upon the newborn beginning to breath shortly after birth, the relative pressure gradient between the left and right atria reverse, with left atrial pressure generally exceeding right atrial pressure. This reversal of the inter-atrial pressure gradient results in the meeting of the septums primum and secundum, closing the foramen ovale and eventually sealing this passage following endothelialization of the tissue (160). However, for reasons that remain poorly understood, this process fails in 25-40% of the population (63, 64), resulting in a patent foramen ovale (PFO). A PFO allows from right-to-left shunt in circumstances where right atrial pressure exceeds left atrial pressure (66). Right-to-left shunt can reduce arterial oxygen content, potentially limiting exercise capacity.

PFO has also been associated with a variety of pathologies. Most significantly, a PFO has been associated increased risk of transient ischemic attacks (TIAs) and stroke (203–205).

This has lead to percutaneous closure to be a treatment option for individuals who have experienced a cryptogenic stroke. Percutaneous closure of the PFO is accomplished by threading a catheter through the femoral vein into the right atrium. The catheter is then used to deliver and place scaffolding on either side of the atrial septum. Once placed, the scaffolding allows for endothelization to occur and closes the PFO. This procedure has been shown to be more effective for the treatment of cryptogenic stroke in those with PFO than medical therapy (i.e. anti-coagulants) (203, 206, 207). While there is strong evidence showing that PFO closure is effective at reducing the risk of cerebrovascular events, little to no data exists examining the effect of PFO closure on pulmonary gas exchange efficiency or exercise capacity. Thus, the purpose of this study was to examine whether percutaneous PFO closure impacted pulmonary gas exchange efficiency or the ability to exercise. We hypothesized that percutaneous PFO closure would improve pulmonary gas exchange efficiency and increase arterial oxygen content.

METHODS

Ethical Approval

The study received approval from the University of Oregon Research Compliance Services (IRB# 12132016.027) and Peacehealth System IRB (#1985991-2). All participants gave written, informed consent prior to participation. The study was performed in accordance with the 2013 Declaration of Helsinki and is registered at ClinicalTrials.gov (NCT03904290).

Participant Recruitment

Participants were recruited from the population of patients undergoing PFO Closure at PeaceHealth Riverbend Hospital (Springfield, OR) or McKenzie-Willamette Hospital (Springfield, OR). Prior to undergoing PFO closure, participants were provided contact information for the laboratory, and encouraged to contact the study team if they wanted more

information about the study. This resulted in the enrollment of n=6 (5 Female) participants in the study. One participant (1 Male) was enrolled in the study and not cleared for exercise, so only resting measures were taken. However, this participant's data is not included as they were diagnosed with an atrial septal defect in addition to patent foramen ovale.

Study Design

After contacting the lab, participants provided informed consent and were enrolled in the study. The study consisted of two sets of three visits (3 pre-closure, 3 post-closure) for a total of six visits to the laboratory. The first visit consisted of comprehensive echocardiogram and bubble study, as well as pulmonary function testing. The second visit consisted of a hypercapnic ventilatory response test, 6-minute walk test, and cycle ergometer VO_{2Peak} test. The third visit was the arterial line study day as detailed below. This sequence was repeated 3-6 months following the percutaneous PFO closure procedure. Outcome variables were compared pre- and post-closure.

PFO Screening and Comprehensive Echocardiogram

While participants were confirmed to have PFO by hospital staff, PFO screening was repeated in our lab to ensure consistency in bubble score grading. PFO screening in the lab was conducted via transthoracic saline contrast echocardiography as detailed elsewhere (48, 167). Ultrasound imaging, measurement, and interpretation were conducted by Registered Diagnostic Clinical Ultrasonographers. Briefly, a 22-gauge intravenous catheter was placed into the antecubital vein. Participants were then positioned in a reclined IV chair in the left lateral decubitus position and an apical 4-chamber view was acquired. Saline (3mL) was agitated with air (1mL) to create the contrast and then injected through the intravenous catheter. Contrast appearing in the left heart within three cardiac cycles of injection was considered positive for the

presence of PFO. A "bubble score" was assigned based on the amount of agitated saline contrast that appeared in the left-heart (63). This procedure was conducted with and without the participant performing a Valsalva release maneuver. Following PFO screening, a comprehensive echocardiogram was performed whereby the following parameters were measured according to the standards of the American Society of Echocardiography: right ventricular wall (RV Wall) thickness (cm), right ventricle internal diameter in diastole (RVID), right ventricular end diastolic (RVED) area (cm^2) and right ventricular end systolic (RVES) area (cm^2) to calculate right ventricular area fraction (%RVAF), left ventricular end-diastolic volume (LVEDV, mL), left ventricular end-systolic volume (LVESV, mL), left ventricle internal diameter in diastole (LVIDD), left ventricular posterior wall thickness (LVPW), left ventricle internal diameter in systole (LVIDs), left atrial diameter (LA), pulmonary valve velocity (PV peak velocity, m/s), pulmonary insufficiency end-diastolic (PIED) gradient (mm Hg) to calculate pulmonary artery end diastolic pressure (PAEDP; mm Hg), aortic valve peak velocity (AoV peak velocity, m/s) to calculate aortic valve area (AVA; cm^2), interventricular septum (IVS), left ventricular outflow tract (LVOT) diameter, and tricuspid annular plane systolic excursion (TAPSE) (144, 149, 150).

Pulmonary Function Testing, DL_{CO}, and Hypercapnic Ventilatory Response

Pulmonary function was determined using computerized spirometry (Medgraphics Elite Plethysmograph, St. Paul, MN) according to American Thoracic Society/European Respiratory Society (ATS/ERS) standards (151). Lung diffusing capacity for carbon monoxide (DL_{CO}) was measured by the single-breath, breath-hold method according to ATS/ERS standards (177). Lung volumes and capacities were determined using whole body plethysmography (Elite Plethysmograph, Medgraphics, St. Paul, MN) according to ATS/ERS standards (176). Hypercapnic ventilatory response was evaluated via a hypercapnic rebreathe protocol.

Participants were instrumented with a nose clip and breathed through a mouthpiece connected to a pneumotachometer in turn connected to a T-valve, with one end open to room air and the other attached to a 5L rubber bag containing 93% O_2 and 7% CO_2. Gasses were sampled at the pneumotachometer and analyzed with a metabolic cart (Medgraphics Ultima, Medgraphics, St. Paul, MN) for end-tidal P_{CO2}, P_{O2}, and ventilation. Baseline data was collected for 5 minutes after which participants were coached to voluntarily hyperventilate for min to lower end-tidal P_{CO2} (P_{ETCO2}) to a target of 20-25 mmHg before the T-valve was switched to the rubber bag. Immediately following the switch, participants took three deep breaths to equilibrate the gases in the bag. Participants rebreathed from this bag until P_{ETCO2} reached a target of 55-60 mmHg or the participant ended the test due to discomfort. P_{ETCO2} was smoothed via linear regression, and then ventilation was plotted against smoothed P_{ETCO2}. Ventilatory recruitment threshold (VRT) was determined through segmental non-linear regression after the removal of outliers, as before (208) (Prism 9.5.0, Graphpad, San Diego, CA). Predicted values were calculated using the Global Lung Initiative online calculator for spirometry (178) and TL_{CO} (179).

Exercise Testing

Participants completed a VO_2max test on a magnetically braked cycle ergometer (Lode cycle ergometer, Lode, Groningen, the Netherlands) while breathing on a mouthpiece connected to a metabolic analysis system (Ultima CardiO_2, Medgraphics, St. Paul, MN) for breath-by-breath measurement of end-tidal gasses ($P_{ET}O_2$, $P_{ET}CO_2$), tidal volume (V_T), minute ventilation (V_E), and respiratory rate (RR). Participants were also instrumented with a forehead oxygen saturation monitor (Nellcor, Medtronic, Minneapolis, MN) for continuous tracking of heart rate (HR) and peripheral oxygen saturation (S_PO_2). Participants were instructed to maintain a pedaling rate between 60 and 90 revolutions per minute. Resistance was set to 50W at the onset

of exercise and increased by 25W every minute. Exercise testing was terminated when the participant was no longer to pedal above 60 RPM, exceeded their age-predicted 85% heart rate maximum, or upon volitional fatigue.

Arterial Line Instrumentation

Participants arrived at the lab at approximately 7AM on this visit. Upon arrival at the lab, a cardiologist (JAH) placed a 20-gauge radial artery catheter in the non-dominant wrist (Arrow International, Reading, PA) under local anesthesia (2% lidocaine). An oesophageal probe was place via the nostril to a specified depth beyond the nasal flare based on the subjects sitting height (153). Participants were additionally instrumented with an 18-gauge intravenous catheter placed into the antecubital fossa of the dominant arm, a forehead oxygen saturation monitor and a 3-lead EKG connected to the ultrasound machine. Due to technical complications, some participants were instead connected to a 12-lead EKG connected to a Mortara EKG monitor (Mortara, Milwaukee, WI, USA) which was in turn routed to the ultrasound machine.

Arterial Line Study Exercise Protocol

After instrumentation participants mounted the cycle ergometer and began breathing on a mouthpiece connected to a metabolic cart (Medgraphics Ultima, Medgraphics, St. Paul, MN). Metabolic data was monitored for approximately 5 minutes until respiratory exchange ratio and end-tidal carbon dioxide had stabilized, at which point a pre-exercise arterial sample was taken. After this sample, participants began pedaling on the ergometer. Participants were able to see and monitor their pedaling rate and were instructed to maintain a rate of approximately 70 revolutions per minute. Participants completed continuous exercise stages corresponding to 25%, 50%, 75%, and 90% of the highest resistance achieved during the maximal exercise testing performed at the earlier visit. Between each exercise workload, participants dismounted the

ergometer and rested in an IV chair for 5-10 minutes until they felt recovered. Exercise was terminated if participants were unable to maintain a pedaling cadence of at least 60RPM. If participants felt that they were unable to complete a workload, they were instructed to notify researchers with a "1 minute warning" by raising a finger, at which point measures for that workload were immediately begun. Three of four participants indicated a "1 minute warning" in the 90% workload, and one participant indicated a "1 minute warning" at the 75% workload pre-closure. Otherwise, at three and a half minutes into each workload, arterial blood was anaerobically drawn over ~20 seconds while heart rate, temperature, peripheral oxygen saturation (S_PO_2), and pedaling cadence were recorded. Ultrasound images were captured as described below. Participants rested for approximately 30 minutes before being re-positioned on the cycle ergometer for the hyperoxic exercise bouts. During the hyperoxic exercise bouts, participants breathed a humidified oxygen mixture ($P_IO_2 = 0.40$, $P_B \sim 280$mmHg) through a Hans-Rudolph non-rebreathing valve (Hans Rudolph 2100 Series, HR Inc, Topeka, KS) while repeating all exercise workloads. Following completion of hyperoxic exercise, the participant was de-instrumented. The arterial catheter was removed, an ice pack pressed against the catheter site, manual pressure applied for 5 minutes, and the site elevated above the participant's heart. This was followed by 10 minutes of ice and pressure applied by a moderately tightly wrapped elastic wrap (Ace bandage, 3M, Maplewood, MN). After removal of the ice and elastic wrap, a gauze pad was applied and secured with an elastic adhesive bandage (Elastoplast, Beiersdorf, Hamburg, Germany). Participants were contacted 24 hours after leaving the lab to confirm no complications from the arterial catheter placement or removal. One participant experienced extreme discomfort from the radial catheter after completing normoxic exercise at her post-closure visit, and the participant did not complete any post-closure hyperoxic exercise.

Arterial Sample Analysis

Arterial blood samples were approximately 3 mL in volume and were drawn anaerobically over approximately 20 seconds. Samples were immediately analyzed in triplicate by a blood gas analyzer calibrated with temperature-corrected tonometered whole blood (RapidLab 248, Siemens, Erlangen, Germany) for pH, PO_2, and PCO_2. Arterial blood gases collected were tonometry and body temperature corrected (180–182). Arterial samples were also analyzed by co-oximeter (OSM-3, Radiometer, Denmark) for tHb, HbCO, HbO_2Sat, MetHb, and O_2 content. Samples were analyzed for hematocrit using the capillary tube centrifugation method and for lactate (Lactate+ meter and strips, Nova Biomedical, Waltham, MA) in duplicate.

Exercise Ultrasound Imaging, Pulmonary Artery Systolic Pressure, Cardiac Output, TPR, VA Coupling and Stimulus PO_2

While arterial sampling was occurring, simultaneous ultrasound images were captured. These images were used to measure tricuspid regurgitation velocity (TR_{Vel}), left ventricular outflow tract velocity time integral ($LVOT_{VTI}$), and heart rate. A small volume (<1mL) of air agitated with 3mL of saline was injected to enhance visualization of TR_{Vel} as needed. Pulmonary artery systolic pressure (PASP) was calculated from TR_{Vel} using the modified Bernoulli equation ($4v_2^2 + P_{RA}$), where v is TR_{Vel} and P_{RA} is the right atrial pressure as estimated by IVC collapse during a "sniff test" conducted as part of the ultrasound screening. P_{RA} was estimated according to American Society of Echocardiography guidelines (149). $LVOT_{VTI}$ was used to calculate cardiac output (Q_T) according to the equation ($LVOT_{VTI}$ x $LVOT_{CSA}$) where $LVOT_{CSA}$ is calculated from LVOT measurement collected as part of the ultrasound screening. Total pulmonary resistance (TPR) was calculated as $PASP/Q_T$ recorded in mm hg/L/min and

converted to dynes/sec/cm^{-5} prior to analysis. Ventriculoarterial (VA) coupling was calculated as TAPSE/PASP (209). Stimulus PO_2 was calculated as $PO_{2Stim} = PvO_2^{0.325} \times PaO_2^{0.626}$.

Gas Calculations

Alveolar (PA_{O2}) was calculated as before. (166, 169, 184). Briefly, PA_{O2} was calculated using the ideal gas equation and temperature- and tonometry-corrected PA_{CO2} and a respiratory quotient (RER) averaged over the period of arterial sampling. Pulmonary gas exchange efficiency (Arterial-to-alveolar difference in oxygen; $AaDO_2$) was determined at rest and during exercise as the difference between temperature- and tonometry-corrected arterial PO_2 (PaO_2) and corresponding PAO_2. Arterial oxygen content (CaO_2) were calculated from the standard content equation using co-oximetry measured [tHb]. Pulmonary end-capillary oxygen content ($Cc'O_2$) was calculated based on Kelman's equations for converting PO_2 to saturation (157). Mixed venous O_2 content ($C\bar{v}O2$) was calculated using the Fick principle using measured CaO_2, VO_2, and estimate of Q_T as described earlier. Venous admixture (Q_{VA}/Q_T) was calculated from the shunt equation:

$$\frac{Cc'O2 - CaO2}{Cc'O2 - C\bar{v}O2} \text{ (185).}$$

Equation 3.6 Venous Admixture

The level of hyperoxia used ($F_IO_2 = 0.40$) is high enough to remove the influence of ventilation-perfusion mismatch and diffusion limitation on venous admixture, and the pre-exercise hyperoxic calculations are reported as shunt fraction (Q_s/Q_T) (169, 210).

Statistics

All statistical analyses were conducted in Graphpad Prism 9.5.0 unless otherwise specified. Lower limits of normal and predicted values were calculated utilizing the Global Lung Initiative calculator. $AaDO_2$, PAO_2, PaO_2, $PaCO_2$, VO_2, VCO_2, Q_{VA}/Q_T, CaO_2, CvO_2,

$Cc'O_2$, V_E, V_T, Respiration Rate, RER, Qc, PASP, Ve/VO2, Ve/VCO2, and TPR were analyzed by 2-way RMANOVA (Closure x Workload) with Sidak's post-hoc test to compare differences pre- and post-PFO closure and across workloads. For variables that were missing data, a mixed-effects analysis was performed with Sidak's post-hoc test for this data. This mixed-effects model uses a compound symmetry covariance matrix and is fitted using Restricted Maximum Likelihood. TPR was recorded in mm hg/L/min and converted to dynes/sec/cm^{-5+} prior to analysis (183). Q_s/Q_T, VRT, anthropometrics and pulmonary function were compared pre- and post-closure and were tested for normality. If normality was not violated then these were compared with a two-tailed paired t-test. If normality was violated, Mann-Whitney test was used instead. Due to one participant not completing the hyperoxic trials, only n = 3 participants are compared for Q_S/Q_T. Bubble score during Valsalva release was compared using Wilcoxon matched-pairs signed rank test. Cardiac structure was compared pre- to post-closure using a two-tailed paired t-test in Microsoft Excel.

RESULTS

Anthropometrics, Cardiac Structure. and Pulmonary Function, Q_s/Q_T, HCVR, Bubble Score

Participant anthropometrics and pulmonary function are reported in Table 1. Participant ages ranged from 26 to 68 (ages 26, 33, 62, 63, 68). There were no changes in anthropometrics or pulmonary function following PFO Closure (**Table 5.1**). There was no difference in 40% hyperoxia resting Q_S/Q_T following PFO closure (p = .192), nor was there a change in hypercapnic ventilatory recruitment threshold (p = .9766) or slope (p = .344) (**Table 5.1**). Cardiac structure measurements were consistent from pre- to post-closure with the exception of LVEF% (p = .041) and TR peak gradient (p = .029), both of which were slightly lower following PFO closure (**Table 5.2**). While all participants decreased their bubble score during a resting

Valsalva maneuver following PFO closure, this decrease failed to achieve statistical significance (p = .125) (**Table 5.2**).

Table 5.1 Pulmonary Function, Shunt Fraction, and HCVR Pre- and Post-PFO Closure.			
	Pre-Closure	Post-Closure	P
FVC (L):	3.82 ± 0.39	3.64 ± 0.48	.257
FVC % Predicted	112.2 ± 8.7	108.2 ± 15.6	
FEV1(L):	2.82 ± 0.41	2.73 ± 0.46	.581
FEV1 % Predicted	102.3 ± 8.9	100.6 ± 15.8	
FEV1/FVC:	73.80 ± 6.57	74.60 ± 2.41	.778
FEV1/FVC % Predicted	90.7 ± 5.1	92.2 ± 2.1	
FEF25-75(L/s):	2.12 ± 0.84	2.24 ± 0.57	.763
FEF25-75 % Predicted	77.5 ± 20.0	85.2 ± 18.8	
SVC(L):	3.78 ± 0.38	3.79 ± 0.40	.897
SVC % Predicted	104.9 ± 5.7	106.3 ± 10.4	
IC(L):	2.52 ± 0.32	2.87 ± 0.67	.063
IC % Predicted	101.2 ± 13.4	115.2 ± 22.7	
DL_{CO}:	23.01 ± 3.13	22.97 ± 1.94	>.999
DL_{CO} % Predicted	110.0 ± 9.8	110.8 ± 8.9	
V_A % Predicted	104.5 ± 14.0	100.7 ± 9.3	
DL_{CO}/V_A	4.54 ± 0.68	4.78 ± 0.54	.537
DL_{CO}/V_A % Predicted	104.5 ± 14.0	108.4 ± 6.4	
FRC(L):	2.70 ± 0.60	3.08 ± 0.84	.210
FRC % Predicted	97.8 ± 17.3	111.6 ± 21.7	
TLC(L):	5.47 ± 1.11	5.65 ± 1.52	.784
TLC % Predicted	103.4 ± 14.5	108.1 ± 22.5	
RV(L):	1.35 ± 0.22	1.25 ± 0.26	.038
RV % Predicted	105.6 ± 21.5	83.7 ± 12.0	
ERV(L):	1.41 ± 0.55	1.19 ± 0.29	.261
ERV % Predicted	125.3 ± 23.2	117.4 ± 18.5	
RV/TLC	0.29 ± 0.07	0.25 ± 0.04	.083
RV/TLC % Predicted	93.1 ± 22.8	86.7 ± 11.9	
40% Hyperoxia Resting Q_S/Q_T:	4.09 ± 3.29	1.51 ± 0.64	.192
HCVR VRT:	45.12 ± 2.45	45.17 ± 1.32	.977
HCVR Slope:	1.712 ± 0.758	1.522 ± 0.501	.344

Table 5.1 Pulmonary Function, Shunt Fraction, and HCVR Pre- and Post-PFO Closure. PFO Closure led to a slight decrease in residual volume (p = .038). Data presented as mean ± standard deviation. Comparison made using student's paired t-test.

Table 5.2 Exercise, Cardiac Structure and Function			
	Pre-Closure	Post-Closure	P
6MWT (feet):	2104 ± 268	2088 ± 447	.927
Highest Workload VO2peak (Watts)	161.0 ± 21.0	159 ± 19.5	.391
RV wall (mm)	5.8 ± 1.5	4.3 ± 0.7	.223
IVSd (mm)	6.6 ± 3.0	7.5 ± 0.6	.695
LVIDd (mm)	4.2 ± 0.2	4.4 ± 0.5	.456
LVPWd (mm)	8.8 ± 1.5	5.9 ± 1.2	.146
LVIDs (mm)	27.5 ± 3.4	30.0 ± 2.6	.406
LA s (mm)	32.3 ± 5.8	30.4 ± 5.0	.080
LVOT diam (mm)	2.1 ± 0.1	1.97 ± 0.08	.391
PV pk vel (m/s)	0.9 ± 0.1	1.0 ± 0.2	.691
LVOT vel (m/s)	1.0 ± 0.1	0.8 ± 0.1	.139
LVOT VTI	21.7 ± 2.4	17.3 ± 1.6	.124
AoV vel (m/s)	1.3 ± 0.1	1.2 ± 0.1	.308
AoV VTI	25.9 ± 2.5	26.1 ± 4.4	.996
AVA (cm^2)	2.8 ± 0.4	2.1 ± 0.2	.141
MV-E vel (m/s)	0.68 ± 0.13	0.7 ± 0.2	.387
MV-A vel (m/s)	0.5 ± 0.1	0.6 ± 0.2	.684
LAT e' (m/s)	14.0 ± 4.3	6.8 ± 4.0	.137
E/e' ratio	3.8 ± 1.4	7.2 ± 1.7	.056
RVED area (cm^2)	18.7 ± 7.9	16.3 ± 4.4	.402
RVES area (cm^2)	9.4 ± 4.0	10.1 ± 2.2	.734
%RVAF	50.4 ± 3.4	37.0 ± 6.7	.120
LVED vol (mL)	77.3 ± 15.6	84.2 ± 15.5	.911
LVES vol (mL)	27.8 ± 7.0	33.8 ± 5.8	.244
HR at LV vol meas (bpm)	65.0 ± 4.5	67.6 ± 3.1	.104
%LVEF	63.5 ± 7.4	59.2 ± 6.4	.041
SV (mL)	68.5 ± 7.1	54.0 ± 9.4	.143
CO (L/min)	4.61 ± 0.92	3.7 ± 0.7	.450
TR pk grad (mmHg)	24.0 ± 5.6	17.0 ± 2.8	.029
IVC size supine (cm)	1.7 ± 0.2	2.0 ± 0.5	.562
RA press (mmHg)	3	3	>.999
PASP (mmHg)	28.5 ± 10.0	23.6 ± 2.1	.245
TAPSE	2.6 ± 0.3	2.1 ± 0.3	.260
Valsalva Bubble Score	3.5	0.5	.125

Table 5.2 Exercise, Cardiac Structure and Function. Tricuspid regurgitation peak gradient was slightly lower following PFO closure (p = .029), as was %LVEF (p = .041), but no other differences were observed. Data presented as mean ± standard deviation. RA pressure and Bubble Score presented as median value. All data compared using student's paired t-test except RA Pressure and Bubble Score, which were compared with Wilcoxon ranked signed signature

test.

Normoxia Venous Admixture, $AaDO_2$, Blood Gases, pH

There was a significant effect of Closure on venous admixture ($p = .030$) in normoxia (**Figure 5.1A**). There were significant main effects of Closure ($p = .008$) on $AaDO_2$ with pairwise differences at all workloads (Pre-Ex $p = .026$, 25% $p = .024$, 50% $p = .006$), 75% $p < .001$, and 90% $p = .015$) (**Figure 5.1B**) and $AaDO_2$ increased as exercise workload increased, as would be expected. There was no effect on PAO_2 ($p = .621$) (**Figure 5.1C**). There was a main effect of closure on PaO_2 ($p = .004$) (**Figure 5.1D**), with pairwise differences at all workloads (Pre-Ex $p = .001$, 25% $p = .020$, 50% $p = .004$, 75% $p < .001$, and 90% $p = .029$). As expected, there was a significant main effect of Workload on $PaCO_2$ ($p < .001$), with $PaCO_2$ decreasing as workload increased (**Figure 5.1E**). As expected, pH decreased as Workload increased ($p = .003$)(**Figure 5.1F**).

Figure 5.1 (next page). **Venous Admixture and Blood Gases Sampled Under the Normoxic Condition**. A) Venous admixture while breathing normoxia at increasing workloads was not significantly altered following PFO closure ($p = .052$). B) There was a significant interaction (Closure x Workload) on PAO_2 ($p = .011$), with a significant pairwise difference at Pre-Ex ($p = .024$). PAO_2 was higher at Pre-Ex following PFO closure, but was not difference once exercise commenced. C) There was no effect of PFO closure on $PaCO_2$ ($p = .314$). D) There was a significant effect of PFO closure on $A\text{-}aDO_2$ ($p = .020$) with specific pairwise differences at 50% ($p = .005$), 75% ($p < .001$) and 90% ($p = .018$). E) PaO_2 was significantly increased following PFO closure ($p = .003$) with specific pairwise differences at Pre-Ex ($p < .001$), 25% ($p = .011$), 50% ($p = .003$), 75% ($p < .001$), and 90% (p.029). F) There was no effect of PFO closure on arterial pH under normoxic conditions.

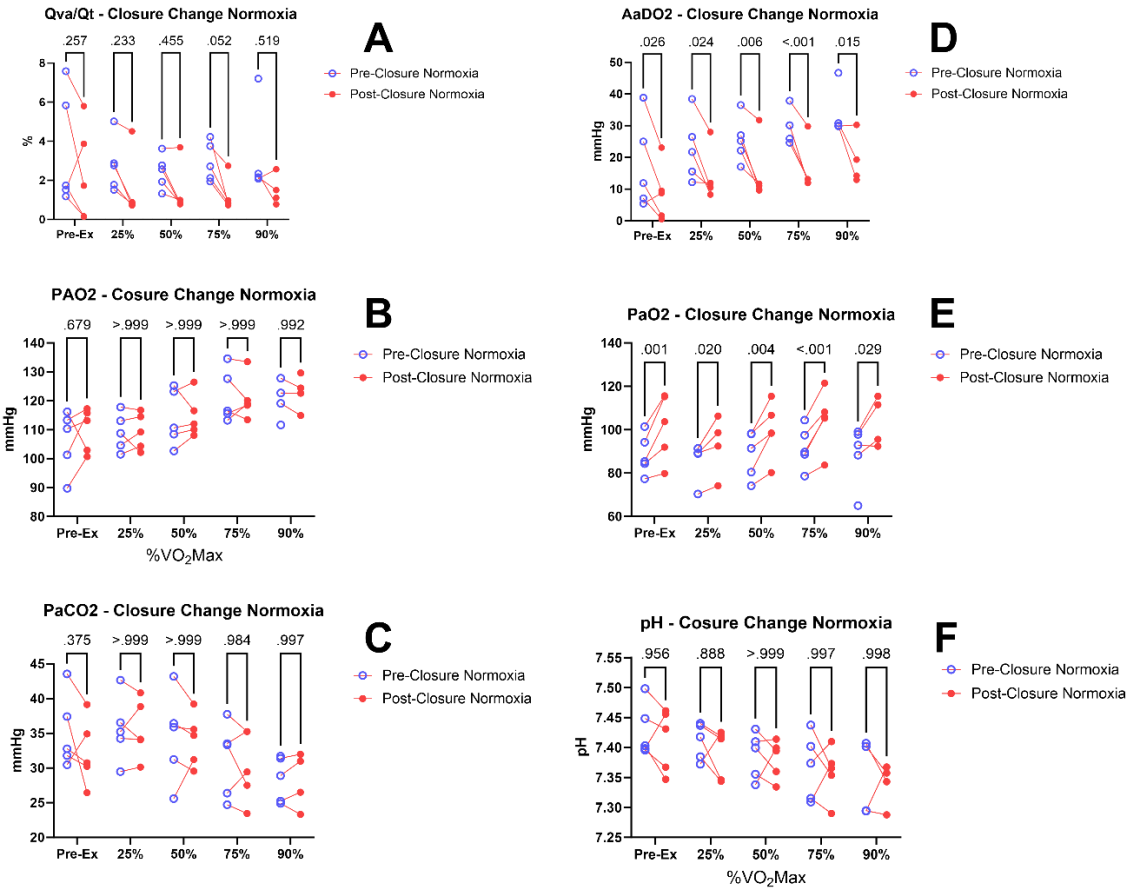

Normoxia Heart Rate, Stroke Volume, Cardiac Output, Pulmonary Pressure, Pulmonary Resistance, VA Coupling

There were no significant changes pre- to post-closure in heart rate (p = .203), stroke volume (p = .797), cardiac output (p = .316), pulmonary pressure (p = .119), or pulmonary resistance (p = .305) (**Table 5.3**). We observed the expected changes in these variables as Workload increased (**Table 5.3**). We observed a significant interaction effect (Closure x Workload) on VA coupling (p = .024) with a pairwise difference at 25% VO_{2Peak} (p = .010) (**Table 5.3**). There were so significant changes in stimulus PO_2 (p = .052) (**Table 5.3**).

Table 5.3 Cardiac Output and Pulmonary Vascular Measurements							
			Pre-Ex	25%	50%	75%	90%
Heart Rate (beats per minute)	Normoxia	Pre-Closure	85 ± 11	116 ± 8	144 ± 15	173 ± 18	167 ± 18
		Post-Closure	80 ± 9	113 ± 12	140 ± 16	159 ± 21	170 ± 16
	Hyperoxia‡	Pre-Closure	97 ± 7	123 ± 12	142 ± 16	160 ± 18	167 ± 18
		Post-Closure	83 ± 12	119 ± 13	142 ± 17	157 ± 26	173 ± 31
Stroke Volume (mL)	Normoxia	Pre-Closure	55.9 ± 6.6	74.9 ± 13.1	73.0 ± 12.8	77.4 ± 11.0	77.9 ± 9.1
		Post-Closure	57.9 ± 9.3	66.5 ± 22.8	74.0 ± 11.3	73.5 ± 7.1	76.3 ± 11.6
	Hyperoxia	Pre-Closure	62.2 ± 6.2	69.3 ± 11.4	77.8 ± 11.4	75.3 ± 6.5	71.8 ± 1.7
		Post-Closure	53.0 ± 7.7	69.7 ± 16.8	80.6 ± 8.6	77.2 ± 14.7	78.0 ± 15.5
Cardiac Output (L/min)	Normoxia	Pre-Closure	4.78 ± 0.94	8.63 ± 0.89	10.58 ± 2.31	13.29 ± 1.84	13.00 ± 1.84
		Post-Closure	4.61 ± 0.89	7.33 ± 1.84	10.23 ± 0.94	11.58 ± 0.52	12.94 ± 2.38
	Hyperoxia	Pre-Closure	6.08 ± 0.69	8.63 ± 1.77	11.09 ±2.27	12.15 ± 0.61	13.22 ±2.23
		Post-Closure	4.40 ± 0.88	8.16 ± 1.62	11.58 ± 2.03	12.01 ± 2.21	13.24 ± 0.26
PASP (mm Hg)	Normoxia	Pre-Closure	25.4 ± 4.0	36.8 ±6.6	43.8 ± 6.2	47.4 ± 9.9	47.5 ±6.5
		Post-Closure	23.5 ± 9.1	26.7 ± 9.7	33.3 ± 12.8	36.1 ± 12.7	38.1 ± 15.0
	Hyperoxia	Pre-Closure	26.5 ± 7.5	37.3 ± 5.4	45.1 ± 11.9	50.7 ± 3.9	50.9 ± 4.8
		Post-Closure	22.5 ± 3.5	31.4 ± 5.8	39.4 ± 5.1	43.6 ± 8.8	46.2 ± 3.8
TPR (dynes/sec/ cm^{-5})	Normoxia	Pre-Closure	435. 3 ± 88.6	348.3 ± 92.2	352.0 ± 124.0	296.3 ± 100.7	300.9 ± 82.7
		Post-Closure	421.6 ±167.3	307.6 ± 144.5	255.3 ± 85.6	251.2 ± 93.0	232.7 ± 79.3
	Hyperoxia	Pre-Closure	349.0 ± 86.9	366.6 ± 136.6	345.2 ± 143.5	334.9 ± 33.3	317.3 ± 85.6
		Post-Closure	432.6 ± 165.4	309.0 ± 23.9	281.2 ± 69.6	293.5 ± 47.7	278.7 ± 17.7

VA coupling	Normoxia‡	Pre-Closure	0.806 ± 0.109	0.534 ± 0.131	0.569 ± 0.047	0.582 ± 0.091	0.619 ± 0.065
		Post-Closure	0.682 ± 0.103	0.929 ± 0.178	0.765 ± 0.171	0.679 ± 0.107	0.666 ± 0.106
	Hyperoxia†	Pre-Closure	0.803 ± 0.154	0.712 ± 0.091	0.638 ± 0.111	0.578 ± 0.093	0.537 ± 0.039
		Post-Closure	0.849 ± 0.206	0.877 ± 0.256	0.717 ± 0.105	0.731 ± 0.217	0.650 ± 0.007
Stimulus PO_2	Normoxia	Pre-Closure	121.5 ± 16.4	79.8 ± 20.1	84.5 ± 15.8	77.9 ± 9.7	72.0 ± 0.0
		Post-Closure	91.8 ± 4.4	72.7 ± 8.6	77.3 ± 4.7	75.8 ± 6.8	67.5 ± 0.0
	Hyperoxia	Pre-Closure	67.4 ± 4.9	58.8 ± 7.7	51.2 ± 12.0	64.1 ± 13.3	53.0 ± 10.4
		Post-Closure	60.2 ± 2.6	51.1 ± 3.5	49.4 ± 4.8	50.8 ± 7.7	48.3 ± 4.2

Table 5.3. Cardiac Output and Pulmonary Vascular Measurements Under the normoxic condition, there were no differences in outcome variables related to cardiac output or pulmonary resistance. Under the hyperoxic condition, we observed a significant interaction effect of PFO Closure x Workload on Heart Rate ($p = .008$), though there were no pairwise differences. We observed expected increases in Heart Rate, Stroke Volume, Cardiac Output, PASP, as well as the expected decrease in total pulmonary resistance as Workload increased. ‡ = significant interaction effect of PFO Closure x Workload. † = significant main effect of PFO Closure. Data presented as mean ± standard deviation.

Normoxia Vt, Respiration Rate, V_E

There was a significant main effect of Closure on tidal volume ($p = .025$), with a specific pairwise difference at 90% workload ($p = .021$) (**Table 5.4**). As expected, there were significant main effect of Workload on respiration rate ($p < .001$) and ventilation ($p < .001$), with both increasing as Workload increased (**Table 5.4)**.

Table 5.4. Ventilatory Parameters							
			Pre-Ex	25%	50%	75%	90%
Tidal Volume (L)	Normoxia †	Pre-Closure	0.86 ± 0.23	1.36 ± 0.32	1.74 ± 0.50	2.13 ± 0.63	2.21 ± 0.59
		Post-Closure	0.73 ± 0.12	1.37 ± 0.38	1.57 ± 0.31	1.84 ± 0.56	1.71 ± 0.54
	Hyperoxia	Pre-Closure	0.83 ± 0.28	1.34 ± 0.28	1.68 ± 0.58	2.02 ± 0.69	1.93 ± 0.60
		Post-Closure	0.80 ± 0.17	1.44 ± 0.27	1.85 ± 0.43	2.06 ± 0.70	2.38 ± 0.61

Table 5.4. Ventilatory Parameters Continued							
			Pre-Ex	25%	50%	75%	90%
Respiration Rate (Breaths/min)	Normoxia	Pre-Closure	12.4 ± 4.0	21.3 ± 4.9	27.8 ± 9.4	38.9 ± 21.1	35.6 ± 9.1
		Post-Closure	12.2 ± 3.5	20.8 ± 5.3	28.6 ± 8.5	38.7 ± 15.4	51.5 ± 9.6
	Hyperoxia	Pre-Closure	11.7 ± 2.7	22.5 ± 5.3	26.4 ± 8.3	35.7 ± 14.0	45.3 ± 10.8
		Post-Closure	13.6 ± 4.1	21.0 ± 4.2	24.2 ± 7.0	38.9 ± 22.4	31.8 ± 13.2
Ventilation (L/min)	Normoxia	Pre-Closure	10.04 ± 2.77	27.85 ± 5.75	44.39 ± 4.99	71.22 ± 9.10	78.42 ± 25.29
		Post-Closure	8.54 ± 3.21	27.03 ± 5.84	42.90 ± 6.24	65.71 ± 12.21	87.23 ± 17.72
	Hyperoxia	Pre-Closure	9.28 ± 4.24	28.78 ± 4.23	40.79 ± 6.25	65.24 ± 10.56	81.82 ± 7.87
		Post-Closure	10.29 ± 2.16	29.88 ± 6.58	42.50 ± 4.27	69.00 ± 15.30	71.14 ± 12.56
VO_2 (L/min)	Normoxia †	Pre-Closure	0.32 ± 0.06	1.02 ± 0.20	1.44 ± 0.18	1.75 ± 0.33	1.95 ± 0.31
		Post-Closure	0.25 ± 0.08	0.97 ± 0.18	1.29 ± 0.19	1.55 ± 0.31	1.68 ± 0.40
	Hyperoxia	Pre-Closure	0.36 ± 0.23	1.15 ± 0.09	1.52 ± 0.08	1.95 ± 0.27	2.06 ± 0.31
		Post-Closure	0.35 ± 0.07	1.23 ± 0.17	1.53 ± 0.09	1.83 ± 0.24	2.39 ± 0.16
VCO_2 (L/min)	Normoxia	Pre-Closure	0.27 ± 0.05	0.93 ± 0.23	1.49 ± 0.14	2.10 ±0.25	2.14 ± 0.58
		Post-Closure	0.22 ± 0.07	0.91 ±0.11	1.37 ± 0.17	1.87 ± 0.33	2.01 ± 0.61
	Hyperoxia	Pre-Closure	0.25 ± 0.13	0.95 ± 0.06	1.44 ± 0.10	2.11 ± 0.23	2.21 ± 0.49
		Post-Closure	0.26 ± 0.05	1.02 ±0.16	1.52 ± 0.07	2.15 ± 0.19	2.24 ± 0.09
V_E/VO_2	Normoxia	Pre-Closure	31.95 ± 7.25	27.54 ± 2.87	31.37 ± 6.57	43.26 ± 16.39	39.52 ± 8.82
		Post-Closure	33.64 ± 4.54	28.53 ± 6.50	33.97 ± 7.11	44.39 ± 15.64	52.25 ± 3.26
	Hyperoxia	Pre-Closure	27.38 ± 4.03	25.30 ± 3.62	26.96 ± 4.43	34.56 ± 10.45	40.51 ± 2.32
		Post-Closure	31.10 ± 4.69	24.34 ± 4.17	27.90 ± 4.08	39.04 ± 14.37	29.72 ± 3.24

V_E/VCO_2	Normoxia †	Pre-Closure	36.59 ± 4.98	30.32 ± 4.23	30.09 ± 4.53	34.62 ± 7.76	36.25 ± 5.86
		Post-Closure	38.95 ± 4.31	29.89 ± 5.09	31.56 ± 5.07	36.07 ± 9.38	43.36 ± 7.25
	Hyperoxia	Pre-Closure	38.44 ± 3.80	30.33 ± 4.03	28.34 ± 4.48	31.17 ± 5.70	37.78 ± 4.87
		Post-Closure	39.81 ± 6.05	29.23 ± 2.67	28.07 ± 3.77	32.27 ± 7.45	31.74 ± 4.31

Table 5.4. Ventilatory Parameters. With normoxia, there was a decrease in tidal volume post-closure compared to pre-closure ($p = .025$), with a pairwise difference at the 90% workload ($p = .021$). There was also a significant decrease in VO_2 following PFO Closure in the normoxic condition ($p = .0$) with pairwise differences at 50% ($p= .025$), 75% ($p = .004$) and 90% ($p = .012$) Workloads. Additionally, we observed the expected changes associated with exercising at increasing workloads. † = Significant effect of PFO closure. * = significant pairwise difference pre- to post-closure.

Normoxia VO_2, VCO_2, V_E/VO_2, V_E/VCO_2

There was a significant effect of Closure on VO_2 ($p = .008$), with pairwise differences at 50% ($p = .025$), 75% ($p = .004$) and 90% ($p = .012$). There was no significant effect of Closure on VCO_2 ($p = .076$), or V_E/VO_2 ($p = .249$). There was a significant effect of closure on V_E/VCO_2 ($p = .038$), with a pairwise difference at 90% ($p = .021$) (**Table 5.4**). We observed the expected effect of Workload on VO_2 ($p < .001$), VCO_2 ($p < .001$), V_E/VO_2 ($p = .006$), and V_E/VCO_2 ($p = .014$) (**Table 5.4**).

Normoxia HbO_2Sat, [Hb], Oxygen Content

There was no effect of closure on HbO_2Sat ($p = .073$) (**Table 5.5**). We observed the expected effects of Workload on [Hb] ($p = .001$), $Cc'O_2$ ($p < .001$), CaO_2 ($p = .002$), and CvO_2 ($p < .001$) (**Table 5.5**).

Table 5.5 (next page). Oxygen Content. We observed no effect of PFO Closure on outcome variables related to oxygen content in the normoxic condition. In the hyperoxic condition, there was a significant interaction on hemoglobin concentration ($p = .012$), and $Cc'O_2$ ($p = .011$), and CaO_2 ($p = .00$) with slight increases following closure, though there were no pairwise differences. As expected, there was a significant effect of Workload on CvO_2 ($p <.001$), with

CvO_2 decreasing as workload increased. ‡ = significant interaction effect of PFO Closure x Workload

Table 5.5. Oxygen Content

			Pre-Ex	25%	50%	75%	90%
[Hb] (g/dL)	Normoxia	Pre-Closure	12.3 ±1.5	12.7 ± 1.7	12.8 ± 1.7	13.4 ± 1.5	13.3 ± 1.2
		Post-Closure	11.7 ± 1.2	12.3 ± 1.4	12.6 ± 1.1	12.4 ± 1.4	12.7 ± 0.9
	Hyperoxia‡	Pre-Closure	12.5 ± 1.6	12.7 ±1.8	13.01 ± 1.5	13.6 ± 1.8	12.6 ± 0.8
		Post-Closure	11.8 ± 1.1	12.5 ± 0.9	12.8 ± 1.0	12.8 ± 0.9	12.9 ± 0.8
$Cc'O_2$ (mL/dL)	Normoxia	Pre-Closure	17.02 ± 2.12	17.55 ± 2.28	17.82 ± 2.28	18.74 ± 2.00	18.97 ± 1.49
		Post-Closure	16.29 ± 1.52	17.05 ±1.92	17.51 ± 1.51	17.28 ± 1.87	17.79 ± 1.23
	Hyperoxia‡	Pre-Closure	17.74 ± 2.08	18.15 ± 2.18	18.53 ± 1.89	19.08 ± 1.89	18.02 ± 0.96
		Post-Closure	17.02 ± 1.58	17.97 ± 1.25	18.48 ± 1.43	18.39 ± 1.32	18.53 ± 1.17
CaO_2 (mL/dL)	Normoxia	Pre-Closure	16.76 ± 1.94	17.18 ± 2.04	17.45 ± 2.09	18.36 ± 1.85	18.06 ± 1.23
		Post-Closure	16.16 ± 1.37	16.84 ± 1.80	17.32 ± 1.39	17.10 ± 1.76	17.80 ± 0.91
	Hyperoxia‡	Pre-Closure	17.51 ± 1.95	17.89 ± 2.07	18.27 ± 1.80	18.83 ± 1.83	17. ± 1.00
		Post-Closure	16.91 ± 1.56	17.88 ± 1.24	18.41 ± 1.44	18.33 ± 1.33	18.40 ± 1.15
CvO_2 (mL/dL)	Normoxia	Pre-Closure	10.06 ± 0.94	5.16 ±1.33	3.10 ±2.45	5.28 ± 3.54	3.23 ± 2.21
		Post-Closure	10.59 ±2.43	4.18 ± 4.10	4.79 ±1.50	3.68 ± 3.29	4.64 ± 2.25
	Hyperoxia	Pre-Closure	11.77 ± 2.43	4.18 ± 4.10	4.79 ± 1.50	3.68 ± 3.30	4.63 ± 2.25
		Post-Closure	8.97± 2.15	2.50 ± 2.50	4.78 ± 1.46	2.64 ± 3.16	0.42 ± 2.04
HbO_2Sat (%)	Normoxia	Pre-Closure	96.6 ± 0.5	96.3 ±0.9	96.1± 1.0	96.1 ± 0.8	95.6 ± 1.4
		Post-Closure	97.4 ± 0.5	97.0 ± 0.4	97.1 ± 0.2	97.2 ± 0.4	96.8 ± 0.5
	Hyperoxia	Pre-Closure	98.4 ± 1.01	98.2 ± 0.5	98.0 ± 0.5	98.0 ± 0.5	97.7 ± 0.2
		Post-Closure	98.3 ± 0.7	98.2 ± 0.6	98.1 ± 0.7	98.2 ± 0.7	97.8 ± 0.1

Hyperoxic Venous Admixture, $AaDO_2$, Blood Gases, pH

There was a significant effect of Closure on venous admixture while breathing 40% oxygen ($p = .030$), with a pairwise difference at Pre-Ex ($p = .007$). (**Figure 5.2A**). There was a significant interaction on $AaDO_2$ ($p = .025$) where $AaDO_2$ decreased after closure, with pairwise differences at 25% ($p = .038$), 50% ($p = .014$), 75% ($p = .015$), and 90% ($p = .034$) (**Figure 5.2B**). There was no effect of Closure on PAO_2 ($p = .385$) (**Figure 5.2C**). There was a significant interaction on PaO_2 ($p = .016$) with pairwise differences at 25% ($p = .003$), 50% ($p <.001$), and 75% ($p <.001$) and 90% ($p = .013$) (**Figure 5.2D**). There was no effect of Closure on $PaCO_2$ ($p = .628$). (**Figure 5.2E**). As expected, pH decreased as Workload increased ($p = .040$) (**Figure 5.2F).**

Figure 5.2 Venous Admixture and Blood Gases Sampled While Participants Breathed Hyperoxia ($F_IO_2 = 0.40$). One participant did not complete post-closure hyperoxic measures, and their data is not included in the analysis. However, their pre-closure data is displayed on plots for transparency. A) There was a significant effect of PFO closure on venous admixture ($p = .043$) with a pairwise difference at Pre-Ex ($p = .036$). B) There was no effect of PFO closure on PAO_2 ($p = .787$). C) There was no effect of PFO closure on $PaCO_2$ ($p = .628$). D) There was a significant interaction effect (PFO Closure x Workload) on $A\text{-}aDO_2$ ($p = .046$). There was no difference at Pre-Ex, but there were significant differences at 25% ($p = .013$), 50% ($p = .003$), 75% ($p = .002$) and 90% ($p = .016$). E) There was a significant effect of PFO closure on PaO_2 ($p = .009$) with pairwise differences at 25% ($p = .017$), 50% ($p = .005$) and 75% ($p = .004$). F) There was no effect of PFO closure on arterial pH ($p = .964$)

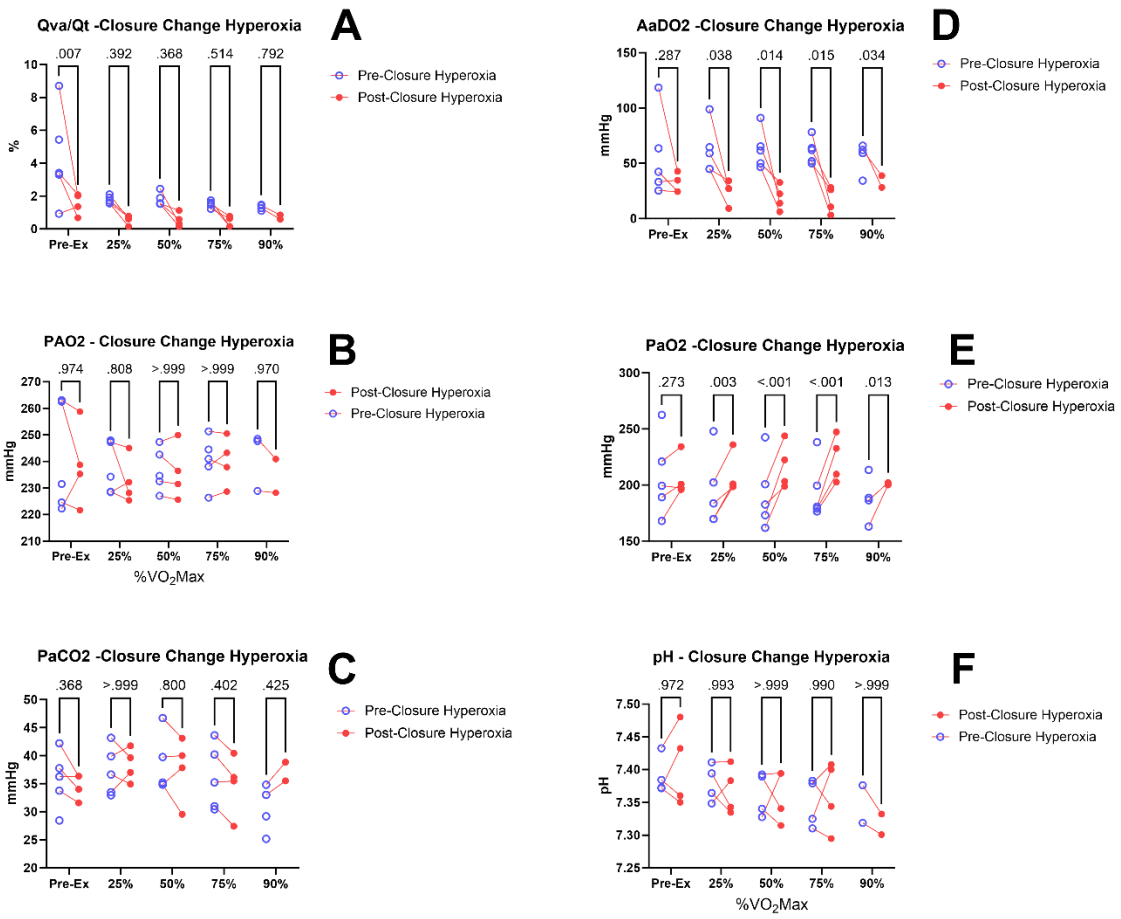

Hyperoxia Heart Rate, Stroke Volume, Cardiac Output, Pulmonary Pressure, Pulmonary Resistance, VA Coupling, Stimulus PO_2

There was a significant interaction effect on heart rate (p = .012), with a pairwise difference at Pre-Ex (p = .002) (**Table 5.3**). We observed the expected increases with Workload in stroke volume (p = .006), cardiac output (p < .001), and PASP (p < .001) (**Table 5.3**). There were no significant findings for TPR (**Table 5.3**). There was a significant effect of PFO Closure on VA coupling (p = .049), but there were no significant pairwise differences (**Table 5.3**). There were no significant findings for stimulus PO_2 (p = .099) (**Table 5.3)**.

Hyperoxia Vt, Respiration Rate, V_E

As expected, as Workload increased we observed increases in tidal volume ($p < .001$), respiration rate ($p < .001$), and ventilation ($p < .001$) (**Table 5.4**).

Hyperoxia VO_2, VCO_2, V_E/VO_2, V_E/VCO_2

As Workload increased, we observed the expected increases in VO_2 ($p < .001$), VCO_2 ($p < .001$), as well as the expected changes in V_E/VO_2 ($p = .033$) and V_E/VCO_2 ($p = .002$) (**Table 5.4**).

Hyperoxia HbO_2Sat, [Hb], Oxygen Content

There was no effect of closure on HbO_2Sat ($p = .791$) (**Table 5.5**). There was not a significant interaction on hemoglobin concentration ($p = .051$). There was a significant interaction on $Cc'O_2$ ($p = .016$) though there were no pairwise differences. There as a significant interaction on CaO_2 ($p = .016$), though there were no pairwise differences (**Table 5.5**). As expected, there was a significant effect of Workload on CvO_2 ($p <.001$), with CvO_2 decreasing as workload increased (**Table 5.5**).

DISCUSSION

The purpose of this study was to evaluate changes in pulmonary gas exchange efficiency following percutaneous closure of PFO. We hypothesized that PFO Closure would reduce shunt fraction, increase arterial PO_2, improve pulmonary gas exchange efficiency, and reduce venous admixture. Our major findings are that 1) Pulmonary gas exchange efficiency and arterial PO_2 improved following percutaneous PFO closure and that these differences were greatest at moderate to high exercise workloads; 2) Venous admixture decreased with exercise following percutaneous PFO closure; 3) There was a trend towards increased oxygen saturation during exercise following percutaneous PFO closure; 4) Oxygen consumption decreased at moderate to high workloads following percutaneous PFO closure; and 5) Tidal volume decreased following

percutaneous PFO closure. This aggregation of findings confirms our hypothesis and shows that PFO closure is effective at improving pulmonary gas exchange efficiency by decreasing intracardiac shunt, thereby leading to an increase in arterial oxygen saturation and arterial PO_2 and decreasing venous admixture.

Following percutaneous closure of PFO, we observed a roughly 50% reduction (corresponding to an approximately 10-15 mmHg decrease) in the A-aDO_2 value under both normoxic and hyperoxic conditions, indicating a meaningful improvement in pulmonary gas exchange efficiency. We saw no change in PAO_2 under either normoxic or hyperoxic conditions following PFO closure but did see a significant increase in PaO_2 following PFO closure with both normoxia and hyperoxia. The normoxic increase in PaO_2 following closure is approximately 10-15 mmHg (**Figure 5.1D)** at all workloads, which is equivalent to the 10-15 mmHg decrease in A-aDO_2 (**Figure 5.1C**) observed following PFO closure. This trend also holds true under the hyperoxic condition, where we observed a roughly 30-40mmHg increase in PaO_2 following PFO closure (**Figure 5.2D**) and a similar magnitude decrease in A-aDO_2 (**Figure 5.2C**). We observed no change in DL_{CO} following PFO closure (**Table 5.1)**, so it is unlikely that this increase in PaO_2 and improvement in pulmonary gas exchange efficiency is due to improvement in diffusing capacity in the lung. Similarly, we administered a level of hyperoxia sufficient to remove the influence of ventilation-perfusion mismatch on pulmonary gas exchange efficiency and still observed improvements in both PaO_2 and A-aDO_2, ruling out the possibility the improved ventilation-perfusion matching following PFO closure was responsible for these observations. Thus, we conclude that the only remaining explanatory variable for these improvements is the reduction in right-to-left shunt following PFO closure.

Right-to-left shunt can reduce arterial PO_2 and saturation through the introduction of poorly oxygenated mixed venous blood into the arterial circulation. At rest, mixed venous blood returning from the systemic circulation to the right atrium has a PO_2 of approximately 40mmhg and a saturation of approximately 75%, (211). As exercise intensity increases, PvO_2 and saturation continue to drop (212). When an intracardiac right-to-left shunt, such as PFO, is present the opportunity for low PO_2 mixed venous blood to pass into the systemic circulation is created. Venous admixture is the calculated portion of cardiac output which must undergo shunt to account for the observed A-aDO_2 (189), and includes contributions from ventilation-perfusion mismatch, diffusion limitation, and shunt. As noted above, sufficient levels of hyperoxia remove the contribution of diffusion limitation and ventilation-perfusion mismatch, leaving only the influence of shunt. While breathing a hyperoxic mixture, approximately 0.5% of venous admixture can be attributed to shunt from bronchial and Thebesian circulations (190, 191), with the remainder coming from intrapulmonary and intracardiac shunt. While we did not evaluate intrapulmonary shunt in this study, it is unlikely that reductions in intrapulmonary shunt were responsible for the observed improvements in PaO_2 and A-aDO_2.

In addition to improvements in pulmonary gas exchange efficiency, we also report an increase in tidal volume following percutaneous PFO closure (**Table 5.4**), and that there was a pairwise difference at the 90% workload. This difference was only present under the normoxia condition and corresponds to a decrease in VO_2 at the same workload (**Table 5.4**). As these differences are only apparent at the highest workloads and only under normoxic conditions, we believe that the most reasonable explanation for these findings is fatigue of participants. While we attempted to limit the influence of fatigue by permitting participants a period of recovery between exercise workloads, the 90% workload represents a very strenuous exercise challenge.

Anecdotally, participants were frequently visibly fatigued and struggling to maintain the pedal cadence towards the end of this workload. As there is a direct linear relationship between power output and oxygen consumption, a parsimonious explanation of these findings is that participants were fatigued, reduced their pedaling rate and power output on the cycle ergometer and displayed a concomitant reduction in oxygen consumption and potentially fatigue of respiratory muscles limiting tidal volume.

Lastly, we report improvements in VA coupling following PFO closure, though this improvement was most pronounced at a relatively low workload (25% workload). Additionally, there was a trend towards improved VA coupling at 50%, 75%, and 90% workloads, though these failed to achieve statistical significance likely due to the small number of participants in the study. The slight increase in VA coupling we report reflects a slightly reduced right ventricular afterload following PFO closure. It should also be noted that the reported improvement in VA coupling occurred in participants who had no evidence of VA decoupling prior to PFO closure. Previous research has associated with PFO with increased degrees of dilation and dysfunction in the right ventricle (213, 216), though authors have speculated that this is due to deformation of the right ventricle "stretching" an otherwise undetectable PFO. We made no direct measures of mixed venous PO_2 and so cannot rule out the possibility that PFO closure led to increases in mixed venous PO_2 in turn leading to reduced pulmonary resistance. However, we report no differences in our calculated venous oxygen content and so it is unlikely that mixed venous PO_2 was altered following PFO closure. Stimulus PO_2 was also not statistically significant different pre- to post-closure, though there was a trend towards increased stimulus PO_2 following closure. This may suggest a statistically insignificant but physiologically meaningful reduction in pulmonary vasoconstriction following PFO closure. However, it remains unclear why VA

coupling improved following PFO closure. Future work which examines changes in mixed venous PO_2 at low to moderate exercise following PFO closure may be helpful in understanding this finding.

LIMITATIONS

The most notable limitation of this study is that we report findings only in women, and it remains unknown whether these findings are generalizable to women. It is known that shunting through PFO is controlled by the pressure gradient between the right and left atria, as well as the size of the PFO. Additionally, changes in intrathoracic pressure can impact venous return and therefore right atrial pressure. As women have smaller airways (and therefor greater resistance to flow), women must create greater intrathoracic pressure changes to achieve the same flow. This may cause greater swings in venous return and right atrial pressure, which could increase flow through the PFO. As such, it is unclear whether men would display similar improvements in PaO_2 of A-aDO_2, as they may have reduced flow through the PFO to begin with.

Not all participants completed the post-closure hyperoxia exercise. One participant experienced significant unexplained pain at the site of the radial arterial catheter after completion of the normoxic exercise bouts but prior to gathering any hyperoxia data. Given the small sample size, this represents a significant loss of data and complicates the interpretability of our results.

We did not force participants to maintain a similar lifestyle before and subsequent to PFO closure. Anecdotally, several participants underwent lifestyle changes following their medical procedure which included increases in physical activity and weight loss. These lifestyle changes may have altered their responses to exercise. However, we observed no significant change in either the highest wattage workload achieved during VO_2peak testing nor 6-minute walk test

(**Table 5.2**). As such, we find it unlikely that lifestyle changes following PFO closure meaningfully affected our findings.

SUMMARY AND CONCLUSION

We investigated how pulmonary gas exchange efficiency was altered 3-6 months following percutaneous closure of a PFO in women. Our results show that, following PFO closure, there was a significant improvement in pulmonary gas exchange efficiency and that this improvement was due to increases in PaO_2. Additionally, we found that while breathing 40% hyperoxia, there was a significant decrease in venous admixture following percutaneous closure of PFO. We interpret these findings to show that reduction of intracardiac shunt through percutaneous closure of PFO is effective at increasing arterial PO_2, improving pulmonary gas exchange efficiency, and reducing venous admixture. However, our conclusions are limited to percutaneous closure in women and future work should examine whether percutaneous PFO closure has similar effects in men.

Chapter VI

HIGH PREVALENCE OF PATENT FORAMEN OVALE IN RECREATIONAL TO ELITE BREATH HOLD DIVERS

This chapter is published in the *Journal of Science and Medicine in Sport* and was co-authored with Alexander Patrician, Mohini Bryant-Ekstrand, Courtney Brown, Christopher Gasho, Hannah G. Caldwell, Rachel N. Lord, Tony Dawkins, Aimee Drane, Michael Stembridge, Tanja Dragon, Otto Barak, Boris Spacjíc, Ivan Drviš, Joseph W. Duke, Glen E. Foster, Philip N. Ainslie, Željko Dujić, and Andrew T. Lovering. All authors aided in data collection. I was solely responsible for data analysis and the writing is entirely mine. Josheph W. Duke, Željko Dujić, and Andrew T. Lovering provided editorial assistance. The manuscript has been edited to comply with the University of Oregon Graduate School Dissertation Formatting requirements.

INTRODUCTION

The foramen ovale is a normal feature of the fetal heart, allowing blood to bypass the lungs during development. Upon delivery and the newborn's first breaths, the drop in right atrial pressure and rise in left atrial pressure closes the foramen ovale, which then seals over the subsequent months via an endothelial-to-mesenchymal transition leading to fibrosis.(160) However, for unknown reasons, the foramen ovale remains patent in 25-35% of adults – resulting in a patent foramen ovale (PFO).(64, 214)

The PFO allows for blood to move left-to-right or right-to-left between the atria following whatever pressure gradient is present in that moment the pathway is open. At times, the PFO acts as a source of right-to-left shunt(44), such as during end inspiration during diastole or following the release of a Valsalva maneuver,(66) when right atrial pressure exceeds left atrial

pressure. The PFO may also act as a pressure relief pathway during condition of high pulmonary arterial and/or right heart pressures whereby pressures may still be higher than normal, yet lower than they would be in the absence of a PFO.(213) Interestingly, there are known pathophysiological associations of PFO with conditions of high pulmonary arterial pressure such as high altitude pulmonary edema (HAPE)(214, 215) and exaggerated pulmonary pressures with exercise in those with chronic mountain sickness.(216) The presence of a PFO is also associated with impaired ventilatory acclimatization to altitude(214), impaired hypercapnic ventilatory responses(214), impaired pulmonary gas exchange efficiency at rest(44, 214), and a higher core body temperature at rest and during exercise.(214, 217) Thus, the presence of PFO is associated with numerous physiological and pathophysiological consequences.

PFO has been shown to be highly common in recreational SCUBA divers experiencing decompression syndrome (DCS).(218) SCUBA diving can result in the formation of venous gas emboli, even when SCUBA divers adhere to recreational dive ascension rates and perform appropriate decompression stops on the ascent or perform no-decompression dives.(219) Due to the presence of a PFO, these venous gas emboli have the potential to bypass the pulmonary circuit and enter systemic and cerebral circulation resulting in neurological decompression symptoms.(219) Percutaneous closure of PFO has been shown to reduce the occurrence of SCUBA divers experiencing DCS, further supporting the link between the presence of PFO and DCS.(220) The prevalence of PFO has not been previously investigated in apnea divers – a pervasive profession/sport, characterized by transient bouts of hydrostatic- and arterial hypertension subsequent to peripheral vasoconstriction. This combination also increases central venous volume during deep dives, leading to an increase in central venous and right atrial pressure. Upon ascent, alveolar hypoxia would lead to hypoxic pulmonary vasoconstriction

resulting in a continued increase in right heart pressures during the dive even as the hydrostatic forces are decreasing. This increase in right atrial pressure may allow for right to left blood flow through a PFO which would act to preserve cardiac output and reduce capillary pressures during the descent and ascent phases of an apnea dive. The repetitive nature of apnea diving and therefore increased right pressures may also stretch open an incompletely sealed foramen ovale, allowing it to be more readily detected. Thus, we hypothesized that PFO prevalence may be greater in apnea divers.

METHODS

The study received approval from the University of Oregon Research Compliance Services and University of Split School of Medicine. Each participant provided written, informed consent before participation (University of Oregon IRB# 07302018.031; University of Split School of Medicine Ethics Committee #2181-198-03-04-19-0052). All studies were performed in accordance with the 2013 Declaration of Helsinki except for registration in a database. Apnea divers (n = 36, 9 female) were recruited from the apnea diver communities surrounding Split, Croatia and an international training camp in Cavtat, Croatia. Control participants (n = 36, 13 female) were recruited from the general population of Split, Croatia and Eugene, Oregon. Control participants had no significant apnea-diving history (e.g., no history of spearfishing or competitive apnea diving or similar history). Some Control participants (n=19, 10 female) were prospectively enrolled from other studies which required them to be screened for PFO and undergo spirometry. The PFO status of these subjects was not known at the time of their enrollment in this study or other studies (University of Oregon IRB# STUDY00000174; STUDY00000019; 04302018.049).

Participants had spirometry assessed prior to participation. They performed forced vital capacity and slow vital capacity maneuvers utilizing a desktop spirometry system (CPFS/D USB Spirometer, Medgraphics Corporation, Saint Paul, MN, USA; Hypair, Medisoft, Sorinnes, Belgium) or plethysmograph (Elite Series Plethysmograph, Medgraphics Corporation).

Participants were instrumented with an intravenous catheter and underwent PFO screening using transthoracic saline contrast echocardiography as described in detail elsewhere.(44, 163) Briefly, transthoracic ultrasound was used to achieve an apical 4-chamber view of the participant's heart while saline contrast was injected into the antecubital vein. Saline contrast was created by vigorously agitating ~3mL of saline with ~1mL air between two syringes connected via three-way stopcocks. This procedure was completed while the participant was at rest and breathing normally and repeated with the participant performing a Valsalva maneuver. Participants were considered PFO-positive if contrast bubbles appeared in the left heart within 3 cardiac cycles of saline contrast appearing in the right ventricle either with or without Valsalva. Ultrasound measures and bubble study evaluations in Croatia were conducted by three experienced ultrasonographers (T.D., R.N.L., A.D.) and reviewed by a Clinical Cardiac Physiologist accredited by the British Society of Echocardiography (A.D.). In Eugene, these measures were conducted and reviewed by Registered Diagnostic Cardiac Ultrasonographers. and we have shown excellent agreement in assigning bubbles scores in blinded physicians and ultrasonographers.(168)

All statistical analyses were conducted via GraphPad Prism version 8.4 (GraphPad Software, San Diego, CA, USA). Spirometry was compared between Divers and Controls utilizing students unpaired t-test. PFO prevalence was compared using a Chi-square analysis with significance set at *a priori* as $p<0.05$.

RESULTS

Apnea divers had a significantly higher PFO prevalence (19 of 36, 53%) than Controls [9 of 26, 25%; $X^2(1, N = 72) = 5.844$, $p = 0.0156$]. Divers were significantly taller and had larger FVC and FEV1, but similar FVC/FEV1 ratio to controls (**Table 6.1**).

Table 6.1. Anthropometric and Spirometric Evaluation of Divers and Controls

	Divers n = 36 **PFO Prevalence: 53%**	**Control n = 36** **PFO Prevalence: 25%**
Height: (cm)	181.2± 7.6***	175.1 ± 7.2
Weight: (kg)	77.8 ± 15.3	72.5 ± 12.6
Age: (yr)	35.5 ± 10.0	28.1 ± 8.6
BMI: (kg/m^2)	23.5 ± 3.5	23.6 ± 3.3
FVC: (L)	6.1 ± 1.4**	5.2 ± 1.0
FEV1: (L)	4.8 ± 1.0†	4.1 ± 0.8
FEV1/FVC:	0.79 ± 0.07	0.80 ± 0.10

****p = .0008*, ***p=.0025*, †*p=.0016*, two-tailed unpaired Student's t-test

DISCUSSION

The elevated prevalence of PFO in breath-hold divers, compared to non-diver controls, provides new insight into a potentially new role of PFO in the unique physiology of apnea divers. The prevalence of PFO in the general population has previously been reported to be approximately ~35%.(63) The prevalence of PFO has been shown to be greater, compared to

the general population, in a variety of pathologies including those diagnosed with obstructive sleep apnea(221). It is unclear why the rate of detection of PFO is greater in apnea divers than the general population, or whether the apparent increase reflects benefit or detriment to apnea divers. Explanations for this finding remain speculative at this time. The prevalence of PFO was also found to be greater in HAPE-susceptible individuals at low altitude.(215) The rate of PFO detection increased further (from 56% to 69%) with ascent to altitude and concomitant increases in pulmonary pressure associated with and exaggerated hypoxic pulmonary vasoconstriction(215) confirming that a PFO may act as a pressure relieve pathway and yet pulmonary pressure would still be elevated, though not as much as it would be in the absence of a PFO.

While an in-depth review of the physiology of apnea diving is beyond the scope of this work, it is important to note some of the physiological responses to an apneic dive. The combination of peripheral vasoconstriction from the mammalian dive reflex and increased hydrostatic pressure results in significant translocation of blood into the thorax, increasing central venous volume and central venous pressure as well as stroke volume and pulmonary capillary hydrostatic pressure.(222) The combination of chemoreceptor stimulation from acidotic hypercapnic hypoxia elicits a significant sympathetic response, likely dramatically increasing mean arterial pressure, though data to confirm this is lacking.(31) Simulated dives in a pressure chamber showed a substantial increase in mean arterial pressure.(223) As depth increases, lungs compress in response to increased hydrostatic pressure, and can result in reduction of lung volume below residual volume at relatively modest depths (40-50m), further increasing pulmonary pressure.(31) At the nadir of the dive, the diver is hyperoxic due to increased barometric pressure increasing PO_2 in accordance with Boyle's law. However, the

diver is still consuming oxygen while submerged, gradually decreasing alveolar PO_2. As the diver ascends from the nadir of their dive, compression of the lung decreases as does barometric pressure. During the ascent phase, the combination of oxygen consumption and decreasing barometric pressure leads to a rapid decrease in alveolar and arterial PO_2. At the cessation of the dive, arterial PO_2 has been measured as low as 27 mmHg,(34) and as low as ~20 mmHg after "dry" apneas.(224) This severe level of hypoxemia may result in a significant hypoxic pulmonary vasoconstriction resulting a prolongation of elevated right heart pressures during the ascent portion of the dive.

While SCUBA-diving in general is not associated with a greater prevalence of PFO, SCUBA-associated DCS is associated with a highly increased prevalence of PFO.(218) Compared to ascending to high altitude or apneic diving to significant depths, SCUBA-diving has relatively modest increases in pulmonary vascular pressure due to the absence of a hypoxic stimulus and associated hypoxic pulmonary vasoconstriction. In contrast, both apneic diving and ascending to altitude cause an increase in pulmonary vascular pressure caused at least in part by hypoxic pulmonary vasoconstriction. This would be particularly true in apnea divers who train in swimming pools and become gradually more and more hypoxic as their lungs are depleted of oxygen. In addition to hypoxic pulmonary vasoconstriction, apneic divers who are diving to great depths have the added impact of lung compression, which can result in reduction of lung volume to below residual volume beyond the relatively routine depths of 40-50m(31), providing a further cause for elevated pulmonary pressure. Additionally, breath hold diving has been shown to induce endothelial dysfunction and increased levels of plasma microparticles.(225) Endothelial microparticle levels have been correlated to the hemodynamic severity of pulmonary hypertension.(226)

While the record depths for apneic dives are in excess of 200m, divers regularly achieve depths sufficient enough to induce hyperbaric stress on the cardiopulmonary circuit. For example, a routinely performed dive to 50m, would cause a reduction in lung volume to <20 % of lung volume at the surface. The combination of lung compression and centralization of blood volume from the periphery into the thorax, elicits a substantial increase in pulmonary vascular pressures. Increases in pulmonary arterial pressure result in a buildup of 'backpressure' (increased right ventricular afterload), as structures must generate higher pressures to continue circulating blood, as mean arterial pressures during a simulated dive to 50m can exceed 200 mmHg.(223) This increase in right ventricular afterload may lead to increased pressure in the right atrium(197), resulting in dramatically increased right atrial pressures relative to left atrial pressures.

An alternate explanation is that rather than the act of deep apnea dives exacerbating otherwise minor intracardiac shunts, the pre-existence of such a shunt facilitates the ability of these individuals to better compensate while performing deeper dives. During the late stages of a dive and particularly during the ascent(141), the PO_2 within the alveoli decreases, resulting in hypoxic pulmonary vasoconstriction and increasing pulmonary vascular pressures. A PFO may function as a 'pressure relief valve', reducing the fraction of cardiac output sent to the lungs, thereby limiting the increase in right ventricular afterload, the rise in pulmonary vascular pressure, and aiding in the preservation of left-ventricular cardiac output while protecting fragile pulmonary capillaries from being subjected to extreme hydrostatic pressures. The blood being shunted right-to-left would have a minimal impact on overall arterial oxygenation as the impact of a shunt on pulmonary gas exchange efficiency decreases as the PO_2 of the right atrial venous blood approaches the PO_2 of the arterial blood. Additionally, the PFO functioning as a pressure

relief pathway for pulmonary pressure may even be protective against pulmonary barotrauma, as exaggerated pulmonary pressure has been proposed as a contributing factor to pulmonary hemorrhage/edema following diving. PFO functioning as a pressure relief pathway may allow for increased frequency or depth of apneic dives without complications and therefore may explain the higher prevalence among individuals who frequently experience extreme hyperbaria associated with apneic diving.(227)

While PFO has been associated with increased risk of DCS in SCUBA diving, the relationship between DCS and PFO in breath-hold is less clear. Similar to SCUBA divers, PFO represents a potential pathway for arterialization of venous gas emboli in breath-hold divers. However, even with very deep breath hold dives we (unpublished observation) and others have found very low venous gas bubble load in breath hold divers (grade 1 on a scale to 5). However, even in SCUBA divers, DCS is not solely dependent on gas bubble load, but also additional factors including endothelial dysfunction(228) and microparticle formation.(229) DCS in breath-hold divers has been linked to these factors.(225) There are also numerous reports of white matter lesions consistent with neurological DCS in Ama divers (traditional Japanese and Korean pearl and seafood divers) as well as DCS in freedivers and spearfishers.(230) Thus, the higher frequency of PFO in breath hold divers may present a risk factor for developing DCS via arterialization of venous gas emboli, but DCS is not solely dependent on this mechanism.
This study has significant limitations. Transcranial doppler can be more sensitive for the detection of PFO compared to transthoracic echocardiography. As such, the rate of detection of PFO reported in this study may be lower than actual prevalence. Similarly, using 1 mL of blood in the agitated saline mixture can also increase sensitivity of the detection method. However, since both Divers and Controls were evaluated using the same ultrasound method and both

groups were evaluated without the addition of 1 mL blood to the saline mixture, it is unlikely that this altered the reported findings. Additionally, in our hands transthoracic saline contrast echocardiography data are strongly associated with TCD data when detecting right-to-left shunt through a PFO, particularly when using TCD to measure both middle cerebral artery and posterior communicating artery microembolic signals.(165) Apnea divers experience significant elevations in pulmonary pressure due to the combined effects of hypoxia and lung compression while diving which may ultimately result in substantial increases in right atrial pressure for an unknown period after the dive. A PFO may be more readily detectable during that period. As the time interval between the last dive and visiting the lab was not standardized, the rate of detection of PFO reported in Divers may underestimate the true PFO prevalence.

CONCLUSION

We found a significantly greater prevalence of PFO in recreational-to-elite apneic divers. This greater prevalence may be either the result of right ventricular afterload caused by lung compression and hypoxic pulmonary vasoconstriction or possibly serves to mitigate barotrauma associated with frequent or extremely deep apneic dives. In either case, PFO presence may lead to a "self-selection" for being an apnea diver and consequently may influence the prevalence of PFO in this population. Whether or not the presence of PFO is beneficial remains unknown. Future studies investigating cardiopulmonary interactions in apnea divers with and without PFO during apneas and/or bouts of hypoxia may provide additional information on the responses of these individuals to arterial hypoxemia and the effect PFO has on exacerbating or mitigating these effects.

CHAPTER VII

BLUNTED HYPOXIC PULMONARY VASOCONSTRICTION IN APNOEA DIVERS

This chapter is published in the *Journal of Experimental Physiology* and was co-authored with Courtney Brown, Mohini Bryant-Ekstrand, Rachel Lord, Tony Dawkins, Aimee Drane, Joel E Futral, Otto Barak, Tanja Dragun, Michael Stembridge, Boris Spajić, Ivan Drviš, Joseph W. Duke, Philip N. Ainslie, Glen E. Foster, Željko Dujić, and Andrew T. Lovering. All authors aided in data collection. Courtney Brown was responsible for the analysis of ventilatory data and associated writing. I was responsible for all other analysis and all other writing is entirely mine. Josheph W. Duke, Željko Dujić, and Andrew T. Lovering provided editorial assistance. The manuscript has been edited to comply with the University of Oregon Graduate School Dissertation formatting requirements.

INTRODUCTION

Elite free divers can hold their breath for an impressive time of ~10 minutes, and can reach depths exceeding 200 meters (31). During training, divers experience bradycardia, which helps to reduce myocardial oxygen consumption (231) and peripheral vasoconstriction to perfuse other organs such as the brain and adrenal glands (133, 232), as well as reductions of coronary blood flow by 50% as measured with contrast MRI scanning (233). Apnoea trained divers have also been shown to have lower mitochondrial oxygen consumption (234). While prolonged apnoea results in significant chemoreflex activation of sympathetic vasoconstriction (235, 236) allowing for optimal O_2 delivery and utilization during apnoea and prolonging consciousness (237–239), baseline sympathetic nerve activity and blood pressure are normal in contrast to other forms of intermittent hypoxia such as obstructive sleep apnoea (235, 240–242). Despite the significant impacts of hyperbaria on the cardiopulmonary system, divers do not display chronic

impairment in lung function (31). These data suggest that elite divers are healthy and capable of incredible physiological responses to extreme stress, making them a unique model to study physiology at the extremes of human tolerance such as repetitive short duration but severe hypoxaemia.

The pulmonary vasculature is unique in that it constricts in response to low oxygen which is, presumably, to enhance ventilation and perfusion matching under conditions of regional alveolar hypoxia (11, 87). Hypoxic pulmonary vasoconstriction (HPV) can significantly increase pulmonary arterial pressure (87), which is further potentiated by hypercapnia and/or acidosis (243–245) likely occurring during dives (246). Due to the hydrostatic impact of the depths achieved and resulting lung compression divers are likely to be hyperoxic at the nadir of their dive (33), potentially reducing any stimulus for HPV until the final 10m of the ascent portion of a dive. This profile of hyperoxia for the majority of a dive followed by severe hypoxia during the final phase of ascent has been demonstrated in diving Emperor penguins (247, 248) and in simulated "dry dives" in humans (139). At the end of an apnoea attempt, divers have exhibited end-tidal PO_2 ($P_{ET}O_2$) values less than 30 mmHg without loss of consciousness (34). Additionally, in elite apnoeists under "dry" laboratory conditions, a series of studies utilizing radial artery (246) and jugular venous catheterizations (224, 249, 250) have measured end-apnoea PO_2's of 29.6 ± 6.6 mmHg and 25 ± 6 mmHg, respectively. Incredibly, an extreme end-apnoea PaO_2 of 23 mmHg following a 435 s breath-hold has been achieved without syncope (251). "Dry" apnoeas have similarly been shown to result in significant increases in PCO_2 and decreases in arterial pH (246, 252). This level of alveolar and arterial hypoxaemia combined with hypercapnia and acidosis creates a robust stimulus for hypoxic pulmonary vasoconstriction and thus, may elevate pulmonary vascular pressure and increase right heart

work (34). The hemodynamic changes associated with immersion (i.e. peripheral vasoconstriction and thoracic shift of blood volume) likely alter the cardiac response to total lung capacity apnoea resulting in greater pulmonary vascular pressures. Additionally, repeated hypoxic bouts lead to progressive increases in the degree of hypoxic pulmonary vasoconstriction in a canine model (253). Thus, apnoea divers may have markedly increased vascular reactivity due to the significant hypoxic stimulus experienced during a dive combined with the repetitive nature of their training.

NO synthesized by endothelial nitric oxide synthase (eNOS) can limit this vasoconstriction. Sildenafil is used clinically due to its specificity and ability to augment this pathway by impeding the function of phosphodiesterase-5, an esterase which degrades cGMP and prevents phosphorylation of protein kinase G (254). Sildenafil is also effective to prevent hypoxic pulmonary vasoconstriction by increasing levels of cGMP. In turn, reduction of hypoxic pulmonary vasoconstriction can be expected to reduce right ventricular afterload and reduce right-heart work (255).

After completing a dive and resuming breathing, alveolar gas values rapidly return to normal in apnoeic divers thereby reversing the hypoxic pulmonary vasoconstriction stimulus, though particularly deep dives which result in compressing the lungs to volumes less than surface residual volume may impair pulmonary gas exchange efficiency (256). Accordingly, these cardiopulmonary responses in apnoea divers may provide a unique model by which to study the impacts of repetitive intermittent exposure to hypoxemia while awake. However, it remains unknown as to whether the repetitive hyperbaric hypercapnic acidotic hypoxaemia of breath-hold diving leads to a remodelling of the pulmonary circulation, pulmonary hypertension and right heart dysfunction, as could be expected based on other work (253, 257).

Therefore, the purpose of this study was to compare the cardiopulmonary responses to 20-30 minutes of isocapnic hypoxia with and without sildenafil between apnoea divers and matched controls. Compared to matched controls, we hypothesized that apnoea divers, who experience repetitive bouts of hypoxaemia while awake, would have a greater pulmonary pressure due to a greater pulmonary vascular resistance at rest and with 30 minutes of isocapnic hypoxia. Similarly, we hypothesized that apnoea divers would have a greater reduction in pulmonary pressure with sildenafil administration than controls at all time points.

METHODS

Ethical Approval

The study received approval from the University of Oregon Research Compliance Services and University of Split School of Medicine and each participant gave written, informed consent before participation (University of Oregon IRB# 07302018.031; University of Split School of Medicine Ethics Committee #2181-198-03-04-19-0052). All studies were performed in accordance with the 2013 Declaration of Helsinki and this study is registered at clinicaltrials.gov (#07302018.031).

Participant Recruitment

36 [8 female (21%)] participants aged 18-65, free from any overt heart or lung disease, volunteered to participate in the study. Divers consisted of experienced spearfishers (5 to 30 years of experience), current and former members of national competitive apnoea diving teams including one former world champion and multiple world record holder. Four participants were excluded for reasons detailed below. All participants underwent echocardiographic screening (see below).

Participant Screening and Characterization

On visit #1, pulmonary function was determined using computerized spirometry (MedGraphics, CPFS/D USB spirometer, St. Paul, MN, USA) according to American Thoracic Society/European Respiratory Society Standards (149, 173). Lower limits of normal and percent predicted values were calculates using the Global Lung Initiative online calculator (178). Next, participants were instrumented with an intravenous catheter for injection of agitated saline for enhancement of tricuspid regurgitation velocity measurement. Briefly, a 22-gauge intravenous catheter was placed in the antecubital vein. A three-way stopcock was attached, and two 10-mL syringes were attached to the other ports. One syringe contained approximately 0.5 mL of air, and the other contained approximately 4mL of sterile saline. The contrast bubbles were created by rapidly agitating the saline-air solution from one syringe to the other.

A comprehensive echocardiogram was performed whereby the following parameters were measured according to the standards of the American Society of Echocardiography: right ventricular wall (RV Wall) thickness (cm), right ventricle internal diameter in diastole (RVID), right ventricular end diastolic (RVED) area (cm^2) and right ventricular end systolic (RVES) area (cm^2) to calculate right ventricular area fraction (%RVAF), left ventricular end-diastolic volume (LVEDV, mL), left ventricular end-systolic volume (LVESV, mL), left ventricle internal diameter in diastole (LVIDD), left ventricular posterior wall thickness (LVPW), left ventricle internal diameter in systole (LVIDs), left atrial diameter (LA), pulmonary valve velocity (PV peak velocity, m/s), pulmonary insufficiency end-diastolic (PIED) gradient (mm Hg) to calculate pulmonary artery end diastolic pressure (PAEDP; mm Hg), aortic valve peak velocity (AoV peak velocity, m/s) to calculate aortic valve area (AVA; cm^2), interventricular septum (IVS), aortic root (AORT), left ventricular outflow tract (LVOT) diameter, and tricuspid annular plane

systolic excursion (TAPSE) (144, 149, 150). One Diver was excluded due to echosonographic evidence of aortic stenosis and referred to their physician.

Study Design

At the conclusion of the characterization ultrasound measures, participants were given a capsule to swallow. The capsule contained either sildenafil (50mg, Aurobindo Pharma USA, East Windsor, NJ, USA) or placebo and was administered in a double-blind placebo controlled and balanced design. Timing of measurements were made to allow for peak effect of sildenafil, which occurs 60-90 minutes after ingestion (258, 259). While sildenafil has popularly been known as a treatment for erectile dysfunction, sildenafil has been used to treat pulmonary hypertension and blunt the pulmonary pressor response to hypoxia (260–262) and therefore can be safely be used to prevent hypoxic pulmonary vasoconstriction in apnoea divers as well as controls.

Participants were positioned on a padded exam table in side-lying position and instrumented for lead-II electrocardiogram, forehead sensor to estimate arterial oxygen saturation (SpO_2) sensor (Covidien, Minneapolis, MN, USA), and finger-mounted blood pressure (Finometer Model 1, Finapres Medical Systems, Netherlands). One hour after ingestion of the capsule, the end tidal forcing system was engaged as described below and the study ultrasound measures of pulmonary pressure, cardiac output (Q_T) and TAPSE, were made as detailed below. After a minimum 24-hour washout period, participants returned to the lab for a subsequent visit to take the alternate capsule and repeat the end-tidal forcing protocol and ultrasound measures (**Figure 7.1**).

Figure 7.1. Schematic Diagram of Study Design (Next Page). Subjects were recruited from the diving community of Split, Croatia (Divers) and the general populations of Split, Croatia and

Eugene, Oregon (Controls). Subjects then underwent spirometry, anthropometric measurements, and a comprehensive echocardiogram. After this, subjects were randomly assigned to receive placebo or 50mg sildenafil. 1 hour after ingestion of the drug capsule, subjects underwent a 20-30 minute hypoxic challenge. After a minimum 24 hour washout period, subjects returned to receive the other treatment (IE those who received placebo on visit 1 received 50 mg sildenafil on visit 2) and repeated the 20-30 minute hypoxic challenge.

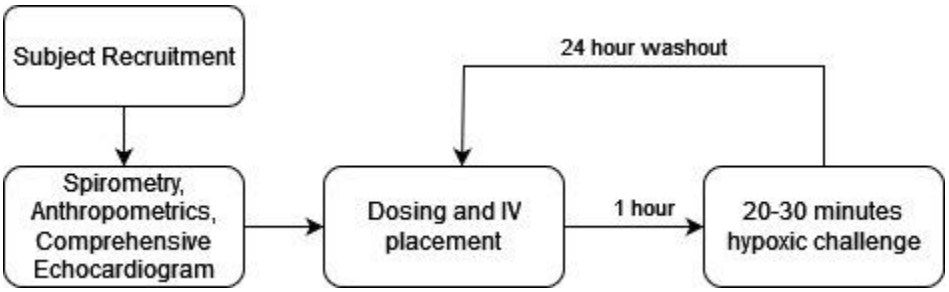

Cardiorespiratory Measurements

All respiratory (i.e. minute ventilation ($\dot{V}_I$), tidal volume (V_T), breathing frequency (f_B), $P_{ET}O_2$, and end-tidal carbon dioxide ($P_{ET}CO_2$). And peripheral oxygen saturation (SpO_2) and cardiovascular (i.e. heart rate (HR), systolic blood pressure (SBP), diastolic blood pressure (DBP) parameters were sampled at 200 Hz using an analogue-to-digital converter (Powerlab/16SP ML 880; ADInstruments, Colorado Springs, CO, USA) interfaced with a personal computer. Commercially available software was used to analyse all variables (LabChart V7.1, ADInstruments). Participants breathed through a mouthpiece and a two-way non-rebreathing valve while wearing a nose clip connected to a pneumotachograph (HR 800L, HansRudolph, Shawnee, KS, USA) and a differential pressure amplifier (ML141, ADInstruments). Partial pressure of end-tidal oxygen and carbon dioxide were sampled at the mouth ($P_{ET}O_2$ and $P_{ET}CO_2$, respectively) (ML206; ADInstruments). SBP and DBP were determined beat-by-beat by finger pulse photoplethysmography (Finometer PRO; Finapress Medical Systems, Amsterdam, Netherlands) and calibrated against the average of three manual

brachial artery blood pressure measurements, while mean arterial pressure (MAP) was calculated as 1/3*SBP + 2/3*DBP. Heart rate (HR) was obtained from a lead-II electrocardiogram (ML132, ADInstruments). Finally, SpO_2 was taken from the forehead pulse oximeter. Technological difficulties with the finger pulse plethysmography device resulted in blood pressure data not being recorded at all time points in some subjects.

Dynamic End-Tidal Forcing

Participants breathed through a mouthpiece connected to a 2-way non-rebreathing valve (2700 series, Hans Rudolph, Shawnee, KS, USA) for collection of end-tidal gases before and during the entire end-tidal forcing procedure. Prior to initiating the end-tidal forcing system, participants breathed on the mouthpiece for 10 minutes to establish baseline values. Once baseline was established, the end-tidal forcing system was engaged to replicate the participant breathing room air and to allow the participant to acclimate to the forcing system. After replicating room-air breathing for 5 to 10 minutes, the end-tidal forcing system was utilized to reduce the $P_{ET}O_2$ to 45 mmHg, which resulted in SpO_2 of approximately 75%, while maintaining baseline $P_{ET}CO_2$ for 30 minutes. Gases were sampled from the mouthpiece and analysed by a calibrated gas analyser (Split: ML206, ADInstruments, Colorado Springs, CO, USA; Eugene: Model 17515^A CO_2 Analyzer, Vacumed, Ventura, CA, USA; N-22M Oxygen Sensor, R-2 Flow Control, S-3A/I Oxygen Analyzer, AEI Technologies, Bastrop, Texas, USA) and respiratory flows were measured using a linear pneumotachograph (Model 4813, Hans Rudolph, Kansas City, MO, USA). Custom software (developed in Labview, Austin, TX, USA) determined breath-by-breath tidal volumes, $P_{ET}O_2$, and $P_{ET}CO_2$. The end-tidal forcing system prospectively delivered inspired gasses to clamp $P_{ET}O_2$ and $P_{ET}CO_2$ at desired levels. Independent solenoid valves delivered the necessary volumes of O_2, CO_2 and N_2 as determined by an error reduction

algorithm incorporating $P_{ET}O_2$, $P_{ET}CO_2$, and inspiratory and expiratory tidal volume from the last breath (154, 155). Three participants (1 Diver, 2 Control) were excluded due to difficulty breathing on a mouthpiece or an extremely exaggerated hypoxic ventilatory response which was not compatible with the end-tidal forcing system.

Echocardiographic Measures During End-Tidal Forcing

Measures of heart rate, TAPSE, left-ventricular outflow tract velocity time integral (LVOT VTI), and tricuspid regurgitation velocity were made by trained ultrasonographers before hypoxia and were repeated at 5-minute intervals through the 30-minutes of hypoxia. Three participants (3 Divers) only had measurements up to 20 minutes of hypoxia due to discomfort associated with hypoxemia, and the 20-minute measures were utilized in place of 30-minute measures in analysis for those participants. Stroke volume was calculated from the LVOT VTI and LVOT cross-sectional area (determined during the comprehensive echocardiogram) and Q_T was calculated as HR x SV (263, 264). SV, and therefore Q were allometrically scaled ($SV/BSA^{0.93}$) to body surface area (BSA) (265–267). Pulmonary artery systolic pressure (PASP) was calculated using the simplified Bernoulli equation (144). Additional saline-contrast bubbles were injected as necessary to enhance measurement of tricuspid regurgitation velocity as previously described (163). PASP measures were not made in one diving participant due to inability to identify a tricuspid regurgitation jet on ultrasound. Total pulmonary resistance was calculated as TPR = PASP / Q_T. Systemic Vascular Resistance (SVR) was calculated as ($MAP - RA_{Pres}$)/Q_T.

Statistical Analyses

All statistical analysis performed in GraphPad Prism 9 (GraphPad Software Version 9.1.1, San Diego, CA, USA), except for ventilatory data ($\dot{V}_I$, V_T, f_B) which utilized the R

statistical language (R Foundation for Statistical Computing, Vienna, Austria) using *The R Stats Package* (R Core Team, 2019) for extraction of dynamic end-tidal forcing system data and analysis. Results are reported as mean ± standard deviation (SD). Divers and Controls were matched by age and sex resulting in *n*=16 matched Diver/Control pairs. One Diver was unable to tolerate the hypoxic challenge beyond 15 minutes, and only their anthropometric, cardiac structure, and acute hypoxic ventilatory response data is reported. Anthropometric data, i.e., height, age, cardiac structure, pulmonary function, etc., were tested for normality with the Shapiro-Wilk test and compared between groups using independent samples t-tests if normality was not violated. If normality was violated, Mann-Whitney test was used instead. SV and Q_T were analysed before and after being indexed to body surface area prior to analysis (SVI and CI, respectively). TPR was recorded in mm mg/L/min and converted to dynes/sec/cm^{-5} prior to analysis.(183) We were interested in understanding how group (Control vs. Divers) and treatment (sildenafil vs. placebo) interacted to alter the responses to 20 to 30-minutes hypoxia. Accordingly, the change in SVI, CI, SV, HR, Q_T, TAPSE, PASP and TPR from a baseline timepoint to 20 to 30-minutes hypoxia were analysed using 2-way (group x treatment) RMANOVA with Sidak's post-hoc test. Due to non-systemic technological complications, blood pressure data was incomplete in some participants, and a mixed-effects analysis was performed with Sidak's post-hoc test for this data. This mixed-effects model uses a compound symmetry covariance matrix and is fit using Restricted Maximum Likelihood. $\dot{V}_I$, V_T, f_B, $P_{ET}O_2$, $P_{ET}CO_2$, were analysed using a mixed effects linear model. Following ANOVA or mixed-effects analysis, multiple comparisons testing was performed between data that differed by only one factor. Comparisons between males and females for all variables were performed utilizing an unpaired t-test.

RESULTS

Anthropometric, Pulmonary Function, Cardiac Structure and Function:

Table 7.1 displays the anthropometric and pulmonary function data. **Table 7.2** shows cardiac function and cardiac structure data. There were no statistically significant differences in cardiac structure, baseline function, or haematocrit between Divers and Controls. Divers were taller (**Table 7.1**) and had greater absolute values for FEV1, FEF 75%, FEF 25-75% (p = .047, p = .046, p = .012, p = .026, respectively) (Divers n=16, Controls n=16). However, when pulmonary function was expressed as a percentage of predicted there were no differences.

Table 7.1. Anthropometrics and Pulmonary Function

	Divers	**Controls**	***p***
Height: (cm)	182.3 ± 9.1	175.7 ± 9.0	0.047
Weight: (kg)	81.7 ± 17.6	79.2 ± 13.7	0.815
Age: (yr)	34 ± 10	32 ± 9	0.569
Body mass index: (kg/m^2)	24.4 ± 3.5	25.6 ± 3.4	0.221
Forced vital capacity: (L)	5.90 ± 1.38	5.27 ± 1.27	0.191
Forced Vital Capacity Lower Limit of Normal	4.13 ± 0.79	4.13 ± 0.62	0.633
Forced Vital Capacity Percent of Predicted	104.3 ± 12.19	103.26 ± 12.02	0.763
Forced Expiratory Volume in 1st second: (L)	4.79 ± 1.04	4.05 ± 0.89	0.046
Forced Expiratory Volume Lower Limit of Normal	3.45 ± 0.62	3.36 ± 0.48	0.790
Forced Expiraotyr Volume in 1st second Percent of predicted	103.88 ± 12.36	99.56 ± 11.49	0.418

Table 7.1. Anthropometrics and Pulmonary Function Continued			
	Divers	**Controls**	***p***
Forced Expiratory Volume in 1st Second / Forced Vital Capacity:	0.82 ± 0.07	0.78 ± 0.08	0.278
Forced Expiratory Flow 25%: (L/s)	8.47 ± 2.19	7.17 ± 1.55	0.133
Forced Expiratory Flow 50%: (L/s)	5.31 ± 1.16	4.63 ± 1.32	0.085
Forced Expiratory Flow 75%: (L/s)	2.36 ± 0.82	1.70 ± 0.57	0.012
Forced Expiratory Flow 25-75%: (L/S)	4.65 ± 1.12	3.67 ± 1.08	0.026
Forced Expiratory Flow Max: (L/S)	10.25 ± 2.41	8.77 ± 1.79	0.061
Slow Vital Capacity: (L)	6.11 ± 1.54	5.28 ± 1.27	0.091
Forced Expiratory Flow in 1st Second / Forced Vital Capacity Lower Limit of Normal	0.71 ± 0.03	0.71 ± 0.03	0.278
Forced Expiratory Flow 25-75% Lower Limit of Normal	2.51 ± 0.58	2.57 ± 0.47	0.724
Forced Expiratory Volume in 1st Second / Forced Vital Capacity Percent of Predicted	99.11 ± 5.92	96.17 ± 7.25	0.404
Forced Expiratory Flow 25-75% Percent of Predicted	102.42 ± 24.25	91.16 ± 20.43	0.293

Table 7.1. Anthropometrics and Pulmonary Function. n=32 (Divers n = 16, Controls n = 16)

Table 7.2. Resting Cardiac Structure and Function Taken During Participant Screening			
	BHD	**BHDc**	***p***
RV wall (mm)	3.5 ± 0.60	3.62 ± 0.79	0.651
IVSd (mm)	8.31 ± 1.54	8.41 ± 1.27	0.843
LVIDd (mm)	49.81 ± 5.99	47.78 ± 6.70	0.373
LVPWd (mm)	8.25 ± 1.44	8.32 ± 1.44	0.893
LVIDs (mm)	30.38 ± 5.24	33.06 ± 4.54	0.131
LA s (mm)	33.06 ± 4.14	32.81 ± 4.23	0.867
LVOT diam (mm)	22.97 ± 3.55	20.84 ± 2.66	0.065
PV pk vel (m/s)	1.06 ± 0.25	1.08 ± 0.24	0.846
PIED gradient (mmHg)	3.07 ± 1.28	2.22 ± 1.10	0.085
PAEDP (mmHg)	7.42 ± 1.82	6.41 ± 1.79	0.209
LVOT vel (m/s)	1.05 ± 0.16	1.08 ± 0.18	0.593
LVOT VTI	22.24 ± 3.18	21.20 ± 3.04	0.322
AoV vel (m/s)	1.23 ± 0.17	1.28 ± 0.17	0.584
AoV VTI	24.84 ± 4.03	24.67 ± 2.80	0.888
AVA (cm^2)	3.46 ± 0.99	2.94 ± 0.82	0.121
MV-E vel (m/s)	0.78 ± 0.16	4.29 ± 14.00	0.324
MV-A vel (m/s)	0.53 ± 0.11	2.69 ± 8.78	0.334
LAT e' (m/s)	0.18 ± 0.04	1.54 ± 5.46	0.328
E/e' ratio	4.27 ± 1.21	4.63 ± 0.71	0.322
RVED area (cm^2)	23.69 ± 7.27	20.57 ± 5.00	0.167
RVES area (cm^2)	12.55 ± 3.66	10.58 ± 2.61	0.090
%RVAF	46.33 ± 5.62	48.92 ± 6.38	0.479
LVED vol (mL)	132.88 ± 37.40	124.75 ± 28.04	0.492
LVES vol (mL)	51.88 ± 15.63	48.19 ± 13.20	0.476
HR at LV vol meas (bpm)	61.13 ± 12.21	63.5 ± 11.69	0.578

Table 7.2. Resting Cardiac Structure and Function Taken During Participant Screening Continued			
	BHD	**BHDc**	***p***
%LVEF	60.63 ± 5.86	61.38 ± 5.71	0.717
SV (mL)	81.06 ± 25.19	76.83 ± 13.23	0.691
CO (L/min)	4.74 ± 1.52	4.94 ± 1.18	0.876
TR pk grad (1st) (mmHg)	19.67 ± 4.85	18.52 ± 4.27	0.482
TR pk grad (2nd) (mmHg)	20.79 ± 5.43	18.61 ± 4.50	0.237
IVC size supine (cm)	1.99 ± 0.37	1.74 ± 0.43	0.093
RA press (mmHg)	3.4 ± 1.3	3.9 ± 2.0	0.413
PASP (1st) (mmHg)	22.5 ± 5.9	23.2 ± 5.6	0.740
PASP (2nd) (mmHg)	24.4 ± 5.6	22.8 ± 5.6	0.414
TAPSE	24.00 ± 3.20	23.75 ± 3.32	0.830
Hematocrit	41.6 ± 3.9	40.4 ± 3.0	0.246

Table 7.2. Resting Cardiac Structure and Function Taken During Participant Screening. There were no significant differences in cardiac structure or function between Divers and Controls. n = 32 (Divers n = 16, Controls n=16)

Pulmonary Pressure, Q_T, and TPR:

There were no effects of group (Divers n=15 vs Controls n=16) or treatment (placebo vs sildenafil) on change in Q_T (ΔQ_T) in response to 20 to 30-minutes hypoxia (**Figure 7.2A**) (p = .222).

There was a significant main effect of treatment on the change in PASP (ΔPASP) in response to 20 to 30-minutes hypoxia, $F(1,29) = 11.42$, p = .002. ΔPASP was greater with placebo than with sildenafil (Δ: 9.3 ± 0.1 vs 5.9 ± 1.9 mmHg) (**Figure 7.2B**) (Divers n=15, Controls n=16).

There was a significant interaction effect of group x treatment on change in total pulmonary resistance (ΔTPR) in response to 20 to 30-minutes hypoxia, $F(1,29) = 8.694$, p = .006. There was a blunted ΔTPR in response to 20 to 30-minutes hypoxia in Divers compared to Controls with placebo (Δ: -3.85 ± 72.85 vs 73.74 ± 91.06 dynes/sec/cm^{-5}, p = .022), but there were no differences with sildenafil (Δ: 2.23 ± 81.32 vs 32.99 ± 82.53 dynes/sec/cm^{-5}, p = .5141) (Divers n=15, Controls n=16). (**Figure 2C**)

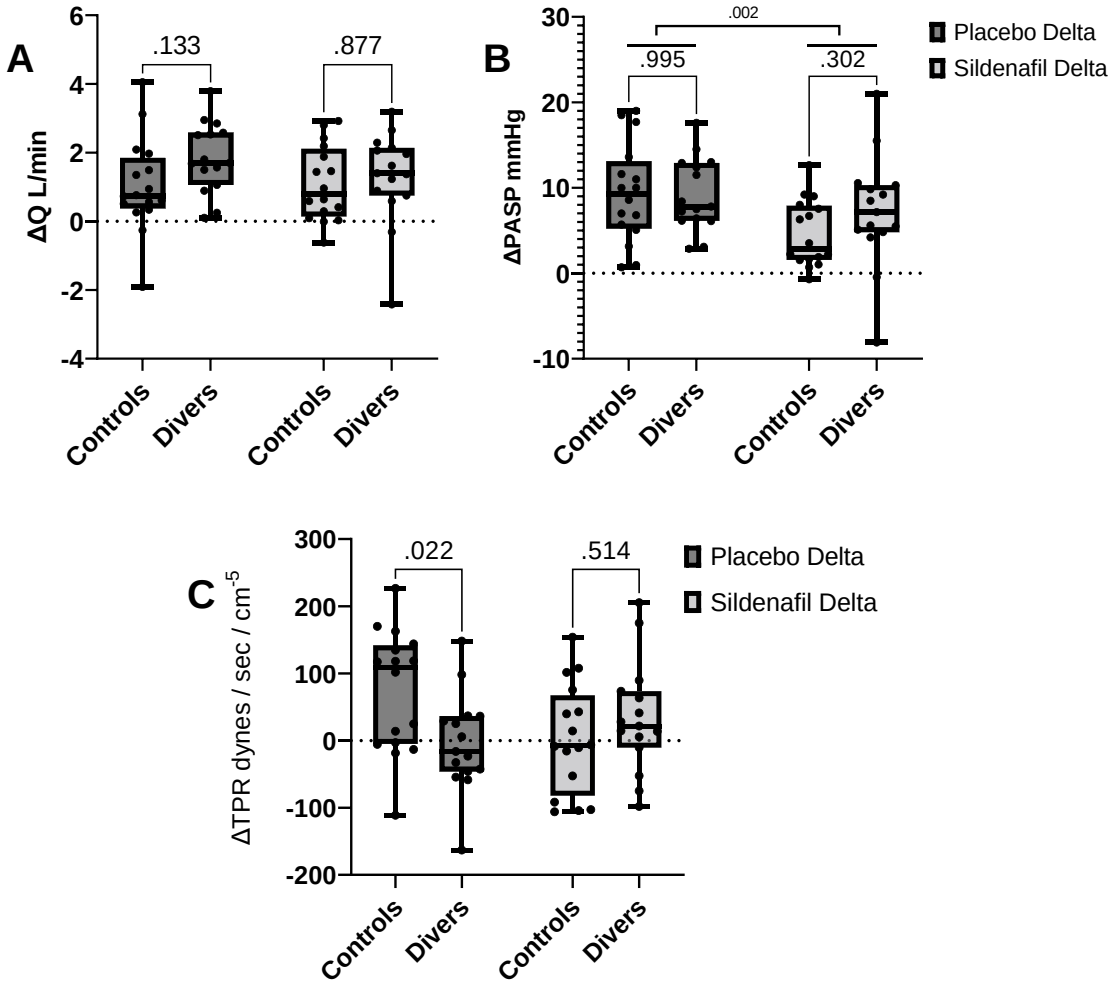

Figure 7.2. Changes in Cardiac Output, PASP and TPR After a Hypoxic Challenge. A*:* There was no difference ΔQ in response to 20 to 30-minutes hypoxia in either Divers or Controls under Placebo or Sildenafil conditions. B: ΔPASP was significantly reduced with sildenafil compared to placebo, but there were no differences in PASP between Divers and Controls. C:

Divers had a significantly smaller ΔTPR in response to 20 to 30-minutes hypoxia under placebo compared to Controls, though there were no differences in TPR in response to 20 to 30-minutes hypoxia between Divers and Controls under the sildenafil condition. *p < .006, **p = .002, ns = not significant. n=31 (Divers n = 15, Controls n=16)

Cardiac Indices, Mean Arterial Pressure, Systemic Vascular Resistance and TAPSE:

There were neither interaction nor main effects of either treatment or group (Divers n=15, Controls n=16) on either ΔHR (p=.472) or ΔSV (p=.079) after 20 to 30-minutes hypoxia and this was not altered when SV was indexed to body surface area (p = .324(**Table 7.3**). There were neither interaction nor main effects of either group or treatment on ΔCI in response to 20 to 30-minutes hypoxia (p= .373) (Divers n=15, Controls n=16) (**Table 7.3).** There were no significant main effects of either group or treatment on ΔTAPSE after 20 to 30-minutes hypoxia (p=.649) (Divers n=15, Controls n=16). (**Table 7.3**)

There were neither significant interaction nor main effects of either group or treatment on ΔMAP (**Figure 7.3**) (Controls placebo delta n = 14, Controls sildenafil delta n = 16, Divers placebo delta n = 14, Divers sildenafil delta n = 14). There was a significant interaction effect of sildenafil x diving on ΔSVR ($F(1,26) = 5.569$, p = .026) showing that Divers had a greater decrease in ΔSVR in response to 20 to 30-minutes hypoxia with placebo compared to sildenafil (ΔSVR with placebo: Controls -98.8 ± 315.7, Divers -362.2 ± 290.6, p = .021) (Controls placebo delta n = 14, Controls sildenafil delta n = 16, Divers placebo delta n = 15, Divers sildenafil delta n = 14). (**Table 7.3**)

Table 7.3. Change in Cardiac Variables After a 20 to 30-Minute Isocapnic Hypoxic Challenge (next page). Divers had a greater magnitude decrease in systemic vascular resistance. * = significant pairwise comparison of Diving on ΔSVR (p = .010). n = 31 (Divers n = 15, Controls n = 16)

Table 7.3. Change in Outcomes After 20 to 30-Minute Isocapnic Hypoxic Challenge

		Placebo	Sildenafil	p
ΔSBP (mmHg)	Control	10.0 ± 16.8	14.0 ± 12.1	.133
	Diver	18.4 ± 25.3	16.2 ± 38.6	
ΔDBP (mmHg)	Control	-2.4 ± 7.1	8.8 ± 26.7	.184
	Diver	4.7 ± 10.5	4.2 ± 17.4	
ΔHR (BPM)	Control	10.8 ± 10.0	11.3 ± 8.7	.472
	Diver	9.1 ± 21.0	7.2 ± 19.6	
ΔSV (mL)	Control	2.0± 12.0	11 ± 9.0	.079
	Diver	3.0 ± 11.0	3.0 ± 14.0	
ΔSVI (mL)	Control	1.3 ± 6.1	1.9 ± 5.5	.324
	Diver	6.2 ± 5.2	1.6 ± 7.1	
ΔCI (L/m^2)	Control	0.57 ± 0.71	0.61 ± 0.63	.373
	Diver	0.99 ± 0.57	0.77 ± 0.86	
ΔTAPSE (mm)	Control	3.1 ± 2.4	2.6 ± 2.1	.649
	Diver	1.9 ± 2.8	1.9 ± 2.4	
ΔSVR (dynes/sec/cm^{-5})	Control	-98.7 ± 315.7	-138.9 ± 217.4	.028
	Diver*	-352.4 ± 298.9	-105.3 ± 205.5	

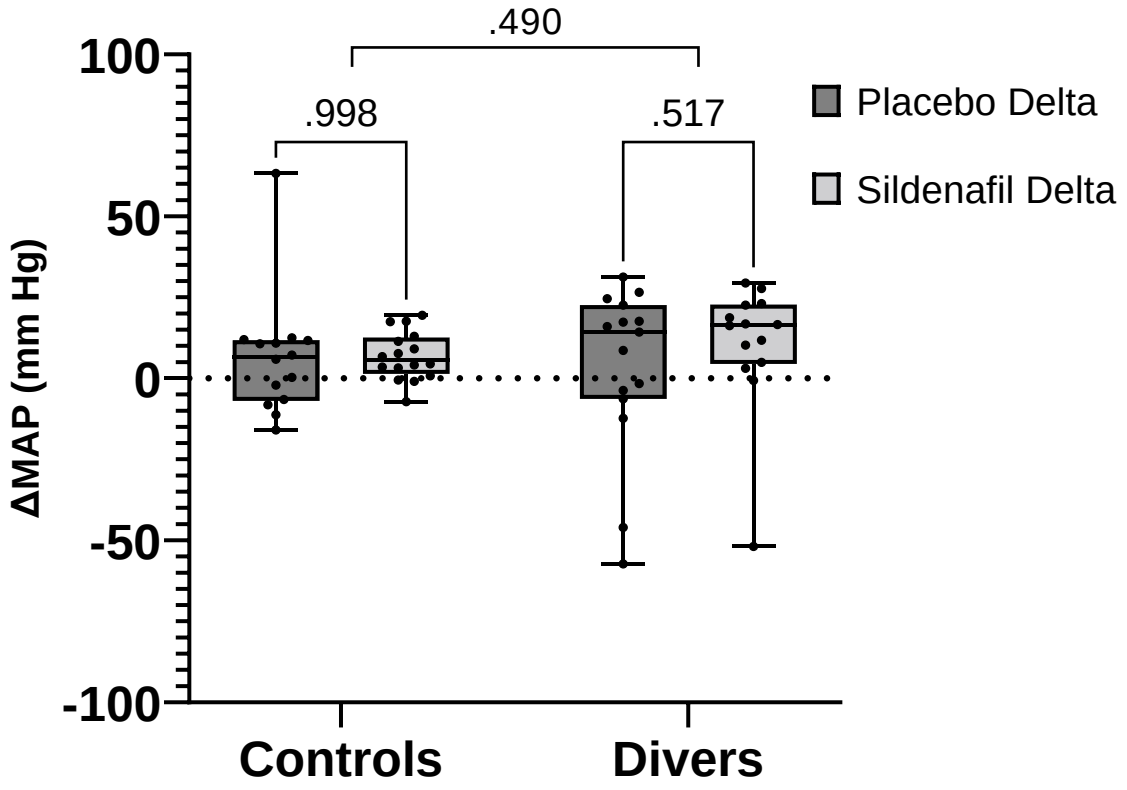

Figure 7.3. ΔMAP. ΔMAP was similar between Divers and Controls after 20 to 30 minutes hypoxic challenge with placebo and sildenafil (p = .490). Control placebo delta n = 14, Control sildenafil delta n = 16, Divers placebo delta n = 15, Divers sildenafil delta n = 14

Ventilatory Response to Isocapnic Hypoxia:

As seen in Table 3 (Divers n=14 , Controls = 16), $\dot{V}_I$, V_T, and f_B were significantly elevated following 20 to 30-minutes of isocapnic hypoxia (p = <.0001 , p = <.0001, p = .003) while $P_{ET}O_2$ was significantly reduced (P < 0.001). $P_{ET}CO_2$ was similar at baseline and following 20 to 30-minutes of isocapnic hypoxia (P = 0.694). There was a main effect of Diving on V_T, with Divers having a larger V_T (1.82 ± 0.3 l) than Controls (1.53 ± 0.4 l; p = 0.0001), while a main effect of Diving on f_B showed that Divers had a significantly lower f_B overall (10.0 ± 2.3 bpm) compared to Controls (12.7 ± 2.4 bpm; p < 0.0001). Although there was a main effect of Diving (p = 0.02) on $P_{ET}O_2$, the difference in $P_{ET}O_2$ (placebo: 53.5 ± 0.8, sildenafil: 53.0 ± 0.8

mmHg; p = 0.02) is not physiologically significant. Additionally, significant interaction of sildenafil x workload on $P_{ET}O_2$ was found, however further interrogation indicated there were no significant differences. There were no differences in the acute hypoxic response between Divers and Controls in either $\dot{V}_I$ or V_T at either the 5-minute or 10-minute time point (**Table 7.4**) (Divers n=16 , Controls = 16). $\Delta \dot{V}_I$ was similar between Divers and Controls in response to 20 to 30-minutes of hypoxia ($F(1,28) = 1.206$, p = .281) (**Figure 7.4**).

Table 7.4. Ventilatory Parameters

		Baseline		**30 Minutes Hypoxia**	
		Placebo	**Sildenafil**	**Placebo**	**Sildenafil**
$\dot{V}_I$	Control	12.1 ± 5.7	12.1 ± 5.7	21.2 ± 5.7*	20.4 ± 5.7*
(l/min)	Diver	10.9 ± 5.7	10.9 ± 5.6	20.0 ± 5.6*	19.1 ± 5.6*
V_T	Control	1.0 ± 0.5	1.0 ± 0.5	1.6 ± 0.5*	1.6 ± 0.5*
(l)	Diver†	1.3 ± 0.5	1.3 ± 0.5	1.9 ± 0.5*	1.9 ± 0.5*
f_B	Control	11.5 ± 3.4	11.4 ± 3.5	13.5 ± 3.5*	12.5 ±3.5*
(bpm)	Diver‡	8.8 ± 3.4	8.8 ± 3.4	10.8 ± 3.4*	9.8 ± 3.5*
$P_{ET}O_2$	Control	98.8 ± 2.4	98.3 ± 2.4	45.6 ± 2.4**	45.0 ± 2.4**
(mmHg)	Diver	100.7 ± 2.1	100.1 ± 2.2	45.7 ± 2.3**	45.1 ± 2.3**
$P_{ET}CO_2$	Control	39.9 ± 2.7	37.9 ± 2.7	39.4 ± 2.7	38.4 ± 2.7
(mmHg)	Diver	41.0 ± 2.6	41.5 ± 2.6	41.5 ± 2.6	42.0 ± 2.7

Table 7.4. Ventilatory Parameters. Ventilatory response to 30 minutes of isocapnic hypoxia in divers and controls on sildenafil and placebo. Abbreviations: f_B, breathing frequency; $P_{ET}CO_2$, end-tidal carbon dioxide; $P_{ET}O_2$, end-tidal oxygen; $\dot{V}_I$, minute ventilation; V_T, tidal volume. * = significantly elevated with hypoxia compared to baseline, p < .0001; ** = significantly decreased with hypoxia compared to baseline, p <.0001. † = significantly larger compared to Controls, p

<.0001, ‡ = significantly smaller compared to Controls, p <.0001 Divers n=15 , Controls = 16, all measures.

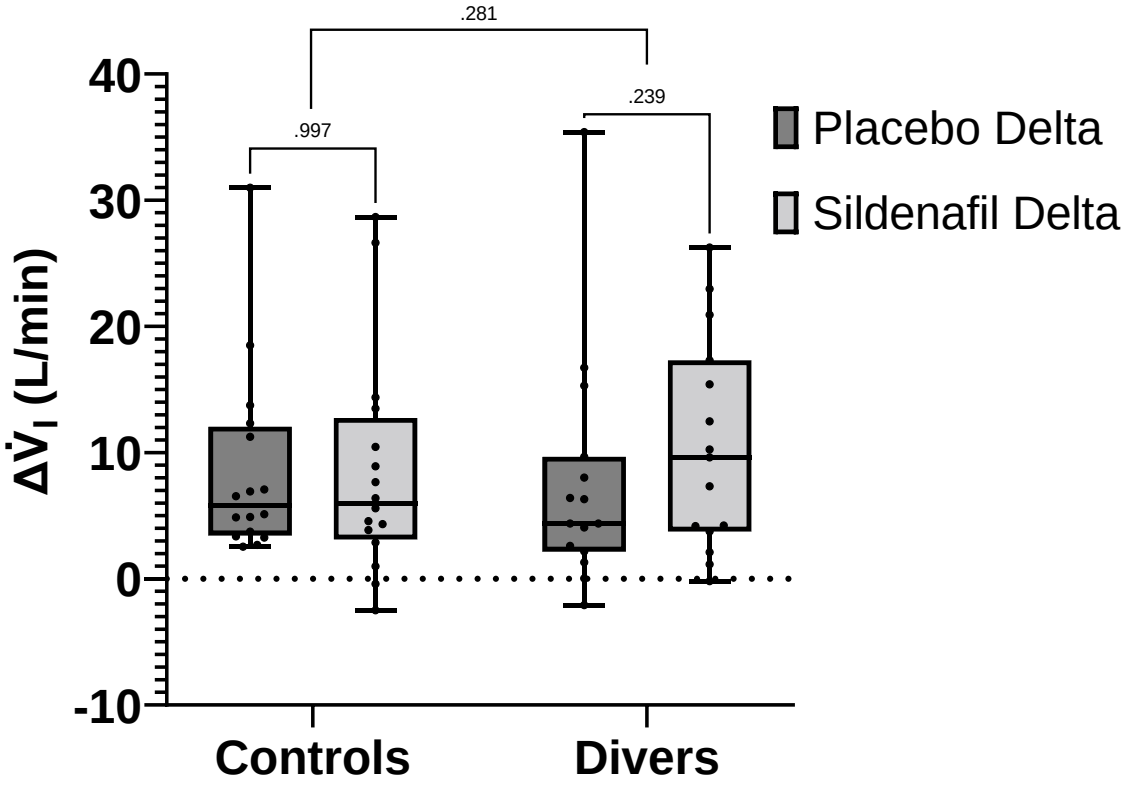

Figure 7.4. $\Delta\dot{V}_I$. $\Delta\dot{V}_I$ was similar between Divers and Controls in response to 20 to 30 minutes hypoxia (p =.281). Sildenafil did not alter Δ V̇I in either Divers or Controls. N = 30 (Divers n = 14, Controls n = 16)

DISCUSSION

The purpose of this study was to compare the cardiopulmonary responses to isocapnic hypoxia with and without sildenafil between apnoea divers and matched controls. The main findings of this study were that 1) Divers had a significantly blunted rise in TPR in response to 20 to 30-minutes hypoxia with placebo, compared to Controls; and 2) with both placebo and sildenafil, Divers had a greater reduction in SVR in response to 20 to 30-minutes hypoxia.

Novel Cardiopulmonary Responses in Apnoea Divers

The above cardiopulmonary characteristics suggest that apnoea divers may have developed a unique set of cardiopulmonary adaptations to the repetitive bouts of hypoxia associated with apnoea diving, independent of any differences in ventilatory chemosensitivity, Divers had a blunted hypoxic pulmonary vasoconstriction in response to isocapnic hypoxia as evidenced by a smaller change in TPR. Divers and Controls had similar changes in PASP, but Divers had a larger (though not statistically significant) increase in Q_T in response to hypoxia that resulted in a significantly blunted change in TPR. This blunted response would allow for the accommodation of increased pulmonary blood flow under hypoxic conditions without an exaggerated increased in pulmonary pressure, as was observed with these Divers, thereby avoiding greater right heart work. Potential explanations for these possibly beneficial adaptive responses to repetitive breath-hold dives may be due to hyperbaria, hypercapnia, hypoxemia, or the combination of all three. This investigation was only designed to investigate the influences of hypoxia associated with apnoea diving, and possible explanations for our findings are discussed below.

Our results indicate that Divers may have a unique cardiopulmonary physiology resulting from months to years of repetitive bouts of hypoxaemia during wakefulness. These results could be explained by a combination of cardiopulmonary adaptations. One possible explanation is that there may be an elevated basal pulmonary artery smooth muscle tone under normoxic conditions in Divers possibly caused by the repetitive hypoxemia of apnoea diving (268, 269). However, Divers had similar total pulmonary resistance at rest compared to Controls (**Table 7.5**) and Divers did not increase pulmonary resistance in response to a 20-to-30 minute hypoxic challenge **(Figure 7.2C**). For there to be normal pulmonary pressures at rest, but no further increase in resistance with hypoxia, and also tonic pulmonary arterial vasoconstriction under normoxia,

Divers would be required to have pulmonary arterioles with larger diameters which allow for tonic vasoconstriction in normoxia but without abnormal pressure elevation for a given Q_T. Intermittent hypoxia has been shown to induce medial thickening (270) and pulmonary hypertension (271). As such, although no direct measures of pulmonary arteriole diameter were made, the authors believe this explanation to be unlikely.

Table 7.5. Mean Values of Cardiopulmonary Outcomes

		Baseline		**30 Minutes Hypoxia**	
		Placebo	**Sildenafil**	**Placebo**	**Sildenafil**
SBP (mmHg)	Control	123.8 ± 9.7	121.6 ± 9.5	140.7 ± 30.5	135.2 ± 19.1
	Diver	123.4 ± 20.1	118.2 ± 14.6	134.3 ± 31.2	134.3 ± 25.5
DBP (mmHg)	Control	80.4 ± 9.9	78.2 ± 5.3	82.5 ± 19.3	80.7 ± 8.8
	Diver	78.4 ± 9.6	72.8 ± 11.7	80.7 ± 13.1	80.4 ± 15.0
MAP (mmHg)	Control	89.7 ± 12.8	87.2 ± 10.3	98.8 ± 22.6	94.1 ± 13.7
	Diver	94.2 ± 15.6	84.5 ± 14.1	100.9 ± 21.0	96.1 ± 24.1
HR (BPM)	Control	65.2 ± 10.2	67.1 ± 13.7	76.0 ± 11.7	78.4 ± 18.7
	Diver	58.8 + 10.7	64.1 + 12.0	72.4 + 17.4	76.1 + 17.3
SV (mL)	Control	79.4 ± 16.6	77.7 ± 19.4	81.6 ± 22.4	80.9 ± 20.9
	Diver	85.3 ± 20.4	94.3 ± 25.1	96.3 ± 22.7	97.3 ± 24.4
SVI (mL/m^2)	Control	42.6 ± 7.7	43.9 ± 11.5	41.6 ± 9.2	43.4 ± 10.5
	Diver	43.9 ± 8.1	50.1 ± 9.3	48.6 ± 10.6	50.7 ± 10.3
Q_T (L/min)	Control	5.11 ± 1.14	6.15 ± 1.82	5.12 ± 1.25	6.22 ± 1.68
	Diver	5.01 ± 1.49	6.83 ± 1.88	5.98 ± 1.82	7.32 ± 2.37

Table 7.5. Mean Values of Cardiopulmonary Outcomes Continued					
CI (L/min/m^2)	Control	2.74 ± 0.53	3.32 ± 0.96	2.77 ± 0.72	3.38 ± 1.05
	Diver	2.59 ± 0.71	3.58 ± 0.90	3.03 ± 0.69	3.84 ± 1.19
TAPSE (mm)	Control	26.1 ± 4.7	26.2 ± 3.4	28.5 ± 2.6	28.4 ± 3.5
	Diver	24.6 ± 2.8	25.2 ± 2.0	26.1 ± 3.1	27.0 ± 2.3
TPR (dynes/sec/cm^{-5})	Control	382.7 ± 96.9	456.4 ± 150.3	368.7 ± 81.7	371.0 ± 121.0
	Diver	401.4 ± 121.7	397.5 ± 111.3	320.1 ± 94.6	353.1 ± 120.5
SVR (dynes/sec/cm^{-5})	Control	1411.6 ± 328.9	1375.5 ± 331.2	1353.6 ± 443.6	1240.4 ± 338.9
	Diver	1405.8 ± 538.0	1070.5 ± 456.0	1088.8 ± 427.5	989.3 ± 423.9

Table 7.5. Mean Values of Cardiopulmonary Outcomes. Mean ± standard deviation. at baseline and after 20 to 30-minutes isocapnic hypoxia under both placebo and sildenafil conditions in Divers and Controls. SBP, DBP, MAP, SVR n = 20 (Divers n = 9, Controls n=11). HR, SV, SVI, Q_T, CI, TAPSE, TPR n = 31 (Divers n =15, Controls n=16)

Another possibility is that the apnoea divers studied had an impairment in the regulation of pulmonary artery smooth muscle tone. While there was a significant main effect of sildenafil in decreasing TPR, this was primarily due to a large decrease in ΔTPR in Controls compared to placebo, i.e. ΔTPR was similar between placebo and sildenafil in Divers (**Figure 7.2C**). Sildenafil acts to augment NO-mediated vasodilation and reduce pulmonary resistance by inhibiting the action of phosphodiesterase 5, an enzyme responsible for catalysing the hydrolysis of cGMP to GMP and leading to reduced phosphorylation of cGMP-dependent protein kinases (272, 273). Reduction in bioavailable NO has been suggested as a potential mechanism of

hypoxic pulmonary vasoconstriction (274). Hypoxia may result in impairment in mitochondrial oxidative phosphorylation, leading to increased generation of reactive oxygen species such as superoxide (87, 275), and subsequent inactivation of K_v channels and activation of L-type calcium channels. Superoxide can bind NO to form peroxinitrite as well as oxidizing tetrahydrobiopterin leading to uncoupling of the eNOS dimer and further generation of reactive oxygen species (87). Some evidence suggests that apnoea diving increases production of reactive oxygen species and peroxinitrites (276) and reduces antioxidant capacity (277) while other evidence suggests that apnoea diving training can reduce oxidative stress in response to exercise while apnoeic (252). We showed that Divers did not have a change in the magnitude of ΔTPR in response to 20 to 30 minutes hypoxia between sildenafil and placebo treatments. This suggests that Divers may generate less ROS in response to hypoxia compared to Controls.

In response to 20 to 30 minutes of hypoxia, there was a larger decrease in ΔSVR with placebo in Divers than in Controls ($p = .021$) (**Figure 7.5**). It should be noted that this effect was primarily driven by one Control subject who a large increase in SVR and one Diver with a large decrease in SVR. Removal of these two subjects from the analysis resulted in the interaction effect no longer being significant ($p = .069$), and also resulting in a significant main effect of sildenafil ($p = .006$) on ΔSVR, (ΔSVR Placebo mean = -223.8 ± 91.2, ΔSVR sildenafil mean = -94.6 ± 36.6). This is consistent with the work of Dinenno, who found that NO is the primary mediator of skeletal muscle vasodilation during hypoxia, as sildenafil acts to augment NO-mediated vasodilation (278).

Figure 7.5. ΔSVR (Next Page). Divers had a larger decrease in ΔSVR with placebo compared to Controls ($p = .021$). (Controls placebo delta n = 14, Controls sildenafil delta n = 16, Divers placebo delta n = 15, Divers sildenafil delta n = 14)

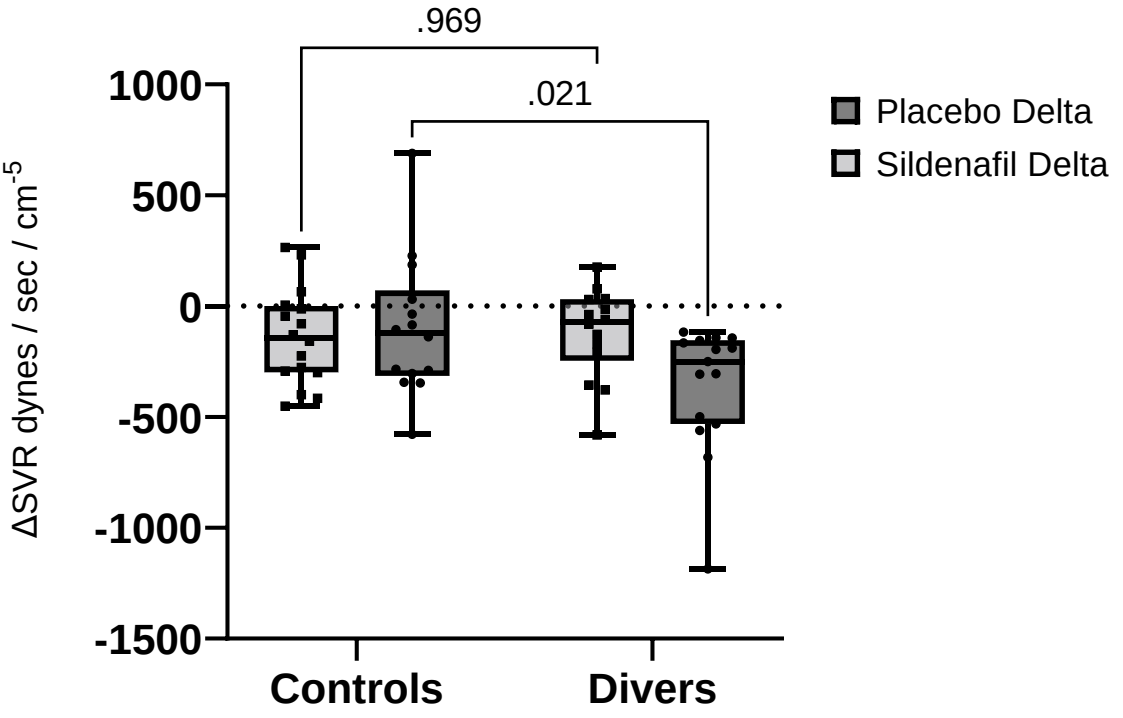

Previous studies have shown that pathological forms of chronic intermittent hypoxia may result in elevated pulmonary vascular pressures and sympathetic activity, though these studies utilized animal models and humans with obstructive sleep apnoea and did not report cardiac output, making it unclear if pulmonary resistance, cardiac output or both were increased (279, 280). Intermittent hypoxia while asleep has been shown to result in increased resting vascular tone, increased mean arterial pressure, and increased MSNA activity which was reversed with decreased frequency of hypoxic episodes (281, 282). However, divers are awake during their intermittent hypoxic episodes, and they do not have a higher resting MAP, which suggests that the consequences of the intermittent hypoxia associated with apnoea diving are less severe. In mouse models, chronic intermittent hypoxia increases left ventricular ejection fraction (283) and cardiac output (284). The lack of difference in left ventricular ejection fraction and cardiac

output between Divers and Controls suggests that Divers do not experience pathological responses to the chronic intermittent hypoxia of diving.

It remains unclear why some forms of chronic intermittent hypoxia such as obstructive sleep apnoea, result in detrimental sequalae, while the chronic intermittent hypoxia of apnoea diving appears to result in beneficial sequelae. These divergent responses to chronic intermittent hypoxia are likely explained by the severity, frequency, and timing of the hypoxia. (27). These results could also be explained if Divers had a weaker stimulus PO_2 due to a relatively higher $P\bar{v}O_2$ compared to Controls. Apnoea divers have been shown to have reduced mitochondrial oxygen consumption in skeletal muscle at rest (234). As the participants were side lying and encouraged to remain still during the hypoxic challenge, Divers may have had lower oxygen consumption. Thus, the reduction in stimulus caused by decreased oxygen consumption and an increased PO_2 would then lead to a reduced degree of hypoxic pulmonary vasoconstriction. However, while direct analysis of blood gasses was not conducted, Divers and Controls showed no differences $P_{ET}O_2$, making it unlikely that there was a meaningful difference in oxygen consumption or $P\bar{v}O_2$ between the groups, and unlikely that the stimulus PO_2 was meaningfully different between Divers and Controls.

The HPV response is also highly variable between individuals (285, 286), with phase 1 of the response usually taking between 20 and 30 minutes to set in (87). As such, it is possible that Divers have a delayed peak pulmonary pressure response, and that this peak may have occurred beyond the 20 to 30 minutes of the hypoxic challenge presented here. Nevertheless, we feel that our findings remain important and useful in that most apnea dives do not last >20 minutes, and therefor these responses would remain a beneficial adaptation for these divers.

Ventilatory Parameters

The present study shows that both Divers and Controls have a similar ventilatory response to 30-minutes of isocapnic hypoxia. In fact, in the present study Divers maintain a comparable $\dot{V}_I$ to Controls under both normoxia and isocapnic hypoxia. These data also indicate that Divers and Controls were exposed to similar hypoxic stimuli (**Table 7.6**). Previous studies interrogating the hypoxic ventilatory response in Divers have yielded mixed results. (241, 287, 288). While previous data suggest that Divers may experience augmented hypoxic ventilatory responses under poikilocapnic conditions (287, 288), when isocapnic hypoxia is used this difference is lost (241). Data from Breskovic et al., (2010) demonstrated that Divers mediate changes in $\dot{V}_I$ primarily through increased V_T, whereas Controls tended to increase f_B. While the present study shows that Divers have a larger V_T and reduced f_B overall compared to Controls, there was no sildenafil x Diving interaction, indicating that increases in both V_T and f_B to 30-minutes of isocapnic hypoxia were comparable between Divers and Controls. The similar recruitment pattern between Divers and Controls in our study may be a result of a longer exposure (i.e. 30-minutes vs 8-minutes of hypoxia) and the use of a single hypoxic step, allowing the psychological response to hypoxia to have subsided by the time of the final measurements. Alternatively, it may be possible that the inclusion of recreational Divers (maximum breath hold < 6 minutes) in the present study may have washed out differences in V_T as they have smaller lung volumes than elite Divers (maximum breath hold > 6 minutes) or utilize different recruitment patterns.

Table 7.6. Acute Hypoxic Ventilatory Response (next page). Divers and Controls had similar acute ventilatory responses to hypoxia. Divers n=16 , Controls = 16, all measures.

Table 7.6. Acute Hypoxic Ventilatory Response				
		Placebo	**Sildenafil**	**p**
Δ $\dot{V}_I$ 5 minutes (L/min)	Control	10.8 ± 7.8	12.2 ± 10.0	.548
	Diver	12.4 ± 9.7	11.5 ± 8.5	
Δ $\dot{V}_I$ 10 minutes (L/min)	Control	9.2 ± 7.7	9.3 ± 9.1	.419
	Diver	8.2 ± 9.5	9.4 ± 6.9	
Δ V_T 5 minutes (L/min)	Control	0.7 ± 0.5	0.7 ± 0.5	.992
	Diver	0.9 ± 0.6	0.8 ± 0.8	
Δ V_T 10 minutes (L/min)	Control	0.6 ± 0.5	0.5 ± 0.4	.339
	Diver	0.7 ± 0.7	0.8 ± 0.9	

LIMITATIONS

Given that hypoxic pulmonary vasoconstriction is not a spatially uniform response (289–291), it is possible that regional changes in pulmonary resistance were not detected. However, this limitation would be true in both Divers and Controls where we and others have detected significant increases in pulmonary pressure and/or pulmonary vascular resistance. Changes in the resistance of the pulmonary circulation can be calculated using either total pulmonary resistance or pulmonary vascular resistance. Total pulmonary resistance includes the contribution from left atrial pressure, whereas pulmonary vascular resistance excludes this contribution. Because left atrial pressure does not increase significantly with hypoxia, using either TPR or PVR should result in different specificities for the vascular resistance value, but

have similar sensitivities. Using right heart catheter data from Operation Everest 2, the specific TPR and PVR were 2.24 and 1.36 respectively, but the change in TPR from room air to breathing 9.5% O_2 was 0.17 Wood units, and the change in PVR was 0.23 (292)

Blood pressure was measured non-invasively using a Finometer device. This device allows for non-invasive tracking of blood pressure, but has been known to result in slightly low measurements of systolic, mean, and diastolic pressures compared to the brachial artery (293). The method utilized by this device correlates well to intra-arterial measures, though systolic (but not diastolic) pressure was significantly different from intra-arterial measures during a cold pressor test only when sign of the difference was considered (294). Reduction in peripheral blood flow would thus be unlikely to impact the measurements that were made utilizing the Finometer device.

PASP and Q_T measurements were measured using ultrasound, an indirect method of assessing pulmonary pressure and pulmonary blood flow. However, these methods have been recommended by the American Society of Echocardiography (201) and shown to be adequate for these measures for the changes expected (256, 295, 296). Furthermore, any error in measurement utilizing these methods would be similar across both Divers and Controls. While TPR was calculated, no direct measurements of left atrial pressure were made, so the contribution of left atrial pressure to pulmonary vascular resistance could not be determined. Nevertheless, hypoxia alone does not increase left atrial pressures (297) so it is unlikely that differences in left atrial pressures would have occurred. While all apnoea divers were experienced, they had achieved differing maximal depths, maximal dive times, dive frequency and dive duration, so represent a heterogenous group in respect to diving. Iron status is known to influence pulmonary vasoreactivity, and iron status was not evaluated. However, there were no

differences in haematocrit between Divers and Controls making differences in iron status unlikely. Maximal apnoeas in well-trained individuals usually last on the order of 5-10 minutes, coinciding with the "fast" component of hypoxic pulmonary vasoconstriction (298). This study did not evaluate, and it is unclear, if repetitive apnoeas modulate the "slow" component of hypoxic pulmonary vasoconstriction, though this is unlikely due to the time course of maximal apnoeas. Trained apnoea Divers regularly experience hyperbaric hypercapnic hypoxia, and the design of this study was unable to explore how repetitive hyperbaria or hypercapnia may have altered the hypoxic pulmonary vasoconstriction response.

While participants were matched on sex and age and were healthy and of similar BMI, it is possible that the differences observed between groups is the result of different fitness levels or athlete lifestyles. It is also possible that Divers self-select into becoming apnoea divers due to having a different physiological response and that these differences are not caused by diving per se. However, Divers represented a homogenous group of athletes and recreational spear-fishers, making it unlikely that lifestyle or self-selection would explain the differences reported.

SUMMARY AND CONCLUSIONS

We evaluated the effect of sildenafil on cardiopulmonary responses to 20-30 minutes of isocapnic hypoxia in 16 practiced apnoea divers and 16 age-, and sex-matched controls. Our findings suggest apnoea divers may have developed unique cardiopulmonary adaptations, including blunted hypoxic pulmonary vasoconstriction and unique systemic vascular responses, in response to a version of chronic intermittent hypoxemia while awake.

CHAPTER VIII

HYPOXIA-INDUCED CHANGES IN TOTAL PULMONARY RESISTANCE ARE NOT ASSOCIATED WITH NITRIC OXIDE, ENDOTHELIN-1, OR INFLAMMATORY CYTOKINES

This chapter was co-authored with Kaitlyn DiMarco, Abigail Cullen, Ashley Walker, and Andrew T. Lovering. Kaitlyn DiMarco performed the multiplex-assay. I was responsible for analysis of multiplex assay results, as well as all other analyses. Abigail Cullen, Ashley Walker, and Andrew T. Lovering assisted in the experimental design. The writing is entirely mine. Editorial assistance was provided by Andrew T. Lovering.

INTRODUCTION

Pulmonary vascular tone is largely regulated via nitric oxide (NO), which is generated by the vascular endothelium. Endothelial nitric oxide synthase (eNOS) converts L-arginine to L-citrulline, and in the process produces NO. NO then diffuses into the vascular smooth muscle cells and initiates a cascade of reactions which ultimately results in vasodilation (299–301). Inflammatory cytokines can interfere with NO-mediated vasodilation as well as serve as markers for other vasoactive substances which oppose vasodilation. This is the case for IL-6, which is increased by the potent vasoconstrictor endothelin-1 (ET-1) (302, 303). TNF-α has been shown to interfere with eNOS expression by downregulating eNOS mRNA (304). TNF-α has also been shown to activate NADPH oxidase, increasing the generation of reactive oxygen species (305), which in turn can interfere with NO-mediated vasodilation by reacting with NO to form peroxynitrite (306), reducing bioavailable NO. Reactive oxygen species can also oxidize tetrahydrobiopterin, leading to eNOS uncoupling (102, 306, 307), which leads to eNOS producing superoxide instead of NO.

We have previously reported that apnea divers have blunted hypoxic pulmonary vasoconstriction in response to a 20- to 30-minute hypoxic challenge (308), which was not altered by the administration of 50mg oral sildenafil. This suggests that apnea divers may have elevated levels of bioavailable nitric oxide, ensuring pulmonary vasodilation even under hypoxic conditions. Additionally, it is well documented that there is significant variability in the hypoxic pulmonary vascular response to hypoxia between individuals, though the reasons for this variability are poorly understood. It is possible that individuals who experience greater increases in pulmonary resistance in response to hypoxia may have increased levels of circulating inflammation which interfere with NO generation by eNOS. Thus, the purpose of this study was twofold. First, we sought to measure the levels of NO, ET-1, and inflammatory cytokines in serum and plasma from apnea divers, non-diving controls, and in participants before and after breathing 11.5% oxygen for 7 to 10 hours. Second, we sought to determine associations between these pulmonary vascular modulators and the pulmonary vascular responses of these individuals to hypoxia. We hypothesized that apnea divers would have greater NO, lower ET-1, and lower inflammatory cytokines compared to non-diving controls because apnea divers have blunted hypoxic pulmonary vasoconstriction. We further hypothesized that in participants breathing 11.5% oxygen for 7 to 10 hours, the participants with the greatest increases in total pulmonary resistance would have the lowest levels of NO, highest levels of ET-1, and highest levels of inflammatory cytokines.

METHODS

Ethical Approval

Ethical approval was secured from the University of Oregon Research Compliance Services and University of Split Medical School (University of Oregon IRB # 07302018.031,

12182010.051, University of Split #2181-198-03-04-19-0052). Each participant gave written informed consent prior to participation and all studies performed after 2013 were performed in accordance with the 2013 Declaration of Helsinki. The Diving study was also registered as a clinical trial (NCT03945643).

Participants

Serum and plasma analyzed in this study were collected from participants in two previous studies. The first study was a 10-hour simulated altitude (FIO2 = .115) study conducted in an environmental chamber. Plasma was collected from participants (n=36, 18 female) prior to (pre-chamber) and at 7-10 hours (during chamber) of exposure to simulated altitude in the environmental chamber, simultaneous with ultrasound measures used to calculate pulmonary artery systolic pressure (PASP) and total pulmonary resistance (TPR). Details regarding participants and methodology have been previously published (44, 309). The second study was a 20- to 30-minute hypoxic challenge (PETO2 ≈ 50 mmHg) in breath-hold divers (n = 16, 4 female) and 16 age- and sex-matched non-diving controls. Serum was collected prior to the hypoxic challenge. Briefly, participants breathed on a dynamic end-tidal forcing system which prospectively delivered a mixture of oxygen, nitrogen, and carbon dioxide to keep end-tidal oxygen at approximately 50 mmHg for 30 minutes. An in-depth explanation of methods and participants of this study has also been previously published (308).

Plasma and Serum Collection

Briefly, a 22 Ga intravenous catheter was aseptically placed into the antecubital vein of the dominant arm. Blood was then drawn into blood collection tubes (VacuTainer, BD). For the chamber study, the blood collection tubes utilized were EDTA-treated for collection of plasma. Tubes were immediately centrifuged at 1500g for 10 minutes. Plasma was then aliquoted and

stored at -80°C until analysis. For the diver study, the blood collection tubes were serum separator tubes (Vacutainer SST, BD). SSTs were allowed to clot at room temperature for 30 minutes, then centrifuged at 1500g for 10 minutes. Serum collected in Eugene, Oregon was then aliquoted and frozen at -80°C until analysis. Serum samples collected in Split, Croatia were stored at -80°C prior to shipment. Samples were shipped to Eugene, Oregon utilizing dry-ice shippers, arrived frozen and were immediately stored at -80°C upon arrival and until analysis.

Pulmonary artery systolic pressure and total pulmonary resistance: Ultrasound measures of tricuspid regurgitation velocity, left ventricular outflow tract velocity time integral, and left ventricular outflow tract cross sectional area were collected in all participants. PASP was calculated from the modified Bernoulli equation: PASP = 4v2 + PRA where v is the velocity of the tricuspid regurgitation jet and PRA is the pressure of the right atrium as measured by collapse of the inferior vena cava during the "sniff test" estimating right atrial pressure (PRA) from the degree of collapse of the inferior vena cava, as has been done previously (44, 308). Stroke volume was calculated as the product of the left-ventricular outflow tract velocity time integral and the left-ventricular outflow tract cross sectional area, and cardiac output (QT) was calculated as the product of stroke volume and heart rate. Total pulmonary resistance (TPR) was calculated as TPR = PASP/QT. Ultrasound images and measurements were made by trained echocardiographers.

Nitric Oxide and Endothelin-1 ELISAs

Prior to analysis, samples were removed from storage at thawed on ice immediately prior to use. Nitric oxide (NO) levels were measured utilizing a nitrate/nitrite assay kit (Total Nitric Oxide and Nitrate/Nitrite Parameter Assay kit, R&D Systems, Inc.). This kit measures endogenous nitrite as well as nitrate utilizing nitrate reductase. This allows for calculation of the

concentration of nitrate, a stable down-stream metabolite of the reactive oxygen species NO. In accordance with manufacturer instructions, samples were purified with a 10kDa centrifugal filter (Amicon Ultra 0.5 Centrifugal Filter Unit, Millipore Sigma) prior to analysis. Plates were read in a microplate reader (Synergy HT, Biotek) at 590nm with a correction reading at 640nm. Two pairs of samples from the Diver study were not included due to insufficient volume of sample after centrifugal filtration.

Endothelin-1 levels were measured utilizing an ELISA kit (Endothelin-1 Human ELISA Kit, Invitrogen) according to the manufacturer's instructions. Per these instructions, samples were purified with the provided extraction solution prior to analysis. Plates were read in a microplate reader at 540nm (Synergy HT, Biotek). Hemolyzed serum and plasma were unsuitable, per the manufacturer's instructions, for use in this assay. Accordingly, 6 samples from the chamber study were not analyzed for ET-1 due to one or both serum samples being hemolyzed and 3 samples from the Diver study were not analyzed due to hemolysis.

Inflammatory Cytokines

Cytokine levels were measured using a bead-based multiplex assay which uses fluorescence-encoded beads suitable for use on flow cytometers (LegendPlex Human Inflammation Panel 1, BioLegend). This assay measures IL-1β, IFN-α2, IFN-γ, TNF-α, MCP-1, IL-6, IL-8, IL-10, IL-12p70, IL-17A, IL-18, IL-23, and IL-33. Briefly, beads are conjugated with specific antibodies for the listed analytes and serve as capture beads. When introduced to the sample, these beads conjugate with their specific analyte. Beads are then washed and a biotinylated detection antibody added, followed by streptavidin-phycoerythrin, which binds to the detection antibody. The bead will then fluoresce at an intensity proportional to the amount of bound analyte. Bead capture was conducted with a flow cytometer (Gallios, Beckman Coulter)

Statistical Analysis

All statistical analysis was performed in GraphPad Prism 10 (v10.0.2; GraphPad, San Diego, CA, USA). Analytes which were below the level of detection for the method of quantification were excluded from analysis. For the environmental chamber study, levels of cytokines, total nitrate, and ET-1 were compared pre- and 7-10 hour exposure utilizing a paired t-test with $\alpha = .05$. Samples which did not have a corresponding time point (i.e. both before and during chamber exposure) were excluded from the analysis (n=8). ET-1, total nitrate, and inflammatory cytokines were analyzed for correlation with PASP and TPR both before and during chamber exposure, as well as the magnitude of change in PASP and TPR between these timepoints (e.g. ΔPASP and ΔTPR) . For the diving study, baseline levels of cytokines, total nitrate, and ET-1 were compared between divers and non-diving controls utilizing a paired t-test with $\alpha = .05$. Additionally, baseline cytokines, total nitrate, and ET-1 were analyzed for correlation with PASP and TPR before and after the hypoxic challenge, as well as the change in these values. Correlation significance was set at $\alpha = .05$.

RESULTS

ET-1, Total Nitrate

ET-1 was significantly elevated post-chamber ($p = .006$) (Table 1). There were no significant correlations of ET-1 with any pulmonary measures. Total nitrate was not different pre- to post-chamber ($p = .093$) (Table 1). Total nitrate was not correlated with any pulmonary measurements before or following chamber exposure.

Table 8.1 (Next Page) Cytokines, ET-1, and Total Nitrate in Plasma Taken From Participants Before and at 7-10 Hours in an Environmental Chamber Breathing 11.5% Oxygen. Pre- and post-chamber values were compared using a paired t-test. Correlations displays Spearman's r-value and according p-value. * = Significant different pre- to post-

environmental chamber. † = Significant correlation between analyte and pulmonary vascular measure

Table 8.1. Cytokines, ET-1, and Total Nitrate in Plasma Taken From Participants Before and at 7-10 Hours in an Environmental Chamber Breathing 11.5% Oxygen

		Value	p	PASP Pre-Chamber		PASP Post-Chamber		ΔPASP		TPR Pre-Chamber		TPR Post-Chamber		ΔTPR	
				r	p	r	p	r	p	r	p	r	p	r	p
IL-1β (pg/mL)	Pre n=24	9.81 ± 11.49	.639	-.152	.467	-.035	.873	-.018	.932	-.161	.453	.223	.307	.299	.167
	Post n=24	9.12 ± 10.09		-.001	.823	-.005	.693	.082	.638	-.254	.141	-.011	.950	-.191	.286
IFN-α2 (pg/mL)	Pre n=30	10.07 ± 9.91	.433	-.310	.090	.035	.862	.154	.415	-.173	.361	.201	.304	.272	.161
	Post n=30	10.99± 11.29		-.104	.552	.028	.875	.103	.555	-.239	.166	.041	.821	.185	.304
IFN-γ (pg/mL)	Pre n=33	4.92 ± 6.53	.051	-.105	.553	-.062	.739	-.042	.815	.013	.944	.011	.955	-.012	.950
	Post n=33	3.23 ± 4.03		-.087	.621	-.040	.825	.040	.820	.078	.654	-.051	.780	-.102	.571
TNF-α (pg/mL)	Pre n=31	6.65 ± 8.06	.491	-.124	.498	.152	.432	.246	.182	-.174	.349	.255	.182	.314	.098
	Post n=31	7.46 ± 11.71		-.162	.353	.050	.784	.139	.425	-.154	.379	.077	.670	.161	.372
MCP-1 (pg/mL)	Pre n=34	90.81± 25.84	.016*	.259	.133	-.125	.497	-.174	.326	.252	.151	-.298	.097	-.417	.018†
	Post n=34	78.84± 20.88		-.009	.959	-.083	.646	-.034	.846	.061	.728	-.105	.563	-.145	.420
IL-6 (pg/mL)	Pre n=29	5.33 ± 7.42	.021*	.039	.836	.049	.810	.035	.859	-.128	.508	.241	.227	.259	.193
	Post n=29	11.10± 12.83		.202	.244	.024	.894	.194	.264	-.056	.751	-.057	.755	.075	.680
IL-8 (pg/mL)	Pre n=33	7.21 ± 8.51	.366	-.055	.836	-.040	.831	-.020	.912	-.025	.892	.110	.554	.085	.648
	Post n=33	8.70 ± 6.15		-.039	.824	-.010	.955	.135	.439	-.192	.269	.110	.542	.206	.250
IL-10 (pg/mL)	Pre n=29	10.2 ± 12.15	<.001*	-.084	.637	.269	.144	.301	.089	-.151	.401	.341	.060	.384	.033†
	Post n=29	17.1 ± 17.56		-.015	.938	.088	.643	.148	.427	-.223	.227	-.007	.971	.157	.407
IL-12p70	Pre n=34	2.44 ± 3.29	<.001*	-.030	.865	.318	.076	.387	.024†	-.094	.598	.451	.010†	.451	.010†
	Post n=34	4.72 ± 5.30		-.071	.687	.081	.654	.208	.230	-.162	.352	.109	.545	.211	.239
IL-17A (pg/mL)	Pre N=32	1.59 ± 1.66	<.001*	-.112	.535	.303	.104	.323	.071	.349	.050	.295	.113	-.032	.867
	Post n=32	3.03 ± 2.65		-.066	.708	-.016	.928	.095	.586	.040	.817	-.002	.993	-.027	.881
IL-18 (pg/mL)	Pre n=34	38.78± 21.91	<.001*	.066	.708	-.056	.760	-.099	.578	.368	.033†	.078	.671	-.361	.043†
	Post n=34	53.90± 19.36		-.102	.561	-.190	.291	-.143	.411	.127	.466	-.099	.584	-.191	.286
IL-23 (pg/mL)	Pre n=34	7.67 ± 7.03	.591	-.255	.139	-.052	.775	-.054	.760	.039	.826	.105	.569	.261	.149
	Post n=34	8.34 ± 6.43		-.070	.688	-.049	.787	.087	.619	-.136	.435	.084	.644	.145	.421
IL-33 (pg/mL)	Pre n=34	129.1± 141.1	.234	-.068	.699	.126	.492	.219	.214	-.138	.438	.215	.238	.261	.149
	Post n=34	104.9± 87.73		.039	.823	-.071	.693	-.013	.941	-.172	.324	-.001	.997	.110	.541

Table 8.1. Cytokines, ET-1, and Total Nitrate in Plasma Taken From Participants Before and at 10 Hours in an Environmental Chamber Breathing 11.5% Oxygen (Continued)

ET-1 (pg/mL)	Pre n=26	13.57 ± 7.35	.006*	-.333	.072	-.094	.636	-.038	.846	-.163	.399	.053	.787	.147	.457
	Post n=26	16.05 ± 7.00		-.010	.957	.019	.918	.024	.897	-.183	.324	.171	.358	.262	.155
Total Nitrate (μmol/L)	Pre n=29	51.45± 38.71	.093	-.171	.334	.095	.613	.206	.249	-.185	.302	.100	.593	.195	.294
	Post n=29	63.50± 33.42		-.163	.381	-.154	.410	-.086	.647	-.172	.356	.016	.934	.128	.493

Neither baseline total nitrate ($p = .884$) nor baseline ET-1 ($p = .632$) were different between divers and non-diving controls (Table 2). Neither baseline total nitrate nor baseline ET-1 were correlated with any pulmonary measurements in either divers or non-diving controls (Table 2).

Table 8.2. (Next page) Cytokines, ET-1, and Total Nitrate in Serum Taken From Apnea Divers and Age- and Sex-Matched Non-Diving Controls. Values were compared between Divers and Controls using a paired t-test. Correlations displays Spearman's r-value and according p-value. * = Significant different pre- to post-environmental chamber. † = Significant correlation between analyte and pulmonary vascular measure

Table 8.2. Cytokines, ET-1, and Total Nitrate in Plasma Taken From Apnea Divers and Age- and Sex-Matched Non-Diving Controls

		Value	p	PASP Pre-Hypoxia		PASP Post-Hypoxia		ΔPASP		TPR Pre-Hypoxia		TPR Post-Hypoxia		ΔTPR	
				r	p	r	p	r	p	r	p	r	p	R	P
IL-1β (pg/mL)	Diver n=4	132.7 ± 168.4	.987	-.418	.409	-.017	.974	.285	.585	.718	.108	.626	.184	-.473	.344
	Control n=4	135.2 ± 158.6		.133	.714	.271	.449	.239	.506	-.130	.722	.109	.764	.434	.210
IFN-α2 (pg/mL)	Diver n=15	10.94 ±9.32	.026*	.067	.811	-.094	.738	-.169	.548	-.092	.743	.022	.936	.189	.500
	Control n=15	36.47 ± 38.55		.345	.208	.261	.347	.024	.932	.057	.840	.081	.774	.075	.792
IFN-γ (pg/mL)	Diver n=12	11.62 ± 13.07	.256	.015	.958	-.253	.384	-.321	.263	.070	.813	.087	.767	.016	.955
	Control n=12	24.22 ± 32.71		.302	.316	.136	.658	-.104	.735	-.145	.636	.043	.889	.199	.515
TNF-α (pg/mL)	Diver n=10	12.61 ± 13.41	.037*	.034	.903	-.091	.747	-.139	.621	-.016	.955	.008	.978	.039	.891
	Control n=10	149.1 ± 173.4		-.066	.848	.024	.945	.086	.802	-.401	.222	-.428	.190	-.259	.441
MCP-1 (pg/mL)	Diver n=15	463.5 ± 324.3	.712	.007	.979	.111	.695	.130	.645	.231	.408	.014	.960	-.364	.182
	Control n=15	425.7 ± 177.0		.085	.763	.103	.715	.057	.841	-.310	.261	-.116	.680	.121	.669
IL-6 (pg/mL)	Diver n=14	10.53 ± 16.89	.124	-.347	.205	-.132	.639	.111	.693	.319	.247	.253	.364	-.147	.602
	Control n=14	25.14 ± 28.93		.208	.475	.010	.736	-.064	.826	.109	.711	.185	.527	.196	.503
IL-8 (pg/mL)	Diver n=2	52.83 ± 53.54	.287	-.455	.306	-.178	.702	.134	.775	.096	.838	-.102	.828	-.550	.201
	Control n=2	310.7 ± 123.3		.190	.652	.578	.137	.614	.105	-.326	.430	-.044	.917	.174	.681
IL-10 (pg/mL)	Diver n=16	20.30 ± 33.56	.131	.080	.776	-.378	.165	-.526	.044	-.452	.091	-.538	.039†	-.066	.814
	Control n=16	54.28 ± 68.05		-.160	.570	.222	.427	.439	.102	.141	.617	.314	.254	.369	.176
IL-12p70 (pg/mL)	Diver n=11	6.77 ± 10.48	.488	.201	.530	.171	.577	.305	.311	-.280	.354	.113	.712	.641	.018
	Control n=11	10.39 ± 12.72		-.122	.502	-.169	.581	-.422	.151	-.015	.960	-.120	.697	-.169	.582
IL-17A (pg/mL)	Diver n=12	2.24 ± 3.23	.193	-.340	.259	-.298	.323	-.131	.669	.302	.316	.133	.666	-.336	.262
	Control n=12	7.81 ± 12.54		.081	.783	.130	.658	.105	.722	-.206	.480	-.177	.546	-.087	.768
IL-18 (pg/mL)	Diver n=15	551.6 ± 527.2	.984	.357	.192	.386	.156	.191	.495	.090	.749	.099	.725	.001	.997
	Control n=15	547.2 ± 645.2		.050	.860	-.018	.950	-.069	.806	-.269	.333	-.095	.736	.114	.687
IL-23 (pg/mL)	Diver n=10	18.76 ± 24.70	.561	-.178	.560	-.290	.337	-.201	.510	.232	.445	.155	.612	-.153	.618
	Control n=10	25.68 ± 25.96		.246	.419	.232	.445	.080	.795	.025	.934	.203	.506	.299	.321

Table 8.2. Cytokines, ET-1, and Total Nitrate in Plasma Taken From Apnea Divers and Age- and Sex-Matched Non-Diving Controls (Continued)

IL-33 (pg/mL)	Diver n=14	716.1 ± 698.6	.122	-.058	.845	-.162	.581	-.160	.585	.189	.517	.158	.590	-.037	.899
	Control n=14	340.2 ± 296.7		.473	.075	.269	.332	-.084	.765	.019	.946	.078	.783	.107	.704
ET-1 (pg/mL)	Diver n=13	17.89 ± 7.33	.632	.069	.806	-.129	.648	-.212	.448	.147	.602	-.074	.793	-.358	.190
	Control n=13	18.92 ± 8.17		.257	.398	.289	.338	.114	.712	-.302	.315	-.056	.857	.206	.499
Total Nitrate (μmol/L)	Diver n=14	28.39 ± 14.97	.883	.115	.683	.124	.659	.062	.827	.164	.559	.159	.572	-.032	.910
	Control n=14	27.27 ± 22.29		-.122	.679	.089	.762	.226	.437	.299	.300	-.247	.396	-.094	.750

Cytokines

Several cytokines were elevated at 7-10 hours of exposure to hypoxia in the environmental chamber (Table 1). IL-12p70 ($p = < .001$), IL-17A ($p < .001$), MCP-1 ($p = .016$), IL-18 ($p < .001$), IL-10 ($p = .001$) and IL-6 ($p = .021$) were all significantly elevated at the post-chamber timepoint compared to the pre-chamber time point. Pre-chamber levels of IL-12p70 were correlated with ΔPASP ($r = .387$, $p = .024$) and ΔTPR ($r = .451$, $p = .001$). Pre-chamber levels of IL-18 were correlated with pre-chamber TPR ($r = .368$, $p = .033$) and ΔTPR ($r = -.361$, $p = .043$). Pre-chamber MCP-1 was correlated with ΔTPR ($r = -.417$, $p = .018$), as was pre-chamber IL-10 ($r = .384$, $p = .033$) (Table 1).

Most baseline cytokines were similar between Divers and Controls. However, IFN-α2 was significantly higher in non-diving controls than divers ($p = .026$), as was TNF-α ($p = .037$) (Table 2). IL-10 was correlated to ΔPASP in Divers ($r = -.526$, $p = .044$) and TPR during hypoxia ($r = -.538$, $p = .039$) in Divers. IL-12p70 was correlated with ΔTPR in Divers ($r = .641$, $p = .018$) (Table 2).

DISCUSSION

In the environmental chamber study, we hypothesized that in response to 7-10 hours in an environmental chamber breathing 11.5% oxygen there would be increased ET-1, lower total nitrate, and an increase in circulating inflammatory cytokines. We also hypothesized that those individuals who displayed the largest increases in PASP and TPR following hypoxia would have the largest changes in ET-1, total nitrate, and inflammatory markers. Our results support our hypothesis that ET-1 and some cytokines would be increased following 7-10 hours breathing 11.5% oxygen. However, our results do not support our hypotheses regarding correlations between PASP, TPR, and the investigated analytes.

In the breath-hold diver study, we hypothesized that apnea divers would have higher levels of total nitrate, lower levels of ET-1, and lower levels of circulating inflammatory cytokines. We found that divers had lower levels of IFN-α2 and TNF-α, as well as that IL-10 and IL-12p70 were correlated to ΔPASP and ΔTPR in breath-hold divers. We interpret these findings as largely unsupportive of our hypotheses.

ET-1

ET-1 is a strong vasoconstrictor released from the vascular endothelium (Yanagisawa et al., 1988) and elevations in plasma ET-1 have previously been associated with exaggerated pulmonary vascular pressure (310). Twenty four hours of moderate hypoxia (FIO2 = 0.10) increased plasma ET-1 in rats (311, 312). ET-1 has also been suggested to "prime" pulmonary arterial smooth muscle cells to contract in response to hypoxia by modulating K+ or Ca2+ channels and sensitivity (313). This has been suggested as an explanation for ET-1's function as a pulmonary vasoconstrictor (314). ET-1 has also been suggested to contribute to increased pulmonary resistance in chronic hypoxia by promoting proliferation of vascular smooth muscle (315, 316). However, this is unlikely to meaningfully contribute to increases in pulmonary pressure after only 7-10 hours of hypoxic exposure. Regardless, our finding that ET-1 increased after 7-10 hours of exposure to 11.5% oxygen is an expected outcome and aligns with our hypothesis.

We unexpectedly found that increases in ET-1 following hypoxia were not correlated with either increases in PASP or TPR following hypoxia. Total nitrate was also not associated with ET-1 levels. There is ample evidence to support that the oxygen sensing mechanism for hypoxic pulmonary vasoconstriction exists within the vascular smooth muscle cells themselves and may directly effect Kv1.5 channels or Ca2+ channels (87). This suggests that while ET-1 is

increased by hypoxia, it has minimal impact on hypoxic pulmonary vasoconstriction in response to short-term moderate hypoxia. ET-1's association with increase pulmonary vascular pressures may be more strongly related to ET-1's mitogenic effects than any meaningful impact on acute pulmonary vasoconstriction. Other studies exposing humans to altitude have shown positive correlations between venous plasma levels of ET-1 and pulmonary PASP, though these studies utilize hypobaric hypoxia and hypoxia measures of ET-1 were taken at 22 hours as opposed to 10 hours (109). However, other studies have shown that endothelin receptor blockade did not inhibit HPV in response to 15 minutes of hypoxia (317), suggesting that ET-1 may have strong vasoconstrictive effects in normoxia but does not have a significant role in HPV. Our findings of elevated ET-1 following 10 hours of moderate hypoxia, but no correlations with pulmonary pressure or resistance, support this interpretation.

We further found that ET-1 levels were not different between apnea divers and non-diving controls and that there was no correlation with ET-1 and pulmonary measures in either group. Other models of chronic intermittent hypoxia, such as obstructive sleep apnea, have shown both higher levels of plasma ET-1 (318), and that ET-1 was correlated with a worse apnea-hypoxia index (319). ET-1 has also been correlated with oxygen saturation and mean arterial pressure (320), though these correlations were only of modest strength. We have previously reported that, unlike OSA, chronic intermittent hypoxia of apnea diving does not appear to lead to negative sequelae. The lack of difference in ET-1 between Divers and Controls may present a potential step in further understanding why these two forms of chronic intermittent hypoxia have divergent physiological outcomes.

Total Nitrate

We found no difference in total nitrate following 10 hours of breathing 11.5% oxygen in an environmental chamber, nor did we find differences in total nitrate between Divers and Controls. NO, produced by NO synthases, can enter the blood where it can rapidly react with oxygen to form nitrite, which in turn can be reduced to nitrate (156). As such, by analyzing the level of total nitrate in the blood, we are able to make reasonable inferences as to the level of NO in the blood. Our findings suggest that, based on total nitrate levels, NO levels are not different following 10 hours breathing 11.5% oxygen in an environmental chamber, and that basal NO levels are not different between apnea Divers and Controls.

NO has been well-established as a potent vasodilator. NO produced by endothelial nitric oxide synthase (eNOS) diffuses from the endothelial cell to the vascular smooth muscle where it activates soluble guanylate cyclase, leading to increased cGMP which in turn activates protein kinase G thereby inhibiting calcium influx. The reduction in calcium then leads to relaxation and vasodilation. Alterations in the activity of downstream regulators of this pathway can alter the vasodilatory response – for example, sildenafil acts as a phosophodiesterase-5 (PDE5) inhibitor, preventing PDE5 from degrading cGMP and thereby augmenting this pathway independent of NO production (321). The effects of hypoxia on the production of NO, and indeed reactive oxygen species in general, has been a matter under significant debate. Some studies have shown increases in NO production in response to hypoxia (322), though this was not associated with changes in the actual diameter of hypoxia-exposed microvessels. Other studies have shown decreases in "exhaled" NO in response to hypoxia in isolated, perfused rabbit lungs (323) and pig lungs (324) suggesting a reduced production of NO in hypoxia. Our findings that NO was not significantly altered by 10 hours of breathing 11.5% oxygen in intact humans suggest that NO is not a major mediator of pulmonary vascular tone in humans exposed to moderate hypoxia.

This is further supported by our finding that NO was not different between Divers and Controls, despite blunted hypoxic pulmonary vasoconstriction in Divers (308).

Cytokines

Following 10 hours of breathing 11.5% oxygen in an environmental chamber, we found increases in IL-12p70, IL-17A, MCP-1, IL-18, IL-10, IL-6, though these differences were generally of a modest magnitude (Table 1). Additionally, pre-chamber IL-12p70 was correlated with ΔPASP and ΔTPR while pre-chamber levels of IL-18, MCP-1, and IL-10 were correlated with ΔTPR.

In general, these cytokines do not appear to have any established relationship with regulation of pulmonary vascular tone, despite associations with hypoxia. IL-12p70 is the bioactive form of IL-12 and is released from dendritic immune cells (325), and hypoxia can alter the phenotypical expression of these cells leading to increased release of IL-12p70 during hypoxia (326). Similarly, IL-17A is associated with release from immune cells under hypoxic conditions (327). IL-17A has also been shown to be associated with hypoxic pulmonary hypertension, and was elevated in humans with COPD-related hypoxic pulmonary hypertension (111). However, this association was primarily related to proliferation of pulmonary artery smooth muscle cells and vascular remodeling seen in chronic hypoxia as opposed to acute changes in pulmonary resistance. Hypoxia has been shown to increase serum MCP-1 levels (328), and increases in MCP-1 have been associated with hypoxia-related increases in pulmonary vascular pressure (329), as has IL-18 (330). Interestingly, a similar cytokine profile has been observed in pediatric acute respiratory distress syndrome (331), suggesting a possible link between these cytokines and pulmonary injury. In conjunction with our findings correlating these cytokines to increases in pulmonary resistance in response to hypoxia, this suggests that

these cytokines may influence pulmonary vasoreactivity in response to the "injury" of hypoxia. However, the effects and interactions of these molecules are highly complex, and this explanation remains highly speculative. Additionally, these correlations are of only moderate strength and may not reflect physiological interactions.

In the Diving study, we found that Divers had significantly lower levels of TNF-α and IFN-α2 compared to non-diving Controls. TNF- α has been show to increase generation of reactive oxygen species through NADPH oxidases (305). Reactive oxygen species can scavenge NO to form peroxinitrite (306), reducing bioavailable NO. Reactive oxygen species can also uncouple the eNOS dimer, leading to the production of superoxide as opposed to NO (102). IFN-α has been shown to oxidize deplete tetrahydrobiopterin, a necessary cofactor for eNOS to produce NO (332, 333). IFN-α has also been implicated in reducing L-arginine availability, the substrate from which NO is synthesized (334, 335). Comparatively lower levels of these cytokines in Divers compared to Controls suggests that Divers may have more bioavailable NO under hypoxic conditions. However, no post-hypoxia blood samples were collected, so this remains speculative.

LIMITATIONS

We utilized an ELISA method to analyze total nitrate in plasma and serum. We assumed the eNOS-generated nitric oxide would be a primary source for nitrate. However, nitrate can be generated from other sources such as digestion of some foods (156). Nitrate is also excreted by kidneys, allowing diuresis to influence blood nitrate level. Neither diet nor diuresis were controlled for, which may have led to over- or under-estimates of total nitrate, respectively. Given that one of the well-documented physiological adjustments to a hypoxic environment is increased diuresis to remove excess bicarbonate from the blood, it is possible that the post-

chamber blood samples underestimated the generation of NO by eNOS due to elevated nitrate excretion as a result of increased diuresis.

Many cytokines follow a circadian pattern with levels of circulating cytokines fluctuating throughout the day. Circadian misalignment and sleep deprivation can increase levels of inflammatory cytokines (336). While the AMS study had participants start and end at approximately the same time every day due to the duration spent in the chamber, the BHD study was less well-controlled due to varying availability of participants. Neither study questioned participants on sleep deprivation or their normal sleep-wake cycle. Additionally, some participants altered their normal sleep-wake cycle in order to undergo lab visits early in the morning, potentially leading to sleep deprivation and elevated cytokine levels in the pre-chamber blood samples. This may potentially have masked a relative increase in cytokines following 10 hours of exposure to hypoxia.

SUMMARY AND CONCLUSION

We examined circulating levels of ET-1, total nitrate, and numerous cytokines before and after 10 hours of breathing 11.5% oxygen as well as in apnea Divers and non-diving Controls and attempted to correlate these bioactive molecules with measures of pulmonary resistance in response to hypoxia. We found that ET-1 increased following 10 hours of breathing 11.5% oxygen, but there was no effect on total nitrate, and ET-1 levels were not associated with any pulmonary vascular measures. We found that some, but not all, of the investigated cytokines were associated with changes in pulmonary resistance though explanations for this finding remain speculative. We additionally found that ET-1 and total nitrate were not different between apnea Divers and non-diving Controls and that these analytes were not correlated with any pulmonary vascular measures.

We interpret our findings to show that increases in pulmonary resistance in response to 10 hours breathing 11.5% oxygen are not mediated by ET-1 or NO, though it remains unclear if the correlations between some inflammatory cytokines and pulmonary vascular measures are indicative of physiological relationships or are simply spurious correlations. We further interpret our findings to show that apnea divers do not have elevated production of NO nor blunted production of ET-1, and that neither of these molecules are explanatory for previous findings of blunted hypoxic pulmonary vasoconstriction in apnea divers. Further research in this area should focus on other molecules which can regulate pulmonary tone, such as bradykinins and prostaglandins, as well as whether other elements of the NO mediated vasodilatory pathway (such as PDE5 activity) are altered in apnea divers.

CHAPTER IX

CONCLUSIONS

The primary objectives of this dissertation were to better understand how 1) a patent foramen ovale may influence pulmonary gas exchange efficiency at rest and during exercise and 2) apnea diving leads to a blunted hypoxic pulmonary vasoconstriction. To achieve the first objective, we examined how sex assigned at birth and PFO size interact to influence pulmonary gas exchange efficiency and we quantified the effect of percutaneous PFO closure on pulmonary gas exchange efficiency. To achieve the second objective, we examined the prevalence of PFO in apnea divers, examined changes in total pulmonary resistance in apnea divers in response to a 20- to 30-minute isocapnic hypoxic challenge, and then investigated whether apnea divers had altered levels of nitric oxide, endothelin-1, or inflammatory cytokines compared to controls as well as investigating whether these same factors were altered in individuals breathing 11.5% O_2 for 7-10 hours.

MAIN FINDINGS

In Chapter IV I tested the hypothesis that individuals with a large PFO, as classified by TTSCE bubble score, would have worse pulmonary gas exchange efficiency compared to those with no or small PFO, and that this difference would be greatest in females. The findings of this study partially supported this hypothesis. The data showed that the presence or size of PFO did not worsen pulmonary gas exchange efficiency in males, but in females the presence of a large PFO was associated with significantly worse pulmonary gas exchange efficiency – particularly at moderate to strenuous exercise workloads. This finding may be related to increased airway resistance in women, secondary to anatomically smaller airways, thereby necessitating more severe changes in intrathoracic pressure to achieve the same alveolar ventilation. The more

dramatic changes in intrathoracic pressure may facilitate greater right atrial pressures relative to left atrial pressure, encouraging right-to-left intracardiac shunt and impaired pulmonary gas exchange efficiency, however this was not directly measured.

In Chapter V I tested the hypothesis that percutaneous closure of PFO would improve pulmonary gas exchange efficiency. Following percutaneous PFO closure, the alveolar to arterial difference in oxygen decreased approximately 50% at rest and during exercise, strongly supporting our hypothesis of improved pulmonary gas exchange efficiency following PFO closure. This improvement in pulmonary gas exchange efficiency was primarily the result of increased arterial PO_2, which I interpret to be caused by reduced right-to-left intracardiac shunt. However, these data were only obtained in females, and it is unclear if these findings are also generalizable to males.

In Chapter VI I tested the hypothesis that patent foramen ovale would be more prevalent in apnea divers compared to non-diving controls. The results of this study show that PFO is significantly more common in apnea divers. It remains unclear as to whether this is a matter of self-selection, whereby the presence of a PFO facilitates apnea diving such as by functioning as a "blow off valve" to partially mitigate increases in pulmonary vascular pressure, or if some facet of diving results in PFO being more detectable in apnea divers.

In Chapter VII I examined the hypothesis that apnea divers would have impaired right-heart function compared to non-diving controls because of increased pulmonary artery pressure related to diving and hypoxia. I unexpectedly found that apnea divers had a significantly blunted increase in total pulmonary resistance in response to a 20- to 30-minutes of an isocapnic hypoxic challenge compared to non-diving controls, and that the administration of sildenafil did not

further reduce pulmonary resistance. I interpret this novel and unexpected finding as evidence of blunted hypoxic pulmonary vasoconstriction in apnea divers.

In Chapter VIII I examined the hypothesis that apnea divers would have lower levels of inflammation, increased levels of total nitrate, and lower levels of endothelin-1 compared to non-diving controls. I additionally hypothesized that after spending 7-10 hours breathing 11.5% oxygen, non-apnea diving participants would have increased levels of inflammation, decreased levels of total nitrate, and increased levels of endothelin-1 and that these vascular mediators would be associated with changes in total pulmonary resistance. The results of this study were largely unsupportive of these hypotheses. I found that total nitrate and endothelin-1 were not different between apnea divers and non-diving controls and that total nitrate was unchanged following 7-10 hours breathing 11.5% oxygen, though there was a slight increase in endothelin-1. I further found that inflammatory cytokines were not associated with changes in pulmonary vascular pressure or resistance in divers, non-diving controls, or after 7-10 hours of breathing 11.5% oxygen. I did find however, that apnea divers had lower levels of TNF-α and IFN-α2 suggesting that apnea divers may produce lower levels of reactive oxygen species in response to hypoxia. I interpreted these findings to show that divers did not have greater levels of bioavailable nitric oxide nor reduced levels of endothelin-1, and that neither nitric oxide nor endothelin-1 were associated with increased total pulmonary resistance after 7-10 hours of breathing 11.5% oxygen.

IMPLICATIONS AND FUTURE DIRECTIONS

This dissertation has shown that patent foramen ovale can negatively impact pulmonary gas exchange efficiency under the right circumstances. However, there is still significant work to be done to understand why patent foramen ovale impairs pulmonary gas exchange in females

but not males. I have hypothesized that this may be due to differences in breathing mechanics in females compared to males, but this remains to be tested, as we made neither measures of intrathoracic pressure nor the power of breathing. Future studies which include these measures may be able to explain why females, but not males, with large PFO have impaired pulmonary gas exchange efficiency during moderate to high intensity exercise.

Similarly, our findings that percutaneous closure of PFO improved pulmonary gas exchange efficiency were the result of data collected only from females. As such, it remains unclear whether males experience similar improvements in pulmonary gas exchange efficiency following PFO closure. This question is particularly interesting given our findings in Chapter IV. It may very well be, given that large PFO only impaired pulmonary gas exchange efficiency in females, percutaneous PFO closure is only effective at improving gas exchange in females but not males. Studies examining changes in pulmonary gas exchange efficiency in males following percutaneous PFO closure would add significantly to this area of knowledge.

The finding that apnea divers have significantly blunted hypoxic pulmonary vasoconstriction was a novel and unexpected result. Chronic intermittent hypoxia is usually associated with a variety of negative sequelae (51, 281, 320) that appear to be absent in apnea divers. It remains unclear why the chronic intermittent hypoxia of apnea diving does not lead to negative sequelae, and there is a tantalizing possibility that apnea training may be the reason. Given the relative simplicity of apnea training, this may be a ripe avenue of research as a treatment for hypoxic pulmonary hypertension (World Health Organization Group 3). Further areas of research to identify the mechanism(s) which allow apnea divers to blunt hypoxic pulmonary vasoconstriction may look at the nitric-oxide mediated vasodilatory pathway,

particularly whether there are differences in the activity of phosphodiesterase-5 may also be fruitful, as sildenafil did not alter HPV in divers.

It is my hope that the information contained in this dissertation will inform future research directions, particularly in better understanding why pulmonary gas exchange efficiency is more negatively affected by the presence of a PFO in females compared to males. Additionally, the information regarding blunted hypoxic pulmonary vasoconstriction in apnea divers may lead to future clinical intervention strategies for some types of pulmonary hypertension, which remains a lethal disease without a cure.

REFERENCES CITED

1. **Aird WC**. Discovery of the cardiovascular system: from Galen to William Harvey. *J Thromb Haemost* 9: 118–129, 2011. doi: 10.1111/j.1538-7836.2011.04312.x.

2. **Rigatelli G**, **Zuin M**. Leonardo da Vinci and patent foramen ovale: An historical perspective. *Int J Cardiol* 222: 826, 2016. doi: 10.1016/j.ijcard.2016.08.079.

3. **da Vinci L**. *Leonardo Da Vinci on the Human Body: The Anatomical, Physiological and Embryological Drawings of Leonardo Da Vinci with Translations, Emendations and a Biographical Introduction*. H. Schuman, 1952.

4. **Shoja MM**, **Agutter PS**, **Loukas M**, **Benninger B**, **Shokouhi G**, **Namdar H**, **Ghabili K**, **Khalili M**, **Tubbs RS**. Leonardo da Vinci's studies of the heart. *Int J Cardiol* 167: 1126–1133, 2013. doi: 10.1016/j.ijcard.2012.09.078.

5. **West JB**. A Century of Pulmonary Gas Exchange. *Am J Respir Crit Care Med* 169: 897–902, 2004. doi: 10.1164/rccm.200312-1781OE.

6. **Krogh A**. On the Oxygen-Metabolism of the Blood 1. *Skand Arch Für Physiol* 23: 193–199, 1910.

7. **Beutner A**. Ueber die Strom-und Druckkräfte des Blutes in der Arteria und Vena pulmonales. .

8. **Young JM**, **Williams DR**, **Thompson AAR**. Thin Air, Thick Vessels: Historical and Current Perspectives on Hypoxic Pulmonary Hypertension. *Front Med* 6: 93, 2019. doi: 10.3389/fmed.2019.00093.

9. **Park MH**. Historical Perspective on the Classification and Nomenclature of Pulmonary Hypertension. In: *Pulmonary Hypertension: Basic Science to Clinical Medicine*, edited by Maron BA, Zamanian RT, Waxman AB. Springer International Publishing, p. 3–15.

10. **Romberg E**. Ueber Sklerose der Lungen arterie. *Dtsch Archiv Klin Med* 48: 197–206, 1891.

11. **Euler US v**, **Liljestrand G**. Observations on the Pulmonary Arterial Blood Pressure in the Cat. *Acta Physiol Scand* 12: 301–320, 1946. doi: 10.1111/j.1748-1716.1946.tb00389.x.

12. **Lumb AB**, **Nunn JF**. Nunn's applied respiratory physiology [Online]. 7th ed. Churchill Livingstone, Elsevier. http://www.123library.org/book_details/?id=46803 [30 May 2023].

13. **Widrich J**, **Shetty M**. Physiology, Pulmonary Vascular Resistance [Online]. In: *StatPearls*. StatPearls Publishing http://www.ncbi.nlm.nih.gov/books/NBK554380/ [11 May 2022].

14. **Marshall BE**, **Marshall C**. A model for hypoxic constriction of the pulmonary circulation. *J Appl Physiol* 64: 68–77, 1988. doi: 10.1152/jappl.1988.64.1.68.

15. **Lovering AT**, **Kelly TS**, **DiMarco KG**, **Bradbury KE**, **Charkoudian N**. Implications of a patent foramen ovale for environmental physiology and pathophysiology: do we know the 'hole' story? *J Physiol* 600: 1541–1553, 2022. doi: 10.1113/JP281108.

16. **Crapo RO**, **Morris AH**, **Clayton PD**, **Nixon CR**. Lung volumes in healthy nonsmoking adults. *Bull Eur Physiopathol Respir* 18: 419–425, 1982.

17. **Schwartz J**, **Katz SA**, **Fegley RW**, **Tockman MS**. Sex and race differences in the development of lung function. *Am Rev Respir Dis* 138: 1415–1421, 1988. doi: 10.1164/ajrccm/138.6.1415.

18. **Torres-Tamayo N**, **García-Martínez D**, **Lois Zlolniski S**, **Torres-Sánchez I**, **García-Río F**, **Bastir M**. 3D analysis of sexual dimorphism in size, shape and breathing kinematics of human lungs. *J Anat* 232: 227–237, 2018. doi: 10.1111/joa.12743.

19. **Romei M**, **Mauro AL**, **D'Angelo MG**, **Turconi AC**, **Bresolin N**, **Pedotti A**, **Aliverti A**. Effects of gender and posture on thoraco-abdominal kinematics during quiet breathing in healthy adults. *Respir Physiol Neurobiol* 172: 184–191, 2010. doi: 10.1016/j.resp.2010.05.018.

20. **Martin TR**, **Castile RG**, **Fredberg JJ**, **Wohl ME**, **Mead J**. Airway size is related to sex but not lung size in normal adults. *J Appl Physiol* 63: 2042–2047, 1987. doi: 10.1152/jappl.1987.63.5.2042.

21. **McClaran SR**, **Harms CA**, **Pegelow DF**, **Dempsey JA**. Smaller lungs in women affect exercise hyperpnea. *J Appl Physiol Bethesda Md 1985* 84: 1872–1881, 1998. doi: 10.1152/jappl.1998.84.6.1872.

22. **Sheel AW**, **Guenette JA**. Mechanics of Breathing during Exercise in Men and Women: Sex versus Body Size Differences? *Exerc Sport Sci Rev* 36: 128, 2008. doi: 10.1097/JES.0b013e31817be7f0.

23. **Guzman CA**, **Summers ED**. Pulmonary Diffusing Capacity during Exercise in Women. *Chest* 64: 678–682, 1973. doi: 10.1378/chest.64.6.678.

24. **Bouwsema MM**, **Tedjasaputra V**, **Stickland MK**. Are there sex differences in the capillary blood volume and diffusing capacity response to exercise? *J Appl Physiol* 122: 460–469, 2017. doi: 10.1152/japplphysiol.00389.2016.

25. **Molgat-Seon Y**, **Peters CM**, **Sheel AW**. Sex-differences in the human respiratory system and their impact on resting pulmonary function and the integrative response to exercise. *Curr Opin Physiol* 6: 21–27, 2018. doi: 10.1016/j.cophys.2018.03.007.

26. **Hopkins SR**, **Harms CA**. Gender and Pulmonary Gas Exchange During Exercise. *Exerc Sport Sci Rev* 32: 50, 2004.

27. **Navarrete-Opazo A**, **Mitchell GS**. Therapeutic potential of intermittent hypoxia: a matter of dose. *Am J Physiol-Regul Integr Comp Physiol* 307: R1181–R1197, 2014. doi: 10.1152/ajpregu.00208.2014.

28. **Lyamina NP**, **Lyamina SV**, **Senchiknin VN**, **Mallet RT**, **Downey HF**, **Manukhina EB**. Normobaric hypoxia conditioning reduces blood pressure and normalizes nitric oxide synthesis in patients with arterial hypertension. *J Hypertens* 29: 2265–2272, 2011. doi: 10.1097/HJH.0b013e32834b5846.

29. **Querido JS**, **Sheel AW**, **Cheema R**, **Van Eeden S**, **Mulgrew AT**, **Ayas NT**. Effects of 10 days of modest intermittent hypoxia on circulating measures of inflammation in healthy humans. *Sleep Breath Schlaf Atm* 16: 657–662, 2012. doi: 10.1007/s11325-011-0555-4.

30. **Serebrovskaya TV**, **Nikolsky IS**, **Nikolska VV**, **Mallet RT**, **Ishchuk VA**. Intermittent hypoxia mobilizes hematopoietic progenitors and augments cellular and humoral elements of innate immunity in adult men. *High Alt Med Biol* 12: 243–252, 2011. doi: 10.1089/ham.2010.1086.

31. **Patrician A**, **Dujić Ž**, **Spajić B**, **Drviš I**, **Ainslie PN**. Breath-Hold Diving – The Physiology of Diving Deep and Returning. *Front Physiol* 12: 582, 2021. doi: 10.3389/fphys.2021.639377.

32. **Sanz J**, **S ánchez-QD**, **Bossone E**, **Bogaard HJ**, **Naeije R**. Anatomy, Function, and Dysfunction of the Right Ventricle. *J Am Coll Cardiol* 73: 1463–1482, 2019. doi: 10.1016/j.jacc.2018.12.076.

33. **Bosco G**, **Rizzato A**, **Martani L**, **Schiavo S**, **Talamonti E**, **Garetto G**, **Paganini M**, **Camporesi EM**, **Moon RE**. Arterial Blood Gas Analysis in Breath-Hold Divers at Depth. *Front Physiol* 9: 1558, 2018. doi: 10.3389/fphys.2018.01558.

34. **Lindholm P**, **Lundgren CEG**. Alveolar gas composition before and after maximal breath-holds in competitive divers. *Undersea Hyperb Med J Undersea Hyperb Med Soc Inc* 33: 463–467, 2006.

35. **Ambler DR**, **Fletcher NM**, **Diamond MP**, **Saed GM**. Effects of hypoxia on the expression of inflammatory markers IL-6 and TNF-a in human normal peritoneal and adhesion fibroblasts. *Syst Biol Reprod Med* 58: 324–329, 2012. doi: 10.3109/19396368.2012.713439.

36. **Hung M-J**, **Cherng W-J**, **Hung M-Y**, **Wu H-T**, **Pang J-HS**. Interleukin-6 inhibits endothelial nitric oxide synthase activation and increases endothelial nitric oxide synthase binding to stabilized caveolin-1 in human vascular endothelial cells. *J Hypertens* 28: 940, 2010. doi: 10.1097/HJH.0b013e32833992ef.

37. **Guzik TJ**, **Korbut R**, **Adamek-Guzik T**. Nitric oxide and superoxide in inflammation and immune regulation. *J Physiol Pharmacol Off J Pol Physiol Soc* 54: 469–487, 2003.

38. **Takeshi S**, **Masashi Y**, **Tomoh M**. Molecular characterization of endothelin receptors. *Trends Pharmacol Sci* 13: 103–108, 1992.

39. **Alonso D**, **Radomski MW**. The Nitric Oxide-Endothelin-1 Connection. *Heart Fail Rev* 8: 107–115, 2003. doi: 10.1023/A:1022155206928.

40. **Nybo L**, **Rasmussen P**. Inadequate Cerebral Oxygen Delivery and Central Fatigue during Strenuous Exercise. *Exerc Sport Sci Rev* 35: 110, 2007. doi: 10.1097/jes.0b013e3180a031ec.

41. **Amann M**, **Calbet JAL**. Convective oxygen transport and fatigue. *J Appl Physiol* 104: 861–870, 2008. doi: 10.1152/japplphysiol.01008.2007.

42. **Hellstrom G**, **Fischer-Colbrie W**, **Wahlgren NG**, **Jogestrand T**. Carotid artery blood flow and middle cerebral artery blood flow velocity during physical exercise. *J Appl Physiol* 81: 413–418, 1996. doi: 10.1152/jappl.1996.81.1.413.

43. **Ogoh S**, **Ainslie PN**. Cerebral blood flow during exercise: mechanisms of regulation. *J Appl Physiol* 107: 1370–1380, 2009. doi: 10.1152/japplphysiol.00573.2009.

44. **Duke JW**, **Beasley KM**, **Speros JP**, **Elliott JE**, **Laurie SS**, **Goodman RD**, **Futral E**, **Hawn JA**, **Lovering AT**. Impaired pulmonary gas exchange efficiency, but normal pulmonary artery pressure increases, with hypoxia in men and women with a patent foramen ovale. *Exp Physiol* 105: 1648–1659, 2020. doi: 10.1113/EP088750.

45. **Lovering AT**, **Stickland MK**, **Amann M**, **O'Brien MJ**, **Hokanson JS**, **Eldridge MW**. Effect of a patent foramen ovale on pulmonary gas exchange efficiency at rest and during exercise. *J Appl Physiol* 110: 1354–1361, 2011. doi: 10.1152/japplphysiol.01246.2010.

46. **Devuyst G**, **Piechowski-Jóźwiak B**, **Karapanayiotides T**, **Fitting J-W**, **Kémeny V**, **Hirt L**, **Urbano LA**, **Arnold P**, **van Melle G**, **Despland P-A**, **Bogousslavsky J**. Controlled Contrast Transcranial Doppler and Arterial Blood Gas Analysis to Quantify Shunt Through Patent Foramen Ovale. *Stroke* 35: 859–863, 2004. doi: 10.1161/01.STR.0000119384.28376.EB.

47. **Dominelli PB**, **Molgat-Seon Y**. Sex, gender and the pulmonary physiology of exercise. *Eur Respir Rev* 31, 2022. doi: 10.1183/16000617.0074-2021.

48. **Kelly T**, **Patrician A**, **Bryant-Ekstrand M**, **Brown C**, **Gasho C**, **Caldwell HG**, **Lord RN**, **Dawkins T**, **Drane A**, **Stembridge M**, **Dragun T**, **Barak O**, **Spajić B**, **Drviš I**, **Duke JW**, **Foster GE**, **Ainslie PN**, **Dujić Ž**, **Lovering AT**. High prevalence of patent foramen ovale in recreational to elite breath hold divers. .

49. **Garvey JF**, **Taylor CT**, **McNicholas WT**. Cardiovascular disease in obstructive sleep apnoea syndrome: the role of intermittent hypoxia and inflammation. *Eur Respir J* 33: 1195–1205, 2009. doi: 10.1183/09031936.00111208.

50. **Rio RD**, **Moya EA**, **Parga MJ**, **Madrid C**, **Iturriaga R**. Carotid body inflammation and cardiorespiratory alterations in intermittent hypoxia. *Eur Respir J* 39: 1492–1500, 2012. doi: 10.1183/09031936.00141511.

51. **Ryan S**, **Taylor CT**, **McNicholas WT**. Selective Activation of Inflammatory Pathways by Intermittent Hypoxia in Obstructive Sleep Apnea Syndrome. *Circulation* 112: 2660–2667, 2005. doi: 10.1161/CIRCULATIONAHA.105.556746.

52. **Lai PFH**, **Mohamed F**, **Monge J-C**, **Stewart DJ**. Downregulation of eNOS mRNA expression by TNFα: identification and functional characterization of RNA–protein interactions in the 3'UTR. *Cardiovasc Res* 59: 160–168, 2003. doi: 10.1016/S0008-6363(03)00296-7.

53. **Wang MC**, **Corbridge TC**, **McCrimmon DR**, **Walter JM**. Teaching an intuitive derivation of the clinical alveolar equations: mass balance as a fundamental physiological principle. *Adv Physiol Educ* 44: 145–152, 2020. doi: 10.1152/advan.00064.2019.

54. **Riley RL**, **Lilienthal JL**. On the determination of the physiologically effective pressures of oxygen and carbon dioxide in alveolar air. *Am J Physiol* 147: 191–198, 1946. doi: 10.1152/ajplegacy.1946.147.1.191.

55. **Warren GL**, **Cureton KJ**, **Middendorf WF**, **Ray CA**, **Warren JA**. Red blood cell pulmonary capillary transit time during exercise in athletes. *Med Sci Sports Exerc* 23: 1353–1361, 1991.

56. **Reeves JT**, **Moon RE**, **Grover RF**, **Groves BM**. Increased Wedge Pressure Facilitates Decreased Lung Vascular Resistance during Upright Exercise. *CHEST* 93: 97S-99S, 1988. doi: 10.1378/chest.93.3_Supplement.97S.

57. **D'Angelo E**, **Salvo Calderini I**, **Tavola M**. The Effects of CO2on Respiratory Mechanics in Anesthetized Paralyzed Humans. *Anesthesiology* 94: 604–610, 2001. doi: 10.1097/00000542-200104000-00013.

58. **Wagner PD**. Ventilation-Perfusion Matching during Exercise. *Chest* 101: 192S-198S, 1992. doi: 10.1378/chest.101.5_Supplement.192S.

59. **Gale GE**, **Torre-Bueno JR**, **Moon RE**, **Saltzman HA**, **Wagner PD**. Ventilation-perfusion inequality in normal humans during exercise at sea level and simulated altitude. *J Appl Physiol* 58: 978–988, 1985. doi: 10.1152/jappl.1985.58.3.978.

60. **Hopkins SR**, **McKenzie DC**, **Schoene RB**, **Glenny RW**, **Robertson HT**. Pulmonary gas exchange during exercise in athletes. I. Ventilation-perfusion mismatch and diffusion limitation. *J Appl Physiol* 77: 912–917, 1994. doi: 10.1152/jappl.1994.77.2.912.

61. **Hammond MD**, **Gale GE**, **Kapitan KS**, **Ries A**, **Wagner PD**. Pulmonary gas exchange in humans during exercise at sea level. *J Appl Physiol* 60: 1590–1598, 1986. doi: 10.1152/jappl.1986.60.5.1590.

62. **Torre-Bueno JR**, **Wagner PD**, **Saltzman HA**, **Gale GE**, **Moon RE**. Diffusion limitation in normal humans during exercise at sea level and simulated altitude. *J Appl Physiol* 58: 989–995, 1985. doi: 10.1152/jappl.1985.58.3.989.

63. **Elliott JE**, **Nigam SM**, **Laurie SS**, **Beasley KM**, **Goodman RD**, **Hawn JA**, **Gladstone IM**, **Chesnutt MS**, **Lovering AT**. Prevalence of left heart contrast in healthy, young, asymptomatic humans at rest breathing room air. *Respir Physiol Neurobiol* 188: 71–78, 2013. doi: 10.1016/j.resp.2013.04.019.

64. **Hagen PT**, **Scholz DG**, **Edwards WD**. Incidence and Size of Patent Foramen Ovale During the First 10 Decades of Life: An Autopsy Study of 965 Normal Hearts. *Mayo Clin Proc* 59: 17–20, 1984. doi: 10.1016/S0025-6196(12)60336-X.

65. **Woods TD**, **Patel A**. A Critical Review of Patent Foramen Ovale Detection Using Saline Contrast Echocardiography: When Bubbles Lie. *J Am Soc Echocardiogr* 19: 215–222, 2006. doi: 10.1016/j.echo.2005.09.023.

66. **Fenster BE**, **Curran-Everett D**, **Freeman AM**, **Weinberger HD**, **Buckner JK**, **Carroll JD**. Saline Contrast Echocardiography for the Detection of Patent Foramen Ovale in Hypoxia: A Validation Study Using Intracardiac Echocardiography. *Echocardiography* 31: 420–427, 2014. doi: https://doi.org/10.1111/echo.12403.

67. **Thurlbeck WM**. Postnatal human lung growth. *Thorax* 37: 564–571, 1982. doi: 10.1136/thx.37.8.564.

68. **Guenette JA**, **Witt JD**, **McKenzie DC**, **Road JD**, **Sheel AW**. Respiratory mechanics during exercise in endurance-trained men and women. *J Physiol* 581: 1309–1322, 2007. doi: 10.1113/jphysiol.2006.126466.

69. **Guenette JA**, **Querido JS**, **Eves ND**, **Chua R**, **Sheel AW**. Sex differences in the resistive and elastic work of breathing during exercise in endurance-trained athletes. *Am J Physiol-Regul Integr Comp Physiol* 297: R166–R175, 2009. doi: 10.1152/ajpregu.00078.2009.

70. **Sheel AW**, **Dominelli PB**, **Molgat-Seon Y**. Revisiting dysanapsis: sex-based differences in airways and the mechanics of breathing during exercise. *Exp Physiol* 101: 213–218, 2016. doi: 10.1113/EP085366.

71. **Dominelli PB**, **Molgat-Seon Y**, **Sheel AW**. Sex Differences in the Pulmonary System Influence the Integrative Response to Exercise. *Exerc Sport Sci Rev* 47: 142, 2019. doi: 10.1249/JES.0000000000000188.

72. **Sheel AW**, **Derchak PA**, **Morgan BJ**, **Pegelow DF**, **Jacques AJ**, **Dempsey JA**. Fatiguing inspiratory muscle work causes reflex reduction in resting leg blood flow in humans. *J Physiol* 537: 277–289, 2001. doi: 10.1111/j.1469-7793.2001.0277k.x.

73. **Smith JR**, **Broxterman RM**, **Hammer SM**, **Alexander AM**, **Didier KD**, **Kurti SP**, **Barstow TJ**, **Harms CA**. Sex differences in the cardiovascular consequences of the inspiratory muscle metaboreflex. *Am J Physiol Regul Integr Comp Physiol* 311: R574-581, 2016. doi: 10.1152/ajpregu.00187.2016.

74. **Nakhjavan FK**, **Palmer WH**, **Mcgregor M**. Influence of Respiration on Venous Return in Pulmonary Emphysema. *Circulation* 33: 8–16, 1966. doi: 10.1161/01.CIR.33.1.8.

75. **Xu Y**, **Yamashiro T**, **Moriya H**, **Tsubakimoto M**, **Tsuchiya N**, **Nagatani Y**, **Matsuoka S**, **Murayama S**. Hyperinflated lungs compress the heart during expiration in COPD patients: a new finding on dynamic-ventilation computed tomography. *Int J Chron Obstruct Pulmon Dis* 12: 3123–3131, 2017. doi: 10.2147/COPD.S145599.

76. **Korth P**, **Bohle RM**, **Corvol P**, **Pinet F**. Cellular distribution of endothelin-converting enzyme-1 in human tissues. *J Histochem Cytochem Off J Histochem Soc* 47: 447–462, 1999. doi: 10.1177/002215549904700403.

77. **Yanagisawa M**, **Kurihara H**, **Kimura S**, **Tomobe Y**, **Kobayashi M**, **Mitsui Y**, **Yazaki Y**, **Goto K**, **Masaki T**. A novel potent vasoconstrictor peptide produced by vascular endothelial cells. *Nature* 332: 411–415, 1988. doi: 10.1038/332411a0.

78. **Davenport AP**. International Union of Pharmacology. XXIX. Update on Endothelin Receptor Nomenclature. *Pharmacol Rev* 54: 219–226, 2002. doi: 10.1124/pr.54.2.219.

79. **Holm P**. Endothelin in the pulmonary circulation with special reference to hypoxic pulmonary vasoconstriction. *Scand Cardiovasc J Suppl* 46: 1–40, 1997.

80. **Ivy DD**, **McMurtry IF**, **Yanagisawa M**, **Gariepy CE**, **Le Cras TD**, **Gebb SA**, **Morris KG**, **Wiseman RC**, **Abman SH**. Endothelin B receptor deficiency potentiates ET-1 and hypoxic pulmonary vasoconstriction. *Am J Physiol-Lung Cell Mol Physiol* 280: L1040–L1048, 2001. doi: 10.1152/ajplung.2001.280.5.L1040.

81. **Griendling KK**, **Tsuda T**, **Alexander RW**. Endothelin stimulates diacylglycerol accumulation and activates protein kinase C in cultured vascular smooth muscle cells. *J Biol Chem* 264: 8237–8240, 1989.

82. **Simonson MS**, **Dunn MJ**. Cellular signaling by peptides of the endothelin gene family. *FASEB J* 4: 2989–3000, 1990. doi: 10.1096/fasebj.4.12.2168326.

83. **Furchgott RF**, **Carvalho MH**, **Khan MT**, **Matsunaga K**. Evidence for Endothelium-Dependent Vasodilation of Resistance Vessels by Acetylcholine. *J Vasc Res* 24: 145–149, 1987. doi: 10.1159/000158689.

84. **Chen C-A**, **Druhan LJ**, **Varadharaj S**, **Chen Y-R**, **Zweier JL**. Phosphorylation of Endothelial Nitric-oxide Synthase Regulates Superoxide Generation from the Enzyme *. *J Biol Chem* 283: 27038–27047, 2008. doi: 10.1074/jbc.M802269200.

85. **Klinger JR**. The Nitric Oxide/cGMP Signaling Pathway in Pulmonary Hypertension. *Clin Chest Med* 28: 143–167, 2007. doi: 10.1016/j.ccm.2006.12.002.

86. **Furchgott RF**. Role of endothelium in responses of vascular smooth muscle. *Circ Res* 53: 557–573, 1983. doi: 10.1161/01.RES.53.5.557.

87. **Sylvester JT**, **Shimoda LA**, **Aaronson PI**, **Ward JPT**. Hypoxic Pulmonary Vasoconstriction. *Physiol Rev* 92: 154, 2012.

88. **Marshall C**, **Marshall B**. Site and sensitivity for stimulation of hypoxic pulmonary vasoconstriction. *J Appl Physiol* 55: 711–716, 1983. doi: 10.1152/jappl.1983.55.3.711.

89. **Archer SL**, **Huang J**, **Henry T**, **Peterson D**, **Weir EK**. A redox-based O2 sensor in rat pulmonary vasculature. *Circ Res* 73: 1100–1112, 1993. doi: 10.1161/01.RES.73.6.1100.

90. **Sommer N**, **Strielkov I**, **Pak O**, **Weissmann N**. Oxygen sensing and signal transduction in hypoxic pulmonary vasoconstriction. *Eur Respir J* 47: 288–303, 2016. doi: 10.1183/13993003.00945-2015.

91. **Aaronson PI**. Hypoxic pulmonary vasoconstriction is/is not mediated by increased production of reactive oxygen species. *J Appl Physiol* 101: 1000–1002, 2006. doi: 10.1152/japplphysiol.00680.2006.

92. **Ward JPT**. Point:Counterpoint: Hypoxic pulmonary vasoconstriction is/is not mediated by increased production of reactive oxygen species. *J Appl Physiol* 101: 993–995, 2006. doi: 10.1152/japplphysiol.00480.2006.

93. **Weir EK**, **Archer SL**. Counterpoint: hypoxic pulmonary vasoconstriction is not mediated by increased production of reactive oxygen species. *J Appl Physiol* 101: 995–998, 2006. doi: 10.1152/japplphysiol.00480a.2006.

94. **Weir EK**, **Archer SL**. Last Word: Point:Counterpoint authors respond to commentaries on "Hypoxic pulmonary vasoconstriction is/is not mediated by increased production of reactive oxygen species." *J Appl Physiol* 101: 1005–1005, 2006. doi: 10.1152/japplphysiol.00707.2006.

95. **Han D**, **Antunes F**, **Canali R**, **Rettori D**, **Cadenas E**. Voltage-dependent Anion Channels Control the Release of the Superoxide Anion from Mitochondria to Cytosol *. *J Biol Chem* 278: 5557–5563, 2003. doi: 10.1074/jbc.M210269200.

96. **Post JM**, **Hume JR**, **Archer SL**, **Weir EK**. Direct role for potassium channel inhibition in hypoxic pulmonary vasoconstriction. *Am J Physiol-Cell Physiol* 262: C882–C890, 1992. doi: 10.1152/ajpcell.1992.262.4.C882.

97. **Yuan XJ**, **Goldman WF**, **Tod ML**, **Rubin LJ**, **Blaustein MP**. Hypoxia reduces potassium currents in cultured rat pulmonary but not mesenteric arterial myocytes. *Am J Physiol-Lung Cell Mol Physiol* 264: L116–L123, 1993. doi: 10.1152/ajplung.1993.264.2.L116.

98. **Stuehr DJ**, **Santolini J**, **Wang Z-Q**, **Wei C-C**, **Adak S**. Update on Mechanism and Catalytic Regulation in the NO Synthases *. *J Biol Chem* 279: 36167–36170, 2004. doi: 10.1074/jbc.R400017200.

99. **Chen W**, **Druhan LJ**, **Chen C-A**, **Hemann C**, **Chen Y-R**, **Berka V**, **Tsai A-L**, **Zweier JL**. Peroxynitrite induces destruction of the tetrahydrobiopterin and heme in endothelial nitric oxide synthase: transition from reversible to irreversible enzyme inhibition. *Biochemistry* 49: 3129–3137, 2010. doi: 10.1021/bi9016632.

100. **Kuzkaya N**, **Weissmann N**, **Harrison DG**, **Dikalov S**. Interactions of Peroxynitrite, Tetrahydrobiopterin, Ascorbic Acid, and Thiols: IMPLICATIONS FOR UNCOUPLING ENDOTHELIAL NITRIC-OXIDE SYNTHASE *. *J Biol Chem* 278: 22546–22554, 2003. doi: 10.1074/jbc.M302227200.

101. **Landmesser U**, **Dikalov S**, **Price SR**, **McCann L**, **Fukai T**, **Holland SM**, **Mitch WE**, **Harrison DG**. Oxidation of tetrahydrobiopterin leads to uncoupling of endothelial cell nitric oxide synthase in hypertension. *J Clin Invest* 111: 1201–1209, 2003. doi: 10.1172/JCI14172.

102. **Yang Y-M**, **Huang A**, **Kaley G**, **Sun D**. eNOS uncoupling and endothelial dysfunction in aged vessels. *Am J Physiol - Heart Circ Physiol* 297: H1829–H1836, 2009. doi: 10.1152/ajpheart.00230.2009.

103. **Radi R**. Peroxynitrite, a Stealthy Biological Oxidant. *J Biol Chem* 288: 26464–26472, 2013. doi: 10.1074/jbc.R113.472936.

104. **Li H**, **Chen SJ**, **Chen YF**, **Meng QC**, **Durand J**, **Oparil S**, **Elton TS**. Enhanced endothelin-1 and endothelin receptor gene expression in chronic hypoxia. *J Appl Physiol* 77: 1451–1459, 1994. doi: 10.1152/jappl.1994.77.3.1451.

105. **Gras E**, **Belaidi E**, **Briançon-Marjollet A**, **Pépin J-L**, **Arnaud C**, **Godin-Ribuot D**. Endothelin-1 mediates intermittent hypoxia-induced inflammatory vascular remodeling through HIF-1 activation. *J Appl Physiol* 120: 437–443, 2016. doi: 10.1152/japplphysiol.00641.2015.

106. **Kanagy NL**, **Walker BR**, **Nelin LD**. Role of Endothelin in Intermittent Hypoxia-Induced Hypertension. *Hypertension* 37: 511–515, 2001. doi: 10.1161/01.HYP.37.2.511.

107. **Shirakami G**, **Nakao K**, **Saito Y**, **Magaribuchi T**, **Jougasaki M**, **Mukoyama M**, **Arai H**, **Hosoda K**, **Suga S**, **Ogawa Y**, **Yamada T**, **Mori K**, **Imura H**. Acute pulmonary alveolar hypoxia increases lung and plasma endothelin-1 levels in conscious rats. *Life Sci* 48: 969–976, 1991. doi: 10.1016/0024-3205(91)90362-F.

108. **Cargill RI**, **Kiely DG**, **Clark RA**, **Lipworth BJ**. Hypoxaemia and release of endothelin-1. *Thorax* 50: 1308–1310, 1995. doi: 10.1136/thx.50.12.1308.

109. **Goerre S**, **Wenk M**, **Bärtsch P**, **Lüscher TF**, **Niroomand F**, **Hohenhaus E**, **Oelz O**, **Reinhart WH**. Endothelin-1 in pulmonary hypertension associated with high-altitude exposure. *Circulation* 91: 359–364, 1995. doi: 10.1161/01.cir.91.2.359.

110. **Morganti A**, **Giussani M**, **Sala C**, **Gazzano G**, **Marana I**, **Pierini A**, **Savoia MT**, **Ghio F**, **Cogo A**, **Zanchetti A**. Effects of exposure to high altitude on plasma endothelin-1 levels in normal subjects. *J Hypertens* 13: 859–865, 1995. doi: 10.1097/00004872-199508000-00006.

111. **Wang L**, **Liu J**, **Wang W**, **Qi X**, **Wang Y**, **Tian B**, **Dai H**, **Wang J**, **Ning W**, **Yang T**, **Wang C**. Targeting IL-17 attenuates hypoxia-induced pulmonary hypertension through downregulation of β-catenin. *Thorax* 74: 564–578, 2019. doi: 10.1136/thoraxjnl-2018-211846.

112. **Yan SF**, **Tritto I**, **Pinsky D**, **Liao H**, **Huang J**, **Fuller G**, **Brett J**, **May L**, **Stern D**. Induction of Interleukin 6 (IL-6) by Hypoxia in Vascular Cells: CENTRAL ROLE OF THE BINDING SITE FOR NUCLEAR FACTOR-IL-6 *. *J Biol Chem* 270: 11463–11471, 1995. doi: 10.1074/jbc.270.19.11463.

113. **Didion SP**. Cellular and Oxidative Mechanisms Associated with Interleukin-6 Signaling in the Vasculature. *Int J Mol Sci* 18: 2563, 2017. doi: 10.3390/ijms18122563.

114. **Ghezzi P**, **Dinarello CA**, **Bianchi M**, **Rosandich ME**, **Repine JE**, **White CW**. Hypoxia increases production of interleukin-1 and tumor necrosis factor by human mononuclear cells. *Cytokine* 3: 189–194, 1991. doi: 10.1016/1043-4666(91)90015-6.

115. **Golden CL**, **Kohler JP**, **Nick HS**, **Visner GA**. Effects of vasoactive and inflammatory mediators on endothelin-1 expression in pulmonary endothelial cells. *Am J Respir Cell Mol Biol* 12: 503–512, 1995. doi: 10.1165/ajrcmb.12.5.7742014.

116. **Michael JR**, **Markewitz BA**. Endothelins and the lung. *Am J Respir Crit Care Med* 154: 555–581, 1996. doi: 10.1164/ajrccm.154.3.8810589.

117. **Yeager ME**, **Belchenko DD**, **Nguyen CM**, **Colvin KL**, **Ivy DD**, **Stenmark KR**. Endothelin-1, the unfolded protein response, and persistent inflammation: role of pulmonary artery smooth muscle cells. *Am J Respir Cell Mol Biol* 46: 14–22, 2012. doi: 10.1165/rcmb.2010-0506OC.

118. **Xin X**, **Cai Y**, **Matsumoto K**, **Agui T**. Endothelin-induced interleukin-6 production by rat aortic endothelial cells. *Endocrinology* 136: 132–137, 1995. doi: 10.1210/endo.136.1.7828523.

119. **Callera GE**, **Touyz RM**, **Teixeira SA**, **Muscara MN**, **Carvalho MHC**, **Fortes ZB**, **Nigro D**, **Schiffrin EL**, **Tostes RC**. ETA receptor blockade decreases vascular superoxide generation in DOCA-salt hypertension. *Hypertens Dallas Tex 1979* 42: 811–817, 2003. doi: 10.1161/01.HYP.0000088363.65943.6C.

120. **Kowalczyk A**, **Kleniewska P**, **Kolodziejczyk M**, **Skibska B**, **Goraca A**. The Role of Endothelin-1 and Endothelin Receptor Antagonists in Inflammatory Response and Sepsis. *Arch Immunol Ther Exp (Warsz)* 63: 41–52, 2015. doi: 10.1007/s00005-014-0310-1.

121. **Forrest JB**, **Fargas-Babjak A**. Variability of the pulmonary vascular response to hypoxia and relation to gas exchange in dogs. *Can Anaesth Soc J* 25: 479, 1978. doi: 10.1007/BF03007410.

122. **Ahmed T**, **Oliver W**, **Wanner A**. Variability of Hypoxic Pulmonary Vasoconstriction in Sheep. *Am Rev Respir Dis* 127: 59–62, 1983. doi: 10.1164/arrd.1983.127.1.59.

123. **Grünig E**, **Mereles D**, **Hildebrandt W**, **Swenson ER**, **Kübler W**, **Kuecherer H**, **Bärtsch P**. Stress doppler echocardiography for identification of susceptibility to high altitude pulmonary edema. *J Am Coll Cardiol* 35: 980–987, 2000. doi: 10.1016/S0735-1097(99)00633-6.

124. **Swenson ER**. Hypoxic Pulmonary Vasoconstriction. *High Alt Med Biol* 14: 101–110, 2013. doi: 10.1089/ham.2013.1010.

125. **Bogaard HJ**, **Abe K**, **Noordegmaf AV**, **Voelkel NF**. The right ventricle under pressure. *Chest* 135: 794–804, 2009. doi: 10.1378/chest.08-0492.

126. **Naeije R**, **Dedobbeleer C**. Pulmonary hypertension and the right ventricle in hypoxia. *Exp Physiol* 98: 1247–1256, 2013. doi: 10.1113/expphysiol.2012.069112.

127. **Brooks D**, **Horner RL**, **Kozar LF**, **Render-Teixeira CL**, **Phillipson EA**. Obstructive sleep apnea as a cause of systemic hypertension. Evidence from a canine model. *J Clin Invest* 99: 106–109, 1997. doi: 10.1172/JCI119120.

128. **Lesske J**, **Fletcher EC**, **Bao G**, **Unger T**. Hypertension caused by chronic intermittent hypoxia--influence of chemoreceptors and sympathetic nervous system. *J Hypertens* 15: 1593–1603, 1997. doi: 10.1097/00004872-199715120-00060.

129. **McGuire M**, **Bradford A**. Chronic intermittent hypercapnic hypoxia increases pulmonary arterial pressure and haematocrit in rats. *Eur Respir J* 18: 279–285, 2001. doi: 10.1183/09031936.01.00078801.

130. **Lavie L**. Obstructive sleep apnoea syndrome – an oxidative stress disorder. *Sleep Med Rev* 7: 35–51, 2003. doi: 10.1053/smrv.2002.0261.

131. **Zoccal DB**, **Bonagamba LGH**, **Oliveira FRT**, **Antunes-Rodrigues J**, **Machado BH**. Increased sympathetic activity in rats submitted to chronic intermittent hypoxia. *Exp Physiol* 92: 79–85, 2007. doi: 10.1113/expphysiol.2006.035501.

132. **Shatilo VB**, **Korkushko OV**, **Ischuk VA**, **Downey HF**, **Serebrovskaya TV**. Effects of intermittent hypoxia training on exercise performance, hemodynamics, and ventilation in healthy senior men. *High Alt Med Biol* 9: 43–52, 2008. doi: 10.1089/ham.2007.1053.

133. **Foster GE**, **Sheel AW**. The human diving response, its function, and its control. *Scand J Med Sci Sports* 15: 3–12, 2005. doi: 10.1111/j.1600-0838.2005.00440.x.

134. **Panneton W**. The Mammalian Diving Response: An Enigmatic Reflex to Preserve Life? *Physiology* 28: 284–297, 2013. doi: 10.1152/physiol.00020.2013.

135. **Hadanny A**, **Efrati S**. The Hyperoxic-Hypoxic Paradox. *Biomolecules* 10: 958, 2020. doi: 10.3390/biom10060958.

136. **Cimino F**, **Balestra C**, **Germonpré P**, **De Bels D**, **Tillmans F**, **Saija A**, **Speciale A**, **Virgili F**. Pulsed high oxygen induces a hypoxic-like response in human umbilical endothelial cells and in humans. *J Appl Physiol* 113: 1684–1689, 2012. doi: 10.1152/japplphysiol.00922.2012.

137. **Semenza GL**. Oxygen Sensing, Homeostasis, and Disease. *N Engl J Med* 365: 537–547, 2011. doi: 10.1056/NEJMra1011165.

138. **Suzuki J**. Endurance performance is enhanced by intermittent hyperbaric exposure via up-regulation of proteins involved in mitochondrial biogenesis in mice. *Physiol Rep* 5: e13349, 2017. doi: 10.14814/phy2.13349.

139. **Muth CM**, **Radermacher P**, **Pittner A**, **Steinacker J**, **Schabana R**, **Hamich S**, **Paulat K**, **Calzia E**. Arterial blood gases during diving in elite apnea divers. *Int J Sports Med* 24: 104–107, 2003. doi: 10.1055/s-2003-38401.

140. **Qvist J**, **Hurford WE**, **Park YS**, **Radermacher P**, **Falke KJ**, **Ahn DW**, **Guyton GP**, **Stanek KS**, **Hong SK**, **Weber RE**, **et al.** Arterial blood gas tensions during breath-hold diving in the Korean ama. *J Appl Physiol* 75: 285–293, 1993. doi: 10.1152/jappl.1993.75.1.285.

141. **Scott T**, **van Waart H**, **Vrijdag XCE**, **Mullins D**, **Mesley P**, **Mitchell SJ**. Arterial blood gas measurements during deep open-water breath-hold dives. *J Appl Physiol Bethesda Md 1985* 130: 1490–1495, 2021. doi: 10.1152/japplphysiol.00111.2021.

142. **Paganini M**, **Moon RE**, **Boccalon N**, **Melloni GEM**, **Giacon TA**, **Camporesi EM**, **Bosco G**. Blood gas analyses in hyperbaric and underwater environments: a systematic review. *J Appl Physiol* 132: 283–293, 2022. doi: 10.1152/japplphysiol.00569.2021.

143. **Ferretti G**. Extreme human breath-hold diving. *Eur J Appl Physiol* 84: 254–271, 2001. doi: 10.1007/s004210000377.

144. **Rudski LG**, **Lai WW**, **Afilalo J**, **Hua L**, **Handschumacher MD**, **Chandrasekaran K**, **Solomon SD**, **Louie EK**, **Schiller NB**. Guidelines for the Echocardiographic Assessment of the Right Heart in Adults: A Report from the American Society of Echocardiography. Endorsed by the European Association of Echocardiography, a registered branch of the European Society of Cardiology, and the Canadian Society of Echocardiography. *J Am Soc Echocardiogr* 23: 685–713, 2010. doi: 10.1016/j.echo.2010.05.010.

145. **Lovering AT**, **Stickland MK**, **Amann M**, **Murphy JC**, **O'Brien MJ**, **Hokanson JS**, **Eldridge MW**. Hyperoxia prevents exercise-induced intrapulmonary arteriovenous shunt in healthy humans. *J Physiol* 586: 4559–4565, 2008. doi: 10.1113/jphysiol.2008.159350.

146. **Bossone E**, **Ferrara F**, **Grünig E**. Echocardiography in pulmonary hypertension. *Curr Opin Cardiol* 30: 574–586, 2015. doi: 10.1097/HCO.0000000000000217.

147. **Currie PJ**, **Seward JB**, **Chan KL**, **Fyfe DA**, **Hagler DJ**, **Mair DD**, **Reeder GS**, **Nishimura RA**, **Tajik AJ**. Continuous wave Doppler determination of right ventricular pressure: a simultaneous Doppler-catheterization study in 127 patients. *J Am Coll Cardiol* 6: 750–756, 1985. doi: 10.1016/s0735-1097(85)80477-0.

148. **Schewel J**, **Schlüter M**, **Schmidt T**, **Kuck K-H**, **Frerker C**, **Schewel D**. Correlation between Doppler echocardiography and right heart catheterization assessment of systolic pulmonary artery pressure in patients with severe aortic stenosis. *Echocardiogr Mt Kisco N* 37: 380–387, 2020. doi: 10.1111/echo.14611.

149. **Lang RM**, **Badano LP**, **Mor-Avi V**, **Afilalo J**, **Armstrong A**, **Ernande L**, **Flachskampf FA**, **Foster E**, **Goldstein SA**, **Kuznetsova T**, **Lancellotti P**, **Muraru D**, **Picard MH**, **Rietzschel ER**, **Rudski L**, **Spencer KT**, **Tsang W**, **Voigt JU**. Recommendations for cardiac chamber quantification by echocardiography in adults: An update from the American society of echocardiography and the European association of cardiovascular imaging. *Eur Heart J Cardiovasc Imaging* 16: 233–271, 2015. doi: 10.1093/ehjci/jev014.

150. **Mor-Avi V**, **Lang RM**, **Badano LP**, **Belohlavek M**, **Cardim NM**, **Derumeaux G**, **Galderisi M**, **Marwick T**, **Nagueh SF**, **Sengupta PP**, **Sicari R**, **Smiseth OA**, **Smulevitz B**, **Takeuchi M**, **Thomas JD**, **Vannan M**, **Voigt JU**, **Zamorano JL**. Current and evolving echocardiographic techniques for the quantitative evaluation of cardiac mechanics: ASE/EAE consensus statement on methodology and indications endorsed by the Japanese society of echocardiography. *Eur J Echocardiogr* 12: 167–205, 2011. doi: 10.1093/ejechocard/jer021.

151. **Graham BL**, **Steenbruggen I**, **Miller MR**, **Barjaktarevic IZ**, **Cooper BG**, **Hall GL**, **Hallstrand TS**, **Kaminsky DA**, **McCarthy K**, **McCormack MC**, **Oropez CE**, **Rosenfeld M**, **Stanojevic S**, **Swanney MP**, **Thompson BR**. Standardization of Spirometry 2019 Update. An Official American Thoracic Society and European Respiratory Society Technical Statement. *Am J Respir Crit Care Med* 200: e70–e88, 2019. doi: 10.1164/rccm.201908-1590ST.

152. **ATS Committee on Proficiency Standards for Clinical Pulmonary Function Laboratories**. ATS statement: guidelines for the six-minute walk test. *Am J Respir Crit Care Med* 166: 111–117, 2002. doi: 10.1164/ajrccm.166.1.at1102.

153. **Mekjavic IB**, **Rempel ME**. Determination of esophageal probe insertion length based on standing and sitting height. *J Appl Physiol* 69: 376–379, 1990. doi: 10.1152/jappl.1990.69.1.376.

154. **Tymko MM**, **Hoiland RL**, **Kuca T**, **Boulet LM**, **Tremblay JC**, **Pinske BK**, **Williams AM**, **Foster GE**. Measuring the human ventilatory and cerebral blood flow response to CO_2 : a technical consideration for the end-tidal-to-arterial gas gradient. *J Appl Physiol* 120: 282–296, 2016. doi: 10.1152/japplphysiol.00787.2015.

155. **Tymko MM**, **Ainslie PN**, **MacLeod DB**, **Willie CK**, **Foster GE**. End tidal-to-arterial CO2 and O2 gas gradients at low- and high-altitude during dynamic end-tidal forcing. *Am J Physiol Regul Integr Comp Physiol* 308: R895-906, 2015. doi: 10.1152/ajpregu.00425.2014.

156. **Lundberg JO**, **Weitzberg E**, **Gladwin MT**. The nitrate–nitrite–nitric oxide pathway in physiology and therapeutics. *Nat Rev Drug Discov* 7: 156–167, 2008. doi: 10.1038/nrd2466.

157. **Kelman GR**. Digital computer subroutine for the conversion of oxygen tension into saturation. *J Appl Physiol* 21: 1375–1376, 1966. doi: 10.1152/jappl.1966.21.4.1375.

158. **Emmanouilides GC**, **Moss AJ**, **Duffie ER**, **Adams FH**. Pulmonary Arterial Pressure Changes in Human Newborn Infants from Birth to 3 Days of Age. *J Pediatr* 65: 327–333, 1964. doi: 10.1016/s0022-3476(64)80395-4.

159. **Gao Y**, **Raj JU**. Regulation of the Pulmonary Circulation in the Fetus and Newborn. *Physiol Rev* 90: 1291–1335, 2010. doi: 10.1152/physrev.00032.2009.

160. **Elliott GC**, **Gurtu R**, **McCollum C**, **Newman WG**, **Wang T**. Foramen Ovale Closure Is a Process of Endothelial-to-Mesenchymal Transition Leading to Fibrosis. *PLoS ONE* 9, 2014. doi: 10.1371/journal.pone.0107175.

161. **Marriott K**, **Manins V**, **Forshaw A**, **Wright J**, **Pascoe R**. Detection of Right-to-Left Atrial Communication Using Agitated Saline Contrast Imaging: Experience with 1162 Patients and Recommendations for Echocardiography. *J Am Soc Echocardiogr* 26: 96–102, 2013. doi: 10.1016/j.echo.2012.09.007.

162. **Patten BM**. Developmental defects at the foramen ovale. *Am J Pathol* 14: 135-162.9, 1938.

163. **Elliott JE**, **Laurie SS**, **Kern JP**, **Beasley KM**, **Goodman RD**, **Kayser B**, **Subudhi AW**, **Roach RC**, **Lovering AT**. AltitudeOmics: Impaired pulmonary gas exchange efficiency and blunted ventilatory acclimatization in humans with patent foramen ovale after 16 days at 5,260 m. *J Appl Physiol* 118: 1100–1112, 2015. doi: 10.1152/japplphysiol.00879.2014.

164. **Johansson MC**, **Eriksson P**, **Peker Y**, **Hedner J**, **Råstam L**, **Lindblad U**. The influence of patent foramen ovale on oxygen desaturation in obstructive sleep apnoea. *Eur Respir J* 29: 149–155, 2007. doi: 10.1183/09031936.00035906.

165. **Lovering AT**, **Lozo M**, **Barak O**, **Davis JT**, **Lojpur M**, **Lozo P**, **Čaljkušić K**, **Dujić Ž**. Resting arterial hypoxaemia in subjects with chronic heart failure, pulmonary hypertension and patent foramen ovale. *Exp Physiol* 101: 657–670, 2016. doi: 10.1113/EP085657.

166. **Lovering AT**, **Laurie SS**, **Elliott JE**, **Beasley KM**, **Yang X**, **Gust CE**, **Mangum TS**, **Goodman RD**, **Hawn JA**, **Gladstone IM**. Normal pulmonary gas exchange efficiency and absence of exercise-induced arterial hypoxemia in adults with bronchopulmonary dysplasia. *J Appl Physiol* 115: 1050–1056, 2013. doi: 10.1152/japplphysiol.00592.2013.

167. **Lovering AT**, **Goodman RD**. Detection of Intracardiac and Intrapulmonary Shunts at Rest and During Exercise Using Saline Contrast Echocardiography. In: *Applied Aspects of Ultrasonography in Humans*.

168. **Elliott JE**, **Choi Y**, **Laurie SS**, **Yang X**, **Gladstone IM**, **Lovering AT**. Effect of initial gas bubble composition on detection of inducible intrapulmonary arteriovenous shunt during exercise in normoxia, hypoxia, or hyperoxia. *J Appl Physiol* 110: 35–45, 2011. doi: 10.1152/japplphysiol.00145.2010.

169. **Elliott JE**, **Duke JW**, **Hawn JA**, **Halliwill JR**, **Lovering AT**. Increased cardiac output, not pulmonary artery systolic pressure, increases intrapulmonary shunt in healthy humans breathing room air and 40% O2. *J Physiol* 592: 4537–4553, 2014. doi: 10.1113/jphysiol.2014.274829.

170. **Laurie SS**, **Yang X**, **Elliott JE**, **Beasley KM**, **Lovering AT**. Hypoxia-induced intrapulmonary arteriovenous shunting at rest in healthy humans. *J Appl Physiol* 109: 1072–1079, 2010. doi: 10.1152/japplphysiol.00150.2010.

171. **Laurie SS**, **Elliott JE**, **Goodman RD**, **Lovering AT**. Catecholamine-induced opening of intrapulmonary arteriovenous anastomoses in healthy humans at rest. *J Appl Physiol* 113: 1213–1222, 2012. doi: 10.1152/japplphysiol.00565.2012.

172. **Norris HC**, **Mangum TS**, **Duke JW**, **Straley TB**, **Hawn JA**, **Goodman RD**, **Lovering AT**. Exercise- and hypoxia-induced blood flow through intrapulmonary arteriovenous anastomoses is reduced in older adults. *J Appl Physiol Bethesda Md 1985* 116: 1324–1333, 2014. doi: 10.1152/japplphysiol.01125.2013.

173. **Miller MR**, **Hankinson J**, **Brusasco V**, **Burgos F**, **Casaburi R**, **Coates A**, **Crapo R**, **Enright P**, **van der Grinten CPM**, **Gustafsson P**, **Jensen R**, **Johnson DC**, **MacIntrye N**, **McKay R**, **Navajas D**, **Pedersen OF**, **Pellegrino R**, **Viegi G**, **Wagner J**. Standardisation of spirometry. *Eur Respir J* 26: 319–338, 2005. doi: 10.1183/09031936.05.00034805.

174. **Knudson RJ**, **Kaltenborn WT**, **Knudson DE**, **Burrows B**. The Single-Breath Carbon Monoxide Diffusing Capacity. *Am Rev Respir Dis* 135: 805–811, 1987. doi: 10.1164/arrd.1987.135.4.805.

175. **MacIntyre N**, **Crapo RO**, **Viegi G**, **Johnson DC**, **van der Grinten CPM**, **Brusasco V**, **Burgos F**, **Casaburi R**, **Coates A**, **Enright P**, **Gustafsson P**, **Hankinson J**, **Jensen R**, **McKay R**, **Miller MR**, **Navajas D**, **Pedersen OF**, **Pellegrino R**, **Wanger J**. Standardisation of the single-breath determination of carbon monoxide uptake in the lung. *Eur Respir J* 26: 720–735, 2005. doi: 10.1183/09031936.05.00034905.

176. **Wanger J**, **Clausen JL**, **Coates A**, **Pedersen OF**, **Brusasco V**, **Burgos F**, **Casaburi R**, **Crapo R**, **Enright P**, **van der Grinten CPM**, **Gustafsson P**, **Hankinson J**, **Jensen R**, **Johnson DC**, **MacIntyre N**, **McKay**

R, **Miller MR**, **Navajas D**, **Pellegrino R**, **Veigi G**. Standardisation of the measurement of lung volumes. *Eur Respir J* 26: 511–522, 2005. doi: 10.1183/09031936.05.00035005.

177. **Graham BL**, **Brusasco V**, **Burgos F**, **Cooper BG**, **Jensen R**, **Kendrick A**, **MacIntyre NR**, **Thompson BR**, **Wanger J**. 2017 ERS/ATS standards for single-breath carbon monoxide uptake in the lung. *Eur Respir J* 49: 1600016, 2017. doi: 10.1183/13993003.00016-2016.

178. **Quanjer, P**, **Stanojevic S**, **Cole T**, **Baur X**, **Hall G**, **Culver B**, **Enright P**, **Hankinson J**, **Zheng J**, **Stocks J**. ERS TASK FORCE REPORT. Multi-ethnic reference values for spirometry for the 3-95-yr age range: the global lung function 2012 equations [Online]. 2012. https://www.ers-education.org/guidelines/global-lung-function-initiative/spirometry-tools.aspx.

179. **Stanojevic S**, **Graham BL**, **Cooper BG**, **Thompson BR**, **Carter KW**, **Francis RW**, **Hall GL**. Official ERS technical standards: Global Lung Function Initiative reference values for the carbon monoxide transfer factor for Caucasians. *Eur Respir J* 50, 2017. doi: 10.1183/13993003.00010-2017.

180. **Dempsey JA**, **Wagner PD**. Exercise-induced arterial hypoxemia. *J Appl Physiol* 87: 1997–2006, 1999. doi: 10.1152/jappl.1999.87.6.1997.

181. **Kelman GR**, **Nunn JF**. Nomograms for correction of blood Po2, Pco2, pH, and base excess for time and temperature. *J Appl Physiol* 21: 1484–1490, 1966. doi: 10.1152/jappl.1966.21.5.1484.

182. **Severinghaus JW**. Blood gas calculator. *J Appl Physiol* 21: 1108–1116, 1966. doi: 10.1152/jappl.1966.21.3.1108.

183. **Kwan WC**, **Shavelle DM**, **Laughrun DR**. Pulmonary vascular resistance index: Getting the units right and why it matters. *Clin Cardiol* 42: 334–338, 2019. doi: 10.1002/clc.23151.

184. **Duke JW**, **Elliott JE**, **Laurie SS**, **Beasley KM**, **Mangum TS**, **Hawn JA**, **Gladstone IM**, **Lovering AT**. Pulmonary gas exchange efficiency during exercise breathing normoxic and hypoxic gas in adults born very preterm with low diffusion capacity. *J Appl Physiol* 117: 473–481, 2014. doi: 10.1152/japplphysiol.00307.2014.

185. **Berggren SM**. *The oxygen deficit of arterial blood cause by non-ventilating parts of the lung*. Norstedt, 1942.

186. **Forster RE**. Exchange of gases between alveolar air and pulmonary capillary blood: pulmonary diffusing capacity. *Physiol Rev* 37: 391–452, 1957. doi: 10.1152/physrev.1957.37.4.391.

187. **Douglas ME**, **Downs JB**, **Dannemiller FJ**, **Hodges MR**, **Munson ES**. Change in pulmonary venous admixture with varying inspired oxygen. *Anesth Analg* 55: 688–695, 1976. doi: 10.1213/00000539-197609000-00016.

188. **Kelman GR**, **Nunn JF**, **Prys-roberts C**, **Greenbaum R**. The Influence of Cardiac Output on Arterial Oxygenation: A Theoretical Study. *Br J Anaesth* 39: 450–458, 1967. doi: 10.1093/bja/39.6.450.

189. **Takala J**. Hypoxemia due to increased venous admixture: influence of cardiac output on oxygenation. *Intensive Care Med* : 908–911, 2007. doi: 10.1007/978-3-642-28270-6_16.

190. **Aviado DM**, **Daly M de B**, **Lee CY**, **Schmidt CF**. The contribution of the bronchial circulation to the venous admixture in pulmonary venous blood. *J Physiol* 155: 602–622, 1961.

191. **Ravin MB**, **Epstein RM**, **Malm JR**. Contribution of thebesian veins to the physiologic shunt in anesthetized man. *J Appl Physiol* 20: 1148–1152, 1965. doi: 10.1152/jappl.1965.20.6.1148.

192. **Cruz JC**, **Rahn H**, **Farhi LE**. Mixed venous PO2, PCO2, pH, and cardiac output during exercise in trained subjects. *J Appl Physiol* 27: 431–434, 1969. doi: 10.1152/jappl.1969.27.3.431.

193. **Perego GB**, **Marenzi GC**, **Guazzi M**, **Sganzerla P**, **Assanelli E**, **Palermo P**, **Conconi B**, **Lauri G**, **Agostoni PG**. Contribution of PO2, P50, and Hb to changes in arteriovenous O2 content during exercise in heart failure. *J Appl Physiol* 80: 623–631, 1996. doi: 10.1152/jappl.1996.80.2.623.

194. **Dominelli PB**, **Molgat-Seon Y**, **Bingham D**, **Swartz PM**, **Road JD**, **Foster GE**, **Sheel AW**. Dysanapsis and the resistive work of breathing during exercise in healthy men and women. *J Appl Physiol* 119: 1105–1113, 2015. doi: 10.1152/japplphysiol.00409.2015.

195. **Mead J**. Dysanapsis in Normal Lungs Assessed by the Relationship between Maximal Flow, Static Recoil, and Vital Capacity. *Am Rev Respir Dis* 121: 339–342, 1980. doi: 10.1164/arrd.1980.121.2.339.

196. **Devendra GP**, **Rane AA**, **Krasuski RA**. Provoked Exercise Desaturation in Patent Foramen Ovale and Impact of Percutaneous Closure. *JACC* 5: 416–419, 2012. doi: 10.1016/j.jcin.2012.01.011.

197. **Fenster BE**, **Nguyen BH**, **Buckner JK**, **Freeman AM**, **Carroll JD**. Effectiveness of Percutaneous Closure of Patent Foramen Ovale for Hypoxemia. *Am J Cardiol* 112: 1258–1262, 2013. doi: 10.1016/j.amjcard.2013.06.022.

198. **Davis JT**, **Boulet LM**, **Hardin AM**, **Chang AJ**, **Lovering AT**, **Foster GE**. Ventilatory responses to acute hypoxia and hypercapnia in humans with a patent foramen ovale. *J Appl Physiol* 126: 730–738, 2019. doi: 10.1152/japplphysiol.00741.2018.

199. **Davis JT**, **Hay MW**, **Hardin AM**, **White MD**, **Lovering AT**. Effect of a patent foramen ovale in humans on thermal responses to passive cooling and heating. *J Appl Physiol* 123: 1423–1432, 2017. doi: 10.1152/japplphysiol.01032.2016.

200. **Stickland MK**, **Tedjasaputra V**, **Seaman C**, **Fuhr DP**, **Collins SÉ**, **Wagner H**, **van Diepen S**, **Byers BW**, **Wagner PD**, **Hopkins SR**. Intra-pulmonary arteriovenous anastomoses and pulmonary gas exchange: evaluation by microspheres, contrast echocardiography and inert gas elimination. *J Physiol* 597: 5365–5384, 2019. doi: 10.1113/JP277695.

201. **Quiñones MA**, **Otto CM**, **Stoddard M**, **Waggoner A**, **Zoghbi WA**. Recommendations for quantification of Doppler echocardiography: A report from the Doppler quantification task force of the nomenclature and standards committee of the American Society of Echocardiography. *J Am Soc Echocardiogr* 15: 167–184, 2002. doi: 10.1067/mje.2002.120202.

202. **Jonk AM**, **Van Den Berg IP**, **Olfert IM**, **Wray DW**, **Arai T**, **Hopkins SR**, **Wagner PD**. Effect of acetazolamide on pulmonary and muscle gas exchange during normoxic and hypoxic exercise. *J Physiol* 579: 909–921, 2007. doi: 10.1113/jphysiol.2006.120949.

203. **Lee PH**, **Song J-K**, **Kim JS**, **Heo R**, **Lee S**, **Kim D-H**, **Song J-M**, **Kang D-H**, **Kwon SU**, **Kang D-W**, **Lee D**, **Kwon HS**, **Yun S-C**, **Sun BJ**, **Park J-H**, **Lee J-H**, **Jeong HS**, **Song H-J**, **Kim J**, **Park S-J**. Cryptogenic Stroke and High-Risk Patent Foramen Ovale: The DEFENSE-PFO Trial. .

204. **Mahtta D**, **Mojadidi MK**, **Tandar A**, **Tobis JM**, **Meier B**. Chapter 12 - Hypoxemia and PFO. In: *Patent Foramen Ovale Closure for Stroke, Myocardial Infarction, Peripheral Embolism, Migraine, and Hypoxemia*, edited by Mojadidi MK, Meier B, Tobis JM. Academic Press, p. 143–154.

205. **Wechsler LR**. PFO and Stroke: What Are the Data? *Cardiol Rev* 16: 53, 2008. doi: 10.1097/CRD.0b013e31815771e4.

206. **Kai Liu MD**, **Bo Song MD**, **Igor F. Palacios MD**, **Ignacio Inglessis-Azuaje MD**, **WenJun Deng P**, **David McMullin P**, **XiaoYing Wang MD**, **Eng H. Lo P**, **YuMing Xu MD**, **Ferdinando S. Buonanno MD**, **MingMing Ning MD**. Patent Foramen Ovale Attributable Cryptogenic Embolism With Thrombophilia Has Higher Risk for Recurrence and Responds to Closure. .

207. **Miranda B**, **Fonseca AC**, **Ferro JM**. Patent foramen ovale and stroke. *J Neurol* 265: 1943–1949, 2018. doi: 10.1007/s00415-018-8865-0.

208. **Duffin J**, **Mohan RM**, **Vasiliou P**, **Stephenson R**, **Mahamed S**. A model of the chemoreflex control of breathing in humans: model parameters measurement. *Respir Physiol* 120: 13–26, 2000. doi: 10.1016/S0034-5687(00)00095-5.

209. **Guazzi M**, **Bandera F**, **Pelissero G**, **Castelvecchio S**, **Menicanti L**, **Ghio S**, **Temporelli PL**, **Arena R**. Tricuspid annular plane systolic excursion and pulmonary arterial systolic pressure relationship in heart failure: an index of right ventricular contractile function and prognosis. *Am J Physiol-Heart Circ Physiol* 305: H1373–H1381, 2013. doi: 10.1152/ajpheart.00157.2013.

210. **Wagner PD**. Influence of mixed venous PO2 on diffusion of O2 across the pulmonary blood: gas barrier. *Clin Physiol* 2: 105–115, 1982. doi: 10.1111/j.1475-097X.1982.tb00013.x.

211. **Korthuis RJ**. Exercise Hyperemia and Regulation of Tissue Oxygenation During Muscular Activity [Online]. In: *Skeletal Muscle Circulation*. Morgan & Claypool Life Sciences https://www.ncbi.nlm.nih.gov/books/NBK57139/ [20 Jun. 2023].

212. **Wagner PD**. The Physiological Basis of Reduced VO2max in Operation Everest II. *High Alt Med Biol* 11: 209–215, 2010. doi: 10.1089/ham.2009.1058.

213. **Sharan L**, **Stackhouse K**, **Awerbach JD**, **Bashore TM**, **Krasuski RA**. Effect of Patent Foramen Ovale in Patients With Pulmonary Hypertension. *Am J Cardiol* 122: 505–510, 2018. doi: 10.1016/j.amjcard.2018.04.014.

214. **Lovering AT**, **Elliott JE**, **Davis JT**. Physiological impact of patent foramen ovale on pulmonary gas exchange, ventilatory acclimatization, and thermoregulation. *J Appl Physiol Bethesda Md 1985* 121: 512–517, 2016. doi: 10.1152/japplphysiol.00192.2015.

215. **Allemann Y**, **Hutter D**, **Lipp E**, **Sartori C**, **Duplain H**, **Egli M**, **Cook S**, **Scherrer U**, **Seiler C**. Patent foramen ovale and high-altitude pulmonary edema. *J Am Med Assoc* 296: 2954–2958, 2006. doi: 10.1001/jama.296.24.2954.

216. **Brenner R**, **Pratali L**, **Rimoldi SF**, **Murillo Jauregui CX**, **Soria R**, **Rexhaj E**, **Salinas Salmón C**, **Villena M**, **Romero C**, **Sartori C**, **Allemann Y**, **Scherrer U**. Exaggerated Pulmonary Hypertension and Right Ventricular Dysfunction in High-Altitude Dwellers With Patent Foramen Ovale. *Chest* 147: 1072–1079, 2015. doi: 10.1378/chest.14-1353.

217. **Davis JT**, **Ng C-YA**, **Hill SD**, **Padgett RC**, **Lovering AT**. Higher oesophageal temperature at rest and during exercise in humans with patent foramen ovale: Higher core temperature in humans with patent foramen ovale. *J Physiol* 593: 4615–4630, 2015. doi: 10.1113/JP270219.

218. **Liou K**, **Wolfers D**, **Turner R**, **Bennett M**, **Allan R**, **Jepson N**, **Cranney G**. Patent Foramen Ovale Influences the Presentation of Decompression Illness in SCUBA Divers. *Heart Lung Circ* 24: 26–31, 2015. doi: 10.1016/j.hlc.2014.07.057.

219. **Ljubkovic M**, **Dujic Z**, **Møllerløkken A**, **Bakovic D**, **Obad A**, **Breskovic T**, **Brubakk AO**. Venous and Arterial Bubbles at Rest after No-Decompression Air Dives. *Med Sci Sports Exerc* 43: 990–995, 2011. doi: 10.1249/MSS.0b013e31820618d3.

220. **Edvinsson B**, **Thilén U**, **Nielsen NE**, **Christersson C**, **Dellborg M**, **Eriksson P**, **Hlebowicz J**. Does persistent (patent) foramen ovale closure reduce the risk of recurrent decompression sickness in scuba divers? *Diving Hyperb Med* 51: 63–67, 2021. doi: 10.28920/dhm51.1.63-67.

221. **Shanoudy H**, **Soliman A**, **Raggi P**, **Liu JW**, **Russell DC**, **Jarmukli NF**. Prevalence of patent foramen ovale and its contribution to hypoxemia in patients with obstructive sleep apnea. *Chest* 113: 91–96, 1998. doi: 10.1378/chest.113.1.91.

222. **Pendergast DR**, **Moon RE**, **Krasney JJ**, **Held HE**, **Zamparo P**. Human Physiology in an Aquatic Environment. In: *Comprehensive Physiology*, edited by Terjung R. Wiley, p. 1705–1750.

223. **Ferrigno M**, **Ferretti G**, **Ellis A**, **Warkander D**, **Costa M**, **Cerretelli P**, **Lundgren CE**. Cardiovascular changes during deep breath-hold dives in a pressure chamber. *J Appl Physiol Bethesda Md 1985* 83: 1282–1290, 1997. doi: 10.1152/jappl.1997.83.4.1282.

224. **Bain AR**, **Ainslie PN**, **Hoiland RL**, **Barak OF**, **Cavar M**, **Drvis I**, **Stembridge M**, **MacLeod DM**, **Bailey DM**, **Dujic Z**, **MacLeod DB**. Cerebral oxidative metabolism is decreased with extreme apnoea in humans; impact of hypercapnia. *J Physiol* 594: 5317–5328, 2016. doi: 10.1113/JP272404.

225. **Barak OF**, **Janjic N**, **Drvis I**, **Mijacika T**, **Mudnic I**, **Coombs GB**, **Thom SR**, **Madic D**, **Dujic Z**. Vascular dysfunction following breath-hold diving. *Can J Physiol Pharmacol* 98: 124–131, 2020.

226. **Amabile N**, **Heiss C**, **Real WM**, **Minasi P**, **McGlothlin D**, **Rame EJ**, **Grossman W**, **De Marco T**, **Yeghiazarians Y**. Circulating Endothelial Microparticle Levels Predict Hemodynamic Severity of Pulmonary Hypertension. *Am J Respir Crit Care Med* 177: 1268–1275, 2008. doi: 10.1164/rccm.200710-1458OC.

227. **Lindholm P**, **Lundgren CE**. The physiology and pathophysiology of human breath-hold diving. *J Appl Physiol* 106: 284–292, 2009. doi: 10.1152/japplphysiol.90991.2008.

228. **Bilopavlovic N**, **Marinovic J**, **Ljubkovic M**, **Obad A**, **Zanchi J**, **Pollock NW**, **Denoble P**, **Dujic Z**. Effect of repetitive SCUBA diving on humoral markers of endothelial and central nervous system integrity. *Eur J Appl Physiol* 113: 1737–1743, 2013. doi: 10.1007/s00421-013-2600-4.

229. **Thom SR**, **Bennett M**, **Banham ND**, **Chin W**, **Blake DF**, **Rosen A**, **Pollock NW**, **Madden D**, **Barak O**, **Marroni A**, **Balestra C**, **Germonpre P**, **Pieri M**, **Cialoni D**, **Le P-NJ**, **Logue C**, **Lambert D**, **Hardy KR**, **Sward D**, **Yang M**, **Bhopale VB**, **Dujic Z**. Association of microparticles and neutrophil activation with decompression sickness. *J Appl Physiol* 119: 427–434, 2015. doi: 10.1152/japplphysiol.00380.2015.

230. **Schipke JD**, **Gams E**, **Kallweit O**. Decompression Sickness Following Breath-hold Diving. *Res Sports Med* 14: 163–178, 2006. doi: 10.1080/15438620600854710.

231. **Hoiland RL**, **Ainslie PN**, **Bain AR**, **MacLeod DB**, **Stembridge M**, **Drvis I**, **Madden D**, **Barak O**, **MacLeod DM**, **Dujic Z**. β1-Blockade increases maximal apnea duration in elite breath-hold divers. *J Appl Physiol* 122: 899–906, 2017. doi: 10.1152/japplphysiol.00127.2016.

232. **Gooden BA**. Mechanism of the human diving response. *Integr Physiol Behav Sci* 29: 6–16, 1994. doi: 10.1007/BF02691277.

233. **Kyhl K**, **Drvis I**, **Barak O**, **Mijacika T**, **Engstrøm T**, **Secher NH**, **Dujic Z**, **Buca A**, **Madsen PL**. Organ perfusion during voluntary pulmonary hyperinflation; a magnetic resonance imaging study. *Am J Physiol-Heart Circ Physiol* 310: H444–H451, 2016. doi: 10.1152/ajpheart.00739.2015.

234. **Kjeld T**, **Stride N**, **Gudiksen A**, **Hansen EG**, **Arendrup HC**, **Horstmann PF**, **Zerahn B**, **Jensen LT**, **Nordsborg N**, **Bejder J**, **Halling JF**. Oxygen conserving mitochondrial adaptations in the skeletal muscles of breath hold divers. *PLOS ONE* 13: e0201401, 2018. doi: 10.1371/journal.pone.0201401.

235. **Heusser Karsten**, **Dzamonja Gordan**, **Tank Jens**, **Palada Ivan**, **Valic Zoran**, **Bakovic Darija**, **Obad Ante**, **Ivancev Vladimir**, **Breskovic Toni**, **Diedrich André**, **Joyner Michael J.**, **Luft Friedrich C.**, **Jordan Jens**, **Dujic Zeljko**. Cardiovascular Regulation During Apnea in Elite Divers. *Hypertension* 53: 719–724, 2009. doi: 10.1161/HYPERTENSIONAHA.108.127530.

236. **Steinback CD**, **Breskovic T**, **Frances M**, **Dujic Z**, **Shoemaker JK**. Ventilatory restraint of sympathetic activity during chemoreflex stress. *Am J Physiol-Regul Integr Comp Physiol* 299: R1407–R1414, 2010. doi: 10.1152/ajpregu.00432.2010.

237. **Dujic Z**, **Breskovic T**. Impact of breath holding on cardiovascular respiratory and cerebrovascular health. *Sports Med Auckl NZ* 42: 459–472, 2012. doi: 10.2165/11599260-000000000-00000.

238. **Mijacika T**, **Dujic Z**. Sports-related lung injury during breath-hold diving. *Eur Respir Rev* 25: 506–512, 2016. doi: 10.1183/16000617.0052-2016.

239. **Bain AR**, **Drvis I**, **Dujic Z**, **MacLeod DB**, **Ainslie PN**. Physiology of static breath holding in elite apneists. *Exp Physiol* 103: 635–651, 2018. doi: 10.1113/EP086269.

240. **Ivancev V**, **Palada I**, **Valic Z**, **Obad A**, **Bakovic D**, **Dietz NM**, **Joyner MJ**, **Dujic Z**. Cerebrovascular reactivity to hypercapnia is unimpaired in breath-hold divers. *J Physiol* 582: 723–730, 2007. doi: 10.1113/jphysiol.2007.128991.

241. **Breskovic T**, **Ivancev V**, **Banic I**, **Jordan J**, **Dujic Z**. Peripheral chemoreflex sensitivity and sympathetic nerve activity are normal in apnea divers during training season. *Auton Neurosci* 154: 42–47, 2010. doi: 10.1016/j.autneu.2009.11.001.

242. **Steinback CD**, **Breskovic T**, **Banic I**, **Dujic Z**, **Shoemaker JK**. Autonomic and cardiovascular responses to chemoreflex stress in apnoea divers. *Auton Neurosci Basic Clin* 156: 138–143, 2010. doi: 10.1016/j.autneu.2010.05.002.

243. **Kiely DG**, **Cargill RI**, **Lipworth BJ**. Effects of Hypercapnia on Hemodynamic, Inotropic, Lusitropic, and Electrophysiologic Indices in Humans. *Chest* 109: 1215–1221, 1996. doi: 10.1378/chest.109.5.1215.

244. **Balanos GM**, **Talbot NP**, **Dorrington KL**, **Robbins PA**. Human pulmonary vascular response to 4 h of hypercapnia and hypocapnia measured using Doppler echocardiography. *J Appl Physiol* 94: 1543–1551, 2003. doi: 10.1152/japplphysiol.00890.2002.

245. **Ketabchi F**, **Egemnazarov B**, **Schermuly RT**, **Ghofrani HA**, **Seeger W**, **Grimminger F**, **Shid-Moosavi M**, **Dehghani GA**, **Weissmann N**, **Sommer N**. Effects of hypercapnia with and without acidosis on hypoxic pulmonary vasoconstriction. *Am J Physiol-Lung Cell Mol Physiol* 297: L977–L983, 2009. doi: 10.1152/ajplung.00074.2009.

246. **Willie CK**, **Ainslie PN**, **Drvis I**, **MacLeod DB**, **Bain AR**, **Madden D**, **Maslov PZ**, **Dujic Z**. Regulation of Brain Blood Flow and Oxygen Delivery in Elite Breath-Hold Divers. *J Cereb Blood Flow Metab* 35: 66–73, 2015. doi: 10.1038/jcbfm.2014.170.

247. **Ponganis PJ**, **Stockard TK**, **Meir JU**, **Williams CL**, **Ponganis KV**, **van Dam RP**, **Howard R**. Returning on empty: extreme blood O2 depletion underlies dive capacity of emperor penguins. *J Exp Biol* 210: 4279–4285, 2007. doi: 10.1242/jeb.011221.

248. **Meir JU**, **Ponganis PJ**. High-affinity hemoglobin and blood oxygen saturation in diving emperor penguins. *J Exp Biol* 212: 3330–3338, 2009. doi: 10.1242/jeb.033761.

249. **Bain AR**, **Ainslie PN**, **Barak OF**, **Hoiland RL**, **Drvis I**, **Mijacika T**, **Bailey DM**, **Santoro A**, **DeMasi DK**, **Dujic Z**, **MacLeod DB**. Hypercapnia is essential to reduce the cerebral oxidative metabolism during extreme apnea in humans. *J Cereb Blood Flow Metab* 37: 3231–3242, 2017. doi: 10.1177/0271678X16686093.

250. **Bain AR**, **Ainslie PN**, **Hoiland RL**, **Barak OF**, **Drvis I**, **Stembridge M**, **MacLeod DM**, **McEneny J**, **Stacey BS**, **Tuaillon E**, **Marchi N**, **Maudave AFD**, **Dujic Z**, **MacLeod DB**, **Bailey DM**. Competitive apnea and its effect on the human brain: focus on the redox regulation of blood-brain barrier permeability and neuronal-parenchymal integrity. *FASEB J* 32: 2305–2314, 2018. doi: 10.1096/fj.201701031R.

251. **Bailey DM**, **Willie CK**, **Hoiland RL**, **Bain AR**, **MacLeod DB**, **Santoro MA**, **DeMasi DK**, **Andrijanic A**, **Mijacika T**, **Barak OF**, **Dujic Z**, **Ainslie PN**. Surviving Without Oxygen: How Low Can the Human Brain Go? *High Alt Med Biol* 18: 73–79, 2017. doi: 10.1089/ham.2016.0081.

252. **Joulia F**, **Steinberg JG**, **Wolff F**, **Gavarry O**, **Jammes Y**. Reduced oxidative stress and blood lactic acidosis in trained breath-hold human divers. *Respir Physiol Neurobiol* 133: 121–130, 2002. doi: 10.1016/S1569-9048(02)00133-7.

253. **Benumof JL**. Intermittent hypoxia increases lobar hypoxic pulmonary vasoconstriction. *Anesthesiology* 58: 399–404, 1983. doi: 10.1097/00000542-198305000-00001.

254. **Corbin JD**. Mechanisms of action of PDE5 inhibition in erectile dysfunction. *Int J Impot Res* 16: S4–S7, 2004. doi: 10.1038/sj.ijir.3901205.

255. **Greyson CR**. Pathophysiology of right ventricular failure. *Crit Care Med* 36: S57-65, 2008. doi: 10.1097/01.CCM.0000296265.52518.70.

256. **Patrician A**, **Spajić B**, **Gasho C**, **Caldwell HG**, **Dawkins T**, **Stembridge M**, **Lovering AT**, **Coombs GB**, **Howe CA**, **Barak O**, **Drviš I**, **Dujić Ž**, **Ainslie PN**. Temporal changes in pulmonary gas exchange efficiency when breath-hold diving below residual volume. *Exp Physiol* 106: 1120–1133, 2021. doi: 10.1113/EP089176.

257. **Ball MK**, **Waypa GB**, **Mungai PT**, **Nielsen JM**, **Czech L**, **Dudley VJ**, **Beussink L**, **Dettman RW**, **Berkelhamer SK**, **Steinhorn RH**, **Shah SJ**, **Schumacker PT**. Regulation of Hypoxia-induced Pulmonary Hypertension by Vascular Smooth Muscle Hypoxia-Inducible Factor-1α. *Am J Respir Crit Care Med* 189: 314–324, 2014. doi: 10.1164/rccm.201302-0302OC.

258. **Mahmud A**, **Hennessy M**, **Feely J**. Effect of sildenafil on blood pressure and arterial wave reflection in treated hypertensive men. .

259. **O'Rourke M**. Arterial stiffening and vascular/ventricular interaction. *J Hum Hypertens* 8 Suppl 1: S9-15, 1994.

260. **Zhao L.**, **Mason N.A.**, **Morrell N.W.**, **Kojonazarov B.**, **Sadykov A.**, **Maripov A.**, **Mirrakhimov M.M.**, **Aldashev A.**, **Wilkins M.R.** Sildenafil Inhibits Hypoxia-Induced Pulmonary Hypertension. *Circulation* 104: 424–428, 2001. doi: 10.1161/hc2901.093117.

261. **Preston IR**, **Hill NS**, **Gambardella LS**, **Warburton RR**, **Klinger JR**. Synergistic effects of ANP and sildenafil on cGMP levels and amelioration of acute hypoxic pulmonary hypertension. *Exp Biol Med Maywood NJ* 229: 920–925, 2004. doi: 10.1177/153537020422900908.

262. **Stembridge M**, **Ainslie PN**, **Boulet LM**, **Anholm J**, **Subedi P**, **Tymko MM**, **Willie CK**, **Cooper SM**, **Shave R**. The independent effects of hypovolaemia and pulmonary vasoconstriction on ventricular function and exercise capacity during acclimatisation to 3800 m. *J Physiol* 597: 1059–1072, 2019. doi: 10.1113/JP275278.

263. **Huntsman LL**, **Stewart DK**, **Barnes SR**, **Franklin SB**, **Colocousis JS**, **Hessel EA**. Noninvasive Doppler determination of cardiac output in man. Clinical validation. *Circulation* 67: 593–602, 1983. doi: 10.1161/01.CIR.67.3.593.

264. **Tan C**, **Rubenson D**, **Srivastava A**, **Mohan R**, **Smith MR**, **Billick K**, **Bardarian S**, **Thomas Heywood J**. Left ventricular outflow tract velocity time integral outperforms ejection fraction and Doppler-derived cardiac output for predicting outcomes in a select advanced heart failure cohort. *Cardiovasc Ultrasound* 15: 18, 2017. doi: 10.1186/s12947-017-0109-4.

265. **de Simone Giovanni**, **Devereux Richard B.**, **Daniels Stephen R.**, **Mureddu GianFrancesco**, **Roman Mary J.**, **Kimball Thomas R.**, **Greco Rosanna**, **Witt Sandra**, **Contaldo Franco**. Stroke Volume and Cardiac Output in Normotensive Children and Adults. *Circulation* 95: 1837–1843, 1997. doi: 10.1161/01.CIR.95.7.1837.

266. **Dewey Frederick E.**, **Rosenthal David**, **Murphy Daniel J.**, **Froelicher Victor F.**, **Ashley Euan A.** Does Size Matter? *Circulation* 117: 2279–2287, 2008. doi: 10.1161/CIRCULATIONAHA.107.736785.

267. **George KP**, **Batterham AM**, **Jones B**. The impact of scalar variable and process on athlete-control comparisons of cardiac dimensions. *Med Sci Sports Exerc* 30: 824–830, 1998.

268. **Shirai M**, **Tsuchimochi H**, **Nagai H**, **Gray E**, **Pearson JT**, **Sonobe T**, **Yoshimoto M**, **Inagaki T**, **Fujii Y**, **Umetani K**, **Kuwahira I**, **Schwenke DO**. Pulmonary vascular tone is dependent on the central modulation of sympathetic nerve activity following chronic intermittent hypoxia. *Basic Res Cardiol* 109: 432, 2014. doi: 10.1007/s00395-014-0432-y.

269. **Dawson CA**, **Grimm DJ**, **Linehan JH**. Influence of hypoxia on the longitudinal distribution of pulmonary vascular resistance. *J Appl Physiol* 44: 493–498, 1978. doi: 10.1152/jappl.1978.44.4.493.

270. **Snow JB**, **Kitzis V**, **Norton CE**, **Torres SN**, **Johnson KD**, **Kanagy NL**, **Walker BR**, **Resta TC**. Differential effects of chronic hypoxia and intermittent hypocapnic and eucapnic hypoxia on pulmonary vasoreactivity. *J Appl Physiol* 104: 110–118, 2008. doi: 10.1152/japplphysiol.00698.2005.

271. **Zieliński J**. Effects of intermittent hypoxia on pulmonary haemodynamics: animal models versus studies in humans. *Eur Respir J* 25: 173–180, 2005. doi: 10.1183/09031936.04.00037204.

272. **Abrams D**, **Schulze-Neick I**, **Magee AG**. Sildenafil as a selective pulmonary vasodilator in childhood primary pulmonary hypertension. *Heart Br Card Soc* 84: E4, 2000. doi: 10.1136/heart.84.2.e4.

273. **Elliott JE**, **Friedman JM**, **Futral JE**, **Goodman RD**, **Lovering AT**. Sildenafil, nifedipine and acetazolamide do not allow for blood flow through intrapulmonary arteriovenous anastomoses during exercise while breathing 100% oxygen. *Exp Physiol* 99: 1636–1647, 2014. doi: 10.1113/expphysiol.2014.081562.

274. **Bailey DM**, **Dehnert C**, **Luks AM**, **Menold E**, **Castell C**, **Schendler G**, **Faoro V**, **Gutowski M**, **Evans KA**, **Taudorf S**, **James PE**, **McEneny J**, **Young IS**, **Swenson ER**, **Mairbäurl H**, **Bärtsch P**, **Berger MM**. High-altitude pulmonary hypertension is associated with a free radical-mediated reduction in pulmonary nitric oxide bioavailability. *J Physiol* 588: 4837–4847, 2010. doi: 10.1113/jphysiol.2010.194704.

275. **Dunham-Snary KJ**, **Wu D**, **Sykes EA**, **Thakrar A**, **Parlow LRG**, **Mewburn JD**, **Parlow JL**, **Archer SL**. Hypoxic Pulmonary Vasoconstriction. *Chest* 151: 181–192, 2017. doi: 10.1016/j.chest.2016.09.001.

276. **Theunissen S**, **Sponsiello N**, **Rozloznik M**, **Germonpré P**, **Guerrero F**, **Cialoni D**, **Balestra C**. Oxidative stress in breath-hold divers after repetitive dives. *Diving Hyperb Med* 43: 63–66, 2013.

277. **Mrakic-Sposta S**, **Vezzoli A**, **Rizzato A**, **Della Noce C**, **Malacrida S**, **Montorsi M**, **Paganini M**, **Cancellara P**, **Bosco G**. Oxidative stress assessment in breath-hold diving. *Eur J Appl Physiol* 119: 2449–2456, 2019. doi: 10.1007/s00421-019-04224-4.

278. **Dinenno FA**. Skeletal muscle vasodilation during systemic hypoxia in humans. *J Appl Physiol Bethesda Md 1985* 120: 216–225, 2016. doi: 10.1152/japplphysiol.00256.2015.

279. **Greenberg HE**, **Sica A**, **Batson D**, **Scharf SM**. Chronic intermittent hypoxia increases sympathetic responsiveness to hypoxia and hypercapnia. *J Appl Physiol* 86: 298–305, 1999. doi: 10.1152/jappl.1999.86.1.298.

280. **Fagan KA**. Selected Contribution: Pulmonary hypertension in mice following intermittent hypoxia. *J Appl Physiol* 90: 2502–2507, 2001. doi: 10.1152/jappl.2001.90.6.2502.

281. **Somers VK**, **Dyken ME**, **Clary MP**, **Abboud FM**. Sympathetic neural mechanisms in obstructive sleep apnea. *J Clin Invest* 96: 1897–1904, 1995. doi: 10.1172/JCI118235.

282. **Narkiewicz Krzysztof**, **Kato Masahiko**, **Phillips Bradley G.**, **Pesek Catherine A.**, **Davison Diane E.**, **Somers Virend K.** Nocturnal Continuous Positive Airway Pressure Decreases Daytime Sympathetic Traffic in Obstructive Sleep Apnea. *Circulation* 100: 2332–2335, 1999. doi: 10.1161/01.CIR.100.23.2332.

283. **Naghshin J**, **McGaffin KR**, **Witham WG**, **Mathier MA**, **Romano LC**, **Smith SH**, **Janczewski AM**, **Kirk JA**, **Shroff SG**, **O'Donnell CP**. Chronic intermittent hypoxia increases left ventricular contractility in C57BL/6J mice. *J Appl Physiol* 107: 787–793, 2009. doi: 10.1152/japplphysiol.91256.2008.

284. **Lucking EF**, **O'Halloran KD**, **Jones JFX**. Increased cardiac output contributes to the development of chronic intermittent hypoxia-induced hypertension. *Exp Physiol* 99: 1312–1324, 2014. doi: 10.1113/expphysiol.2014.080556.

285. **Naeije R**, **Mélot C**, **Mols P**, **Hallemans R**. Effects of vasodilators on hypoxic pulmonary vasoconstriction in normal man. *Chest* 82: 404–410, 1982. doi: 10.1378/chest.82.4.404.

286. **Laks L**, **Lehrhaft B**, **Grunstein RR**, **Sullivan CE**. Pulmonary artery pressure response to hypoxia in sleep apnea. *Am J Respir Crit Care Med* 155: 193–198, 1997. doi: 10.1164/ajrccm.155.1.9001311.

287. **Costalat G**, **Pichon A**, **Coquart J**, **Bauer F**, **Lemaître F**. Cardio-ventilatory responses to poikilocapnic hypoxia and hypercapnia in trained breath-hold divers. *Respir Physiol Neurobiol* 192: 48–54, 2014. doi: 10.1016/j.resp.2013.12.005.

288. **Masuda Y**, **Yoshida A**, **Hayashi F**, **Sasaki K**, **Honda Y**. The ventilatory responses to hypoxia and hypercapnia in the ama. *Jpn J Physiol* 31: 187–197, 1981. doi: 10.2170/jjphysiol.31.187.

289. **Dawson A**. Regional pulmonary blood flow in sitting and supine man during and after acute hypoxia. *J Clin Invest* 48: 301–310, 1969. doi: 10.1172/JCI105986.

290. **Hopkins SR**, **Olfert IM**, **Wagner PD**. Point:Counterpoint: Exercise-induced intrapulmonary shunting is imaginary vs. real. *J Appl Physiol* 107: 993–994, 2009. doi: 10.1152/japplphysiol.91489.2008.

291. **Asadi AK**, **Cronin MV**, **Sá RC**, **Theilmann RJ**, **Holverda S**, **Hopkins SR**, **Buxton RB**, **Prisk GK**. Spatial-temporal dynamics of pulmonary blood flow in the healthy human lung in response to altered FiO2. *J Appl Physiol* 114: 107–118, 2013. doi: 10.1152/japplphysiol.00433.2012.

292. **Groves BM**, **Reeves JT**, **Sutton JR**, **Wagner PD**, **Cymerman A**, **Malconian MK**, **Rock PB**, **Young PM**, **Houston CS**. Operation Everest II: elevated high-altitude pulmonary resistance unresponsive to oxygen. *J Appl Physiol Bethesda Md 1985* 63: 521–530, 1987. doi: 10.1152/jappl.1987.63.2.521.

293. **Staessen JA**, **Fagard R**, **Thijs L**, **Amery A**. A Consensus View on the Technique of Ambulatory Blood Pressure Monitoring. *Hypertension* 26: 912–918, 1995. doi: 10.1161/01.HYP.26.6.912.

294. **Parati G**, **Casadei R**, **Groppelli A**, **Di Rienzo M**, **Mancia G**. Comparison of finger and intra-arterial blood pressure monitoring at rest and during laboratory testing. *Hypertension* 13: 647–655, 1989. doi: 10.1161/01.hyp.13.6.647.

295. **Duke JW**, **Davis JT**, **Ryan BJ**, **Elliott JE**, **Beasley KM**, **Hawn JA**, **Byrnes WC**, **Lovering AT**. Decreased arterial , not O2 content, increases blood flow through intrapulmonary arteriovenous anastomoses at rest. *J Physiol* 594: 4981–4996, 2016. doi: 10.1113/JP272211.

296. **Willie CK**, **Patrician A**, **Hoiland RL**, **Williams AM**, **Gasho C**, **Subedi P**, **Anholm J**, **Drane A**, **Tymko MM**, **Nowak-Flück D**, **Plato S**, **McBride E**, **Varoli G**, **Binsted G**, **Eller LK**, **Reimer RA**, **MacLeod DB**, **Stembridge M**, **Ainslie PN**. Influence of iron manipulation on hypoxic pulmonary vasoconstriction and pulmonary reactivity during ascent and acclimatization to 5050 m. *J Physiol* 599: 1685–1708, 2021. doi: 10.1113/JP281114.

297. **Benumof JL**, **Wahrenbrock EA**. Blunted hypoxic pulmonary vasoconstriction by increased lung vascular pressures. *J Appl Physiol* 38: 846–850, 1975. doi: 10.1152/jappl.1975.38.5.846.

298. **Talbot NP**, **Balanos GM**, **Dorrington KL**, **Robbins PA**. Two temporal components within the human pulmonary vascular response to ~2 h of isocapnic hypoxia. *J Appl Physiol* 98: 1125–1139, 2005. doi: 10.1152/japplphysiol.00903.2004.

299. **Chen J**, **Zacharek A**, **Zhang C**, **Jiang H**, **Li Y**, **Roberts C**, **Lu M**, **Kapke A**, **Chopp M**. Neurobiology of Disease Endothelial Nitric Oxide Synthase Regulates Brain-Derived Neurotrophic Factor Expression and Neurogenesis after Stroke in Mice. .

300. **Govers R**, **Rabelink TJ**. Cellular regulation of endothelial nitric oxide synthase. *Am J Physiol - Ren Physiol* 280, 2001. doi: 10.1152/ajprenal.2001.280.2.f193.

301. **Palmer RMJ**, **Ashton DS**, **Moncada S**. Vascular endothelial cells synthesize nitric oxide from L-arginine. *Nature* 333: 664–666, 1988. doi: 10.1038/333664a0.

302. **Browatzki Joachim Schmidt Wolfgang Kübler Roger Kranzhöfer M**, **Browatzki M**, **Schmidt J**, **Kübler Kranzhöfer WR**. *Endothelin-1 induces interleukin-6 release via activation of the transcription factor NF-B in human vascular smooth muscle cells*. 2000.

303. **Satwiko MG**, **Ikeda K**, **Nakayama K**, **Yagi K**, **Hocher B**, **Hirata K**, **Emoto N**. Targeted activation of endothelin-1 exacerbates hypoxia-induced pulmonary hypertension. *Biochem Biophys Res Commun* 465: 356–362, 2015. doi: 10.1016/j.bbrc.2015.08.002.

304. **Yoshizumi M**, **Perrella MA**, **Burnett JC**, **Lee ME**. Tumor necrosis factor downregulates an endothelial nitric oxide synthase mRNA by shortening its half-life. *Circ Res* 73: 205–209, 1993. doi: 10.1161/01.RES.73.1.205.

305. **Lin C-C**, **Lin W-N**, **Cho R-L**, **Wang C-Y**, **Hsiao L-D**, **Yang C-M**. TNF-α-Induced cPLA2 Expression via NADPH Oxidase/Reactive Oxygen Species-Dependent NF-κB Cascade on Human Pulmonary Alveolar Epithelial Cells. *Front Pharmacol* 7: 447, 2016. doi: 10.3389/fphar.2016.00447.

306. **Gielis JF**, **Lin JY**, **Wingler K**, **Van Schil PEY**, **Schmidt HH**, **Moens AL**. Pathogenetic role of eNOS uncoupling in cardiopulmonary disorders. *Free Radic Biol Med* 50: 765–776, 2011. doi: 10.1016/j.freeradbiomed.2010.12.018.

307. **Xia N**, **Daiber A**, **Förstermann U**, **Li H**. Antioxidant effects of resveratrol in the cardiovascular system. *Br J Pharmacol* 174: 1633–1646, 2017. doi: 10.1111/bph.13492.

308. **Kelly T**, **Brown C**, **Bryant-Ekstrand M**, **Lord R**, **Dawkins T**, **Drane A**, **Futral JE**, **Barak O**, **Dragun T**, **Stembridge M**, **Spajić B**, **Drviš I**, **Duke JW**, **Ainslie PN**, **Foster GE**, **Dujic Z**, **Lovering AT**. Blunted hypoxic pulmonary vasoconstriction in apnoea divers. *Exp Physiol* 107: 1225–1240, 2022. doi: 10.1113/EP090326.

309. **DiMarco KG**, **Beasley KM**, **Shah K**, **Speros JP**, **Elliott JE**, **Laurie SS**, **Duke JW**, **Goodman RD**, **Futral JE**, **Hawn JA**, **Roach RC**, **Lovering AT**. No effect of patent foramen ovale on acute mountain sickness and pulmonary pressure in normobaric hypoxia. *Exp Physiol* 107: 122–132, 2022. doi: 10.1113/EP089948.

310. **J. Stewart D**, **D. Levy R**, **Cernacek P**, **Langleben D**. Increased Plasma Endothelin-1 in Pulmonary Hypertension: Marker or Mediator of Disease? .

311. **Earley S**, **Nelin LD**, **Chicoine LG**, **Walker BR**. Hypoxia-induced pulmonary endothelin-1 expression is unaltered by nitric oxide. *J Appl Physiol* 92: 1152–1158, 2002. doi: 10.1152/japplphysiol.00829.2001.

312. **Elton TS**, **Oparil S**, **Taylor GR**, **Hicks PH**, **Yang RH**, **Jin H**, **Chen YF**. Normobaric hypoxia stimulates endothelin-1 gene expression in the rat. *Am J Physiol* 263: R1260-1264, 1992. doi: 10.1152/ajpregu.1992.263.6.R1260.

313. **Shimoda LA**, **Sham JSK**, **Liu Q**, **Sylvester JT**. Acute and chronic hypoxic pulmonary vasoconstriction: a central role for endothelin-1? *Respir Physiol Neurobiol* 132: 93–106, 2002. doi: 10.1016/S1569-9048(02)00052-6.

314. **Lippton HL**, **Hauth TA**, **Summer WR**, **Hyman AL**. Endothelin produces pulmonary vasoconstriction and systemic vasodilation. *J Appl Physiol* 66: 1008–1012, 1989. doi: 10.1152/jappl.1989.66.2.1008.

315. **Hirata Y**, **Takagi Y**, **Fukuda Y**, **Maruno F**. Endothelin is a potent mitogen for rat vascular smooth muscle cells. *Atherosclerosis* 78: 225–228, 1989. doi: 10.1016/0021-9150(89)90227-X.

316. **Janakidevi K**, **Fisher MA**, **Del Vecchio PJ**, **Tiruppathi C**, **Figge J**, **Malik AB**. Endothelin-1 stimulates DNA synthesis and proliferation of pulmonary artery smooth muscle cells. *Am J Physiol-Cell Physiol* 263: C1295–C1301, 1992. doi: 10.1152/ajpcell.1992.263.6.C1295.

317. **Johnson W**, **Nohria A**, **Garrett L**, **Fang JC**, **Igo J**, **Katai M**, **Ganz P**, **Creager MA**. Contribution of endothelin to pulmonary vascular tone under normoxic and hypoxic conditions. *Am J Physiol Heart Circ Physiol* 283: H568-575, 2002. doi: 10.1152/ajpheart.00099.2001.

318. **Saarelainen S**, **Seppälä E**, **Laasonen K**, **Hasan J**. Circulating Endothelin-1 in Obstructive Sleep Apnea. *Endothelium* 5: 115–118, 1997. doi: 10.3109/10623329709079869.

319. **Gjørup PH**, **Sadauskiene L**, **Wessels J**, **Nyvad O**, **Strunge B**, **Pedersen EB**. Abnormally Increased Endothelin-1 in Plasma During the Night in Obstructive Sleep Apnea: Relation to Blood Pressure and Severity of Disease*. *Am J Hypertens* 20: 44–52, 2007. doi: 10.1016/j.amjhyper.2006.05.021.

320. **Phillips BG**, **Narkiewicz K**, **Pesek CA**, **Haynes WG**, **Dyken ME**, **Somers VK**. Effects of obstructive sleep apnea on endothelin-1 and blood pressure. *J Hypertens* 17: 61, 1999.

321. **Barnett CF**, **Machado RF**. Sildenafil in the treatment of pulmonary hypertension. *Vasc Health Risk Manag* 2: 411–422, 2006. doi: 10.2147/vhrm.2006.2.4.411.

322. **Yamaguchi K**, **Suzuki K**, **Naoki K**, **Nishio K**, **Sato N**, **Takeshita K**, **Kudo H**, **Aoki T**, **Suzuki Y**, **Miyata A**, **Tsumura H**. Response of Intra-acinar Pulmonary Microvessels to Hypoxia, Hypercapnic Acidosis, and Isocapnic Acidosis. *Circ Res* 82: 722–728, 1998. doi: 10.1161/01.RES.82.6.722.

323. **Carlin RE**, **Ferrario L**, **Boyd JT**, **Camporesi EM**, **McGraw DJ**, **Hakim TS**. Determinants of nitric oxide in exhaled gas in the isolated rabbit lung. *Am J Respir Crit Care Med* 155: 922–927, 1997. doi: 10.1164/ajrccm.155.3.9117027.

324. **Cremona G**, **Higenbottam T**, **Takao M**, **Hall L**, **Bower EA**. Exhaled nitric oxide in isolated pig lungs. *J Appl Physiol* 78: 59–63, 1995. doi: 10.1152/jappl.1995.78.1.59.

325. **Bosseto MC**, **Palma PVB**, **Covas DT**, **Giorgio S**. Hypoxia modulates phenotype, inflammatory response, and leishmanial infection of human dendritic cells. *APMIS* 118: 108–114, 2010. doi: 10.1111/j.1600-0463.2009.02568.x.

326. **Yang M**, **Ma C**, **Liu S**, **Shao Q**, **Gao W**, **Song B**, **Sun J**, **Xie Q**, **Zhang Y**, **Feng A**, **Liu Y**, **Hu W**, **Qu X**. HIF-dependent induction of adenosine receptor A2b skews human dendritic cells to a Th2-stimulating phenotype under hypoxia. *Immunol Cell Biol* 88: 165–171, 2010. doi: 10.1038/icb.2009.77.

327. **Moran EM**, **Heydrich R**, **Ng CT**, **Saber TP**, **McCormick J**, **Sieper J**, **Appel H**, **Fearon U**, **Veale DJ**. IL-17A Expression Is Localised to Both Mononuclear and Polymorphonuclear Synovial Cell Infiltrates. *PLOS ONE* 6: e24048, 2011. doi: 10.1371/journal.pone.0024048.

328. **Zaloudikova M**, **Vytasek R**, **Vajnerová O**, **Hnilickova O**, **Vízek M**, **Hampl V**, **Herget J**. Depletion of alveolar macrophages attenuates hypoxic pulmonary hypertension but not hypoxia-induced increase in serum concentration of MCP-1. *Physiol Res* 65: 763–768, 2016.

329. **El Alam S**, **Pena E**, **Aguilera D**, **Siques P**, **Brito J**. Inflammation in Pulmonary Hypertension and Edema Induced by Hypobaric Hypoxia Exposure. *Int J Mol Sci* 23: 12656, 2022. doi: 10.3390/ijms232012656.

330. **Morisawa D**, **Hirotani S**, **Oboshi M**, **Nishimura K**, **Sawada H**, **Eguchi A**, **Okuhara Y**, **Iwasaku T**, **Naito Y**, **Mano T**, **Okamura H**, **Masuyama T**. Interleukin-18 disruption suppresses hypoxia-induced pulmonary artery hypertension in mice. *Int J Cardiol* 202: 522–524, 2016. doi: 10.1016/j.ijcard.2015.09.118.

331. **Wong JJM**, **Tan HL**, **Zhou J**, **Lee JH**, **Leong JY**, **Yeo JG**, **Lee YH**. Large scale cytokine profiling uncovers elevated IL12-p70 and IL-17A in severe pediatric acute respiratory distress syndrome. *Sci Rep* 11: 14158, 2021. doi: 10.1038/s41598-021-93705-8.

332. **Felger JC**, **Li L**, **Marvar PJ**, **Woolwine BJ**, **Harrison DG**, **Raison CL**, **Miller AH**. Tyrosine metabolism during interferon-alpha administration: Association with fatigue and CSF dopamine concentrations. *Brain Behav Immun* 31: 153–160, 2013. doi: 10.1016/j.bbi.2012.10.010.

333. **Kitagami T**, **Yamada K**, **Miura H**, **Hashimoto R**, **Nabeshima T**, **Ohta T**. Mechanism of systemically injected interferon-alpha impeding monoamine biosynthesis in rats: role of nitric oxide as a signal crossing the blood–brain barrier. *Brain Res* 978: 104–114, 2003. doi: 10.1016/S0006-8993(03)02776-8.

334. **Fekkes D**, **Van Gool AR**, **Bannink M**, **Sleijfer S**, **Kruit WHJ**, **van der Holt B**, **Eggermont AMM**, **Hengeveld MW**, **Stoter G**. Nitric oxide production and monoamine oxidase activity in cancer

patients during interferon-α therapy. *Amino Acids* 37: 703–708, 2009. doi: 10.1007/s00726-008-0191-x.

335. **Fekkes D**, **Bannink M**, **Kruit WHJ**, **Van Gool AR**, **Mulder PGH**, **Sleijfer S**, **Eggermont AMM**, **Stoter G**. Influence of pegylated interferon-α therapy on plasma levels of citrulline and arginine in melanoma patients. *Amino Acids* 32: 121–126, 2007. doi: 10.1007/s00726-006-0284-3.

336. **Wright KP**, **Drake AL**, **Frey DJ**, **Fleshner M**, **Desouza CA**, **Gronfier C**, **Czeisler CA**. Influence of sleep deprivation and circadian misalignment on cortisol, inflammatory markers, and cytokine balance. *Brain Behav Immun* 47: 24–34, 2015. doi: 10.1016/j.bbi.2015.01.004.